CURRENT GEOLOGIC ISSUES IN NEW YORK STATE: FROM CARBON DIOXIDE STORAGE TO LANDSLIDING

A Dissertation
Presented to the Faculty of the Graduate School
of Cornell University
in Partial Fulfillment of the Requirement for the Degree of
Doctor of Philosophy

by
Kathryn Lydia Tamulonis
May 2010

CURRENT GEOLOGIC ISSUES IN NEW YORK STATE: FROM CARBON DIOXIDE STORAGE TO LANDSLIDING

Kathryn Lydia Tamulonis, Ph.D.

Cornell University, 2010

The work in this dissertation explores two topics: 1) the local and regional geologic carbon dioxide storage potential in the Upper Ordovician Queenston Formation, and 2) the causes of current displacement at two active landslides, as well as assess past landslide activity. The study site for both projects is central New York State.

A site-specific CO_2 storage assessment of the Queenston Formation is performed for a particular coal-fired power plant in central New York, and this formation is also regionally evaluated for CO_2 storage potential in central New York. Well log, core, seismic, and outcrop data comprise the Queenston Formation data set. In Tompkins and Cayuga Counties, the Queenston Formation was deposited in a distributary fluvial system with mobile channels and no stable, long-lived flood plains. A static CO_2 storage calculation reveals that a 25 mile^2 area of the formation underlying a particular coal-fired power-plant in northern Tompkins County could store on average 18 years of CO_2 emissions from that particular plant. Several regional interpretations of the Queenston Formation depositional system are constructed, but regardless of the depositional model, the Queenston Formation does not have porosity necessary for CO_2 storage in western New York. A static CO_2 storage calculation for the central New York study area reveals that the portion of the Queenston Formation with >10% porosity can store approximately 5×10^9 metric tons of CO_2, which is the equivalent of 120 years of state-wide power plant CO_2 emissions.

Data collected at two active landslides in glacio-lacustrine sediment in the Tully Valley, New York, reveal that several factors affect current landslide movement, including heavy rainstorms, the associated rise in ground-water levels with precipitation events, and stream-generated erosion of the landslide toe. Dendrogeomorphic techniques suggest that past landslide activity also results from a sequence of factors, including: (1) periods with below-average precipitation followed by persistent above-average precipitation, (2) the attendant increase in streamflow eroding the landslide toe, resulting in upslope slump propagation, and (3) the harvesting of trees within the landslide.

BIOGRAPHICAL SKETCH

Kathryn Tamulonis was born on January 27, 1980 in Reading, Pennsylvania. She lived in Pottsville, Pennsylvania until she was 6 years old, when her relocated to Orwigsburg, Pennsylvania. Katie attended Blue Mountain High School, where she was on the volleyball and soccer teams, participated in a state champion Environthon team, edited the school yearbook, and participated in art club.

After high school, Katie went to Dickinson College in Carlisle, Pennsylvania to pursue her undergraduate degree. During her time at Dickinson College, Katie majored in geology, and in the summer of 2001, she spent the summer doing fieldwork in Mono Lake, California with Susan Zimmerman (now at Lawrence Livermore National Laboratory). Katie worked as a geologist for Groundwater Sciences Corporation, an environmental consulting firm in Fishkill, New York, between undergraduate and graduate school.

Katie entered the graduate program in the Earth and Atmospheric Sciences Department at Cornell University in 2004 to pursue a Ph.D. under the guidance of Teresa Jordan. Katie was awarded the Olin Fellowship from Cornell University her first year of graduate school, and was funded for two years as a graduate student intern at the Ithaca USGS office (in conjunction with the New York State Water Research Institute). Katie spent the summer of 2008 as an intern with Schlumberger Carbon Services in Houston, Texas, and in May 2009, Katie was given the Estwing Award from Cornell's Earth and Atmospheric Sciences Department. During her free time, Katie enjoys skiing, biking, the Philadelphia Eagles and Phillies, and Bruce Springsteen. This dissertation represents the results of research conducted throughout Katie's 5.5 years as a graduate student at Cornell University. After defending her

Ph.D., Katie moved to Houston, Texas, where she is employed as a geologist by Schlumberger Carbon Services.

Dedicated to my family

ACKNOWLEDGMENTS

Many people have helped me attain my goals at Cornell University, including advisors, professors, fellow graduate students, friends, and family. All of these individuals have provided me with the guidance, inspiration, and support necessary to complete my Ph.D. degree over the past five years.

First and foremost, I thank Teresa Jordan, my principal advisor at Cornell University. Since my first day at Cornell, Terry has been generous with her time, encouragement, constructive feedback, and financial support. She has humbly taught me to be an effective scientist, and I enjoy growing as a geologist under her kind and outstanding guidance. In addition to Terry, the rest of my committee, Lou Derry and Tammo Steenhuis, have aided me in the classroom, committee meetings, and exams. Without the guidance and support of my committee, I would not have been able to complete this dissertation.

Other university faculty and staff members have also helped me throughout my years as a graduate student. The staff of Cornell's Malcolm and Carolyn Wiener Laboratory for Aegean and Near Eastern Dendrochronology was very helpful in the completion of my landslide dendrogeomorphology study. Sturt Manning, Carol Griggs, Jenn Watkins, and Brita Lorentzen shared their dendrochronology expertise and helped me develop a method for historically modeling landslide activity from tree ring growth patterns. Maura Weathers was patient when teaching me to operate the XRD machine, Michelle Goman allowed me to use her lab for various sample preparation procedures, Bill Bassett generously donated some of his microscope equipment to our lab, and Dan Karig was my personal guide to landslides in the Six Mile Creek. Rick Allmendinger generously invited me into the field with him and was

always willing wager football bets. Chris Andronicus was helpful with mineral identification, and Muawia Barazangi and Art Bloom made sure I was nourished and productive in the lab. Sequestration conversations with Jason Phips Morgan were enlightening and entertaining. Steve Gallow saved me from many a technology-related disaster, and the ladies in the front offices, Linda Hall, Amy Colvin, and Carolyn Clark always provided assistance when needed.

The USGS Ithaca office, along with the New York State Water Research Institute, provided me with a two year internship, which included financial support. I had a wonderful time working in this office. Dave Eckhardt, my supervisor, was a patient teacher and enthusiastic boss. Jim Reddy, my ground-water sampling partner, was always available to help me with GIS problems or talk football. Will Hackett was an effective field assistant in the Tully Valley, and Stephen Shaw helped me wrap up the landslide projects after my internship ended. Bill Kappel was a wonderful mentor who helped me develop the Tully Valley landslide projects. I truly enjoyed every minute I spent with Bill, and his advice and support are greatly appreciated.

The Reservoir Characterization Group at the New York State Museum provided all well log, core, and cuttings data. Aside from supplying data, Rich Nyahay, Taury Smith, Brian Slater, Alexa Storolow, and Joe Bamberger provided assistance with well log interpretation, sample location, and Petra software problem-solving. Without the help of this group, the CO_2 sequestration portion of my dissertation would not have been possible. Anschutz Exploration Corporation collected 3D seismic data from our sequestration study area and generously offered to share this data with our group. Discussions with Dan Bean, Scott Hajicek, and Margot Timbel were very insightful, and Elaine Bateman's help with Kingdom Suites software was invaluable during our visit with Anschutz. Dan Krygowski of the Discovery Group provided help with well log analysis, and Jeff Over aided in trace

fossil identificaton. Meetings and phone conferences with our NYSERDA CO_2 sequestration grant co-workers proved to be enlightening and entertaining experiences. I thank Marta Castagna, Matt Becker, Bob Jacobi, and Rick Frappa for their collaboration.

I spent the summer of 2008 interning with Schlumberger Carbon Services division, where I will be employed after I complete my degree. I thank John Tombari for offering me the internship and future career. Alan Brown was my immediate supervisor during my internship, and he never hesitated to share his knowledge and expertise with me. I look forward to working with him and John in Houston.

I am grateful for the financial support I received throughout the years. My first year of graduate school was funded by Cornell University's Olin Fellowship, and my second and third years were funded by an internship through the New York State Water Research Institute with the USGS Ithaca office. I have most recently been funded as a research assistant through carbon sequestration research grants award by the Engineering College and NYSERDA. The Cornell University Graduate School and the S. Kaufman Travel Fund provided conference travel funds.

I first became interested in geology at Dickinson College in Carlisle, Pennsylvania thanks to the energetic atmosphere of the Dickinson College campus and a lively and enthusiastic geology department. Marcus Key, Noel Potter, Jeff Neimitz, and Gene Yogodzinski instilled the confidence, curiosity, and work ethic needed to become a successful geologist, and they showed me how fun geology can be.

I enjoyed developing my dissertation alongside my fellow Snee Hall graduate students. I entered graduate school with Tiffany Tcharkirides, Holly Caprio, Rachel Shannon, Ursula Smith, and Gaby Depine, and it was a pleasure to begin this journey alongside such a clever group of women. Aside from being a classmate, Gaby Depine was a wonderful housemate and supportive friend throughout my years at Cornell.

Labmates Greg Hoke, Brian Ruskin, Peter Nester, Joey Rosario, Naomi Kirk-Lawlor, and Ceren Karaca provided interesting scientific exchange through the years. I particularly thank Peter Nester and Stephanie Devlin for creating a workspace full of laughter, fun, and science, and Louise McGarry for her invaluable friendship. Other relationships with graduate students have been influential during my time at Cornell. I thank Jacob Moore, Jack Loveless, Adam Goss, Mary Kosloski, Greg Kirkpatrick, Chen Chen (CC), Danielle Glasgow, Bill Barnhart, Phoebe Judge, Amanda Baker, Chao Shi, Gregg McElwee, and Chen Chen for their support and reassurance that we are all in this together.

The Philadelphia Eagles and Phillies provided much distraction, fun, and pain throughout my entire life. I am very, very thankful that the Phils finally brought a trophy to back to Philly in 2008, and I look forward to seeing the Lombardi trophy at the Linc.

Thanks to all my friends outside the department for their support, particularly Lindsay Kift, Anna Posner, Andréa Campbell, and Mackenzie Mady. Art Kasson provided companionship, patience, fun, love, and support during my time at Cornell, for which I am grateful.

Finally, my immediate and extended family has been a constant source of encouragement and enthusiasm. I thank my parents, Frank and Jane Tamulonis, for instilling in me the desire to pursue my dreams, teaching me the value of giving my best effort, and providing me the means to do so. My brother, Frankie, is a shining source of laughter and support. My aunt, Jeanie Troutman, and my grandparents, (Mimi, Pops, Cis, and Tam) were and are wonderful influences who valued the importance of quality education. I extend my deepest gratitude to my family for building the framework for this dissertation.

TABLE OF CONTENTS

LIST OF FIGURES

LIST OF TABLES

INTRODUCTION

The geology of central New York is controlled by sedimentary Paleozoic bedrock, and the relatively recent glacial history of the region produced some of the most visually remarkable surface features in the eastern United States. The Paleozoic bedrock records various mountain building events and sea level fluctuations, and significant work defining North American geology occurred in this region in the 19th and 20th centuries (i.e., Conrad, 1843; Grabau, 1908 and 1913**)**. Aside from providing clues to Earth's evolution throughout the Paleozoic, central New York sedimentary rocks are economically valuable, as natural gas has been produced for over a century (Smith, 2006) and salt mined from the area was the Nation's largest salt source in the 19th century (Yager et al., 2007). The Pleistocene movement of ice sheets over central New York bedrock carved the region and deposited moraines, drumlins, glacio-lacustrine sediment, and gravel (Rogers, 1991).

The study of sediments and the rocks they form provides useful insight into present and historic processes on Earth's surface. These materials can serve informative and practical purposes, such as revealing clues about depositional history and functioning as subsurface reservoirs, respectively, but they also pose risks, as the interaction among unconsolidated sediment exposed on a slope, ground-water flow, precipitation, and erosion may trigger landslides. This dissertation discusses two different topics: 1) the potential for a Paleozoic siliciclastic formation in central New York to serve as a geologic carbon dioxide storage reservoir (Chapters 1 and 2), and 2) sediments involved in landslides in the Tully Valley, New York and the factors affecting present and historic displacement of these landslides (Chapters 3 and 4).

Carbon dioxide is a greenhouse gas believed to be a major factor in global warming (IPCC, 2005). In order to mitigate global warming, regulations such as the

Regional Greenhouse Gas Initiative (RGGI, www.rggi.org), were established to motivate member states to investigate methods to reduce carbon dioxide emissions into the atmosphere. New York State joined RGGI in 2006 and is currently investigating the feasibility of carbon capture and storage potential as a means of dealing with CO_2 emissions from point sources. Technology must improve and storage options must be developed in order for carbon capture and storage to happen. Subsurface geologic CO_2 storage in New York State offers a promising storage option (Smith, 2007).

Numerous topics must be thoroughly evaluated prior to installation of any geologic CO_2 storage operation in a sedimentary basin, inclusive of technical aspects, engineering design, and risk factors, but the starting point must be to evaluate if there is sufficient void space in the target area rocks to hold the volume of CO_2 projected to be injected. Furthermore, the suitable void volume in one or more CO_2 storage reservoirs must exist at depths great enough to be sealed below the minimum depth at which CO_2 can be maintained in a supercritical state (IPCC, 2005). Depending on the details of the geothermal gradient, the minimum depth is greater than 2600 feet (800 meters; IPCC, 2005). Primary and secondary sealing units must exist above the reservoir unit. Pursuing the long list of other technical parameters is worthwhile to do only in the rocks that have adequate void space.

The New York Reservoir Characterization Group of the New York State Museum identified as potential carbon dioxide reservoirs numerous Paleozoic sedimentary formations in the Appalachian basin sector of New York State because of their regionally favorable porosity (Smith, 2007). After a preliminary data assessment, we focus our study on the Upper Ordovician Queenston Formation. Other important factors to consider when assessing a potential geologic storage reservoir

(aside from porosity) that are not addressed in this dissertation are flow and geochemical modeling, geomechanical properties, and seals.

Chapter 1 presents a site-specific geologic CO_2 storage estimate for the Queenston Formation at a particular AES coal-fired power plant in central New York (the AES Cayuga power plant). Well log examination reveals that the petrophysical properties of the Queenston Formation vary laterally and with depth. Based on these properties, I divide the formation into petrophysical zones; examine sedimentary characteristics from well core; divide the core into distinct lithfacies; examine macroscale formation structure and variability distinguished in seismic data; conduct thin section point counts; describe cement; and compare various porosity data sets in order to determine the most accurate porosity measurement. A geologic interpretation (inclusive of depositional environment and base level fluctuations) of the Queenston Formation from data surrounding the AES Cayuga power plant site indicates that the formation offers the potential to store CO_2 in its pore space. Potential static CO_2 storage mass is estimated for a defined Queenston Formation reservoir area underlying and adjacent to the AES power plant, though numerous uncertainties are with this calculation affect the error measurements.

Chapter 2 uses the depositional environment results from Chapter 1, along with additional well core and outcrop data, to perform a regional CO_2 storage calculation for the Queenston Formation of central New York. I map regional petrophysical zones based on well log variations and construct isopachs of these zones. Integration of petrophysical zones with well core reveal that the gamma log signature records base level cycles, which are mapped throughout the study area. I then calculate net feet of sand with porosity greater than 10% for wells using neutron porosity and gamma logs and assemble contour maps of the porous sand feet. Variations in base level trends recorded by gamma logs are noted. Based on well log, core, seismic, and outcrop

data, several depositional and stratigraphic models are constructed, all of which affect CO_2 storage potential in the Queenston Formation. A hypothesis concerning how Queenston Formation sediment was supplied and how this sediment supply interacted with western New York fault systems is addressed. I calculate the static CO_2 storage potentials for the entire Queenston Formation. Based on facies changes detected from well logs, cutting, and outcrops, favorable locations for geologic CO_2 storage are determined.

Landslides in central New York are primarily composed of glacio-lacustrine sediment and move generally slowly, though fast-moving landslides have been recorded. The largest landslide in New York State since the early 1900's occurred in the glacio-lacustrine sediment of the Tully Valley in the Finger Lakes region in 1993. There is evidence of at least four other historic landslides in the Tully Valley, and currently, two active, slow-moving landslides are located in the Tully Valley, the Rattlesnake Gulf and Rainbow Creek landslides. These active landslides are composed of sediment similar to that involved in the 1993 Tully Valley landslide. In order to understand these landslides, it is necessary to study the causes of current landslide displacement, as well as examine possible historic landslide triggers. Chapters 3 investigates present day landslide triggers and Chapter 4 models past landslide activity using dendrogeomorphology techniques, respectively.

Chapter 3 addresses the causes of displacement at the two active landslides in the Tully Valley. For both Rattlesnake Gulf and Rainbow Creek landslides, I mapped the area of active and historic landsliding and described the composition of the landslide sediment. Data on soil displacement (landslide movement), ground-water levels, and precipitation are collected. Examination of the data sets reveals that precipitation and ground-water levels affect landslide movement and indicates there are at least several displacement mechanisms working on the landslide. Historic

landslide activity is examined from aerial photographs dating back to 1937, and from this data, I construct a conceptual progression of degradation of the Rainbow Creek channel. Geotechnical sediment properties of the two landslides are collected and compared to those of the fast moving 1993 Tully Valley landslide.

Chapter 4 discusses dendrogeomorphic techniques used to assess historic landslide movement within the Rattlesnake Gulf landslide in the Tully Valley during the last century. Dendrogeomorphology is based on the premise that landmass movement, expressed as slope failure, can cause trees to tilt, which in turn can trigger a response in tree growth (i.e, Aestello, 1971). Increment cores are obtained from hemlock trees (*Tsuga canadensis)* across the active part of the landslide and from three control sites to interpret the soil-displacement history. Annual growth rings are measured and reaction wood is identified to indicate years in which ring growth changed from concentric to eccentric, on the premise that soil movement triggered compensatory growth in displaced trees. These data provided a basis for an "event index" to identify years of landslide activity over the 108 years of record represented by the oldest trees. Event-index values are related to total annual precipitation records with multiple-regression and residual-values. A sequence of factors, including precipitation, streamflow, and the harvesting of trees above the landslide, all trigger landslide displacement.

REFERENCES

Aestello, J. 1971. Dendrochronological interpretation of geomorphic processes. Fennia. 105: 1-140.

Conrad, T.A. 1843. Description of fossils from the Helderberg Division of New York. *In* Geology of New York; Part I, Comprising the geology of the first geological district. Albany, New York. 349 pp.

Fickies, R.H. 1993. A large landslide in Tully Valley, Onondaga County, New York. Association of Engineering Geologists News. 36(4): 22-24.

Grabau, A.W. 1908. A revised classification of the North American Silurian. Science. 27: 622-623.

Grabau, A.W. 1913. Early Paleozoic delta deposits of North America. Geological Society of America. 24: 299-528.

Intergovernmental Panel on Climate Change (IPCC). 2005. Carbon Dioxide Capture and Storage. 442 pp.

Pair, D.L., Kappel, W.M., and Walker, M.S. 2000. History of landslides at the base of Bare Mountain, Tully Valley, Onondaga County, New York: U.S. Geological Survey Fact Sheet 190-99. 6 pp.

Rogers, W. B. 1991. The missing record - Tertiary Period, *In* Isachsen, Y.W., Landing, E., Lauber, J.M., Rickard, L.V., and Rogers, W.B., Eds. Geology of New York - A simplified account: Albany, N.Y., New York State Museum, Educational Leaflet 28: 157-160.

Smith, L.B., Jr. 2006. Origin and reservoir characteristics of Upper Ordovician Trenton-Black River hydrothermal dolomite reservoirs in New York. AAPG Bulletin. 90(11): 1691-1718.

Smith, L.B., Jr. 2007. Carbon dioxide capture and storeage (CCS) potential in New York State. PowerPoint slides. Retreived from http://esogis.nysm.nysed.gov/esogis/talks.cfm.

Yager, R.M., Kappel, W.M., and Plummer, L.N. 2007. Halite brine in the Onondaga Trough near Syracuse, New York: Characterization and simulation of variable-density flow: U.S. Geological Survey Scientific Investigations Report 2007–5058. 40 pp.

CHAPTER 1

SITE-SPECIFIC CARBON DIOXIDE STORAGE POTENTIAL FOR THE QUEENSTON FORMATION NEAR THE AES CAYUGA COAL-FIRED POWER PLANT IN TOMPKINS COUNTY, NEW YORK

Abstract

We evaluate the pore volume available for a specific potential geologic carbon dioxide storage site in the Queenston Formation near the AES Corporation Cayuga coal-fired power plant in Tompkins County, New York. Well core data collected 25 miles (40 kilometers) from the AES Cayuga plant reveal that the Queenston Formation is a relatively homogenous fine to medium grained sandstone with hematite cement. Cross and planar bedding are the dominant sedimentary structures, and mudstone rip-up clasts are common. Based on observed core characteristics, the Queenston Formation was divided into six lithofacies, and base level cycles were interpreted from the characteristics of these lithofacies.

Gamma, neutron porosity, and electron density well logs collected near the AES site reveal four stacked petrophysical zones (Queenston B (top) to E (base)) that can also be related to seismic and core data. Seismic data record likely unconformities within these zones. Well core and log signatures imply that petrophysical zones B and C each represents a cycle of base level fall followed by base level rise. An isopach map generated from the seismic data reveals that the Queenston Formation is thickest in a NNW trending depocenter. This trend is similar to the paleocurrent direction recorded in the Juniata Formation, the Pennsylvania equivalent to the Queenston Formation, which suggests these depocenters may coincide with channels cut during base level fall and then subsequently filled during base level rise. Seismic and core

data indicate that the Queenston Formation was deposited in a distributary fluvial system with mobile channels and no stable, long-lived flood plains.

Porosity is a major factor affecting geologic CO_2 storage potential, and it is important to understand discrepancies among porosity measured from core-plug, neutron porosity, density-derived porosity (from electron density log data), and thin section point-count values. Porosity and air permeability data vary systematically with petrophysical zones, as well as with lithofacies. Assuming that core-plug derived porosity represent the most accurate porosity values, data sets reveal that the neutron porosity log is more reliable than the electron density porosity values. Thin section examination reveals that hematite cement content is the primary factor affecting porosity.

A site-specific static CO_2 storage calculation has been made for the AES Cayuga power plant. Seismic, core, and well log data suggest that in a 5 mile × 5 mile area surrounding this AES power plant, the Queenston Formation can sequester 18 million metric tons (+/- 11 million metric tons) of CO_2 (approximately 8 years (with a range considering uncertainties of 3 to 12 years) of CO_2 emission from the AES Cayuga power plant. Uncertainties, such as CO_2 density, reservoir porosity, and formation storage efficiency factor, must be better constrained in order to obtain a more accurate estimate. Because the Queenston Formation near the AES Cayuga power plant is relatively homogenous with little differentiation between sheet flood sands and channel sands, a majority of this formation at this location offers the potential for CO_2 storage in its pore space. This potential decreases west of the AES Cayuga site where the formation is more variable and clay content increases. Existing permeability data suggest that portions of the Queenston Formation are tight sands (permeability less than 1 mD) and reservoir stimulation would be needed to access much of the pore volumes. Much additional data, particularly fracture permeability

data, must be collected in order to further assess the CO_2 sequestration potential of the Queenston Formation.

Introduction

New York State joined the Regional Greenhouse Gas Initiative (RGGI) in August 2006, under which ten Northeast and Mid-Atlantic USA states agreed to implement a CO_2 cap-and-trade system in order to reduce greenhouse gas emissions into the atmosphere. These regulations make it necessary that New York State, as well as the power and industrial sectors, investigate the feasibility of carbon capture and storage potential as a means to deal with CO_2 emissions from point sources, such as coal-fired power plants (Figure 1.1). Independent of efforts needed to improve the technology of carbon capture, storage options must be developed and studied (IPCC, 2005). Subsurface geologic CO_2 storage in New York State offers a promising storage option (Smith, 2007).

Numerous topics must be thoroughly evaluated prior to installation of any geologic CO_2 storage operation, including technical factors, engineering design, and risk factors. But the starting point must be to evaluate whether there is sufficient void space in the target area rocks, either in pores or fractures, to hold the volume of CO_2 projected to be injected. Furthermore, the suitable void volume in one or more CO_2 storage reservoirs must exist at depths great enough to be sealed below the minimum depth at which CO_2 can be maintained in a supercritical state (IPCC, 2005). Depending on the details of the geothermal gradient, the minimum depth is greater than approximately 2,600 feet (800 meters; IPCC, 2005). In order to assure that primary and secondary sealing units exist above the reservoir unit yet below 2,600 feet (800 meters), we adopt the practice of seeking reservoirs in New York State at depths greater than 3,000 feet (900 meters) below the ground surface. Pursuing the long list

Figure 1.1. Map of New York State. Data was consulted from 269 wells (acquired from New York State Museum database at www.esogis.com,) from an 11 county area (yellow) surrounding five AES power plants (not all of these wells have Queenston Formation data). The north-south cross section is located from A-A' (Figure 2). Anschutz Exploration Corporation provided seismic data in Tompkins and Cayuga counties. The Silurian Syracuse Salt, considered to be a prospective secure seal unit (Smith, 2007), exists south of green line. The black dashed line marks the northern extent of area in which the top of the Queenston Formation occurs at depths greater than 3,000 feet. Wells used for the N-S cross section (Figure 1.2) and the petrophysical zone cross section (Figure 1.4) are filled with black and numbered: 1 – Wasielewski Well, 2 – Venice View Dairy Well, 3 – Fee Richarson Well, 4 – Kesselring Well.

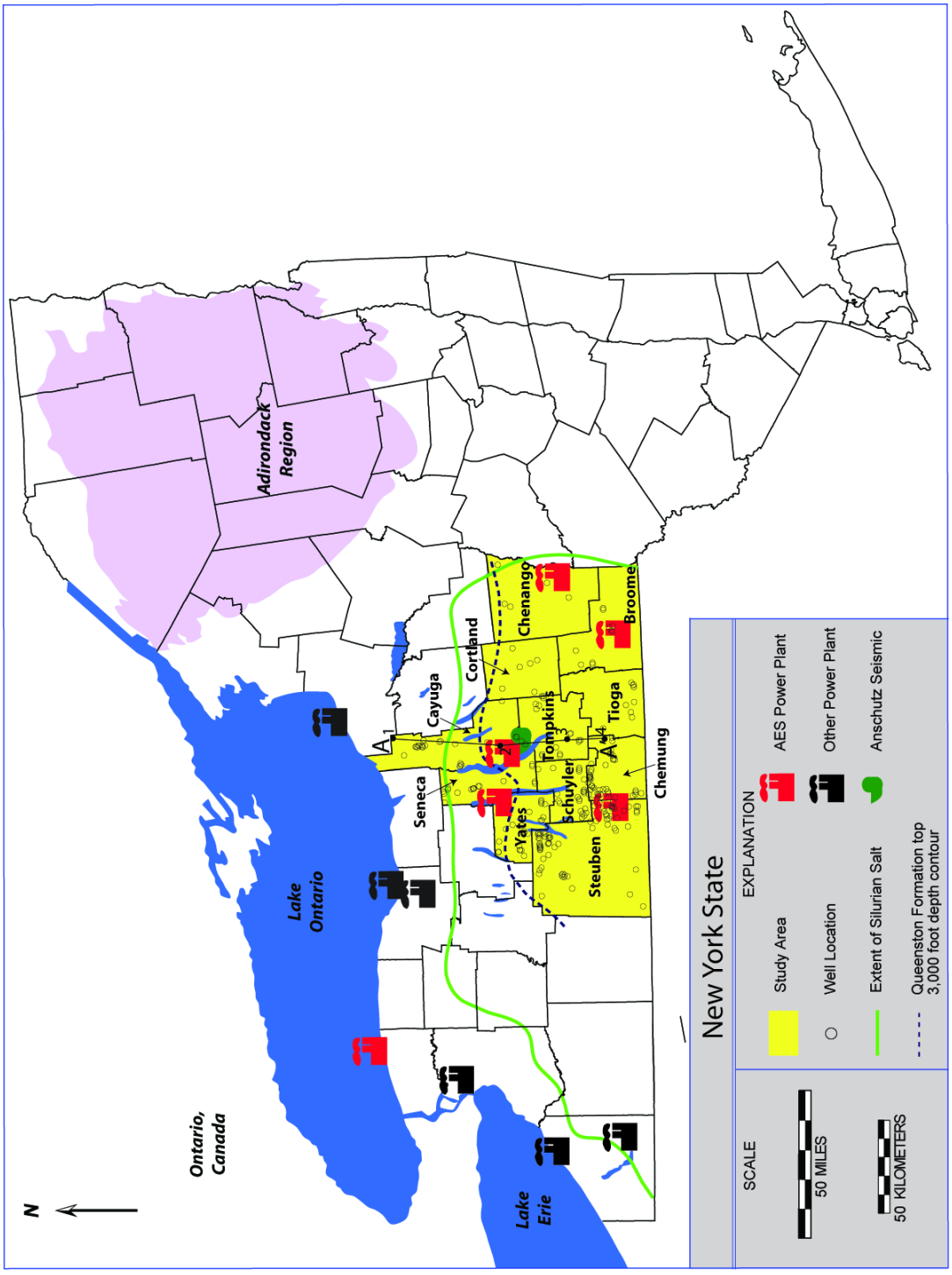
New York State
EXPLANATION
Study Area
Well Location
Extent of Silurian Salt
Queenston Formation top
3,000 foot depth contour
AES Power Plant
Other Power Plant
Anschutz Seismic
SCALE
50 MILES
50 KILOMETERS
N
Ontario,
Canada
Lake
Ontario
Lake
Erie
Adirondack
Region
Seneca
Cayuga
Cortland
Chenango
Broome
Tioga
Tompkins
Schuyler
Yates
Steuben
Chemung
A1
A2
A3
A4

of other technical requirements is worthwhile only in the rocks that have adequate void space.

The New York State Reservoir Characterization Group of the New York State Museum initially highlighted the Cambrian Potsdam Formation, the Cambro-Ordovician Beekmantown Group, Upper Ordovician Black River, Trenton, Oswego, and Queenston Formations, and the Lower Silurian Clinton Formation as potential CO_2 storage formations in the Appalachian basin sector of New York State because of their regionally favorable porosity (Smith, 2007; Figure 1.2). For seals, they proposed that the Upper Silurian Syracuse Salt Formation would serve as an ultimate seal above these potential storage formations. A regional assessment of well log data reveals the Upper Ordovician Queenston Formation of central New York could potentially serve as a subsurface storage reservoir for carbon dioxide (Tamulonis, 2010).

We calculate a potential CO_2 storage mass for a specific point-source site, the AES Cayuga power plant. This location was chosen for focus because a relatively abundant data set is available near that location (Figures 1.1 and 1.3) and because the volume of the approximate 600 feet (800 meters) of Queenston Formation thickness is large enough to potentially store a significant amount of CO_2. Anschutz Exploration Corporation collected seismic and well log data in the immediate vicinity of the AES Cayuga plant for natural gas exploration that focused on the underlying Trenton and Black River Formations, and the New York State Museum has additional digital well logs that surround the power plant. Also available is a four inch (10 centimeter) diameter core through 324 feet (99 meters) of the Queenston Formation from a well approximately 25 miles (40 km) north of the study area (the Delaney well). Comparison of the Delaney well log to other well log signatures, as well as comparison of the core to well cuttings from a well approximately 13 miles (21

Figure 1.2. North-south cross section in study area, illustrating the 1-2°S regional dip. Gamma logs (GR) were used to identify the formation tops, which are mapped on the cross section. The Queenston Formation (highlighted orange) reaches the 2,500 foot depth contour below the gray dashed line, which is the absolute minimum depth necessary for supercritical CO_2 storage. The intersection of the top of the Queenston Formation with the more conservative 3,000 feet below surface horizon is mapped on Figure 1.1 (black dashed line) and occurs below the black dashed line in this figure. Devonian geology is approximate because these formations were not a focus of this study. The unit names are placed just below the top of the corresponding unit.

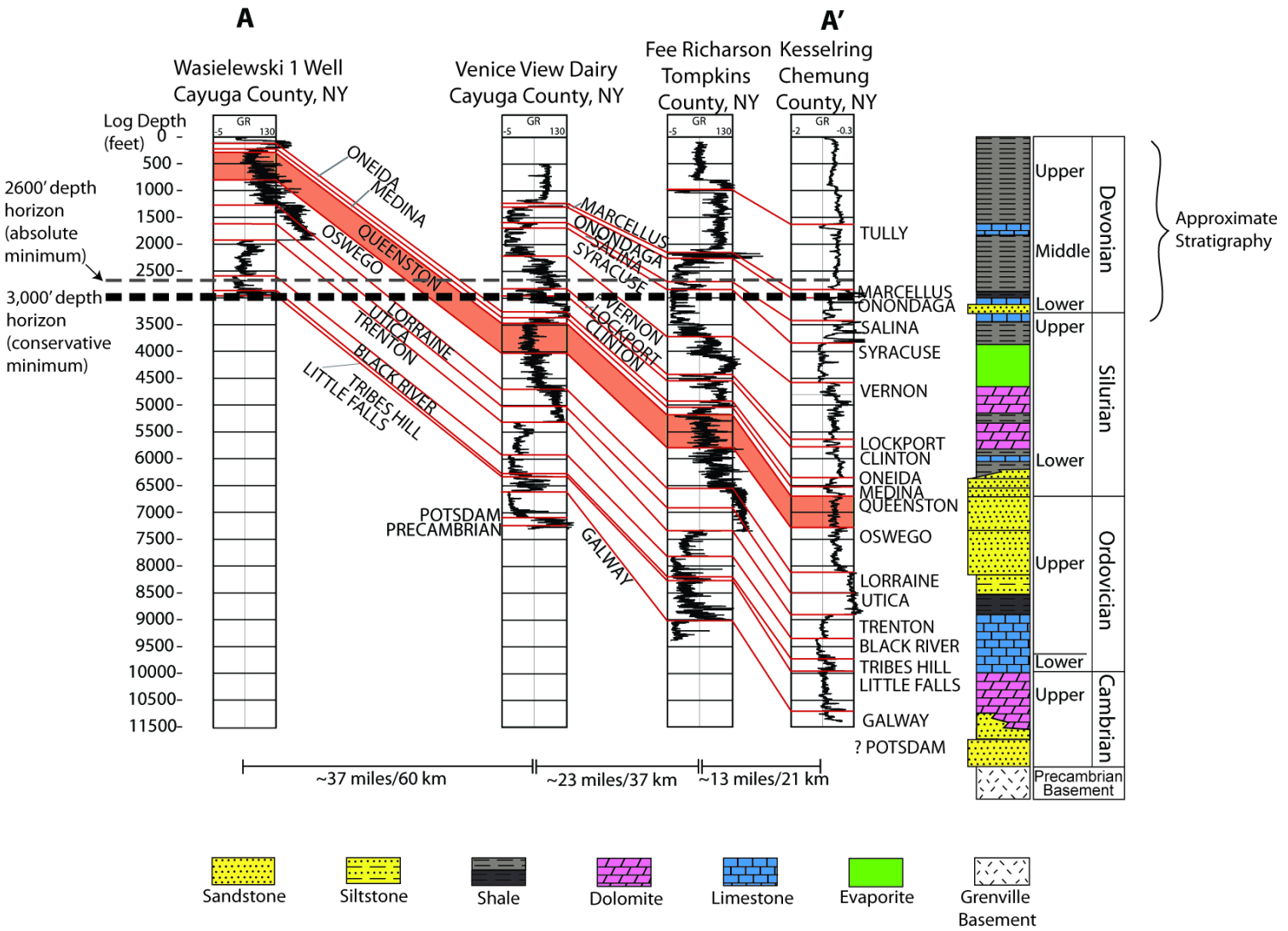
A
A'
Wasielewski 1 Well
Cayuga County, NY
Venice View Dairy
Cayuga County, NY
Fee Richarson
Tompkins
County, NY
Kesselring
Chemung
County, NY
Log Depth
(feet)
2600' depth
horizon
(absolute
minimum)
3,000' depth
horizon
(conservative
minimum)
ONEIDA
MEDINA
QUEENSTON
OSWEGO
LORRAINE
UTICA
TRENTON
BLACK RIVER
TRIBES HILL
LITTLE FALLS
POTSDAM
PRECAMBRIAN
MARCELLUS
ONONDAGA
SALINA
SYRACUSE
VERNON
LOCKPORT
CLINTON
GALWAY
TULLY
MARCELLUS
ONONDAGA
SALINA
SYRACUSE
VERNON
LOCKPORT
CLINTON
ONEIDA
MEDINA
QUEENSTON
OSWEGO
LORRAINE
UTICA
TRENTON
BLACK RIVER
TRIBES HILL
LITTLE FALLS
GALWAY
? POTSDAM
~37 miles/60 km
~23 miles/37 km
~13 miles/21 km
Upper
Middle
Lower
Devonian
Upper
Lower
Silurian
Upper
Lower
Ordovician
Upper
Cambrian
Precambrian
Basement
Approximate
Stratigraphy
Sandstone
Siltstone
Shale
Dolomite
Limestone
Evaporite
Grenville
Basement

Figure 1.3. An isopach map from well log data in central New York indicates that the Queenston Formation thickens to the southwest portion of the study area. The top of the Queenston Formation reaches depths greater than 3,000 feet south of the black dashed line, and the top of the Syracuse Formation reaches depths greater than 3,000 feet south of the orange dashed line. Trenton-Black River and Queenston gas fields are located, as well as the AES Cayuga power plant. Wells used for petrophysical zone cross section are mapped on line B-B', and the Shepard well is also mapped.

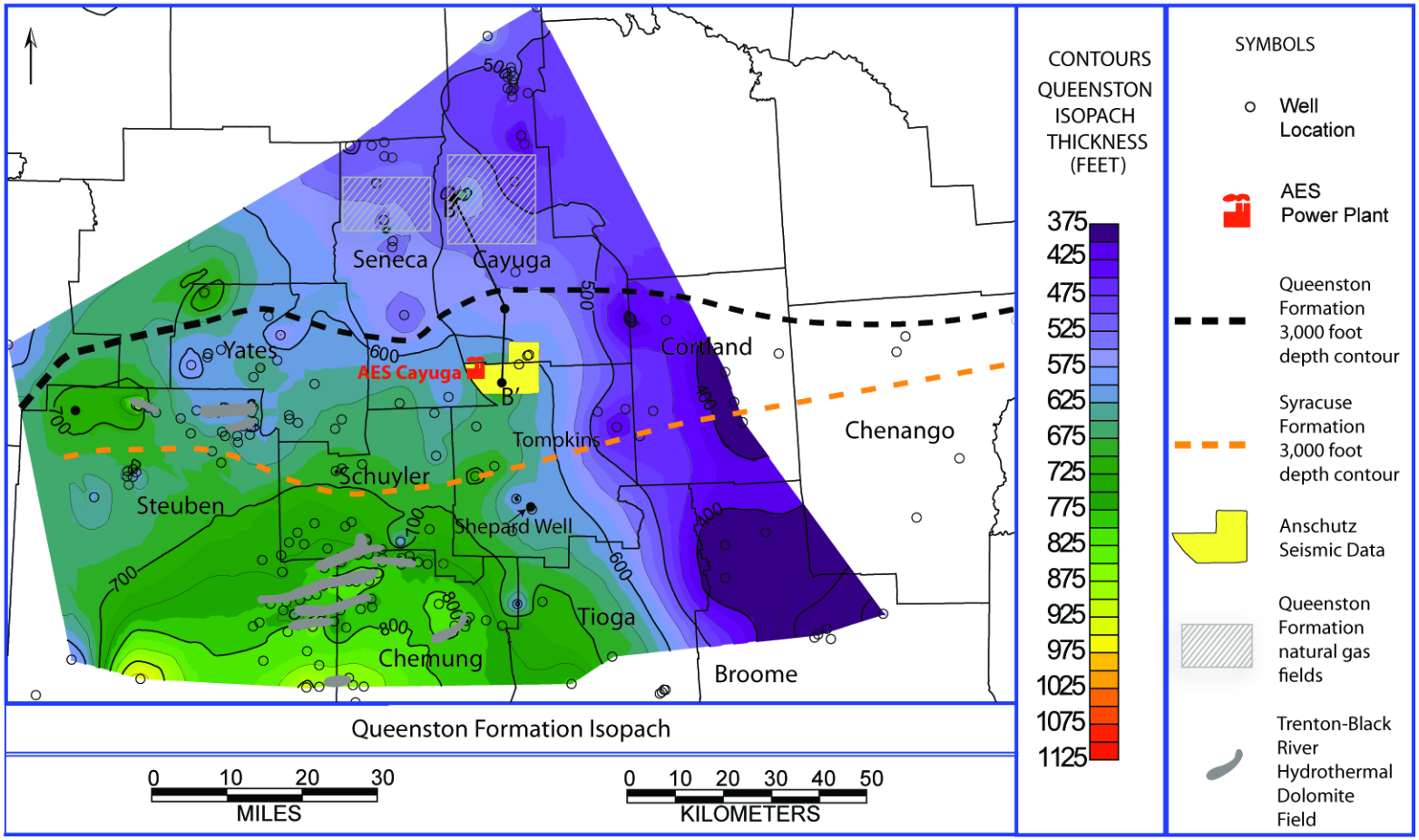
Seneca
Cayuga
Yates
AES Cayuga
B′
Cortland
Tompkins
Chenango
Schuyler
Steuben
Shepard Well
Tioga
Chemung
Broome
500
600
700
800
400
Queenston Formation Isopach
0 10 20 30
MILES
0 10 20 30 40 50
KILOMETERS
CONTOURS
QUEENSTON
ISOPACH
THICKNESS
(FEET)
375
425
475
525
575
625
675
725
775
825
875
925
975
1025
1075
1125
SYMBOLS
Well Location
AES Power Plant
Queenston Formation 3,000 foot depth contour
Syracuse Formation 3,000 foot depth contour
Anschutz Seismic Data
Queenston Formation natural gas fields
Trenton-Black River Hydrothermal Dolomite Field

kilometers) south of the AES Cayuga power plant, imply that the characteristics of this core are likely similar to those of the Queenston Formation underlying the plant (Figure 1.4). The ensemble of data indicate that the Queenston Formation potentially offers the porosity necessary for CO_2 storage at the AES Cayuga site. An important follow-up step in evaluation of the site must be a much more extensive study of the permeability of the unit. Our preliminary data suggest that reservoir stimulation would likely be needed to increase permeability. This paper primarily characterizes the Queenston Formation stratigraphy, porosity, and static CO_2 storage potential for the AES Cayuga power plant. Understanding the variability within the formation throughout New York State has important implications for Queenston Formation carbon storage potential at other point sources. Tamulonis (2010) uses the data presented in this paper plus additional well logs, outcrop, and previously published work, to develop several stratigraphic models for the Queenston Formation, which are integrated into a regional assessment of carbon storage potential for the Queenston Formation.

Geologic Setting

The Upper Ordovician to Lower Silurian sandstones of central New York were deposited in the Appalachian foreland basin and record a complex pattern of deposition, erosion, and facies changes (Robinson, 1987). The Upper Ordovician Queenston Formation is a clastic foreland basin wedge which was deposited westward during Phase V of the Taconic Orogeny (Fisher, 2006) and is part of the Queenston Delta Complex – a regional redbed complex which extends from Ontario to Alabama and collectively is comprised of the Queenston and Oswego Formations in New York (Colton et al., 1970). The formation crops out on the south shore of Lake Ontario and the Niagara Gorge in western New York, where it is siltstone to fine grained quartz sandstone with clay interbeds, and in Ontario, where it is composed of red to gray

Figure 1.4. Cross section B-B' shows the variations in the Queenston Formation petrophysical zones. Location of cross section is mapped in Figure 1.3. Gamma (black line), neutron porosity (blue line, axis reversed), and electron density (red line) logs of the Queenston petrophysical zones Queenston B-E. A porosity log was not available for the Venice View Dairy well. The zone names occur within the corresponding zone.

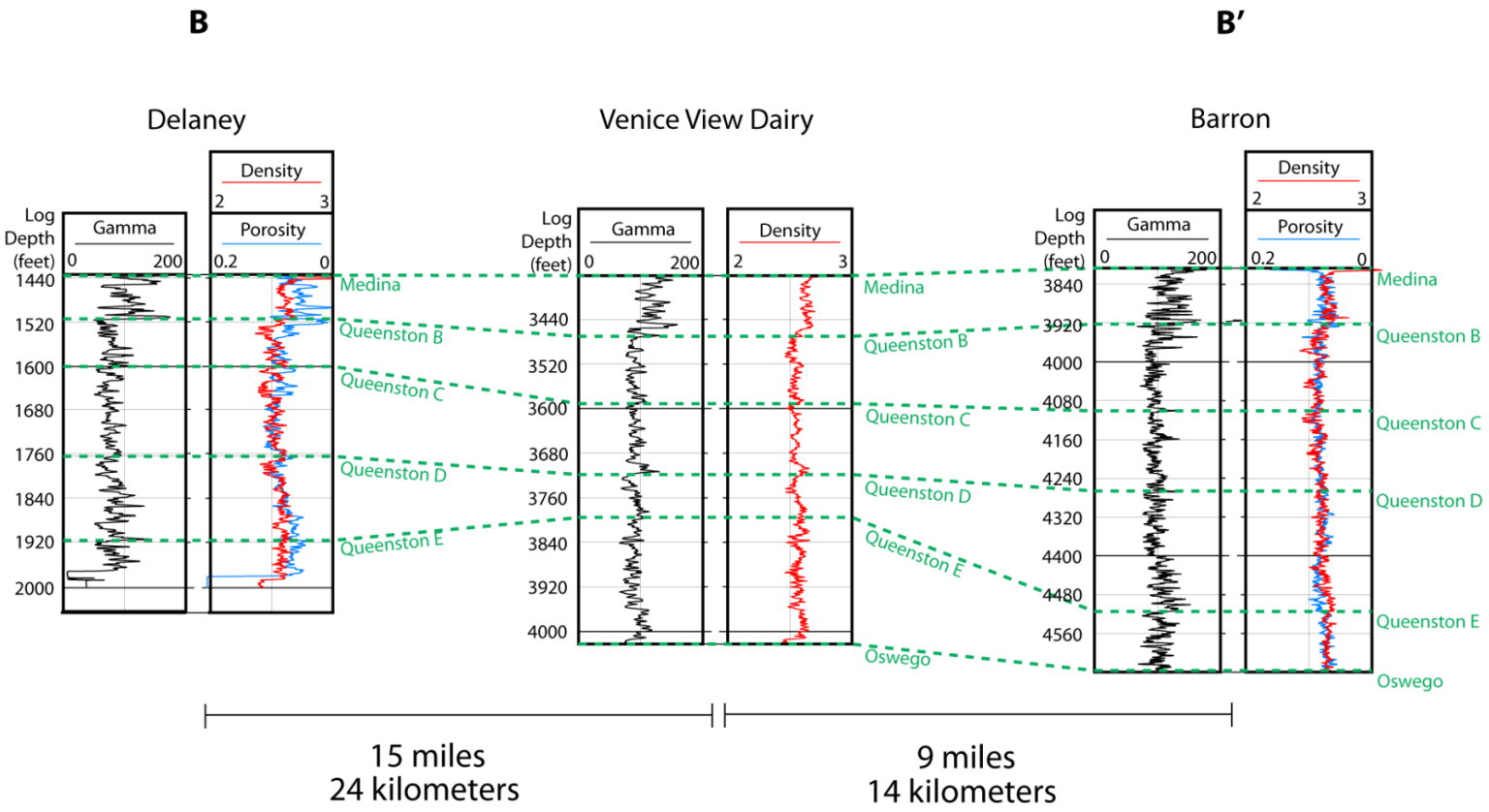
B
B′
Delaney
Venice View Dairy
Barron
Log Depth (feet)
Gamma
0
200
Density
2
3
Porosity
0.2
0
1440
1520
1600
1680
1760
1840
1920
2000
3440
3520
3600
3680
3760
3840
3920
4000
3840
3920
4000
4080
4160
4240
4320
4400
4480
4560
Medina
Queenston B
Queenston C
Queenston D
Queenston E
Oswego
15 miles
24 kilometers
9 miles
14 kilometers

shales and bioclastic limestone (Brett et al., 1996; Brogly et al., 1988). In the subsurface of central New York, the Queenston Formation is primarily red, fine to medium grained sandstone with hematite cement and ranges from 350 to 800 feet (110 to 240 meters) in thickness (Figure 1.3).

The Oswego Formation conformably underlies the Queenston Formation in New York State and is interbedded fine to coarse sandstone, siltstone, and shale. This formation grades into shale and siltstone westward (Robinson, 1987) and forms the transition between the deep water Lorraine shales, which conformably underlie the Oswego Formation, and the Queenston Formation. This sequence (Lorraine, Oswego, Queenston) formed from northward marine regression and uplift of the eastern source area (Robinson, 1987). The Cherokee Unconformity separates the Queenston Formation from the overlying Medina Group (Brett et al., 1996).

Several shallow (less than 1,600 feet) Queenston Formation natural gas fields exist in Cayuga and Seneca counties. Their reservoirs are fine-grained quartz sandstone with subangular quartz grains and clay content averaging 20%. These have been producing natural gas since 1940 (Robinson, 1987).

The top of the Queenston Formation becomes shallower to the north due to the 1-2° regional southward dip of the bedrock (Figure 1.2). It reaches the 3,000 foot (900 meter) depth contour that we adopt as a reasonable minimum for supercritical CO_2 storage north of the Seneca/Schuyler and Cayuga/Tompkins counties border (Figures 1.1 and 1.3). At the AES Cayuga power plant, the top of the Queenston Formation is at approximately 4,200 feet (1280 meters) depth. The top of the unit identified by the New York State Museum as the ultimate seal, the Syracuse Formation, is at approximately 2,200 feet (670 meters) depth. This makes assessment of intermediate seals between the Queenston Formation and the Syracuse Formation vital to identify

existing primary and secondary sealing below the 2,600 foot (800 meter) depth horizon necessary for supercritical CO_2 storage.

Previous Work

Lugert et al. (2006) studied the Queenston Formation core from the Delaney Well in Cayuga County to assess its brine disposal potential. In this study, the physical properties of the core were thoroughly investigated, though the depositional setting from core features was not interpreted. In general, Lugert et al. (2006) described the core as a red, fine to medium-grained sandstone with cross and planar bedding, rip-up clasts, and reduced zones. Based on thin section and porosity data, Lugert et al. (2006) concluded that the formation could potentially store brine.

Robinson (1987), Saroff (1987), and Schlumberger (1996) investigated the nature of the Queenston Formation in Seneca and Cayuga counties for natural gas reservoir potential. Saroff (1988) described the Cayuga County Auburn field to be a fractured, low permeability reservoir with best production in highly fractured zones with high sand content (greater than 75%). Approximately 145 gas wells were drilled into the Cayuga County field since 1960, and in the late 1980's, commercial annual gas production averaged one billion cubic feet per two years (Saroff, 1987). Schlumberger (1996) describes the upper sandstone of this field to be naturally fractured. Robinson (1987) described the fields in Cayuga and Seneca counties as composed of fine-grained subangular quartz sandstone with up to 20% clay content, in which porosity and permeability increase where the formation is fractured. More regionally, the Queenston Formation is interpreted to have been deposited in non-marine conditions (Grabau, 1913; Rodgers, 1971; Brett et al., 1996; Robinson, 1997), though there has been some dispute to that claim (Hughes, 1976; Saroff, 1987).

Materials and Methods

Oil and gas have been produced from Ordovician formations in New York

State for over a century. Recently, in central New York, exploration has been focused on Upper Ordovician Black River and Trenton Formations (Smith, 2006), as well as the Middle Devonian Marcellus Formation (Engelder and Gash, 2008). As a result of this gas exploration and production, hundreds of well logs document the subsurface Queenston Formation in central New York. The gas exploration data summed with data collected to investigate the Queenston Formation for brine disposal comprise a relatively rich data set, to which we apply techniques similar to those used in oil and gas reservoir characterization to study CO_2 storage potential in the Queenston Formation. Though there are several Queenston Formation natural gas fields north of the AES Cayuga power plant (Figure 1.3), the Queenston Formation is not considered to be a major gas producer in New York State. Our Queenston Formation data set consists of borehole logs, core, cuttings, and seismic data. The New York State Museum Reservoir Characterization group stores all digital well logs, cuttings, and cores collected throughout New York State. They have digitized all well logs, to which we had access through the Empire State Oil and Gas Information System database (www.esogis.com), and they also supplied cutting and core samples to this project. Anschutz Exploration Corporation provided access to proprietary seismic data collected in the study area.

Well Logs

Throughout an 11 county area in central New York, 157 of the 269 wells drilled in the region contain digital borehole data from the Queenston Formation, collected as early as 1948 (Figure 1.1). In the four county area surrounding the AES Cayuga power plant (Tompkins, Cayuga, Seneca, and Schuyler counties), 72 wells have Queenston Formation digital log data (Figure 1.3). From this data set, primarily gamma, neutron porosity, and electron density logs were used, though wells with Queenston Formation log data do not necessarily have all three logs. Log

measurements exist on a regular 0.5 foot interval. Where data are available, formation tops between the Salina Formation and the Precambrian basement were identified (Figure 1.2). Petra © software was used in well log interpretation and analysis.

Tamulonis (2010) mapped regionally six distinct petrophysical zones (Queenston A (top) – Queenston F (bottom)) based on gamma, neutron porosity, and electron density signatures. Zones B-E exist in the proximity of the AES Cayuga plant (Figure 1.4). Gamma logs measure rock shale content by measuring natural radioactivity, neutron porosity logs quantify porosity by measuring the hydrogen content in pore space, and electron density logs measure the electron density of a formation by emitting gamma rays into the rock. More specifically, neutron porosity values are calculated from the difference of energy loss from neutrons emitted into a formation by the log tool and neutrons detected by the tool. The underlying phenomenon is that neutrons lose energy when they collide with hydrogen nuclei because the mass of a neutron is approximately equivalent to the mass of a hydrogen nucleus. The neutron energy decline is then converted into porosity units. The density logging tool emits gamma rays that then collide with electrons in the formation and lose energy (defined as Compton Scattering). Returned, scattered rays are then counted by a detector, which is located at a fixed distance from the emitting source. This count is an indicator of formation density (Asquith and Krygowski., 2004).

Seismic Data and Interpretations

Anschutz Exploration Corporation collected approximately 45 miles^2 (115 kilometers^2) of 3D seismic data and 11 N-S trending 2D seismic lines in Tompkins and Cayuga counties (Figure 1.3). Fortuitously, the AES Cayuga power plant is located on the western edge of the seismic data set. This data acquisition was associated with gas exploration targeted for the Trenton and Black River Formations. A mixed source of dynamite and vibroseis was used to collect the 3D data. Dynamite

charges were two pounds in 20 foot (six meter) deep holes, except in areas where depth to groundwater was shallow, in which case one pound dynamite charges were used in 10 foot (three meter) deep holes. The vibroseis source consisted of three 44,000 pound vibroseis trucks which used a sweep frequency of 10-120 Hz, summing eight sweeps of eight seconds per vibration point. Source line spacing was 1,500 feet (450 meters), and receiver line spacing was 1,118 feet (341 meters), at an angle of 26.75° to the source lines. Vibroseis was the source for the 2D lines and had the same sweep parameters as the 3D data, with a shot interval of 180 feet (55 meters). Anschutz Exploration Corporation processed the data, which was deconvoluted, filtered, and migrated.

The Venice View Dairy well log is located approximately six miles (10 kilometers) north of the seismic grid in Cayuga County and is the closest well that has borehole data extending to the Precambrian basement. Sonic velocity and electron density logs from this well were used by Anschutz to calculate synthetic seismic waveforms, which aided in mapping formation tops throughout the seismic data set.

The data were interpreted using Kingdom Suite © software. The authors mapped formation tops between the Syracuse Formation (salt) and the crystalline Precambrian basement on five N-S trending 2D seismic lines and 10 lines within the 3D seismic grid (7 NE-trending lines, and 3 SE-trending cross lines). Nearly half of the mapped lines were chosen for proximity to the AES Cayuga power plant (Figures 1.5, 1.6, and 1.7). In order to convert from two-way travel time, we used sonic velocities calculated by Anschutz Exploration Corporation from electron density logs in the Venice View well (Figures 1.1 and 1.2). The average Queenston Formation sonic velocity is 13441 feet (4096 meters) per second.

Figure 1.5. A seismic line integrated with a gamma well log for the Queenston Formation. This line intersects the Barron well, for which the tops of Queenston petrophysical zones B (Queenston top to top of Queenston C (QC)), C (QC), D (QD), and E (QE) are mapped. On this scale, reflectors in the Queenston Formation generally appear to be flat lying. See Figure 1.7 for approximate location of this line.

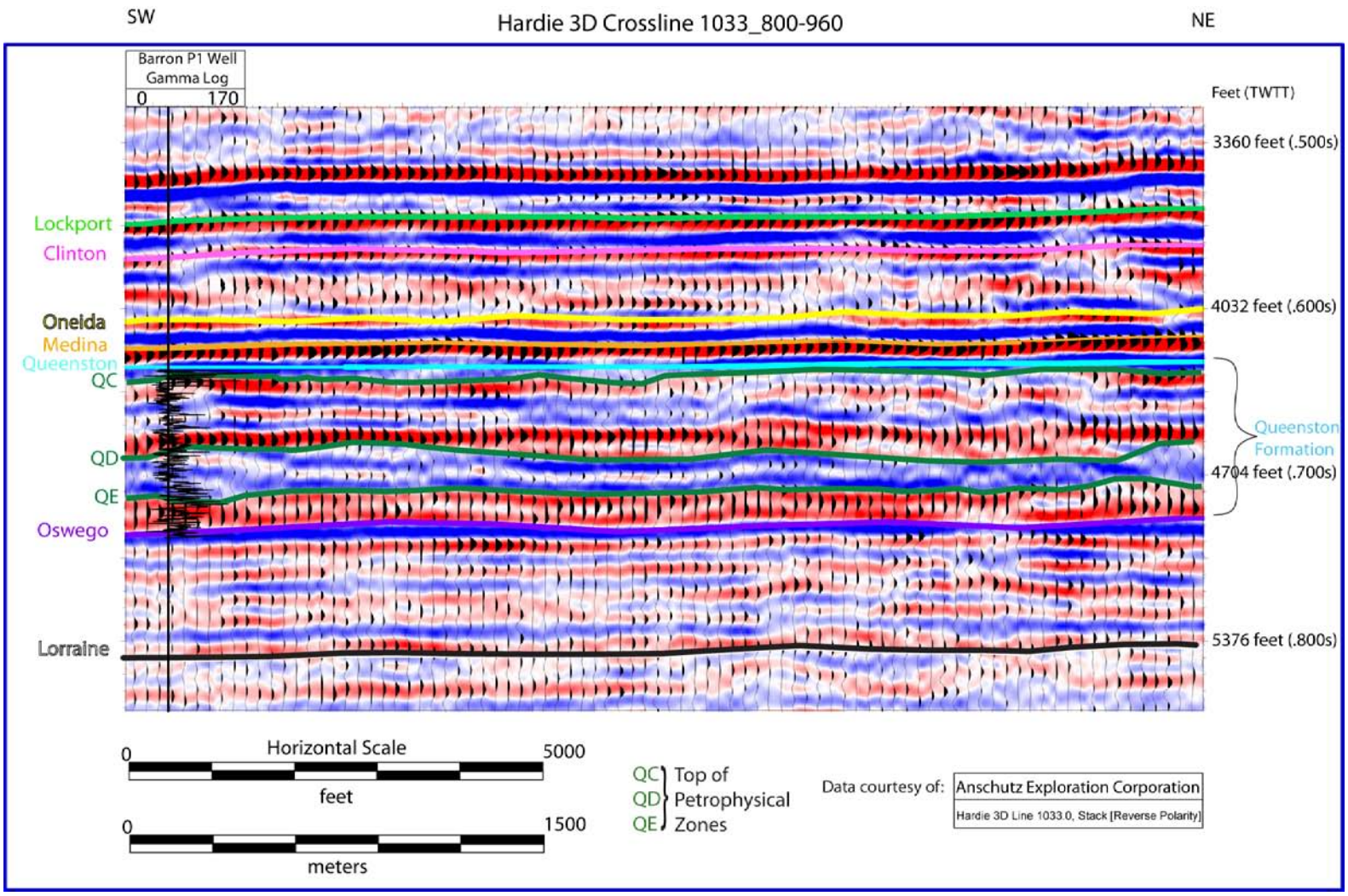
SW
Hardie 3D Crossline 1033_800-960
NE
Barron P1 Well
Gamma Log
0
170
Feet (TWTT)
3360 feet (.500s)
Lockport
Clinton
4032 feet (.600s)
Oneida
Medina
Queenston
QC
QD
QE
Oswego
Queenston
Formation
4704 feet (.700s)
Lorraine
5376 feet (.800s)
Horizontal Scale
0
5000
feet
0
1500
meters
QC
QD
QE
Top of
Petrophysical
Zones
Data courtesy of:
Anschutz Exploration Corporation
Hardie 3D Line 1033.0, Stack [Reverse Polarity]

Figure 1.6. Seismic facies reveal that the Queenston Formation in northern Tompkins and southern Cayuga counties was deposited in a channelized setting. In the seismic data, petrophysical zones Queenston C (QC) and Queenston D (QD) appear to have several erosional surfaces. Queenston reflections are outlined in black line and the top of petrophysical zones are mapped with green lines. See Figure 1.7 for the location of this seismic line.

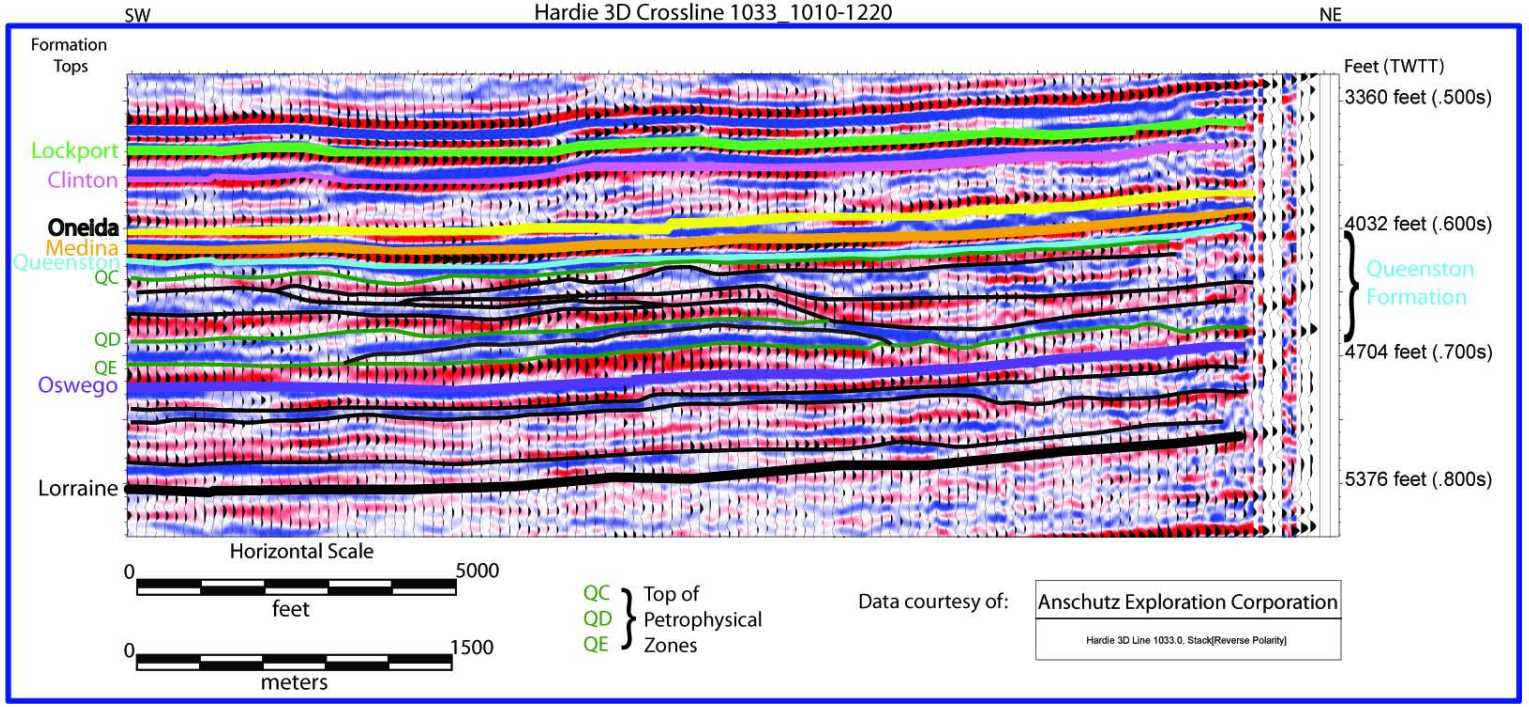
SW
Hardie 3D Crossline 1033_1010-1220
NE
Formation Tops
Lockport
Clinton
Oneida
Medina
Queenston
QC
QD
QE
Oswego
Lorraine
Feet (TWTT)
3360 feet (.500s)
4032 feet (.600s)
Queenston Formation
4704 feet (.700s)
5376 feet (.800s)
Horizontal Scale
0
5000
feet
0
1500
meters
QC
QD
QE
Top of Petrophysical Zones
Data courtesy of:
Anschutz Exploration Corporation
Hardie 3D Line 1033.0, Stack[Reverse Polarity]

Figure 1.7. A high resolution Queenston Formation isopach map from the 2D and 3D seismic data. The location of the AES Cayuga power plant and approximate position of the Hardie seismic line 1033 are displayed. 2D seismic line surveys are mapped with gray line, and every fourth shotpoint is located by a black circle. The red square outlines a 5 mile x 5 mile area surrounding AES Cayuga within which the static CO_2 storage capacity of the Queenston Formation is calculated. The time to depth conversion is based on sonic velocities calculated by Anschutz Exploration Corporation for the Venice View Dairy Well (Figure 1.3).

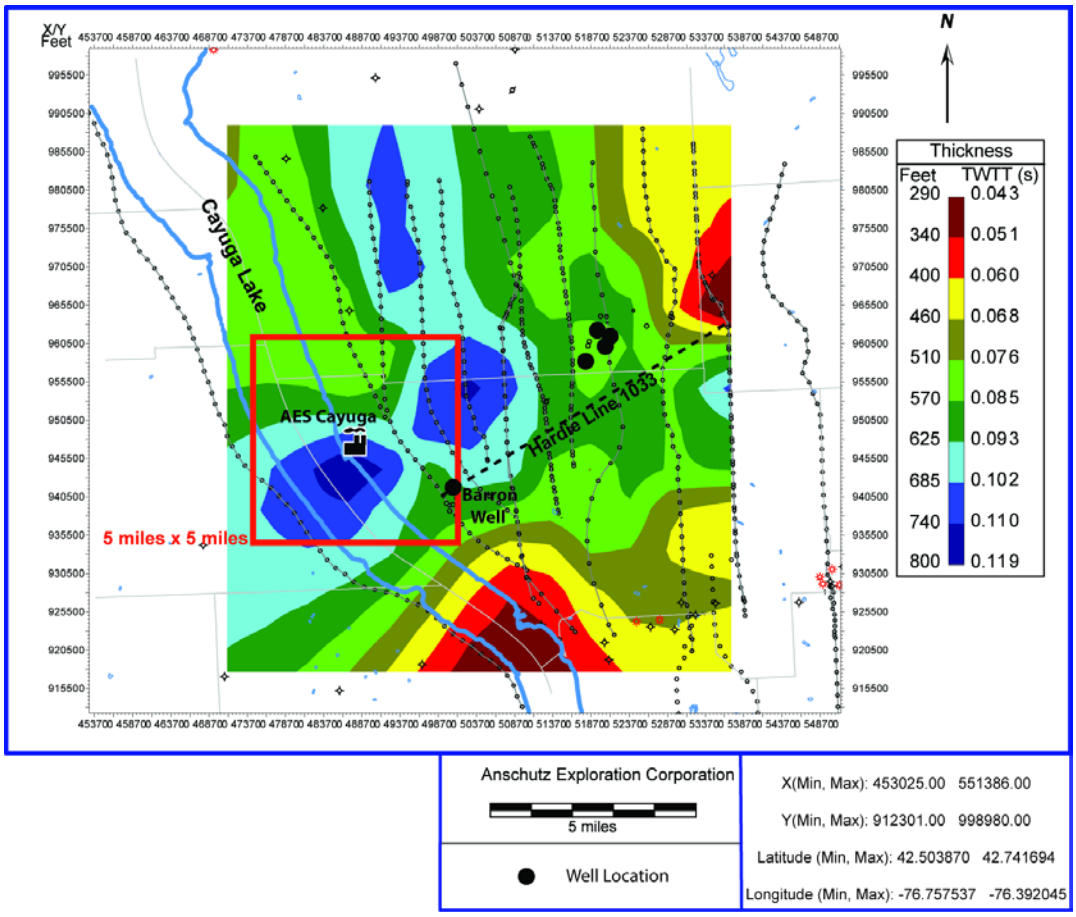
X/Y Feet
453700 458700 463700 468700 473700 478700 483700 488700 493700 498700 503700 508700 513700 518700 523700 528700 533700 538700 543700 548700
995500 990500 985500 980500 975500 970500 965500 960500 955500 950500 945500 940500 935500 930500 925500 920500 915500
N
Thickness
Feet TWTT (s)
290 0.043
340 0.051
400 0.060
460 0.068
510 0.076
570 0.085
625 0.093
685 0.102
740 0.110
800 0.119
Cayuga Lake
AES Cayuga
Harris Line 1033
Barron Well
5 miles x 5 miles
Anschutz Exploration Corporation
5 miles
Well Location
X(Min, Max): 453025.00 551386.00
Y(Min, Max): 912301.00 998980.00
Latitude (Min, Max): 42.503870 42.741694
Longitude (Min, Max): -76.757537 -76.392045

Core , Core-plug Measurements, and Core Thin Sections

The Delaney Well is located in the West Auburn gas field in Cayuga County, and 324 feet (99 meters) of Queenston Formation four inch (ten centimeter) diameter core were collected from this borehole (Figures 1.8 and 1.9). The cored portion extends from the top of the Queenston Formation to a position within petrophysical zone D, but does not penetrate into petrophysical zone E. For this well, core-plug porosity and permeability data were analyzed by Lugert et al. (2006), who also described the physical characteristics of the core. For the current study, core lithofacies were described, and lithofacies, petrophysical zones, core-plug porosity, and core-plug permeability were related (Figures 1.8, 1.9, 1.10, and 1.11). Neutron porosity data (calculated by logging tool based on the formation's hydrogen content) and density porosity data (derived by logging tool from formation bulk density obtained from the electron density log, estimated formation fluid density, and an assigned matrix density, for which the value used in this case is unknown) from boreholes was available in the ESOGIS database for the Delaney well. The various porosity data were compared in order to determine the most accurate porosity measurement for wells without core data (Figure 1.12).

Core thin sections were collected from the Delaney well in Cayuga County by Lugert et al. (2006), and these thin sections were further examined in this study (Figures 1.13 and 1.14). Spacing between Delaney core thin sections range from 0.1 feet to 9 feet (0 to 3 meters), depending on lithologic varations, and were not collected at the regular 0.5 foot interval of the well log measurements. Grain and cement compositions of 71 thin sections were quantified by point-counting. On a grid at greater than 400 points per thin section, quartz grains, lithic fragments, hematite, clay, quartz cement, carbonate cement, and muscovite were enumerated. Mineralogical data were collected by the author and by Miller Brewing Company by XRD analysis

Figure 1.8. Delaney Well (Cayuga County) core description, lithofacies interpretation, and relation to petrophysical zones Queenston B (QB), Queenston C (QC), and Queenston D (QD). Flood deposits (FD) and lowstand system tracts (LST) were identified by core properties. Trends in base level (arrows) were drawn based on well log and core variations. Lithofacies are described in Table 1.

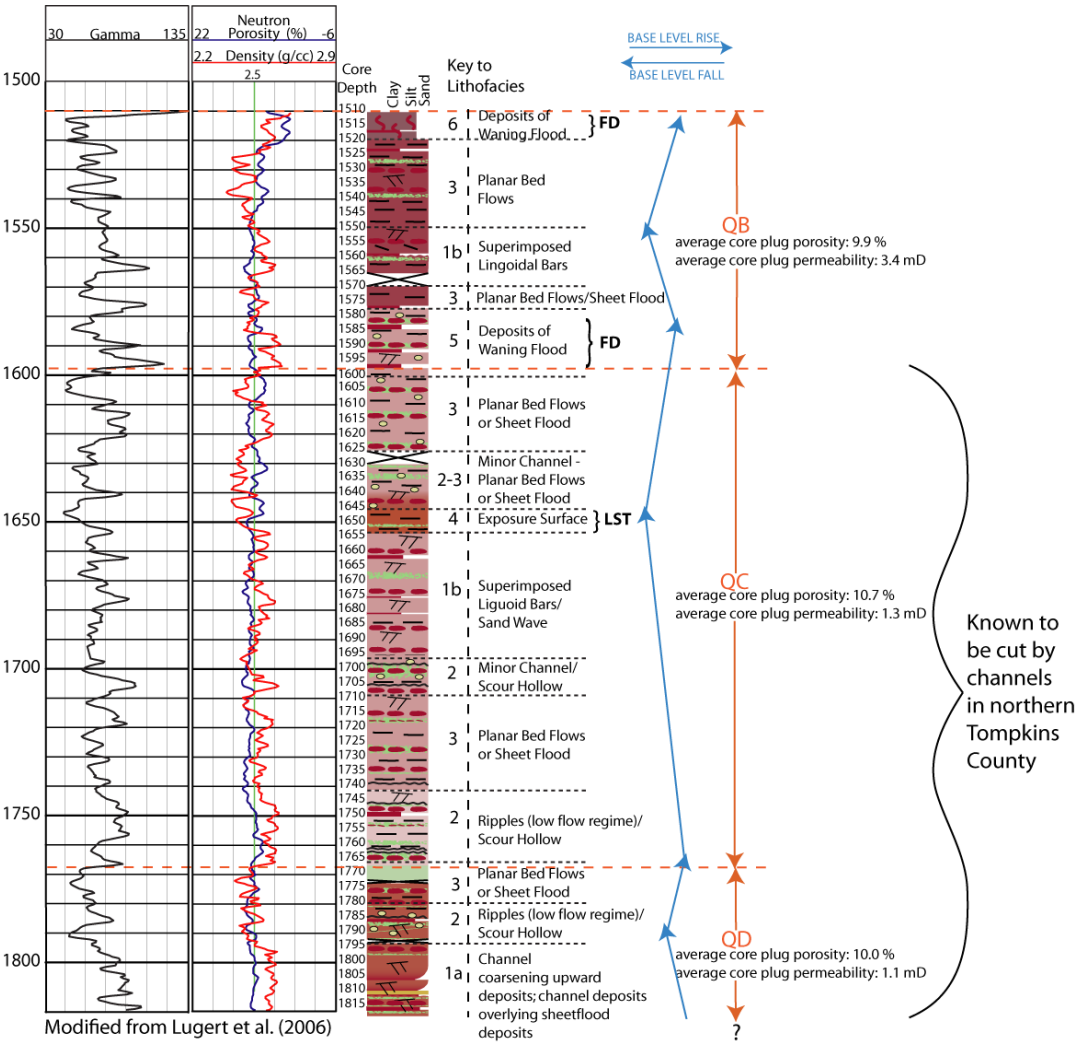

EXPLANATION

- Burrows
- Planar Beds
- Cross Beds
- Mottling
- Rip-up Clasts
- Petrophysical Zone
- Lithofacies Boundary

Figure 1.9. Photographs of Delaney core lithofacies and average values of core-plug porosity and permeability for the corresponding lithofacies depth intervals (Core Lab data). Lithofacies description is included in Table 1. Photographs taken by Lugert et al. (2006). Sections of missing core are the result of core-plug collection.

9a) Lithofacies 1a -1805 feet

porosity: 7.9
permeability: 0.2

9b) Lithofacies 1b -1677 feet

porosity: 9.6
permeability: <0.1

9c) Lithofacies 2 -1750 feet

porosity: 7.4
permeability: 0.2

9d) Lithofacies 3 -1769 feet

porosity: 2.4
permeability: 0.2

9e) Lithofacies 4 -1647 feet

porosity: 15.5
permeability: 23

9f) Lithofacies 5 -1593 feet

porosity: 7.7
permeability: 0.4

9g) Lithofacies 6 -1515 feet

porosity: 4.2
permeability: 0.4

Scale: 4 inches

Figure 1.10. Porosity distribution frequency graph for core-plug porosity data from the Delaney well (total of 295 data points). A Gaussian normal distribution probability density function best fits the porosity frequency distribution when the porosity mean is 10% and standard deviation is 2.5%.

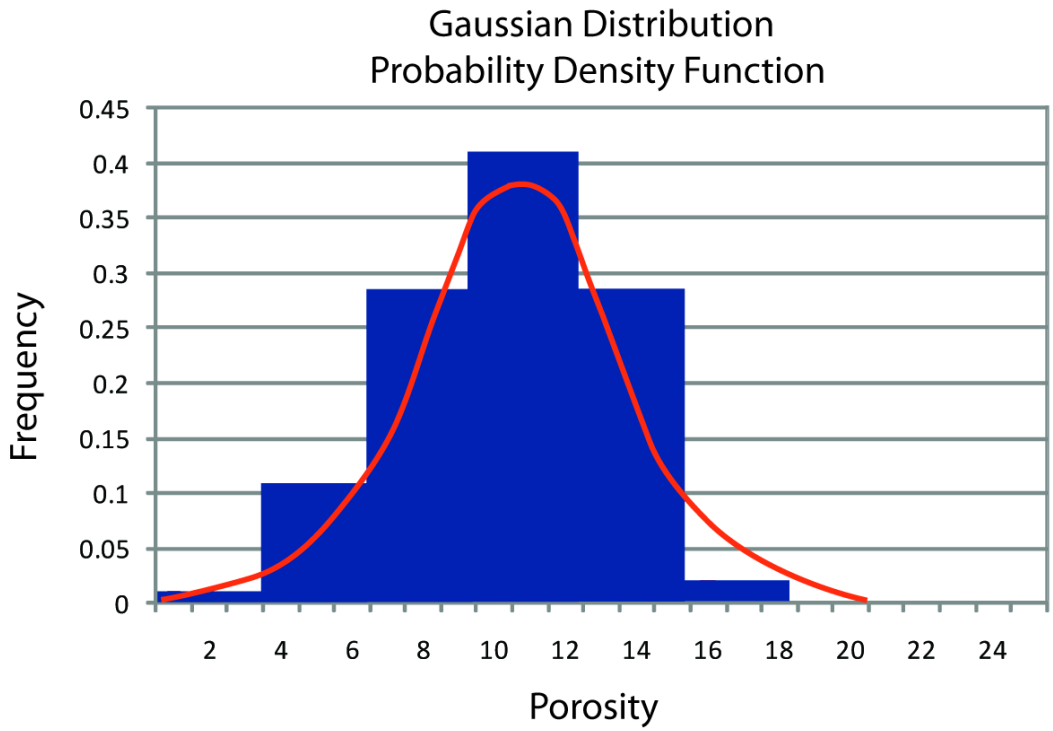

$$f(x) = \frac{1}{\sqrt{2\pi\sigma^2}} e^{-\frac{(x-\mu)^2}{2\sigma^2}}$$

π (mean) = 10

σ (standard deviation) = 2.5

Figure 1.11. A) Core-plug porosity (%) and permeability (mD) graph with exponential best-fit curve for the Delaney core. These data were collected by Core Laboratories (1979) for Miller Brewing Company and provided by the New York State Museum Reservoir Characterization Group. B) Core plug porosity (%) and permeability (mD) graph with exponential best-fit curve for Delaney core petrophysical zone Queenston B.

A.

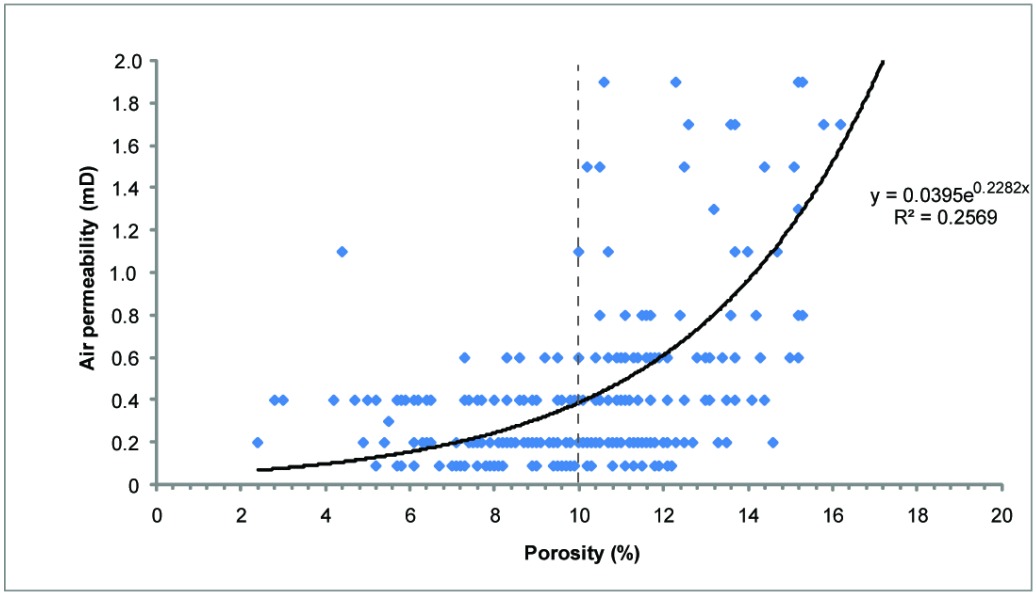
Air permeability (mD)
Porosity (%)
y = 0.0395e^0.2282x
R² = 0.2569

B.

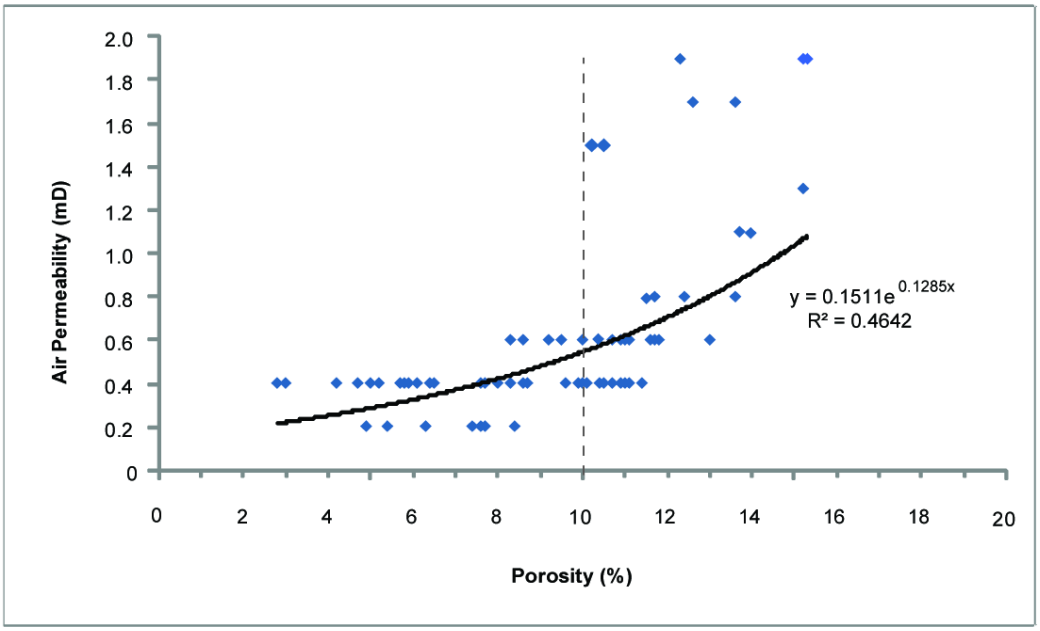
Air Permeability (mD)
Porosity (%)
y = 0.1511e^0.1285x
R² = 0.4642

Figure 1.12. Neutron Porosity (NPHI), density porosity (DPHI), core-plug porosity, and point-count porosity values for the Delaney well. NPHI and DPHI are petrophysical log derived porosities, core-plug values were collected on one-inch diameter core-plugs, and the point-count values were collected from thin section point-counts (at least 400 points counted in a grid pattern per thin section).

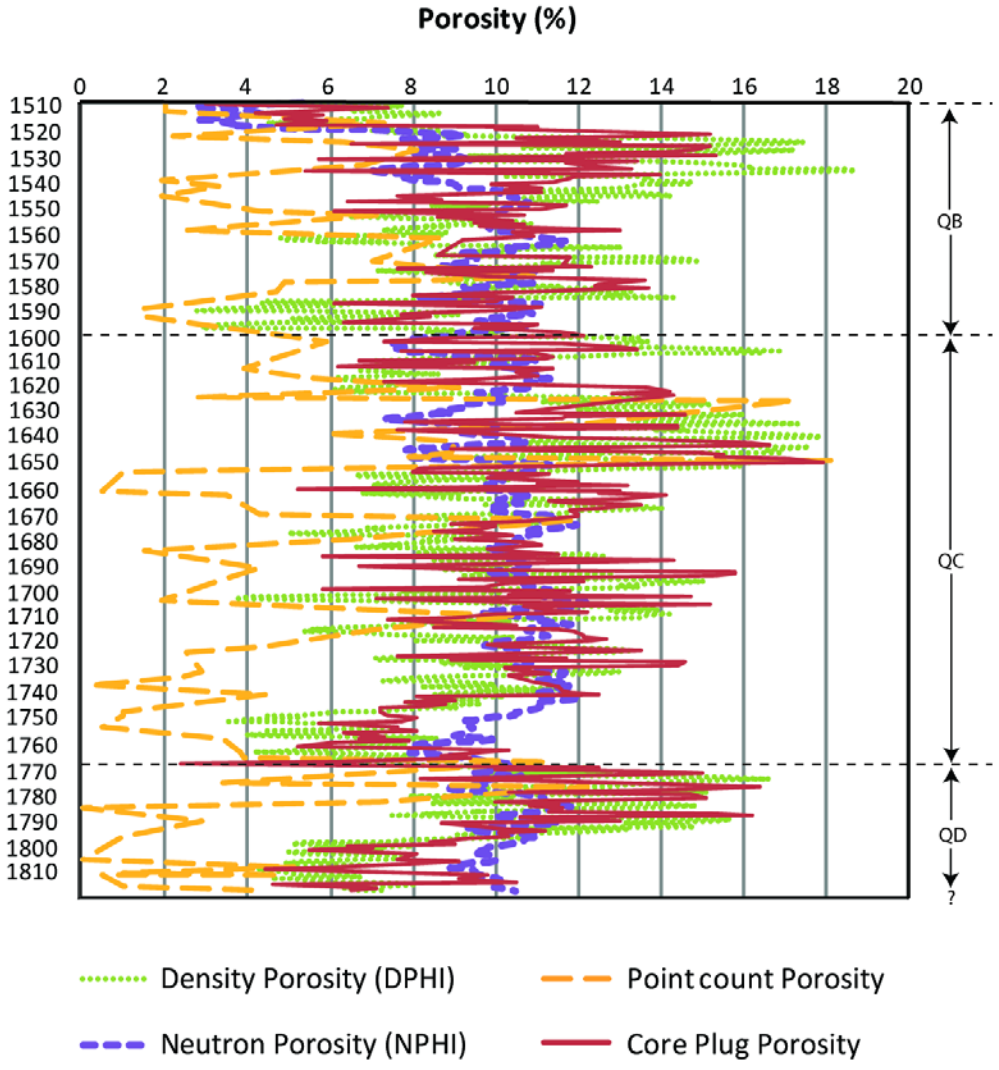
Porosity (%)
0
2
4
6
8
10
12
14
16
18
20
1510
1520
1530
1540
1550
1560
1570
1580
1590
1600
1610
1620
1630
1640
1650
1660
1670
1680
1690
1700
1710
1720
1730
1740
1750
1760
1770
1780
1790
1800
1810
QB
QC
QD
?
Density Porosity (DPHI)
Point count Porosity
Neutron Porosity (NPHI)
Core Plug Porosity

Figure 1.13. Thin section photographs of Delaney well lithofacies 1a, 1b, 2, and 3. Each lithofacies has a thin section picture under plane polarized light (left) and cross polarized light (right, labeled xp). Irregular, large hematite patches (about the size of quartz grains) are present in lithofacies 1b and 2. Blue in plane polarized light shows pore space.

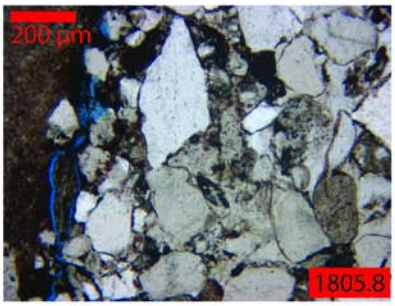

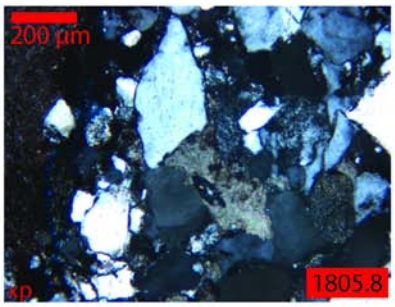

Lithofacies 1a

Fine-medium sand. Subround-angular quartz grains with large rip-up clast on left; silica overgrowth, carbonate and hematite cement; fracture porosity.

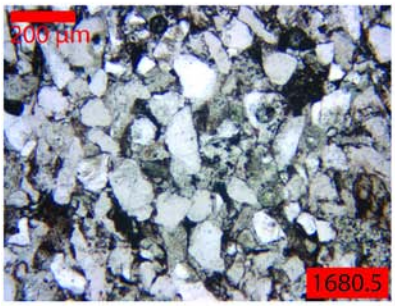

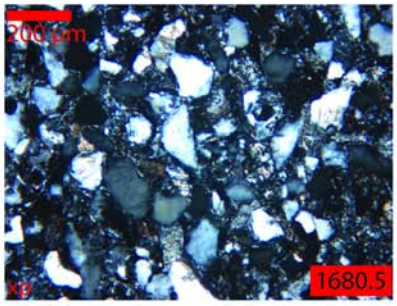

Lithofacies 1b

Fine sand. Subound-angular quartz grains with clay matrix and hematite cement.

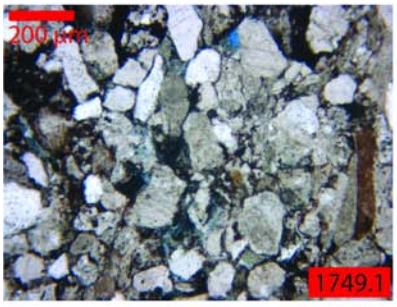

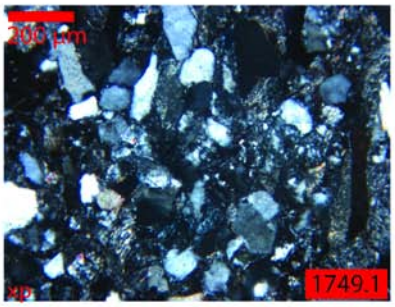

Lithofacies 2

Fine sand. Subangular-round quartz grains with lithic clast, hematite and carbonate cement, and intergranular porosity.

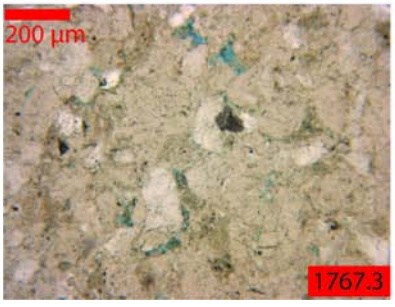

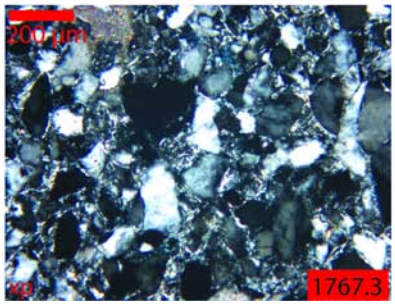

Lithofacies 3

Fine sand. Subround-angular quartz grains with clay matrix, carbonate cement, and intergranular porosity.

Figure 1.14. Thin section photographs of Delaney well lithofacies 4, 5, and 6. Each lithofacies has a thin section picture under plane polarized light (left) and cross polarized light (right, labeled xp). Inter-granular porosity is visible in lithofacies 4 and a rip-up clast is visible in lithofacies 5. Blue in plane polarized light shows pore space.

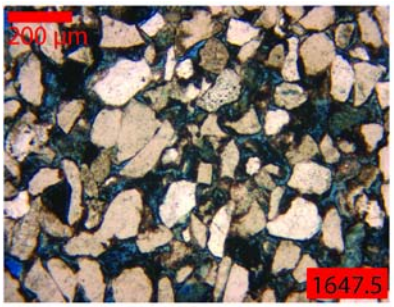

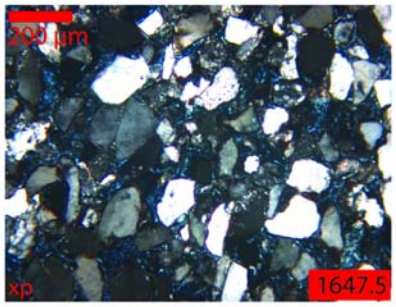

Lithofacies 4
Fine sand. Round-subangular quartz grains with hematite cement and intergranular porosity.

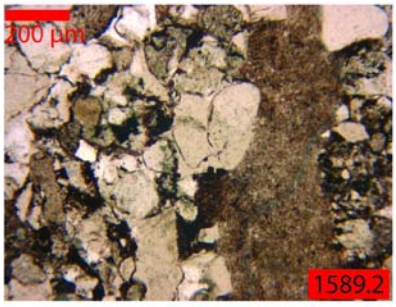

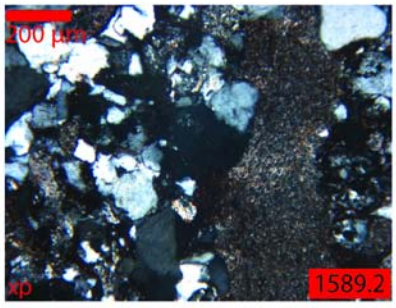

Lithofacies 5
Fine-medium sand. Round-subangular quartz grains with large rip-up clasts, silica overgrowth and hematite cement.

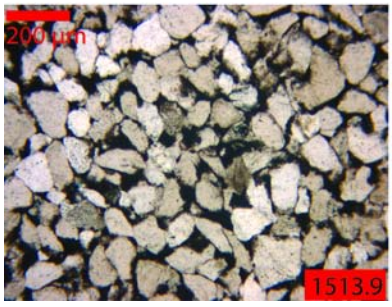

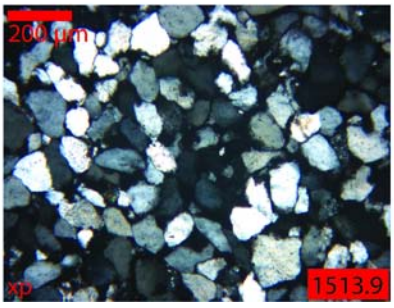

Lithofacies 6
Silt-fine sand.Round-subangular quartz grains with hematite cement.

for samples within each petrophysical zone of the Delaney core. The core was divided into lithofacies based on grain size and sorting, color, and sedimentary structures. Depositional environments of the lithofacies were interpreted based on Miall's (1977, 1996) and Todd's (1996) classifications.

Cuttings

Over 600 feet of the Queenston Formation are logged in the Shepard well in southern Tompkins County, and cuttings were collected every five feet throughout the formation. These cuttings were examined with 10× magnification, and seven samples for thin sectioning were selected at apparent changes in lithology. Only a small proportion of intact rock fragments occur in the cuttings, amidst a high proportion of single detrital grains. The point-count procedure used for the Delaney well thin sections was also used on the Shepard well thin sections. Because the Shepard well cuttings material is partially disaggregated, mineralogy and cement type can be determined but cement texture and porosity cannot be thoroughly evaluated.

Results

Well Logs

Petrophysical zones B-E were identified in well logs surrounding the AES Cayuga plant (Figure 1.4). Zones A and F do not extend far enough northeast in central New York to be mapped in the logs surrounding the plant (Tamulonis, 2010). The tops of these zones were determined based on distinct gamma, electron density, and neutron porosity variations within the Queenston Formation that can be mapped throughout central New York, with gamma peaks being the primary factor influencing where the top of each zone is picked. The following describes each petrophysical zone in the Cayuga/Tompkins County area surrounding the AES Cayuga power plant, though this petrophysical zone description varies slightly throughout central New York particularly where the formation becomes more variable. Zone Queenston B

(top of Queenston Formation to top of Queenston C) has distinctly lower gamma and density values compared to the overlying Medina Formation. Queenston C has less varied gamma values compared to Queenston B, with peaks at the top and bottom of the zone, and its density and porosity values are similar to those of Queenston B. The top of Queenston D is defined by a drop in gamma and neutron porosity values, and an increase in density values. Queenston D density generally increases with depth and porosity decreases with depth. Relative to the bottom of zone D, the top of Queenston E has decreased gamma, density, and porosity log patterns. The log signature of the Barron Well is somewhat inconsistent with this petrophysical zone description (Figure 1.5), which may be due to the fact that it is located within the depocenter described in the section below.

Local Scale Lateral Variability

The seismic reflections at depths corresponding to the Queenston Formation reveal lateral variability at a horizontal scale of hundreds of feet to several miles (kilometers), a much higher resolution than detectable in the available well data. Though reflections in the Queenston Formation are generally horizontal and laterally continuous (Figure 1.5), this formation has more seismic variability and erosional truncations than occur in the underlying and overlying formations. Channel geometries and channel fill are distinguishable locally (Figure 1.6).

The Barron well intersects Hardie 3D Crossline 1033_800-960 (Figure 1.5). Petrophysical zones B-E in the well log data were recognized using the criteria described above (Figure 1.4) and then mapped into the seismic reflections by linearly scaling the top of the Queenston and Oswego Formations from the borehole data to mapped formation tops in the seismic reflections. In Figure 1.5, seismic reflection tops coincide with the tops of Queenston petrophysical zones B-E (with the Queenston B top being equivalent to the Queenston Formation top in light blue), and the

reflections generally appear to be laterally continuous interfaces in this seismic line. However, Figure 1.6 displays numerous unconformities defined by the Queenston Formation seismic reflections, which extend over one mile (1.6 kilometers) laterally and display hundreds of feet (meters) of relief. There is at least one prominent surface of internal unconformity located in Queenston C zone, marked by erosional truncation of underlying units and a strong horizontal reflection above the truncation surface. This strong reflection appears in all seismic lines studied, though the seismic reflector truncations are not observed in all lines. It is difficult to determine if channel features are present in zone B seismic facies (Queenston top to top of zone C) because it is relatively thin. The lower vertical resolution of the seismic data (tens of feet) compared to the well log (one foot) lends uncertainty to the association of the petrophysical zones with the unconformities, and the vertical position of a seismic reflector depends on the accuracy of the velocity model from borehole correlation.

A high resolution isopach map (Figure 1.7) was generated from the 3D and 2D seismic data and converted to thickness using the Venice View Dairy velocity data. This map shows that the thickness of the Queenston Formation ranges between 300-800 feet near AES Cayuga. A thick, elongate Queenston Formation depocenter trends NNW through the study area and is well constrained by the data. However, an ENE trending depocenter that appears to be located beneath the AES Cayuga plant and Lake Cayuga may be an artifact of the lack of seismic data below the lake. Compared to the regional Queenston Formation isopach from well log data (Figure 1.3), this higher resolution isopach better illuminates local variations of Queenston Formation thickness.

Petrology, Texture, Porosity, and Permeability of the Queenston Formation

The cored strata are primarily composed of well-sorted, fine to medium-grained quartz sandstone with hematite cement and some silica overgrowth cement.

Cross and planar beds are the dominant sedimentary structures throughout the core and mudstone rip-up clasts are common (Figures 1.8 and 1.9). There is a 10 foot (3 meter) thick silt-dominated burrowed interval at the top of the core, and a five foot (1.5 meter) thick interbedded sandstone and siltstone zone at 1580 to 1585 feet (481 to 483 meters) below the surface. Fossils are not observed, and trace fossils (burrows) are rare. Colors depicted in Figure 1.8 approximate actual colors in the core. Relatively low gamma values correspond to the sandstone lithofacies, and higher gamma log values are primarily associated with silt and clay-rich layers. Layers rich in rip-up clasts also cause increased gamma values. The electron density and neutron porosity logs generally have an inverse relationship to each other, as is expected if they are accurately reflecting mineral density and water-filled void spaces, respectively.

Based on our core observations, we divided the Delaney Queenston core into six lithofacies (lithofacies 1a,1b, 2-6, Table 1). Lithologic changes visible in the Delaney well core coincide with the distinct log-defined petrophysical zones B, C, and D (Figure 1.8). Zone Queenston B is primarily composed of red, fine to medium grained sandstone with planar bedding and some cross bedding. The top of zone Queenston B is a 10 foot (3 meter) thick burrowed mudstone to fine sandstone, and the bottom of the zone is interbedded sandstone and siltstone. Zone Queenston C contains fine to medium grained reddish sandstones with planar horizontal beds and cross beds, and there are several reduced intervals (greenish color with carbonate cement and lacking hematite cement) and scoured surfaces throughout this zone. This zone also has an 8 foot (2.5 meter) thick massively bedded, medium grained sandstone with visible porosity. Zone Queenston D is generally a brownish red medium-grained sandstone with a reduced section at the top of the zone. Scoured surfaces, coarsening upward intervals, planar horizontal bedding, and ripples are observed locally in zone

Queenston D. The zones in the Delaney well core with the highest average core-plug porosity and permeability are Queenston B and Queenston C, though zones Queenston B, C, and the part of D in the core only vary within +/- 0.8%.

Table 1.1. Delaney core lithofacies description and interpreted depositional environment based on Miall (1977) and Todd (1996) (Figure 1.8).

LITHOFACIES		
	Description	Interpreted Depositional Environment
1a	-Medium grained sandstone -Reddish brown with some tan layers -Well laminated cross beds and cross laminae -Coarsening upward sequences -Not bioturbated: one long burrow -Rip-up clasts, some reduced (reduced prior to rip-up) -Scours	Channel coarsening upward suggests coarser channel deposits overlying finer sheet flood deposits
1b	-Fine-medium grained sandstone -Dark red -Low to high angle planar cross beds	Ripples/ Lingoidal Bars
2	-Medium grained sandstone -Reddish purple brown -Planar horizontal bedding -Scours -Rip-up clasts, some reduced (reduced prior to rip-up) -Mottling	Minor Channel/ Scour Hollow
3	-Medium grained sandstone -Reddish purple brown to dark red with pale greenish tan reduced zones (up to 6 inches thick -Planar horizontal bedding -Rip-up clasts -Mottling -Visible porosity	Planar Bed Flows or Sheet Flood
4	-Medium grained sandstone -Brownish red -Massive bedding	Paleosol
5	-Interbedded medium grained sandstone and siltstone (individual beds inches thick) -Reddish purple brown and dark brown -Planar horizontal bedding -Rip-up clasts -Mottling	Overbank Flood Deposits
6	-Fine grained sandstone with clay interbeds -Very dark red-brown -Rippled -Burrows	Flood/Marine Deposits

Petrographic examination of the Delaney core thin sections reveals that the Queenston Formation is a fairly homogenous fine to medium-grained, sub-round to sub-angular, well-sorted quartz sandstone with hematite cement. Quartz was overwhelmingly the dominant mineral present (Table 1.2). A number of boundaries between quartz grains are convex/concave or straight, illustrating compaction influence (Figures 1.13 and 1.14, lithfacies 1a, 2, 5, and 6). Lithic fragments are also present locally, and there are several silt and clay rich zones, though only lithofacies 5 has clay matrix percents comparable to the clay percents reported in the Cayuga and Seneca Queenston gas fields by Robinson (1987). Porosity is intergranular, intragranular, and in fractures. Except for lithofacies 5 and 6, which contain some clay and siltstone, all lithofacies are dominantly fine to medium quartz sandstone.

Table 1.2. Thin section point-count results in percent.

Lithofacies	Quartz	Lithic Fragment	Hematite	Quartz Cement	Carbonate Cement	Clay Matrix	Pore
1a	43	25	17	3	3	5	4
1b	54	10	18	3	2	9	4
2	49	9	18	4	3	10	5
3	51	10	18	2	8	4	7
4	51	0	11	6	8	7	17
5	44	7	22	4	1	20	3
6	71	0	18	1	2	3	3

Hematite is present in all the lithofacies of the Delaney core, primarily as cement. In general, hematite is absent at points of grain contact **(**Figure 1.14, lithofacies 4, 5, and 6), and large (quartz grain-sized), irregular hematite patches are also present in thin sections. Horneblende and other iron-bearing minerals besides hematite are not identified in the thin section.

Silica overgrowth cement (Figures 1.13 and 1.14, lithofacies 1a and 5) and carbonate cement (Figure 1.13, lithofacies 1a, 2, and 3) coexist with hematite cement (Table 1.2). Hematite generally was not present in reduced zones (portions of lithofacies 3), where carbonate cement content is high. Clay matrix content is relatively high in lithofacies 1b, 2, and 5, and rip-up clasts are abundant in lithofacies 1a and 5. Lithofacies 3, 4, and 5 have visible porosity in thin sections, though lithofacies 3 and 5 do not have relatively high porosity point-counts. XRD results indicate muscovite and siderite are also present in the Delaney core.

Because the Shepard well thin sections were made from well cuttings, it was difficult to study cement patterns. Generally for the Shepard well, cutting samples were composed of individual grains, suggesting that at this location, the Queenston Formation may have been poorly cemented. Shepard well grain compositions, sizes, and its cement types are similar to those of the Delaney Well.

For the Delaney well core, a histogram of core-plug porosity data set is best fit by a Gaussian or normal distribution curve, whose mean porosity and standard deviation are 10% and 2.5%, respectively (Figure 1.10). Core-plug porosity does not exceed 18%.

The relationship between the core-plug porosity and permeability data can be crudely approximated by an exponential curve ($R^2 = 0.26$, Figure 1.11A), and suggests that 10% porosity is a threshold for effective permeability. Below 10% porosity, permeability is less than 0.8 mD and permeability values correlate poorly with porosity. Above 10% porosity, there is only a weak correlation of porosity to permeability, but the permeability for 25% of these samples exceeds 1mD. Porosity averaged for each of the petrophysical zones does not vary greatly, ranging between 9.9%-10.7% (Figure 1.8). Average permeability is greatest in zone Queenston B at 3.4 mD, and the strongest porosity and permeability correlation occurs in this zone,

though there is still only a week correlation above 10% porosity (Figure 1.11B). Average core-plug permeabilities are 1.3 mD and 1.1 mD for zone C and zone D, respectively (Figure 1.9 and 1.12).

Systematic patterns of porosity and permeability change are dependent on lithofacies (Table 1.3). Lithofacies 4, which is a massively bedded medium-grained sandstone, has the highest average porosity and permeability, as well as a relatively low porosity standard deviation. Lithofacies 1a (medium grained sandstone with cross beds and rip-up clasts) and lithofacies 6 (fine grained sandstone with clay interbeds) have the lowest porosity and permeability values. Lithofacies 4 has the highest permeability standard deviation due to a permeability value of 110 mD at 1540 feet depth.

Table 1.3. Average porosity and permeability for each lithofacies with standard deviations (StDev).

Lithofacies	**Porosity (%)**		**Permeability (mD)**	
	Average	StDev	Average	StDev
1a	8.1	1.9	0.3	0.7
1b	10.8	2.2	0.8	1.4
2	10.2	2.9	1.5	3.4
3	11.2	2.5	2.9	10.9
4	15.8	1.4	16.0	9.3
5	10.1	2.1	0.7	0.7
6	4.9	1.4	0.4	0.1

Porosity Correlation

Porosity greatly affects geologic CO_2 storage potential, and it is important to understand discrepancies among core-plug, well log neutron porosity (NPHI), density porosities (DPHI) derived from the electron density log, and thin section point-count values. In order to gain accurate porosity values for wells with only logged data (no core), causes for porosity discrepancies among data sets must be determined and the most accurate porosity well logs should be used. Assuming porosity and permeability values derived from core-plug measurements are the most accurate data, as it is collected directly from the rock in a controlled environment, Delaney core porosity and permeability can be related to the respective well log suite and variations between log and core data can be determined.

Visual inspection of the NPHI, DPHI, core-plug, and thin section point-count porosity data suggests that DPHI and core-plug porosity values have a similar pattern of change (Figure 1.12). The magnitude of change for the NPHI is less than that of the DPHI and core-plug values, and the point-count values are consistently lower than other porosity values. Correlation coefficients indicate the strength and direction of a linear relationship between two random variables and were calculated for the relationships between density porosity (DPHI), neutron porosity (NPHI), core-plug porosity, point-count porosity, and core-plug permeability (Table 1.4).

The relationship between core porosity and neutron porosity has the highest positive correlation coefficient for porosity values of 0.45, and permeability and point-count porosity have the highest positive correlation coefficient of 0.46. This suggests that although visually the core porosity and neutron porosity data sets do not appear similar (Figure 1.11), they follow the same trends, though the NPHI value range is less than the core porosity range. The relationship between point-count porosity and

Table 1.4. Neutron porosity (NPHI), density porosity (DPHI), core-plug porosity (core), point-count porosity (point), and permeability (perm) correlation coefficients for the Delaney well.

	DPHI	NPHI	Core	Point	Perm
DPHI	--	0.18	0.35	0.30	0.30
NPHI	0.18	--	0.45	-0.12	-0.12
Core	0.35	0.45	--	0.37	0.22
Point	0.30	-0.12	0.37	--	0.46
Perm	0.30	-0.12	0.22	0.46	--

neutron porosity has a negative correlation coefficient of -0.12. One possible factor influencing this relationship is that the thin sections used for the point-count are not at the exact locations of well log measurements. Hematite cement may affect adversely density porosity values that are derived from the formation bulk density, formation fluid density, and an assigned rock density for an assumed lithology due to hematite's relatively high density (5 g/cm^3). The assigned matrix density used in the Delaney density porosity log calculation is unknown, and it may have underestimated the hematite rich sandstone density. The relationship between point-count porosity and permeability suggests that the macropores accounted for in thin section point-count affect porosity, and micropores that may be accounted for in petrophysical and core-plug porosity measurements to do not influence permeability.

Correlation coefficients for point-count porosity and all other point-count components were calculated in order to gain insight into factors affecting porosity in

the Delaney Well. These results are reported in Table 1.5. According to these results, the increased hematite content decreases porosity, and samples with carbonate cement, which is most abundant in reduced zones, appear to have increased porosity, perhaps due to subsequent dissolution of some calcite cement (Abdel-Wahab, 1998).

Table 1.5. Correlation coefficients for Delaney well point-count porosity and grain, hematite, clay, and cement content.

	Quartz Grain	Hematite	Clay	Silica Cement	Carbonate Cement
Point Count Porosity	-0.11	-0.45	0.04	0.05	0.24

Geologic Interpretation

Based on the geometry of seismic reflections, sedimentary structures revealed in core, and lack of fossils, we determine that the Queenston Formation of central New York was primarily deposited in a fluvial setting. The criteria for fluvial environments published by Allen (1970), Miall (1977, 1996), and Todd (1996) lead us to interpret that the Queenston Formation is the product of steady stream flow and sheet flooding with almost little evidence of waning flow. The key criteria for this classification are: fine- to medium- grained sandstone; high occurrence of cross beds and cross lamination; planar horizontal bedding, and rip-up clasts (Figures 1.8 and 1.9 and 1.11); general lack of fining-upward series in core that are typical of meandering stream deposits; lack of mudstone interbeds in core; and evidence of mound-like features (hundreds of feet wide, tens of feet thick) in seismic sections that are interpreted as longitudinal or lingoidal bars (Figure 1.6). Stream banks during the Ordovician would have been relatively unstable due to a lack of vegetation, encouraging the development

of weakly channelized bed load rivers, leading to sandstone sheetflood deposits (Miall, 1996). The NNW trending depocenter recorded in the seismically derived isopach map coincides with the direction of Juniata Formation paleoflow direction in Pennsylvania (Yeakel, 1962). This suggests that the depocenters represent channels cut during base level fall, which were then subsequently filled during a rise in base level.

Small scale depositional environments of the Delaney core lithofacies were interpreted based on Miall's (1977, 1996) and Todd's (1996) classifications (Table 1). Lithofacies 1, a fine- to medium-grained, reddish-brown sandstone with cross beds and cross laminae, is subdivided into 1a and 1b, with 1a having coarsening upward sequences and 1b lacking these sequences. Lithofacies 1a is interpreted to be relatively finer grained sheet flood deposits overlain by coarser grained channel deposits (Miall, 1977), though the change in grain size is relatively subtle. This suggests there is not a strong differentiation between floodplains and channel sediment. Lithofacies 1b is interpreted to be the product of low-flow mesoform ripples (i.e., dunes controlled by boundary-layer thickness or flow depth) or macroform (widths and heights comparable to depth of flow) lingoidal bar migration (Miall, 1977; Miall, 1996). Cross laminated fine sand is a common expression of low-flow regime ripple microform migration and may be superimposed on upper surfaces of bars (Todd, 1996).

Lithofacies 2 and 3 both were deposited in relatively high discharge environments. Due to planar horizontal bedding and scours, lithofacies 2 is interpreted to be a sand-filled scour (Miall, 1996). Lithofacies 3 has planar horizontal bedding and rip-up clasts suggesting it was deposited as sheetfloods (Todd, 1996), which are very common in little channelized distributary systems or planar river bed flows (Miall, 1977; Todd, 1996; Beer and Jordan, 1989). Sandstone sheet deposits

develop in a series of coalescing, broad, virtually unconfined flows for which even small discharge events can cause deposition in a broad region (Beer and Jordan, 1989). These sheetfloods form a system of continuous sandstone sheets, and there is no differentiation of channel and overbank facies (Campbell, 1976; Miall, 1996). In general, the planar bedding in lithofacies 2 and 3 is interpreted to be a product of upper-phase flow, rather than slower moving flows, due to the presence of scours and rip-up clasts. These upper-flow phase beds are generally deposited from high velocity flows of shallow depths (Beer and Jordan, 1989).

The lack of sedimentary structures and horizonation, distinct brownish red color, massive bedding, and the friable nature of lithofacies 4 suggest it is a chemically weathered exposure surface. Well-developed red, calcareous, burrowed paleosols with pedogenic carbonate are reported in the correlative Juniata Formation in Pennsylvania (Retallack, 2001), though no such features are observed in this core. Modern soil classification techniques do not necessarily apply to lithofacies 4 due to its lack of soil stratification and biogenic features. Many early Paleozoic soils lack such features because land vegetation did not exist (Retallack, 1986). Precambrian paleosols are also rarely stratified for the same reason, and in order to define a Precambrian exposure surface, disruption of the parent rock, macro- and micro-sedimentary structures, and mineralogy must be studied (Gall, 1999). This line of reasoning may be applicable to Ordovician exposure surfaces. The massive, structureless bedding of lithofacies 4 is unique in the Delaney Core. Point-count indicates lithofacies 4 has less iron oxide (11%, compared to 21% from the rest of the core) and greater porosity relative to the remainder of the core (16%, compared to 9% in the rest of the core). Both porosity and permeability decrease with depth within this lithofacies. While none of the properties of lithofacies 4 are highly diagnostic, we conclude that lithofacies 4 is a paleosol.

Due to the presence of silt and clay, both lithofacies 5 and 6 are interpreted to have been deposited in waning flood conditions. Lithofacies 5 is located at the bottom of petrophysical zone Queenston B and is composed of interbedded sandstone and siltstone with planar bedding. This lithofacies has relatively high gamma and electron density log values, and low neutron porosity log values. Lithofacies 6 is located at the top of the core, which is the top of Queenston B, and is a burrowed mudstone to fine sandstone with ripples, suggesting this could have been deposited during a marine incursion. The burrows appear to be vertical, and lining in the burrow is not visible. The vertical burrow is indicative of a suspension feeder in a marginal marine setting (Pemberton et al., 1992). The gamma log values generally increase with height in this interval. Both the electron density and neutron porosity logs are relatively high, though the high neutron porosity logs are probably influenced by the shale content of this lithofacies, as there is little visible porosity in thin section. The log character of these zones can be traced to surrounding wells and into the seismic data. Both of these lithofacies are located in zone B, which has uninterrupted seismic reflections and no evidence of channelization.

The vertical succession of these lithofacies is interpreted to define a series of base level cycles (Wheeler, 1964). There are three distinct surfaces recorded in the Delaney Well. Below lithofacies 4 (1652 to1816 feet depth; 504 to 554 meters), deposits of channelized flow and sheet flood occur throughout the core and reveal that the fluvial sediments were aggrading. Lithofacies 4 (1646-1652 feet depth; 502 to 504 meters; Table 1) is interpreted to be an exposure surface. The existence of this exposure surface suggests that the paleogeographic location of the surface was either some distance from a river channel or topographically raised above the fluvial channels (Todd, 1996). The change from an underlying environment of fluvial aggradation to an exposure surface is interpreted as a base level fall. Above the

paleosol, fluvial channel features or sheetflood deposits again occur until approximately 1,600 feet (488 meters) depth, above which approximately 20 feet (6 meters) of interbedded sandstone and siltstone (lithofacies 5) are interpreted to be waning flood deposits that would be more typical of a flood plain. This suggests a base level rise occurred after the deposition of the paleosol, while the floodplain sediments accumulated. Lithofacies 6 is a burrowed, interbedded fine sand, silt, and clay interval and is located at the top of the core. This is also interpreted to be a flooding surface (possibly marine), implying that a cycle of base level fall and rise occurred between the lithofacies 5 and the top of the core. Among lithofacies 4, 5, and 6, definitive base level changes are recorded, but it is difficult to indentify base level changes within the more uniform sandstones (below 1652 feet (504 meters) depth).

The tops of petrophysical zones Queenston B, C, and D correspond to some of the boundaries between lithofacies (Figure 1.8), though there is an uncertainty of +/- 2 feet associated with the locations of the petrophysical zones. The top of Queenston B corresponds to the top of the burrowed flooding surface (lithofacies 6) at the top of the core. The Queenston C top is located just below lithofacies 5. The top of Queenston D is located at a rip-up clast-rich layer with planar horizontal beds, interpreted to have been deposited in a high-flow regime, channelized setting. This vertical succession of lithofacies in petrophysical Queenston D (channel deposits overlain by low-flow regime deposits overlain by high-flow regime deposits) may represent another cycle of base level fall followed by a base level rise. We deduce that the base level cycles generated the facies variations that are responsible for the systematic physical property variations expressed in the petrophysical zones. These petrophysical zones can be mapped in well logs throughout central New York.

Based on the Delaney core thin section data, the origin of hematite in the Queenston Formation is difficult to determine, particularly due to the sparse data set.

Three possibilities exist for the oxidized state of the Queenston Formation hematite cement: 1) the sediment was originally drab colored and diagenetically oxidized, 2) the hematite formed prior to burial of the sediment through pedogenesis and portions were diagenetically reduced, or 3) the hematite pigmentation on individual detrital grains is a primary characteristic. Most prior studies conclude that the sediments were oxidized during diagenesis, but some contradictory data exist.

Hughes (1976) concludes that the color boundary separating the Queenston and Oswego Formations vertically varies more than 400 feet (120 meters) throughout western and central New York, and it cuts across lithofacies, which is also observed by Tamulonis (2010). This evidence supports a diagenetic origin of the color boundary, because the color change should be parallel to time lines if the pigment change was primary. If oxidation was a diagenetic reaction, the section was initially reduced and drab in color (gray-green), iron was leached from horneblende, clays, and/or other ferrous iron-bearing minerals, and Eh-pH conditions then caused oxidation. The absence of: a) hematite at points of grain contact, b) other iron-bearing minerals, and c) abrasion scars on hematite coated quartz grains suggest that hematite may be diagenetic or pedogenic in origin and formed from *in situ* alteration of iron-bearing detrital grains (Walker, 1967), rather than pedogenic or coming from a hematite-rich source rock. Hornblende or other iron bearing silicates were not identified in the Queenston Formation thin sections, but irregular patches of hematite approximately the size of surrounding quartz grains (Figure 1.13, lithofacies 1b and 2) are observed. These irregular large patches may be what was once hornblende or another iron-bearing mineral and then altered to hematite (Thompson, 1970). Also, there is no evidence of hematite abrasion, which may be evident if a hematite coating was present during sediment transport (Walker, 1967; Thompson, 1970). Oxidation likely occurred as a near-surface phenomenon in the aerated zone above the water

table (pedogenesis), which is a possibility suggested by Thompson (1970) for the Juniata Formation (Queenston Formation equivalent) in Pennsylvania. Mottled color patches (reduction spots) are commonly found in red beds (Burley, 1984: Surdam et al., 1993) and are present in portions of the Delaney core (Figure 1.8). Generally, it is believed that these reduction spots results from a later reduction of the red pigment (i.e., Walker, 1976; Burley, 1984), though it is possible the reduction spots are preserved during oxidation of initially drab strata (Durrance et al., 1978)

One factor that does not support this pedogenic or diagenetic oxidation theory is that reduced rip-up clasts are embedded in hematite-rich sand layers, and these reduced rip-up clasts occur in the same horizons as oxidized rip-up clasts. This implies that the rip-up clasts were reduced prior to being ripped-up and then deposited in an all red section. Preferential flow of aerated water through the sand particles (and not through mudstone rip-up clasts) may have caused oxidation of iron bearing minerals in the sand, but the presence of oxidized and reduced rip-up clasts in the same horizon does not support this hypothesis and instead suggests that pigmentation may be detrital or pedogenic. Based on the sparse data set from the Delaney core, it is difficult to determine whether diagenesis and cementation involved oxidation or reduction, or if the ferrous pigmentation is a primary or pedogenic characteristic.

Discussion

Based on core, seismic, well log, and cuttings data, the Upper Ordovician Queenston Formation appears to have the characteristics necessary to serve as a CO_2 storage reservoir for the AES Cayuga power plant. The Queenston Formation top is at an approximate depth of 4,200 feet (1280 meters) below the surface, so CO_2 would be in a supercritical state at the AES Cayuga site. At a distance of approximately 12 miles (19 kilometers) north of the AES Cayuga power plant the Queenston Formation rises above the 3,000 foot (915 meter) depth contour. Intermediate sealing units need

to be investigated at the AES Cayuga power plant because the Syracuse Formation is only at 2,200 feet (670 meters) depth. Other possible seals are the overlying Grimsby siltstone of the Medina Formation and shales of the Clinton Group (Figure 1.2). Saroff (1988) described Queenston Formation natural gas fields in Cayuga County to have best production in sand-rich highly fractured zones, indicating fracture permeability could play a major factor in migration and must be further investigated. The permeability of the Queenston Formation north of the AES Cayuga power plant must be determined to investigate whether up-dip migration to the north would be confined by low permeability.

Many conceptual uncertainties are associated with this storage reservoir assessment and geologic interpretation. Our data set consists of only one core, from which we can examine sedimentary structures and access small samples. Seismic data provide clues to Queenston Formation macrostructure, but there are many uncertainties associated with mapping seismic facies, such as depth conversion, tracing seismic reflectors, and processing choices. Both seismic and well log data provide clues to the Queenston Formation rock properties, but these properties cannot be verified without additional core evidence. With supplementary core and well log data collected within the potential storage site, we could increase the certainty of our current geologic interpretation.

The relative homogeneity of the Queenston Formation suggests there would be few internal primary barriers to restrict fluid flow through the reservoir, though cementation variations may influence migration. In a broad scope, early Paleozoic fluvial deposits may potentially be good geologic CO_2 storage targets due to their relative homogeneity. Pre-Devonian stream banks were unstable due to lack of vegetation, which encouraged the development of weakly channelized bed load rivers and sandstone sheetflood deposits (Miall, 1996). Core data indicate there is little

differentiation between channel and overbank facies in the Queenston Formation. Based on this generalized interpretation of an Ordovician fluvial system, the entire Queenston Delta complex (including the Juniata and Bald Eagle Formations in Pennsylvania, Maryland, and West Virginia; and the Sequatchie Formation in Kentucky, Tennessee, and Alabama (Dennison, 1976)) and other pre-Devonian fluvial systems with sheet-like geometries (i.e, Whirlpool sandstone of the lower Silurian Clinton Group in western New York (Cheel and Middleton, 1993; Johnson, 1998); cratonic Ordovician St. Peter Sandstone in the northern Mississippi Valley, USA (Dott et al., 1985); Ordovician Disi Formation in Jordan (Amireh et al., 2001)) that developed prior to land vegetation may be favorable for geologic CO_2 storage due to relative homogeneity. These should be considered for preliminary storage reservoir assessment.

Carbon Dioxide Storage Calculation

Methods used for estimating subsurface volumes are routinely used in the petroleum industry, and the standard methodology for calculating CO_2 storage potential has been documented by the Department of Energy (DOE, 2008). CO_2 storage can be divided into static and dynamic categories. Calculation of the static CO_2 storage capacity is governed by volumetrics and supercritical CO_2 compressibility. In contrast, dynamic storage capacity calculations incorporate reservoir homogeneity, permeability, and capillarity, and require reservoir simulation, injection rate data, and the treatment of interactions of the CO_2 with the formation fluid.

From seismic, core, and well log data, the static CO_2 storage capacity for a 5 mile × 5 mile (65 kilometer^2) area is estimated for the Queenston Formation surrounding the AES Cayuga power plant in Tompkins County (Figure 1.7), and uncertainties are reported in Table 1.6.

Table 1.6. CO_2 storage capacity variables and uncertainties (see equation 1.1).

Parameter	Average	Uncertainty (%)	Range
CO_2 Density (lbs/ft^3)	46	9%	42-50
Reservoir Thickness (feet)	600	17	500-700
Reservoir Area (acres)	16,000	--	--
Porosity (%)	10	25	7.5-12.5
Reservoir Storage Efficiency Factor	0.025	60	0.01-0.04

Log patterns for wells located within the seismic grid indicate that the Queenston Formation under the AES Cayuga power plant has similar properties to that of the Delaney core in Cayuga County (Figure 1.4), which has a bulk average porosity of 10% (+/- 2.5% from standard deviation in Figure 1.10, also from Schlumberger (1991)). Estimated reservoir temperature and pressure at the top of the Queenston Formation, which is approximately 4,200 feet (1280 meters) depth, are 100°F (38°C) and 1850 psi (128 bars) with errors of approximately +/- 10°F (5°C) (Beardsmore et al., 2001) and +/- 100 psi (Jarrell et al., 2002), respectively. These estimates assume a pressure gradient of 0.44 psi/foot (0.1 bars/meter), a temperature gradient of 42°F/mile (19°C/km), and a surface temperature of 60°F (16°C). Data were obtained from

temperature and pressure surveys from the Barron Well, which is located approximately six miles (10 kilometers) south of AES Cayuga. At this temperature and pressure, CO_2 at the top of the Queenston Formation will be in supercritical state and have a density of 46 lbs/ft^3, though based on the errors associated with subsurface gradients, the density may range from 42 lbs/ft^3 to 50 lbs/ft^3 (Table 1.6, Jarrell et al., 2002).

Many uncertainties about the properties of the rock are encompassed in a term referred to as the reservoir storage efficiency factor (Table 1.7, DOE, 2008). Reservoir storage efficiency is a function of reservoir area, porosity, and the interconnectedness of the pore spaces. Optimistically, CO_2 will replace up to 4% of the formation water constituting a reservoir storage efficiency factor of 0.04, though typical reservoir storage efficiency is generally estimated to range from 0.01 to 0.04 (Burruss et al., 2009; Zhou et al., 2007; DOE, 2008; Medina and Rupp, 2009). For the Queenston Formation at the AES Cayuga site, average reservoir storage efficiency is 0.025 (Table 1.7), which is similar to an assessment done by Medina and Rupp (2009) on the carbon sequestration potential of Cambrian Mount Simon Sandstone in Illinois. Though the reservoir storage efficiency factor could theoretically range over several orders of magnitude, we use a conservative reservoir storage efficiency average of 0.025 and a range of 0.01 to 0.04. Using these values and associated errors and an average Queenston Formation thickness of 600 feet +/-100 feet (180 meters +/- 30 meters) from the seismic data, we can calculate the static CO_2 storage mass with Equation 1.1 below (Jarrell et al., 2002; DOE, 2008). This calculation does not consider how much CO_2 will dissolve in formation fluid, which is dependent on temperature, pressure, and formation fluid composition.

Table 1.7. Reservoir storage efficiency parameter description with averages and ranges.

Terms	Average	Range	Description
Terms used to define the entire basin or region pore volume			
Net to total area	0.7	0.2-0.8	Fraction of total basin or region that has a suitable formation present. From facies map (Chapter 2, Figure 2.4).
Net to gross thickness	0.25	0.25-0.75	Fraction of total geologic unit that meets minimum porosity and permeability requirements for injection. Fraction of formation with NFSG10
Effective to total porosity ratio	0.6	0.6-0.95	Fraction of total porosity that is effective, i.e., interconnected. From percentage of Delaney well with >10% porosity.
Terms used to define the pore volume immediately surrounding a single well CO_2 injector			
Areal displacement efficiency	0.8	0.5-0.8	Fraction of immediate area surrounding an injection well that can be contacted by CO_2; most likely influenced by areal geologic heterogeneity such as faults or permeability anisotropy. Estimated to be 0.8 due to formation's areal homogeneity in the study area.
Vertical displacement efficiency	0.6	0.6-0.9	Fraction of vertical cross section (thickness), with the volume defined by the area (A) that can be contacted by the CO_2 plume from a single well; most likely influenced by variations in porosity and permeability between sublayers in the same geologic unit. If one zone has higher permeability than others, the CO_2 will fill this zone quickly and leave the other zones with less CO_2 or no CO_2 in them. From Delaney well with >10% porosity.
Gravity	0.9	0.2-0.9	Fraction of net thickness that is contacted by CO_2 as a consequence of the density difference between CO_2 and in-situ water. In other words, 1-Eg is that portion of the net thickness not contacted by CO_2 because the CO_2 rises within the geologic unit. Assuming CO_2 is injected into bottom of the Queenston Formation
Microscopic displacement efficiency	0.5	0.5-0.8	Portion of the CO_2-contacted, water-filled pore volume that can be replaced by CO_2. E_d is directly related to irreducible water saturation in the presence of CO_2. From water saturation reported by Lugert et al. (2006)for Queenston Auburn gas field.
	0.025 Average	0.001-.3 Range	

Equation 1.1. Equation for calculating CO_2 storage mass (Jarrell et al., 2002; DOE, 2008).

$$CO_2 \text{ Sequestration Mass (metric tons)} = \frac{(CO_2 \text{ Density}) \times (\text{Reservoir Thickness}) \times (\text{Reservoir Area}) \times (\text{porosity}) \times (\text{Reservoir Storage Efficiency Factor})}{2200}$$

42-50 lbs/ft^3; 500-700 feet; 16,000 acres; 7.5%-12.5%; 0.01-0.04

2200: Conversion factor (1 metric ton = 2200 lbs)

= 18 million metric tons (range 7 to 29 million metric tons)

Average formation properties (100°F (38°C), 1850 psi (128 bars), 0.025 storage efficiency, 600 feet (180 meters) thick, 10% porosity) indicate that this area of the Queenston Formation could hold 18 million metric tons of CO_2. Error was propagated independently throughout the calculation and gives a range of 7 to 29 million metric tons. AES Cayuga emits 2.4 million metric tons of CO_2 each year. Based on the static storage capacity estimate, a 25 square mile area of the Queenston Formation could theoretically sequester approximately 8 years of CO_2 output in its pore space, though error and uncertainties in the measurements cause this to range from 3 to 12 years of CO_2 output.

Conclusion

Seismic, core, and thin section examination indicate that the Queenston Formation of central New York is a homogenous fine- to medium-grained, well-sorted quartz sandstone with hematite cement that was deposited in a distributary fluvial system with mobile channels and no stable, long-lived flood plains. Increased hematite cement content decreases formation porosity. Four stacked petrophysical zones Queenston B (top) to Queenston E (bottom) were mapped near the AES Cayuga coal-fired power plant from well log, seismic, and core data. Seismic data suggest

there are internal unconformities within zones C and D, and locally the contact of C and D is erosional. Well core implies that zones B and C represent a series of base level changes, and an exposure surface is located in zone C in the Delaney Core. Core, cutting, and well log data show that the Queenston Formation is relatively homogenous surrounding the power plant. The two fine-grained lithofacies (5 and 6) only comprise 10% of the cored strata. There is little differentiation of channel and sheetflood overbank facies, which collectively comprise 90% of the Queenston Formation. This lack of significant lithologic change enhances the potential of the Queenston Formation for carbon dioxide storage near the AES Cayuga site.

In a 5 mile × 5 mile (65 kilometers^2) area surrounding the AES Cayuga power plant in Tompkins County, for the approximate parameters stated above, the Queenston Formation could store 18 million metric tons (+/- 11 million metric tons) of CO_2. Hence, if CO_2 can be effectively injected and the necessary seals exist, the Queenston Formation could theoretically sequester approximately 8 years of CO_2 output from the AES Cayuga coal-fired power plant. Uncertainties associated with this calculation, particularly values of formation porosity, storage efficiency (which includes porosity), CO_2 density, and fracture patterns, must be better constrained to obtain a more accurate estimate.

REFERENCES

Abdel-Wahab, A. 1998. Diagenetic history of Cambrian quartzarenites, Ras Dib-Zeit Bay area, Gulf of Suez, eastern Desert, Egypt. Sedimentary Geology. 121(1-2): 121-140.

Allen, J.R.L. 1970. Studies in fluviatile sedimentation; a comparison of fining-upwards cyclothems, with special reference to coarse-member composition and interpretation. Journal of Sedimentary Petrology. 40(1): 298-323.

Amireh, B.S., Schneider, W., and Abed, A.M. 2001. Fluvial-shallow marine-glaciofluvial depositional environments of the Ordovician System in Jordan. Journal of Asian Earth Sciences. 19: 45-60.

Asquith, G., and Krygowski. 2004. Basic well log analysis. In collaboration with S. Henderson and N. Hurley. AAPG Methods in Exploration Series. 16. 224 pp.

Beardsmore, G.R., and Cull, J.P. 2001. Crustal heat flow; a guide to measurement and modelling. Cambridge University Press. 324 pp.

Beer, J.A., and Jordan, T.E. 1989. The effects of Neogene thrusting on deposition in the Bermejo Basin, Argentina. Journal of Sedimentary Petrology. 59(2): 330-345.

Brogly, P.J., Martini, I.P., and Middleton, G.V. 1998. The Queenston Formation; shale-dominated, mixed terrigenous-carbonate deposits of Upper Ordovician, semiarid, muddy shores in Ontario, Canada. Canadian Journal of Earth Sciences. 35(6): 702-719.

Brett, C.E., Goodman, W.M., LoDuca, S.T., and Lehmann, D.F. 1996. Upper Ordovician and Silurian strata in western New York; sequences, cycles and basin dynamics. *In* Upper Ordovician and Silurian sequence stratigraphy and depositional environments in western New York: a field guide for the James

Hall Symposium, second international symposium on the Silurian System. C.E. Brett and W.M. Goodman, Co-leaders. 71-120 pp.

Burley, S.D. 1984. Patterns of diagenesis in the Sherwood Sandstone Group (Triassic), United Kingdom. Clay Mineralogy. 19: 403–440.

Burruss, R.C., Brennan, S.T., Freeman, P.A., Merrill, M.D., Ruppert, L.F., Becker, M.F., Herkelrath, W.N., Kharaka, Y.K., Neuzil, C.E., Swanson, S.M., Cook, T.A., Klett, T.R., Nelson, P.H., and Schenk, C.J. 2009. Development of a probabilistic assessment methodology for evaluation of carbon dioxide storage: U.S. Geological Survey Open-File Report 2009–1035. 81 pp. Available only online at *http://pubs.usgs.gov/of/2009/1035/*.

Campbell, C.V. 1976. Reservoir geometry of a fluvial sheet sandstone. America Association of Petroleum Geologists Bulletin. 60(7): 1009-1020.

Cheel, R.J., and Middleton, G.V. 1993. Directional scours on a transgressive surface: examples from the Silurian Whirlpool sandstone. Journal of Sedimentary Petrology. 63(3): 392-397.

Colton, G.W. 1970. The Appalachian Basin; its depositional sequences and their geologic relationships. *In* Studies of Appalachian geology: central New York. G.V. Fisher, F.J. Pettijohn, and K.N. Weaver Eds. 5-47 pp.

Core Laboratories, Inc. 1978. Special core analysis study for the Miller Brew Company, Delaney No. A-124-5 Well, West Auburn Field, Cayuga County, New York. 38 pp.

Dennison, J. 1976. Appalachian Queenston Delta related to eustatic sea level drop accompanying late Ordovician glaciation centered in Africa. *In* The Ordovician System; Proceedings of a Palaeontological Association Symposium, Birmingham, UK. University of Wales Press and National Museum of Wales. Cardiff, Wales, United Kingdom. 107-120.

Department of Energy (DOE). 2008. Methodology for Development of Geological Storage Estimates for Carbon Dioxide. http://www.netl.doe.gov/technologies/carbon_eq/refshelf/methodology2008.pdf.

Dott, R.H., Jr., Byers, C.W., Fielder, G.W., Stenzel, S.R., and Winfree, K.E. 1985. Aeolian to marine transition in Cambro-Ordovician cratonic sheet sandstones of the northern Mississippi valley, U.S.A. Sedimentology. 33(3): 345-367.

Engelder, T., and Gash, G. 2008. Marcellus shale play's vast resource potential creating a stir in Appalachia. The American Oil and Gas Reporter. 51(6): 76-87.

Fisher, D.W. 2006. The Rise and Fall of the Taconic Mountains: a geological history of eastern New York. In collaboration with Stephen L. Nightingale. Black Dome Press Corporation. 184 pp.

Gall, Q. 1999. Precambrian Palaeosols; a view from the Canadian Shield. In Palaeoweathering, Palaeosurfaces, and Related Continental Deposits. M. Thiry and R. Simon-Coinçon Eds. 207-221 pp.

Grabau, A.W. 1913. Early Paleozoic delta deposits of North America. Geological Society of America. 24: 299-528.

Hughes, S.E.M. 1976. The paleogeography and subsurface stratigraphy of the Late Ordovician Queenston Coastal Complex in New York. Master's of Science Thesis, Cornell University. 127 pp.

Intergovernmental Panel on Climate Change (IPCC). 2005. Carbon Dioxide Capture and Storage. 442 pp.

Jarrell, P., Fox, C., Stein, M., and Webb, S. 2002. Practical Aspects of CO_2 Flooding. SPE Monograph Series. 22. 220 pp.

Johnson, M.F. The sedimentology of the Lower Silurian Whirlpool sandstone in the subsurface Lake Erie, Ontario. Master's of Science Thesis, Brock University (Ontario). 186 pp.

Lugert, C., Smith, L., and Nyahay, R. 2006. Systematic technical innovations initiative for brine disposal in the northeast. New York State Energy Research and Development Authority (NYSERDA) Report, Contract number 6940. 269 pp.

Medina, C.R., and Rupp, J.A. 2009. Carbon Dioxide Storage Capacity in the Upper Cambrian Basal Sandstone of the Midwest Region: A County-Based Analysis. AAPG Eastern Section 2009 meeting, Evansville Indiana. Poster.

Miall, A.D. 1977. A review of the braided-river depositional environment. Earth-Science Reviews. 13(1): 1-62.

Miall, A.D. 1996. The geology of fluvial deposits: sedimentary facies, basin analysis, and petroleum geology. Berlin, Springer-Verlag, Federal Republic of Germany, 582 pp.

Pemberton, S.G., MacEachern, J.A., and Frey, R.W. 1992. Trace fossil facies models: envirnonmental and allostratigraphic significance. *In* Facies models; response to sea level change. R.G. Walker and N.P. James, Eds. Geological Association of Canada, Alberta, Canada. pp. 47-72.

Retallack, G.J. 1986. Fossil soils as grounds for interpreting long-term controls on ancient rivers. Journal of Sedimentary Petrology. 56(1): 1-18.

Retallack, G.J. 2001. *Scoyenia* burrows from Ordovician palaeosols of the Juniata Formation in Pennsylvania. Palaeontology. 44: 209-235.

Robinson, J.E. 1987. Upper Ordovician and Silurian sandstone facies of central New York State. Twelfth Appalachian Basin Industrial Associates Program, spring meeting. 12: 93-106.

Rodgers, J. 1971. The Taconic Orogeny. Geological Society of America Bulletin. 81(5): 1141-1177.

Saroff, S.T. 1987. Subsurface structure and nature of gas production of the Upper Ordovician Queenston Formation, Auburn gas field, Cayuga County, New - York. Thirteenth Appalachian Basin Industrial Associates Program, fall meeting. 13: 38-58.

Schlumberger. 1991. Formation Log Interpretation Principles/Applications. Schlumberger Educational Services. 198 pp.

Schlumberger. 1996. Improved recovery in the naturally-fractured Queenston Formation using geologic/engineering analysis and deviated well technology. New York State Energy Research and Development Authority (NYSERDA) Report, Contract number 4307. 58 pp.

Smith, L.B. Jr. 2006. Origin and reservoir characteristics of Upper Ordovician Trenton-Black River hydrothermal dolomite reservoirs in New York. AAPG Bulletin. 90(11): 1691-1718.

Smith, L.B. Jr. 2007. Carbon dioxide capture and storeage (CCS) potential in New York State. PowerPoint slides. Retrieved from http://esogis.nysm.nysed.gov/esogis/talks.cfm.

Surdam, R.C., Jiao, Z.S., MacGowan, D.B. 1993. Redox reactions involving hydrocarbons and mineral oxidants: a mechanism for significant porosity enhancement in sandstones. American Association of Petroleum Geologist Bulletin. 77: 1509–1518.

Tamulonis, K. 2010. Regional stratigraphy of the Queenston Formation in central New York and its implications for geologic carbon storage potential. Chapter 2 of this dissertation.

Thompson, A.M. 1970. Geochemistry of color genesis in red-bed sequence, Juniata and Bald Eagle Formations, Pennsylvania. Journal of Sedimentary Petrology. 4: 599-615.

Todd, S.P. 1996. Process deduction from sedimentary structures. *In* Advances in fluvial dynamics and stratigraphy. P.A. Carling and M.R. Dawson, Eds. 109. pp. 299-350.

Walker, T.R. 1967. Formation of red beds in modern and ancient deserts. Geological Society of America Bulletin. 78: 353-368.

Walker, T.R. 1976. Diagenetic origin of continental red beds. *In* The Continental Permian in Central, West, and South Europe. Falke, H., Ed. Reidel, Dordrecht. pp. 240–282.

Wheeler, H.E. 1964. Baselevel, lithosphere surface, and time-stratigraphy. Geological Society of America Bulletin. 75(7): 599-609.

Yeakel, L.S., Jr. 1962. Tuscarora, Juniata, and Bald Eagle paleocurrents and paleogeography in the Central Appalachians. Geological Society of America Bulletin. 73(12): 1515-1539.

Zhou, Q., Birkholzer, J., Rutqvist, J., and Tsang, C. 2007. Sensitivity study of CO_2 storage capacity in brine aquifers with closed boundaries: Dependence on hydrogeologic properties. Sixth annual conference on carbon capture and sequestration –DOE/NETL. 37 pp.

CHAPTER 2

REGIONAL STRATIGRAPHY OF THE QUEENSTON FORMATION IN CENTRAL NEW YORK AND ITS IMPLICATIONS FOR GEOLOGIC CARBON DIOXIDE STORAGE POTENTIAL

Abstract

The Upper Ordovician Queenston Formation is among potential targets for subsurface geologic carbon dioxide storage in New York State. We explore the total pore volume and lateral variability of the Queenston Formation in central New York and assess the potential of this formation as a carbon dioxide storage reservoir. In this study area, the Queenston Formation is a sequence of southwestward-thickening subsurface sandstones. In contrast, in western New York and Ontario, Canada, the Queenston Formation crops out, and it is composed of shale, siltstone, and sandstone that thin into Canada.

The available data sets reveal six stacked petrophysical zones (Queenston A (top) to F (base)) that range from 5 to 300 feet (2 to 90 meters) in thickness in central New York. Log and core data indicate that zones B, C, and D are laterally continuous throughout the study area and have higher porosity values than the other subunits in the formation. Seismic data reveal likely internal unconformities within zones C and D, and rock samples (from core) suggest that zones B and C each represents a cycle of base level fall followed by base level rise. Zones B, C, and D are thickest in NW-SE trending “channels” in the study area. For wells with neutron porosity and gamma logs, maps of net feet sandstone thickness with greater than 10% porosity reveal that zones B, C, and D have greatest thickness of porous sandstone coinciding with the depocenter ‘channels.’

Several interpretations of the Queenston Formation depositional system may be made based on sparse well log, core, outcrop, and seismic data from central and western New York. We believe the strongest hypothesis is that the Queenston Formation in central New York is non-marine and accumulated in a mobile-bed stream system. Western New York outcrops appear to be primarily lower energy subaerial coastal plain distributary channel to tidal flat deposits which grade westward into beach and marine deposits. Nevertheless, there is some controversy as to whether the western New York Queenston Formation shale and siltstone were deposited in a fluvial coastal plain environment or a shallow marine environment. Due to ambiguities in the data set, several models for Queenston Formation depositional environments were constructed. Regardless of the depositional model used, the Queenston Formation does not appear to have the porosity necessary for CO_2 storage west of Livingston County.

Regionally, controls on the accommodation space for the Queenston Formation seem to have varied across New York State and neighboring Ontario, judging by dissimilar patterns of base level change recorded in the strata and petrophysical logs. In the central New York study area, accommodation space for the Queenston Formation appears to have been controlled by tectonic activity, as the well log signatures primarily record regressive vertical trends even while 600 feet (180 meters) of non-marine strata aggraded. In western New York, the Queenston Formation log signature is dominated by transgressive trends, suggesting that sea level rise produced accommodation, modified by sea level fluctuations that dominated small-scale depositional patterns. The transition from regressive vertical trends in the east to transgressive vertical trends in the west suggests that the Queenston Formation may not be laterally continuous from east to west. Western New York fault systems, which

were active during the Ordovician, may have limited sediment supply to the west, as well as controlled accommodation potential.

The static CO_2 storage potential for the central New York study area has been calculated for the portion of the Queenston Formation at depths greater than 3,000 feet (900 meters) and intervals with porosity >10%. The volume of the Queenston Formation with depths greater than 3,000 feet (900 meters) for which porosity exceeds 10% can sequester approximately 5×10^9 metric tons of CO_2, which is the equivalent of 120 years of state wide power plant CO_2 emissions. For those intervals meeting this greater than 10% porosity criteria, pore volume calculations indicate that zones B, C, D, and E have the greatest potential for CO_2 storage. Existing permeability data suggest that approximately three quarters of the Queenston Formation is tight sands (permeability less than 1 mD) and reservoir stimulation would be needed to access much of the pore volumes. The environmental interpretation is highly generalized, due to the paucity of seismic, core, and outcrop data. This lends a degree of uncertainty to any evaluation, as do uncertainties associated with subsurface data collection and contouring methods.

Introduction

According to the Intergovernmental Panel on Climate Change (IPCC), geologic storage is a relatively well-developed carbon dioxide storage option because the technology has been advanced and used by the petroleum industry for enhancing oil recovery from producing reservoirs (IPCC, 2005). At emission point sources such as industrial sites and coal-fired power plants, CO_2 can be separated from other flue gases and then concentrated into a stream of pure, high pressure CO_2. The CO_2 collected from the flue stream is transformed to the supercritical phase (temperatures greater than 31.1°C (88°F) and pressures greater than 73 atmospheres (1073 psi)) for storage, and can then be injected through a well into a subsurface rock formation.

Storage formations must have a minimum depth of approximately 2,600 feet (800 m) in order for the CO_2 to remain in a supercritical phase (IPCC, 2005). Ideally, the supercritical CO_2 will be isolated from the atmosphere for a geologically significant time period (thousands to millions of years; IPCC, 2005). In the rock, CO_2 entrapment mechanisms include physical and residual trapping, solubility storage, mineralization, and adsorption onto organic matter, and a combination of these mechanisms is an ideal storage scenario (IPCC, 2005). Generally, a porous and somewhat permeable reservoir rock is needed to store significant amounts of CO_2, and it is preferred that this reservoir rock have saline formation fluids, as opposed to potable water. An overlying seal above the storage formation is necessary to prevent upward migration of CO_2 to the surface or to potable aquifers.

Recent policy initiatives, such as the Regional Greenhouse Gas Initiative (RGGI), make it necessary for New York State to investigate the feasibility of carbon capture and storage potential as a means of dealing with CO_2 emissions from power and industrial point sources. Existing data sets collected primarily for natural gas exploration throughout New York allow geologists to explore the potential for geologic CO_2 storage in subsurface formations. The New York State Reservoir Characterization Group of the New York State Museum reported on the general suitability of rocks throughout the state for storage (Smith, 2007). In New York's Appalachian basin, they initially highlighted the Cambrian Potsdam Formation, the Cambro-Ordovician Beekmantown Group, Upper Ordovician Black River, Trenton, Oswego, and Queenston Formations, and the Lower Silurian Clinton Formation as potential state-wide CO_2 storage formations because of their regionally favorable porosity. According to Smith (2007), the Upper Silurian Syracuse Salt Formation would serve as an ultimate seal above these potential storage formations. The Syracuse salt exists only south of the green line in Figure 2.1 (north of the Venice

Figure 2.1. Map of study area. Data were consulted from 269 wells (acquired from New York State Museum database www.esogis.com) from an 11 county area (yellow) surrounding five AES power plants. Anschutz Exploration Corporation provided seismic data in Tompkins and Cayuga Counties. The Silurian Syracuse Salt is considered to be a prospective secure seal unit (Smith, 2007). This salt exists south of the green line. The black dashed line marks the northern extent of area in which the top of the Queenston Formation occurs at depths greater than 3,000 feet. The north-south cross section is located from A-A' (Figure 2.2). Regional cross section (B-B', Figures 2.15 and 2.18) relates our central New York study area to western New York and Ontario outcrops. Wells used for the N-S and W-E cross sections are filled with black and numbered: 1 – Wasielewski Well, 2 – Venice View Dairy Well, 3 – Fee Richarson Well, 4 – Kesselring Well, 5 – Milton, Ontario Core, 6 – Hooker Chemical Well, 7 – Fee Well, 8 – Foss Well, 9 – Howes Well, 10 – Hilts Well, 11 – Kennedy Well, 12 – Button Well, 13 – Schaffer Well, 14 – Delaney Core. Outcrop locations marked with X and numbered: 15 – Lewiston, 16 – Lockport, 17 – Golden Hills State Park.

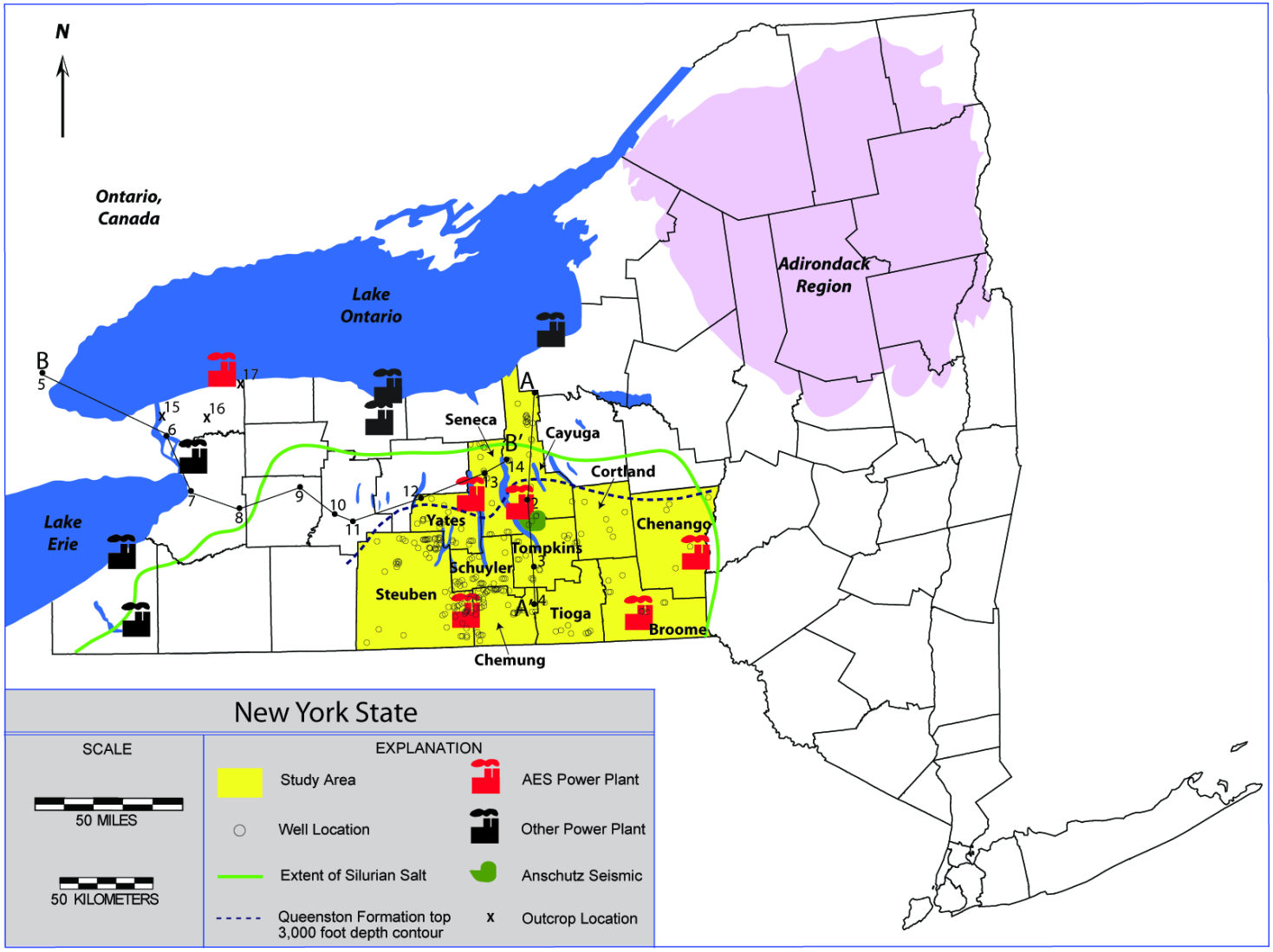
N
Ontario,
Canada
Lake
Ontario
Adirondack
Region
Lake
Erie
Seneca
Cayuga
Cortland
Yates
Chenango
Tompkins
Schuyler
Steuben
Tioga
Broome
Chemung
A
A'
B
B'
New York State
SCALE
50 MILES
50 KILOMETERS
EXPLANATION
Study Area
Well Location
Extent of Silurian Salt
Queenston Formation top
3,000 foot depth contour
AES Power Plant
Other Power Plant
Anschutz Seismic
Outcrop Location

View Dairy well in Figure 2.2) and reaches depths necessary to maintain CO_2 in a supercritical phase south of the northern borders of Steuben, Tompkins, and Schuyler counties (Figure 2.3).

As previously stated, the minimum depth necessary to store CO_2 in a supercritical state is approximately 2,600 feet (800 meters, IPCC, 2005), with variations dependent on the geothermal gradient of a basin. In order to assure that primary and secondary sealing units can exist above the reservoir unit, the practice of seeking reservoirs in New York State at depths greater than 3,000 feet (900 meters) below the ground surface is adopted. We specifically investigate geologic CO_2 storage potential for reservoirs greater than 3,000 feet (900 meters) depth in an eleven county area in central New York surrounding five coal-fired power plants owned by AES Corporation (Greenridge, Hicklng, Cayuga, Jennison, and Westover power plants). The study area includes Steuben, Yates, Schuyler, Chemung, Seneca, Cayuga, Tompkins, Tioga, Cortland, Broome, and Chenango counties (several well logs from Livingston County were also used; Figure 2.1). This investigation is based on archived well log, core, and seismic data and is approached in the same manner a reservoir characterization team investigates oil and gas reservoirs.

After a preliminary data assessment of siliciclastic formations at depths greater than 3,000 feet (900 meters), we determined that the Queenston Formation potentially offers the porosity necessary to be a CO_2 storage formation in central New York. This result is in conflict with outcrops and log data from western New York, which suggests there is not sufficient porosity for CO_2 storage. The Queenston Formation in central New York has not been extensively studied in the past because it is not considered to be a major gas producer. Regardless, a relatively abundant subsurface data set exists for the Queenston Formation due to the collection of data for natural gas

Figure 2.2. North-south cross section in study area, illustrating the 1-2°S regional dip (location in Figure 2.1). Gamma logs (GR) were used to identify the formation tops, which are mapped on the cross section. The Queenston Formation (highlighted orange) reaches the 3,000 foot depth contour necessary for supercritical CO_2 storage south of the black dashed line in Figure 2.1 and below the black dashed line in Figure 2.2. Formation names are placed just below the top of the corresponding unit.

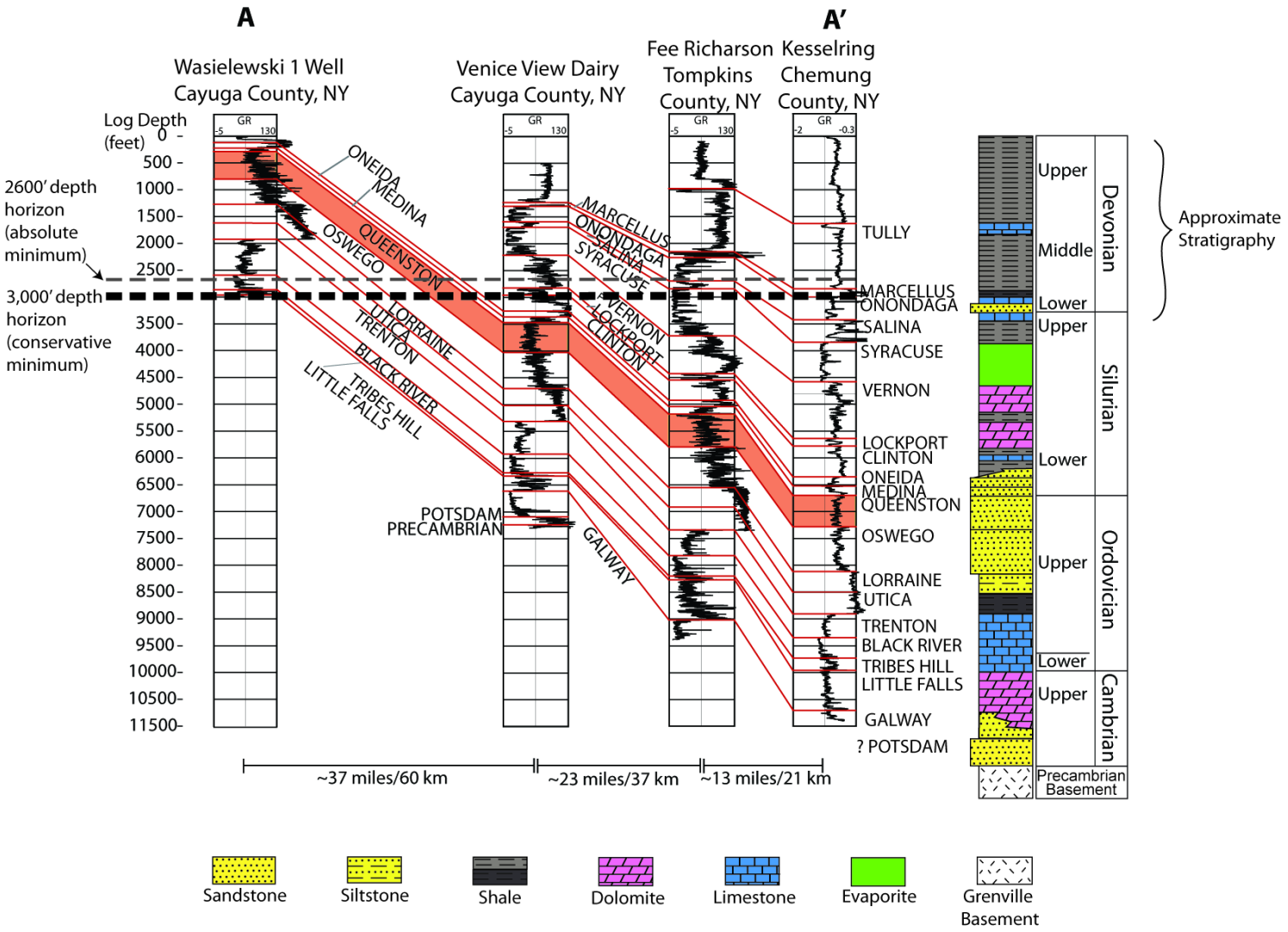
A
A'
Wasielewski 1 Well
Cayuga County, NY
Venice View Dairy
Cayuga County, NY
Fee Richarson
Tompkins
County, NY
Kesselring
Chemung
County, NY
Log Depth
(feet)
2600' depth
horizon
(absolute
minimum)
3,000' depth
horizon
(conservative
minimum)
ONEIDA
MEDINA
QUEENSTON
OSWEGO
LORRAINE
UTICA
TRENTON
BLACK RIVER
TRIBES HILL
LITTLE FALLS
POTSDAM
PRECAMBRIAN
GALWAY
MARCELLUS
ONONDAGA
SALINA
SYRACUSE
VERNON
LOCKPORT
CLINTON
TULLY
MARCELLUS
ONONDAGA
SALINA
SYRACUSE
VERNON
LOCKPORT
CLINTON
ONEIDA
MEDINA
QUEENSTON
OSWEGO
LORRAINE
UTICA
TRENTON
BLACK RIVER
TRIBES HILL
LITTLE FALLS
GALWAY
? POTSDAM
~37 miles/60 km
~23 miles/37 km
~13 miles/21 km
Upper
Middle
Lower
Devonian
Upper
Lower
Silurian
Upper
Lower
Ordovician
Upper
Cambrian
Precambrian
Basement
Approximate
Stratigraphy
Sandstone
Siltstone
Shale
Dolomite
Limestone
Evaporite
Grenville
Basement

Figure 2.3. Basin-wide isopach for the Queenston and Juniata Formations, partially modified from Brett et al. (1996) and Brogly et al. (1998). The study area is highlighted in yellow, and the regional cross section (B-B') is marked with a black dashed line. Contour intervals are in feet.

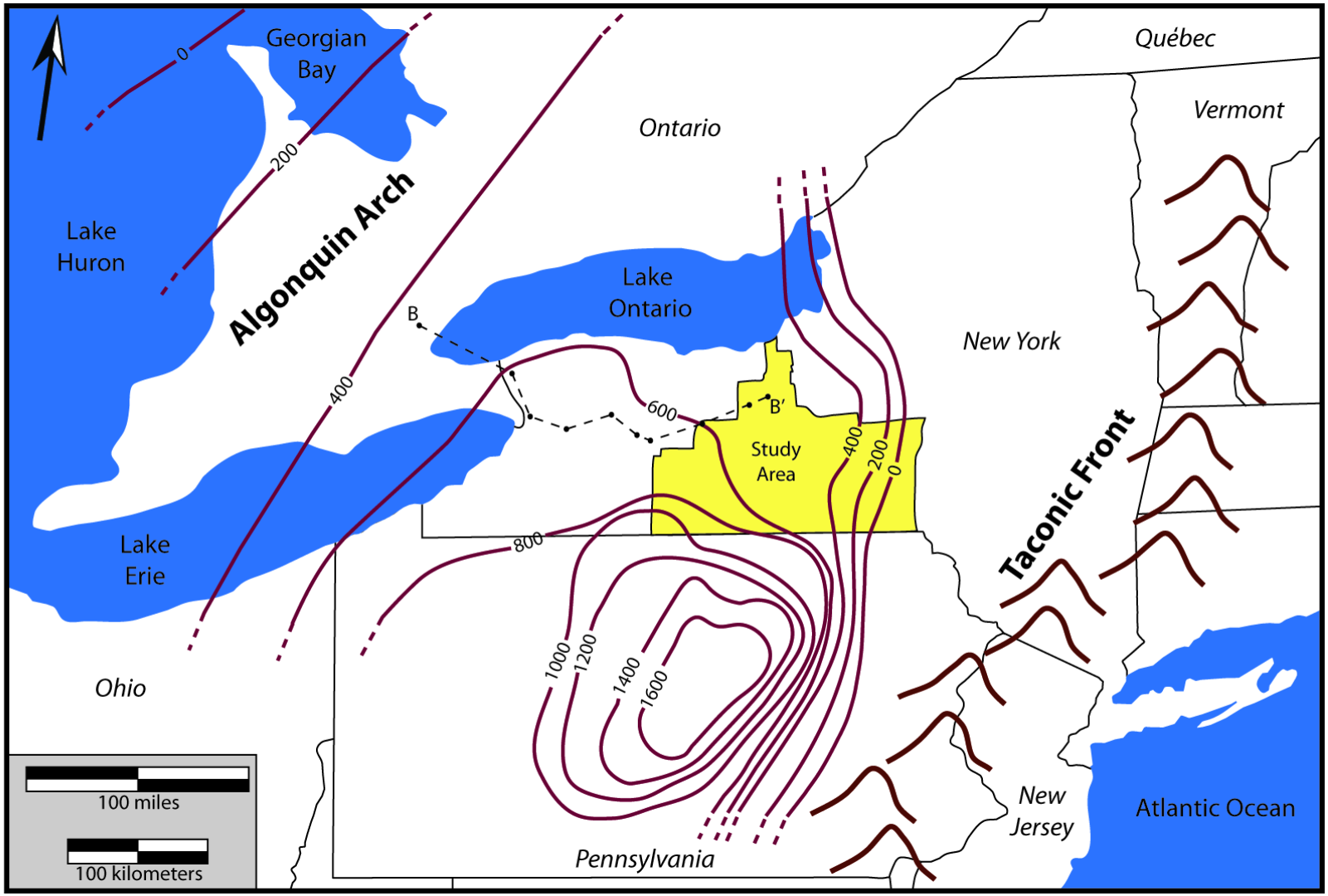
Georgian Bay
Québec
Ontario
Vermont
Lake Huron
Algonquin Arch
Lake Ontario
New York
B
B′
Study Area
Taconic Front
Lake Erie
Ohio
Pennsylvania
New Jersey
Atlantic Ocean
0
200
400
600
800
1000
1200
1400
1600
100 miles
100 kilometers

exploration in the underlying and relatively widely explored Trenton and Black River Formations (Smith, 2006).

Queenston Formation regional stratigraphy, porosity, permeability, and static CO_2 storage potential in central New York are characterized in this paper. The Grimsby Siltstone of the Medina Group could serve as an immediate seal overlying the Queenston Formation in central New York (Saroff, 1987), with the Syracuse Salt serving as the ultimate seal (Figure 2.2). This paper does not present seal characterization, geochemical transport, or flow modeling, though all of these aspects are currently being investigated. Numerous uncertainties are associated with the stratigraphic models, log data, and thus the CO_2 storage calculation. These uncertainties are identified, quantified when possible, and propagated throughout the CO_2 storage calculation. The geologic model of the Queenston Formation and the porosity associated with the formation's facies forms the basis for all subsequent carbon storage assessment steps, and uncertainties associated with this model may result in an unsuccessful storage project.

Geologic Setting

Regional

The Upper Ordovician Queenston Formation is a clastic foreland basin wedge which was deposited westward during Phase V of the Taconic Orogeny (Fisher, 2006; Colton et al., 1970; Figure 2.3). The western boundary of the Queenston Formation is the Algonquin Arch, a low forebulge that was intermittently uplifted during the Taconic Orogeny (Brett et al., 1996; Figure 2.3). Its facies patterns and thickness variations record a complex pattern of deposition and erosion throughout New York State (Robinson, 1987). The Queenston Formation is part of the Queenston Delta – a regional redbed complex which extends from Ontario to Alabama and collectively is comprised of the Queenston and Oswego Formations in New York, Ohio, and Ontario;

the Juniata and Bald Eagle Formations in Pennsylvania, Maryland, and West Virginia; and the Sequatchie Formation in Kentucky, Tennessee, and Alabama (Dennison, 1976). West of New York State, the Queenston Formation grades into carbonates in the Michigan Basin (Johnson, 1985).

During Queenston Formation deposition, the northern Appalachian Basin was located in a subtropical climate belt at approximately 20°-25°S latitude (Van der Voo, 1988). In Ontario, the Queenston Formation is composed of red to gray shales and bioclastic limestone (Brogly et al., 1988). The formation crops out in western New York at the Niagara Gorge and at or near the south shore of Lake Ontario, where it is a reddish quartz siltstone with considerable amounts of sand and clay. In the subsurface of central New York, the Queenston Formation is primarily a well-sorted, red, fine to medium grained sandstone (Brogly et al., 1998; Woodrow, 1989). Friedman (1987) calculated that the Ordovician strata in western New York and Ontario was buried to a maximum depth of 2.5 to 3 miles (4 to 5 km) prior to Mesozoic and Cenozoic denudation.

In New York, the Oswego Formation conformably underlies the Queenston Formation and is a north-south trending lens of interbedded fine to coarse sandstone, siltstone, and shale that grades westward into shale and siltstone (Robinson, 1987). The Oswego Formation consists of un-fossiliferous greenish-gray sandstones, siltstones, mudstones, and shales, which were deposited in offshore shelf to intertidal environments (Hughes, 1976; Patchen, 1965; Robinson, 1987). The lowest Oswego beds were deposited in deep, offshore waters, and overlying beds were deposited in progressively shallower environments, including bars and lagoons (Patchen, 1965). In outcrop, the Queenston/Oswego contact is generally defined by the lowest occurrence of red beds (Brett et al., 1996). In central New York, the Oswego Formation is over 1,000 feet (300 meters) thick in the southern part of the study area

and thins to the north to 400 feet (120 meters) in Cayuga County (Figure 2.2). The Oswego Formation coarsens and increases upward in roundness and sorting of the constituent grains (Patchen, 1965). In outcrop, these upper sandstones are tight (permeability < 1 mD, Robinson, 1987). Oswego Formation geophysical log porosity values remain fairly constant throughout the formation, with an average porosity of 9% in Seneca County increasing southward to 13% in Schuyler County.

The Oswego Formation forms the transition between the deep water Lorraine shales, which conformably underlie the Oswego Formation, and the Queenston Formation. This sequence (Lorraine, Oswego, Queenston) formed from northward sea regression and uplift of the eastern source area (Robinson, 1987). Generally, it is believed the Queenston Formation was deposited in a semi-arid environment (Brett et al., 1996; Brogly et al., 1998; Grabau, 1913) during a time of glacio-eustatic sea level fall due to glaciation centered in Africa (Brett et al., 1996; Dennison, 1976). This sea level fall, along with the terminal compressional event of the Taconic Orogeny, produced the Cherokee Unconformity, which separates the Queenston Formation from the overlying Medina Group and represents the regressive maximum (Brett et al., 1996) .

Study Area

Well log data from the study area show that the Queenston Formation thickness ranges from approximately 350 feet (100 meters) in Broome County to greater than 800 feet (240 meters) in Steuben County (Figure 2.4). There is erosional and depositional thinning of the Queenston Formation in the eastern portion of the study area, and the formation is erosionally truncated in a north-south trending zone east of Chenango, Madison, and Broome counties (Robinson, 1987). The top of the Queenston Formation is shallowest in the northern portion of the study area at approximately 300 feet (90 meters) below the surface (Figure 2.2). The unit dips

Figure 2.4. An isopach map from well log data indicates that the Queenston Formation thickens to the southwest portion of the study area. The top of the Queenston Formation reaches depths greater than 3,000 feet south of the black dashed line, and the top of the Syracuse Formation reaches depths greater than 3,000 feet south of the orange dashed line. Trenton-Black River and Queenston gas fields are located, as well as AES power plants. Contours (pink and yellow dashed lines) defining sand, sand and silt, and sand, silt, and mud dominated zones were drawn based on average Queenston Formation gamma log values (sand dominated: < 80 gamma API; sand and silt: 80-150 API; sand, silt, and mud: > 150 API).

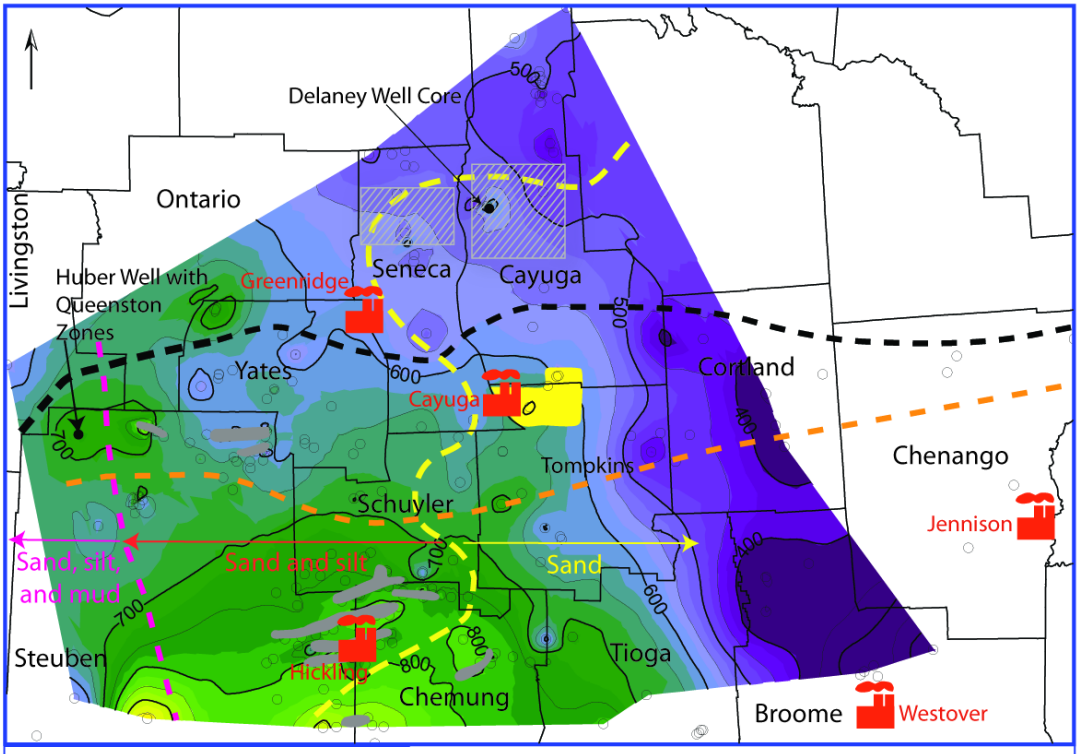

Queenston Formation Isopach

0 10 20 30
MILES

0 10 20 30 40 50
KILOMETERS

CONTOURS

QUEENSTON ISOPACH THICKNESS

contour interval = 50 feet

375 425 475 525 575 625 675 725 775 825 875 925 975 1025 1075 1125

SYMBOLS

- Well Location
- AES Power Plant
- Queenston Formation 3,000 foot depth contour
- Syracuse Formation 3,000 foot depth contour
- Queenston Formation sand dominated east of yellow dashed line
- Queenston Formation mud dominated west of pink dashed line
- Trenton-Black River Hydrothermal Dolomite Field
- Approximate Location of Queenston Formation Seneca and Cayuga County Fields
- Anschustz Exploration Corporation Seismic Data

1-2°S reaching the 3,000 foot (900 meter) depth contour necessary for supercritical CO_2 storage in an east–west trending zone between the AES Greenridge and Cayuga power plants (Figures 2.2 and 2.4). Depth to the Queenston Formation top approaches 8,000 feet (2,400 meters) at the New York/Pennsylvania border. This study focuses on the CO_2 storage potential for the area south of the dashed black line in Figure 2.3.

Reservoirs for several shallow (less than 1,600 feet; 490 meters) Queenston Formation natural gas fields in Cayuga and Seneca counties are fine-grained quartz sandstone with subangular quartz grains and clay content averaging 20% (Robinson, 1987). Saroff (1988) described the Cayuga County field to be a fractured, low permeability reservoir with best production in zones with greater than 75% sand content that have been highly fractured. Our well cuttings and core data show that the Queenston Formation in central New York is a sub-round to sub-angular, fine- to medium-grained, well-sorted sandstone with hematite cement. The cuttings show that Oswego Formation grain size and roundness decrease with depth, which is a sub-angular to angular siltstone to fine-grained sandstone with lithic fragments and quartz overgrowth and carbonate cement.

Previous Work

Studies of the Queenston Formation in central New York have been conducted since the early part of the twentieth century, and it was Grabau (1913) who first recognized that large clastic wedges were deposited in the Appalachian Basin as the landmass to the east was uplifted during the Taconic Orogeny (Figure 2.3). The Queenston Formation in Ontario, Canada and western New York has been extensively studied by numerous geologists (Brett et al., 1996; Brogly et al., 1998; Caley, 1940; Dyer, 1925), and it is generally believed to have been deposited in a muddy deltaic environment, though there is some dispute as to whether the formation is marine or non-marine (Hughes, 1976; Saroff, 1987). Brogly et al. (1998) studied Queenston

Formation outcrop and core from southern Ontario, concluding that features of the formation are indicative of prograding muddy, storm and tide affected shores. A series of at least three base level cycles are also noted in the southern Ontario/Western New York Queenston section (Brett et al., 1996; Brogly et al., 1998). Robinson (1987) describes the Queenston Formation in New York State to be fluvial to shallow water deltaic deposits that spread westward. It is believed that the Queenston Delta was deposited during the late stages of the Taconic Orogeny and is composed of detritus shed from a highland (Ettensohn, 1991). Portions of this highland were composed of somewhat older strata, which resulted in recycled detritus that was relatively fine grained and lacks conglomerate deposits (Ettensohn, 1991).

The Juniata Formation is a sandstone and conglomerate of the central Appalachians (Thompson, 1970) and is the southern counterpart of the Queenston Formation. The Juniata Formation is over 1,500 feet (450 meters) thick in central Pennsylvania (Figure 2.3; Brett et al., 1996). This formation has been more widely studied because it has relatively widespread outcrops, particularly in central Pennsylvania. Due to the presence of laterally extensive genetic units of sandstone and conglomerate with planar horizontal beds, cross beds, and trough cross lamination, Cotter (1978) concluded that sediment was deposited in a low sinuosity, fluvial setting with sheet flooding. Juniata Formation paleocurrent direction was to the northwest (Yeakel, 1962), suggesting that, compared to the Queenston Formation, the sandstones and conglomerates of the Juniata Formation were deposited in a higher energy environment closer to the source area.

Relatively little is known about the Queenston Formation in central New York, primarily because it is in the subsurface and has only minor natural gas production in Cayuga and Seneca County fields (Robinson, 1987). Hughes (1976) studied well cuttings from the Queenston and Oswego Formations in central and western New

York and interpreted the formations to have been deposited in marine and beach environments. Hughes (1976) stated that the color boundary separating the two formations varies and is not consistently located at the Queenston/Oswego contact defined by well logs. These results were interpreted to imply that the Oswego Formation is the diagenetically reduced portion of an initially all-red section.

Several studies of the Queenston Formation in Seneca and Cayuga counties have been conducted to assess natural gas fields and the potential for the Queenston Formation to be a reservoir for brine disposal (Lugert et al., 2006; Robinson, 1987; Saroff, 1987; Schlumberger, 1996). These studies concluded that the Queenston Formation has the porosity necessary to serve as a reservoir, and permeability is greatest in sandstones that are highly fractured. Saroff (1987) deduced that better producing wells lie along a NE-SW linear trend, which parallels Precambrian basement faults interpreted from Bouguer gravity anomaly, and concludes that abundant fracture sets surrounding the basement faults improve reservoir permeability. Tamulonis (2010) conducted a site-specific CO_2 storage assessment for the Queenston Formation surrounding an AES power plant on the border of Tompkins and Cayuga counties. She concluded that the Queenston Formation was deposited in a distributary fluvial system with no stable, long-lived flood plains, and that the formation offers the porosity necessary to store a commercially significant mass of supercritical CO_2.

Materials and Methods

The Ordovician formations of New York State have been producing natural gas for over a century. Recently, the Trenton and Black River Formation have been a focus of exploration (Smith, 2006), as well as the Devonian Marcellus Formation (Engelder and Gash, 2008). As a result of this exploration and production, subsurface data are available for certain locations, but available types of data vary among the many stratigraphic units. Data types are most comprehensive in several Queenston

Formation natural gas fields that are located in the study area (Figure 2.4). Our Queenston Formation data set consists of widely distributed borehole logs, core, and cuttings, as well as localized seismic reflection data. The New York State Museum Reservoir Characterization group stores digital well logs, cuttings, and core collected throughout New York State. They have digitized all the well logs, to which we had access through the Empire State Oil and Gas Information System database (www.esogis.com), and they also supplied cutting and core samples to this project. Anschutz Exploration Corporation provided access to seismic data collected in Tompkins and Cayuga counties.

Well Logs

Because gas exploration in central New York has not been focused on the Queenston Formation, nearly half of the existing well log suites from the study area do not have data pertaining to the Queenston Formation. Either wells did not penetrate the Queenston Formation or logging equipment did not collect data from the formation. A total of 157 wells in the study area contain digital borehole data from the Queenston Formation, and these digital logs were imported into Petra software, where they were analyzed and maps were constructed from the data. Log data were collected as early as 1948. From this data set, gamma, neutron porosity, and electron density logs were primarily used, though wells with Queenston Formation log data do not necessarily have all three logs. Gamma logs measure rock shale content by measuring the decay of radioactive atoms incorporated in clay structure, neutron porosity logs quantify porosity by measuring the hydrogen content of water or hydrocarbons in pore space, and electron density logs emit gamma rays into the rock, which measures the density of electrons in a formation (Asquith and Krygowski, 2004). Figure 2.4 shows the location of wells used in this study. Where data are available, formation tops between the Salina Formation and the Precambrian basement were identified (Figure

2.2), and distinct petrophysical zones were mapped within the Queenston Formation based on gamma, neutron porosity, and electron density logs (Asquith and Krygowski, 2004; Figure 2.5).

All well logs were examined and the gamma log was used to identify the top of the Queenston Formation, which was defined to be the first significant decrease in gamma value below the Medina Formation top (Figures 2.2 and 2.5). The Oswego Formation top was picked where there is a relatively subtle increase in gamma values (Figures 2.2 and 2.5). Isopach maps from well log data were constructed for the entire Queenston Formation (Figure 2.4) and for individual zones (Figure 2.6).

Seven well logs from western New York and data from a core in Ontario, Canada (Brogly et al., 1996) were also consulted to aid in correlation between Queenston outcrops and central New York subsurface data (Figure 2.1). Using the same techniques and criteria as in the 11 county study area, these wells logs were divided into petrophysical zones based on variations in gamma, neutron porosity, and electron density logs (Figure 2.7).

Porosity from Well Log Data

In order to understand the spatial distribution of rock with a large volume of high porosity sandstone within the study area, a quantity termed the "net feet of sandstone with greater than 10% porosity" (NFSG10) was calculated using Petra software for 49 wells with neutron porosity and gamma logs. This quantification sums, for each location with suitable data, the thickness of rock in which the average porosity exceeds 10%. The spatial distribution of the NFSG10 values was mapped for the entire Queenston Formation (Figure 2.8), as well as for each petrophysical zone (Figure 2.9).

Neutron porosity logs were chosen because it was the log type from which

Figure 2.5. Gamma (black line), neutron porosity (blue line), and electron density (red line) logs display the variations in values that are the criteria used to identify the contacts between the Medina-Queenston and Queenston-Oswego Formations, as well as the six petrophyscal zones, Queenston A-F. The labels indicate the tops of each named unit. The Medina-Queenston boundary coincides with the top of petrophysical zone Queenston A. From the Huber Well in Steuben County (Figure 2.4).

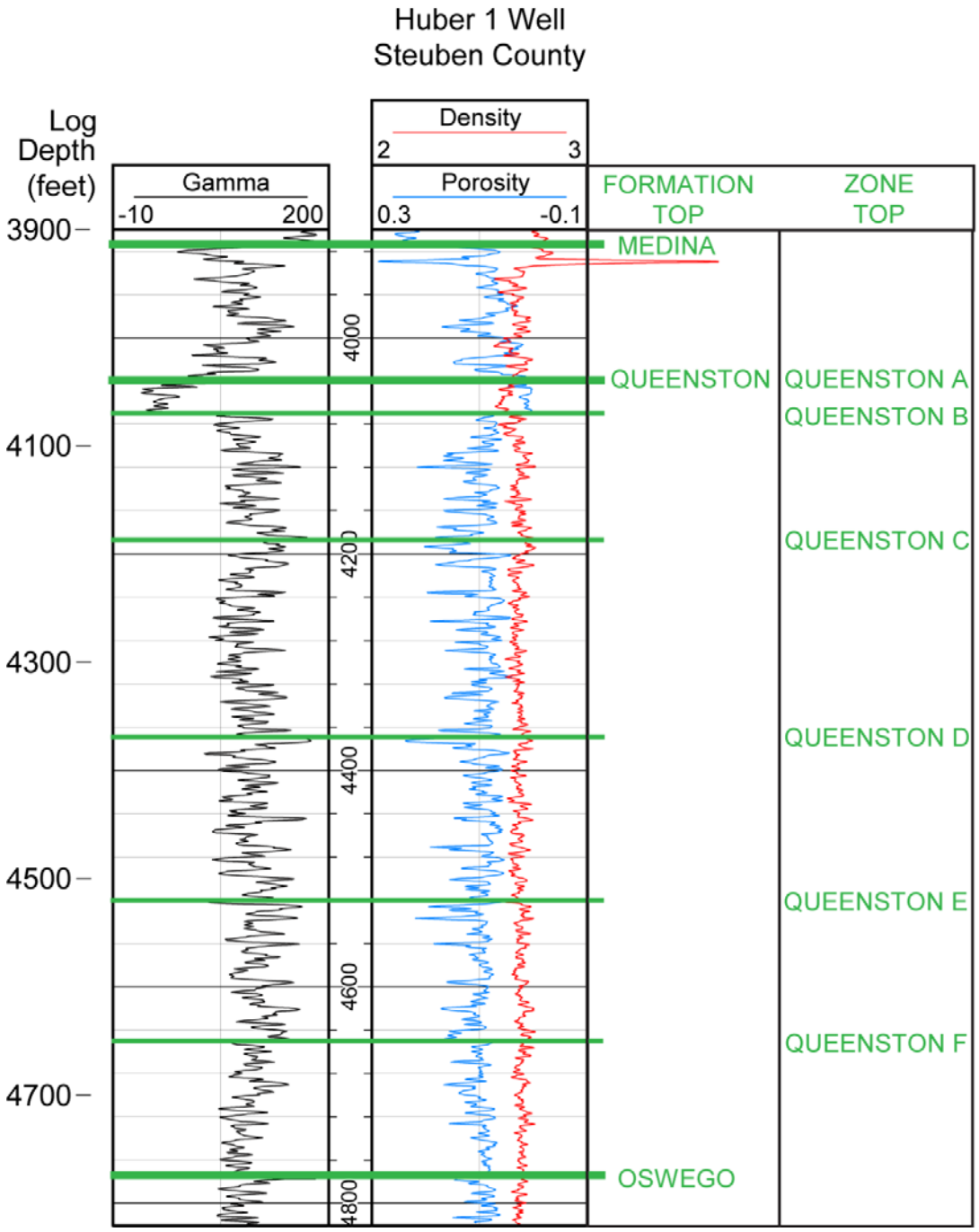
Huber 1 Well
Steuben County
Log Depth (feet)
Gamma
-10
200
Density
2
3
Porosity
0.3
-0.1
FORMATION TOP
ZONE TOP
3900
4100
4300
4500
4700
4000
4200
4400
4600
4800
MEDINA
QUEENSTON
QUEENSTON A
QUEENSTON B
QUEENSTON C
QUEENSTON D
QUEENSTON E
QUEENSTON F
OSWEGO

Figure 2.6. Isopach maps of Queenston petrophysical zones A-F based on well log data for central New York.

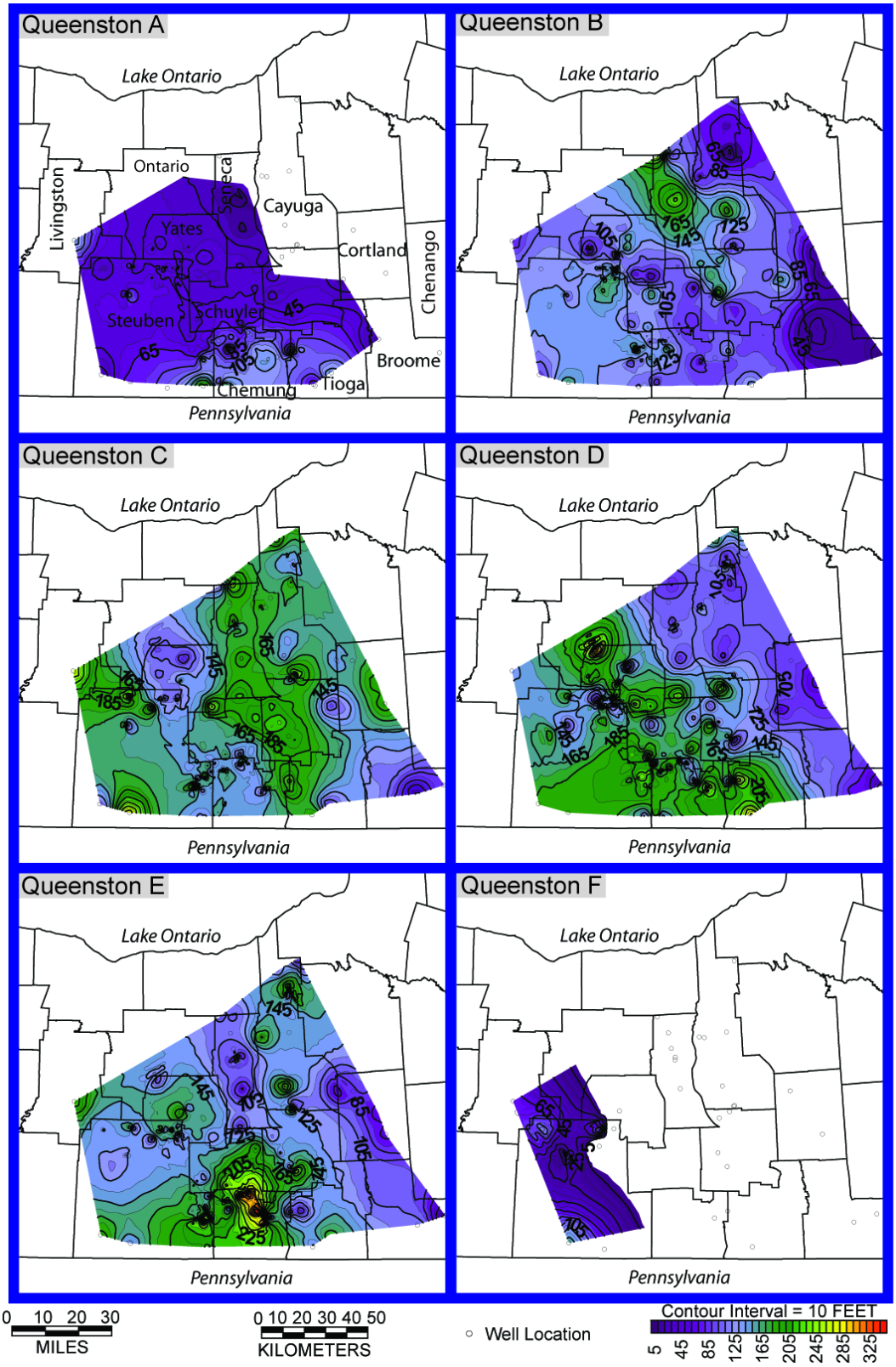
Queenston A
Lake Ontario
Ontario
Seneca
Cayuga
Livingston
Yates
Cortland
Chenango
Steuben
Schuyler
Broome
Chemung
Tioga
Pennsylvania
Queenston B
Lake Ontario
Pennsylvania
Queenston C
Lake Ontario
Pennsylvania
Queenston D
Lake Ontario
Pennsylvania
Queenston E
Lake Ontario
Pennsylvania
Queenston F
Lake Ontario
Pennsylvania
0 10 20 30
MILES
0 10 20 30 40 50
KILOMETERS
Well Location
Contour Interval = 10 FEET
5 45 85 125 165 205 245 285 325

Figure 2.7. Gamma (black line), neutron porosity (blue line), and electron density (red line) logs of the western New York petrophysical zones Queenston V-Z, from the Howes Well in Wyoming County (Figure 2.1). The labels indicate the tops of each named unit. The Medina-Queenston boundary coincides with the top of petrophysical zone Queenston V.

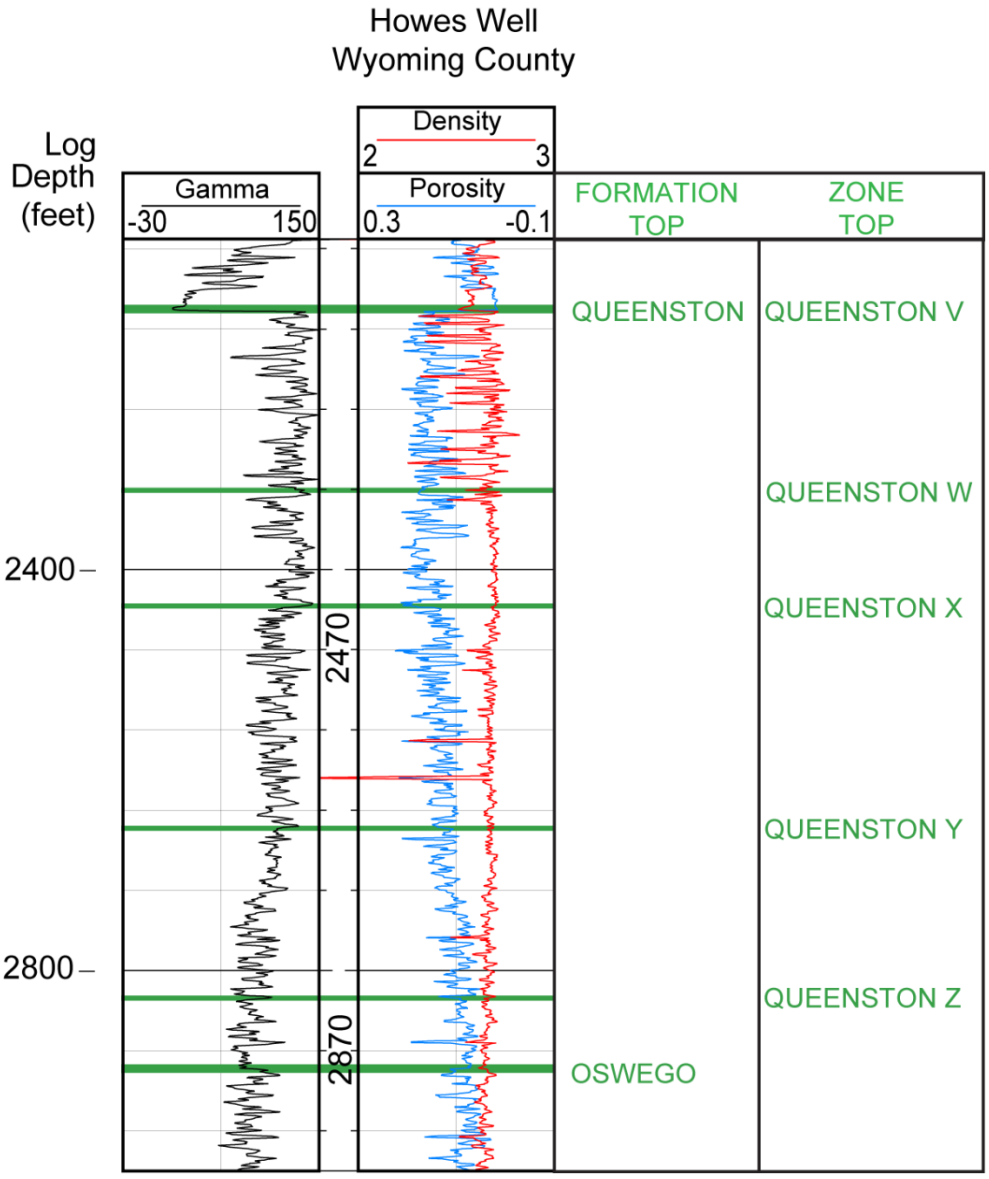
Howes Well
Wyoming County
Log
Depth
(feet)
Gamma
-30
150
Density
2
3
Porosity
0.3
-0.1
FORMATION
TOP
ZONE
TOP
QUEENSTON
QUEENSTON V
QUEENSTON W
QUEENSTON X
QUEENSTON Y
QUEENSTON Z
OSWEGO
2400
2800
2470
2870

Figure 2.8. Isopach map of the net thickness (in feet) of rock with greater than 10% porosity (NFSG10) for the entire Queenston Formation. The contoured values were obtained from neutron porosity logs, with gamma values used as a discriminator to avoid the 'shale effect.'

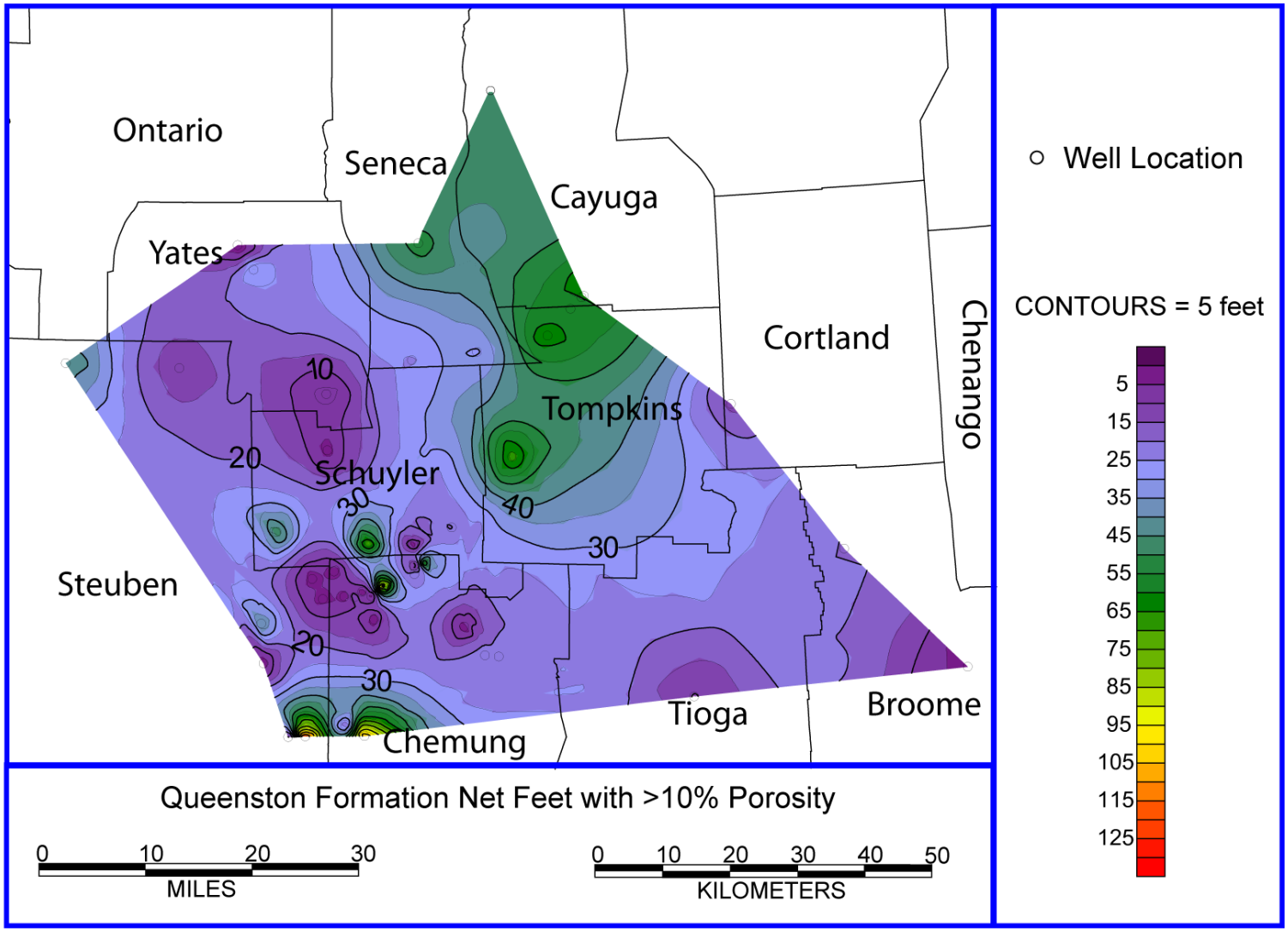
Ontario
Seneca
Cayuga
Yates
Cortland
Chenango
Tompkins
Schuyler
Steuben
Tioga
Broome
Chemung
10
20
30
40
30
20
30
Well Location
CONTOURS = 5 feet
5
15
25
35
45
55
65
75
85
95
105
115
125
Queenston Formation Net Feet with >10% Porosity
0 10 20 30
MILES
0 10 20 30 40 50
KILOMETERS

Figure 2.9. Isopach maps of the net thickness (in feet) of rock with greater than 10% porosity for each Queenston Formation petrophysical zone. The contoured values were obtained from neutron porosity logs, with gamma values used as a discriminator to avoid the ‘shale effect.’

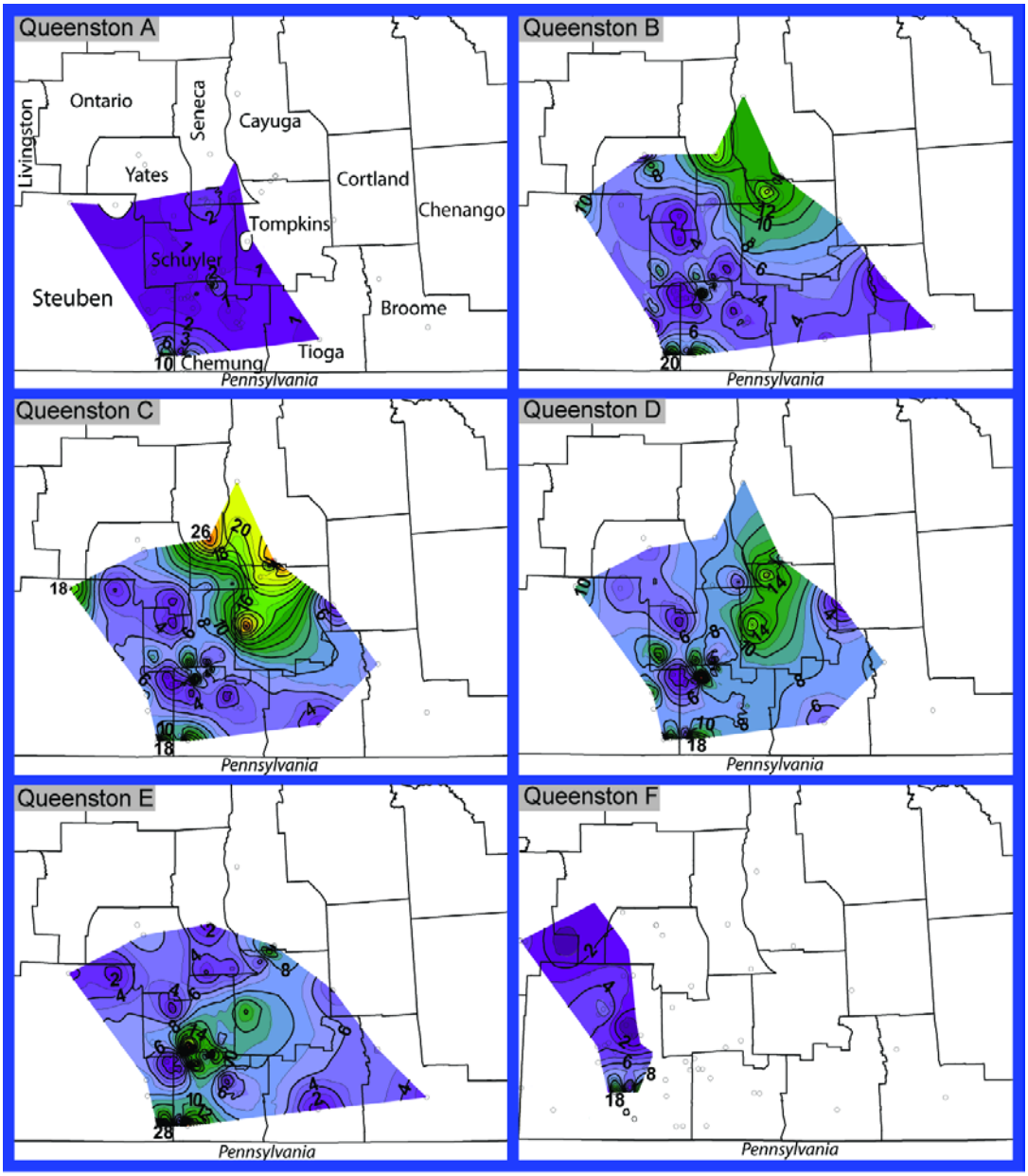
Queenston A
Ontario
Seneca
Cayuga
Livingston
Yates
Cortland
Chenango
Tompkins
Schuyler
Steuben
Broome
Chemung
Tioga
Pennsylvania
Queenston B
Pennsylvania
Queenston C
Pennsylvania
Queenston D
Pennsylvania
Queenston E
Pennsylvania
Queenston F
Pennsylvania
0 10 20 30
MILES
0 10 20 30 40 50
KILOMETERS
Well Location
CONTOUR INTERVAL = 1 FOOT
2 4 6 8 10 12 14 16 18 20 22 24 26 28

porosity can be deduced that was available for the largest number of wells, and because Tamulonis (2010) determined that this was the most accurate log porosity measurement compared to core porosity data collected from the Queenston Formation in Cayuga County. A neutron porosity log is a measure of a formation's hydrogen content and is used to quantify the porosity of a formation (Asquith and Krygowski, 2004). The tool emits neutrons into a formation, and because the mass of a neutron is approximately equivalent to the mass of a hydrogen nucleus, the neutrons lose energy when they collide with hydrogen nuclei. The degradation of neutron energy, measured at a detector that is also located on the tool, is an approximation of the number of hydrogen atoms along the neutron flux path (Asquith and Krygowski, 2004). These formation hydrogen atoms may be incorporated as hydrocarbons in pore space, as water in pore space, or as bound hydrogen in minerals such as clay. The neutron porosity tool calculates the hydrogen index of the formation, which is the quantity of hydrogen per unit volume of rock, and this value is then directly converted to neutron porosity units (Asquith and Krygowski, 2004). A problem with this method is the 'shale effect,' where hydrogen bound in the clay mineral structure will cause a false increased "porosity" value in the neutron logs. One way to correct for this effect is to use electron density logs to correct neutron porosity values for a specific lithology (Asquith and Krygowski, 2004), but unfortunately density logs are not available for all wells with neutron porosity logs. A common practice among petroleum geologists is to exclude shale-rich horizons from calculations of neutron porosity on the premise that a shale horizon will have low porosity. This approach relies on using the gamma values as a discriminator to determine shale-rich horizons. In practice, formation lithology is identified by normalizing gamma curves to a common clean sand value and a common high shale value, and then using a single arbitrary cutoff to classify and then exclude shale layers (Asquith and Krygowski,

2004). In this case, gamma values had to be normalized, because log data were collected over several decades with various equipment. The low gamma value is normalized to 15 API units and the high gamma value is normalized to 230 API units. An industry standard shale cutoff is typically 80 API (Krygowski, 2009), so zones with shale gamma values greater than 80 API were excluded from computing NFSG10. For the entire Queenston Formation and for each petrophysical zone within the formation, contour maps of NFSG10 were constructed for 49 wells (Figures 2.8 and 2.9).

The frequency distribution for every porosity measurement from each well in the study area was compiled, and the best fit probability density function for the porosity distribution was calculated (Figure 2.10).

Western New York Outcrops

The Queenston Formation crops out in western New York and is not exposed in central New York. Three outcrop locations were visited for this study (Figure 2.1). These outcrops are located in the Niagara Gorge in Lewiston, Niagara County; Lockport, Niagara County (Figure 2.11); and Golden Hills State Park on the border of Niagara and Orleans counties (Figure 2.12). Sedimentological information, primarily lithology and sedimentary structures, was collected from the outcrop for paleoenvironmnetal interpretation.

Core and Seismic Data

The Delaney core in Cayuga County was collected for a brine disposal study (Figure 2.4) and is a vertical penetration of 324 feet (99 meters) from the Queenston Formation (Figure 2.13). Seventy-one thin sections and 82 core plug porosity and permeability measurements were obtained for this core (Lugert et al., 2006). The cored interval was divided into seven lithofacies, petrophysical zones were picked

Figure 2.10. Porosity distribution frequency graph for every porosity data point from each well with Queenston Formaton neutron porosity data (total of 293,088 data points). A gamma distribution probability density function best fits the porosity frequency distribution when $k = 8$ and $\theta = 1.3$.

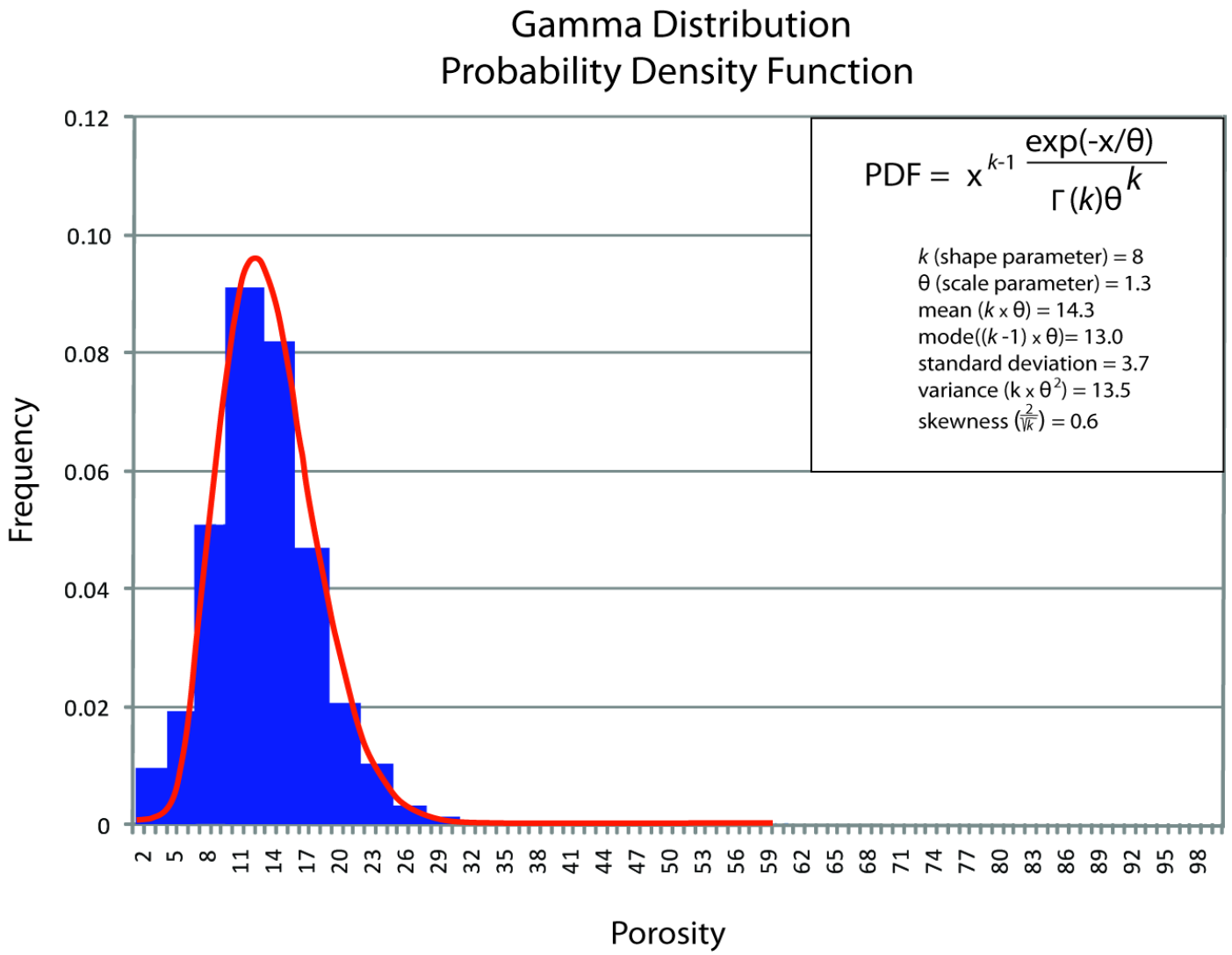
Gamma Distribution
Probability Density Function
PDF = $x^{k-1} \frac{\exp(-x/\theta)}{\Gamma(k)\theta^k}$
k (shape parameter) = 8
θ (scale parameter) = 1.3
mean (k x θ) = 14.3
mode((k -1) x θ)= 13.0
standard deviation = 3.7
variance (k x θ²) = 13.5
skewness ($\frac{2}{\sqrt{k}}$) = 0.6
Frequency
0.12
0.10
0.08
0.06
0.04
0.02
0
2 5 8 11 14 17 20 23 26 29 32 35 38 41 44 47 50 53 56 59 62 65 68 71 74 77 80 83 86 89 92 95 98
Porosity

Figure 2.11. Lockport, New York Queenston Formation outcrop (located in Figure 2.1). The overlying Whirlpool sandstone of the Medina Group is separated from the Queenston Formation by the Cherokee Unconformity. At Lockport, the Queenston Formation is similar to the lower portion of the Lewiston outcrop, with massively bedded red siltstone interbedded with fine-grained sandstone layers (some reduced) and some mudstone layers.

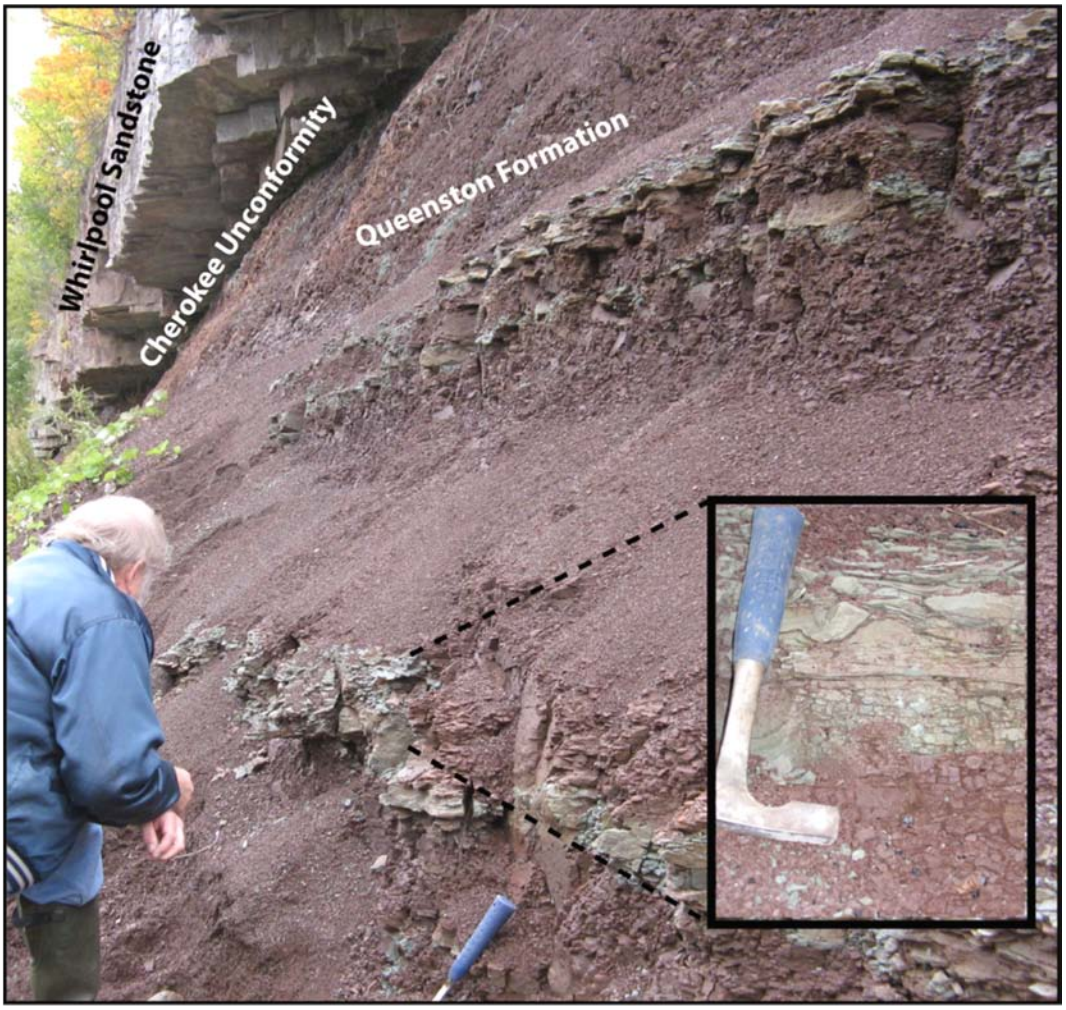
Whirlpool Sandstone
Cherokee Unconformity
Queenston Formation

Figure 2.12. Golden Hills State Park, New York Queenston Formation outcrop (located in Figure 2.1). The Queenston Formation is primarily a brownish red, laminated fine-grained sandstone interbedded with siltstone layers. Some layers are reduced, and long, parallel ripples up to eight inches in length are present (inset photograph), as well as rip-up clasts.


~ 5 feet
6 inches

Figure 2.13. Delaney Well (Cayuga County) core description, lithofacies interpretation, and relation to petrophysical zones Queenston B (QB), Queenston C (QC), and Queenston D (QD) (Tamulonis, 2010). Trends in base level (arrows) were drawn based on well log and core variations, and three distinct deposits are highlighted. Lithofacies are described by Tamulonis (2010). FD – flood deposit, LST – low-stand system track.

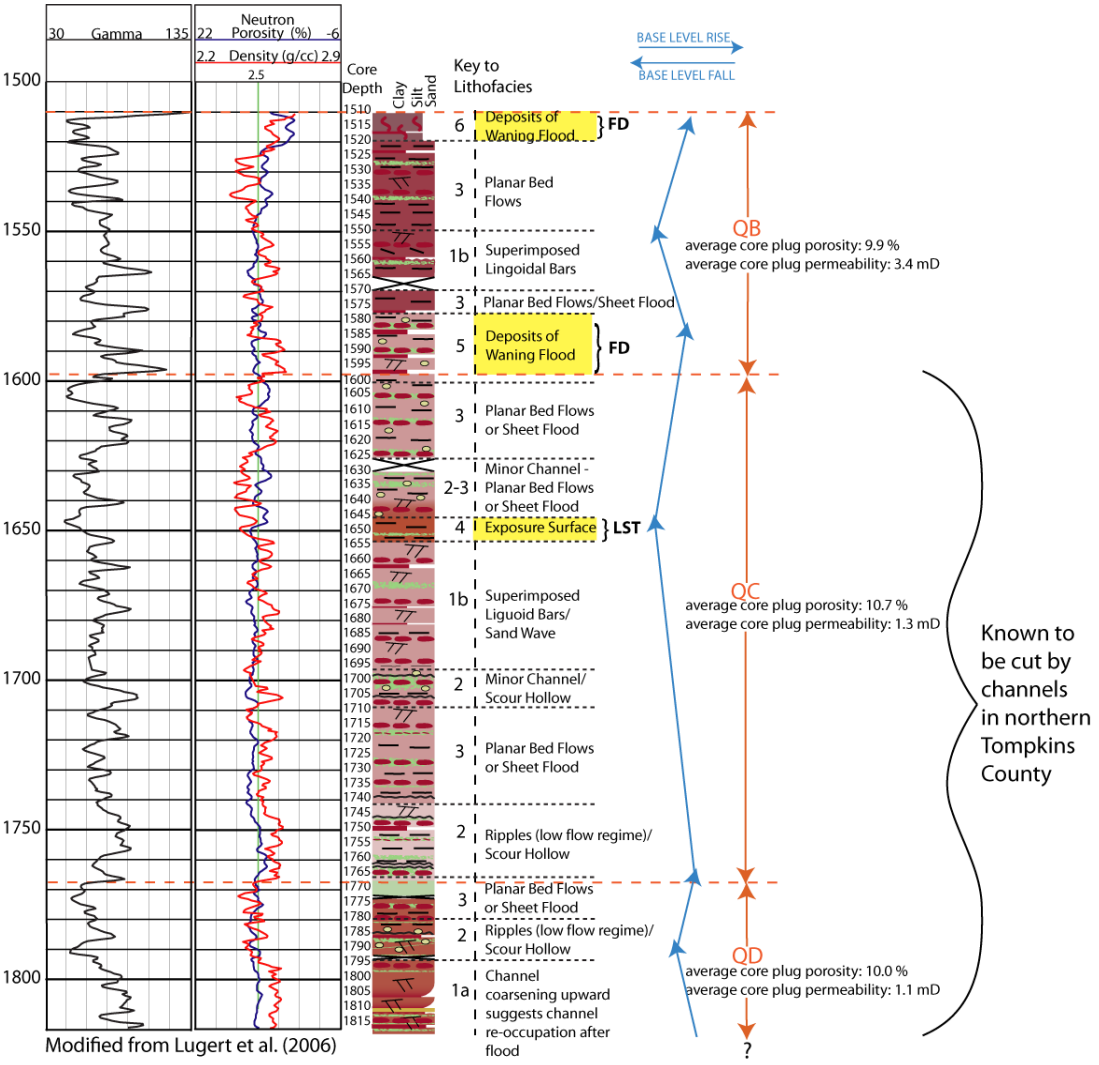
30 Gamma 135
Neutron Porosity (%) 22 -6
Density (g/cc) 2.2 2.9
2.5
Core Depth
Clay
Silt
Sand
Key to Lithofacies
BASE LEVEL RISE
BASE LEVEL FALL
1500
1550
1600
1650
1700
1750
1800
6 Deposits of Waning Flood } FD
3 Planar Bed Flows
1b Superimposed Lingoidal Bars
3 Planar Bed Flows/Sheet Flood
5 Deposits of Waning Flood } FD
3 Planar Bed Flows or Sheet Flood
2-3 Minor Channel - Planar Bed Flows or Sheet Flood
4 Exposure Surface } LST
1b Superimposed Liguoid Bars/ Sand Wave
2 Minor Channel/ Scour Hollow
3 Planar Bed Flows or Sheet Flood
2 Ripples (low flow regime)/ Scour Hollow
3 Planar Bed Flows or Sheet Flood
2 Ripples (low flow regime)/ Scour Hollow
1a Channel coarsening upward suggests channel re-occupation after flood
QB
average core plug porosity: 9.9 %
average core plug permeability: 3.4 mD
QC
average core plug porosity: 10.7 %
average core plug permeability: 1.3 mD
QD
average core plug porosity: 10.0 %
average core plug permeability: 1.1 mD
?
Known to be cut by channels in northern Tompkins County
Modified from Lugert et al. (2006)
EXPLANATION
Burrows
Planar Beds
Cross Beds
Mottling
Rip-up Clasts
Petrophysical Zone
Lithofacies Boundary

based on log signature variations, and base level cycles were interpreted by lithofacies stacking (Tamulonis, 2010).

Anschutz Exploration Corporation collected approximately 45 miles^2 (117 kilometers^2) of 3D seismic data and 11 N-S trending 2D seismic lines in Tompkins and Cayuga counties (Figure 2.4), focusing on natural gas exploration in the Trenton and Black River Formations. Formation tops from the Silurian Syracuse Formation to the Precambrian basement were identified along one seismic line that crossed a well location for which formation tops were known (Tamulonis, 2010; Figure 2.14). The formation tops were mapped on 15 seismic lines, and Queenston petrophysical zones were mapped on two seismic lines that intersected boreholes. Data collection methods for the core and seismic data are discussed extensively by Tamulonis (2010).

Results

Regional Variations in Thickness and in Petrophysical Properties in Central and Western New York

Gamma log data show that the Queenston Formation of central New York thickens to the southwest and reaches a maximum thickness of nearly 1,000 feet (300 meters) in Steuben County (Figure 2.4). The formation thins to the east and is approximately 350 feet (100 meters) thick in Broome County. In wells east of Broome County, either the Queenston Formation was not recorded in well logs, the Queenston-Oswego contact was missing, or the criteria for recognizing the formation top is not suitable due to erosion and/or non-deposition.

Generally in central New York, Queenston Formation gamma values increase with depth, and neutron porosity and electron density values are fairly uniform, although subtle variations are observed in all logs (Figures 2.2 and 2.5). Based on these subtle gamma, neutron, and density log variations, the Queenston Formation was visually divided into six stacked petrophysical zones, Queenston A (top)-F (base)

Figure 2.14. Seismic facies reveal that the Queenston Formation in northern Tompkins and southern Cayuga Counties was deposited in a channelized setting. In the seismic data, petrophysical zones Queenston C (QC) and Queenston D (QD) appear to have several erosional surfaces. Queenston reflections are outlined with black and the tops of petrophysical zones are mapped with green (Tamulonis, 2010). Seismic data courtesy of Anschutz Exploration Corporation.

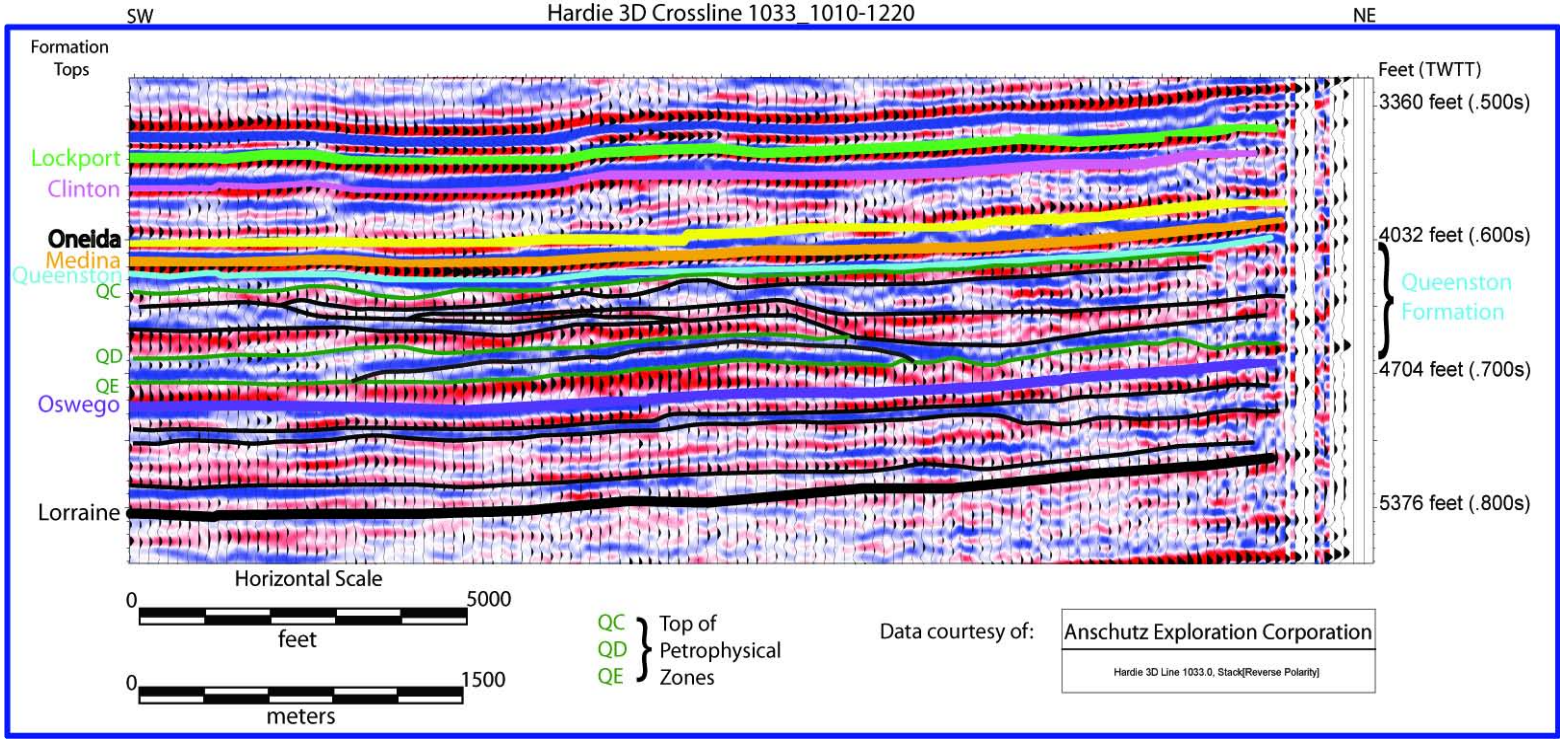
SW
Hardie 3D Crossline 1033_1010-1220
NE
Formation Tops
Lockport
Clinton
Oneida
Medina
Queenston
QC
QD
QE
Oswego
Lorraine
Feet (TWTT)
3360 feet (.500s)
4032 feet (.600s)
Queenston Formation
4704 feet (.700s)
5376 feet (.800s)
Horizontal Scale
0
5000
feet
0
1500
meters
QC
QD
QE
Top of Petrophysical Zones
Data courtesy of:
Anschutz Exploration Corporation
Hardie 3D Line 1033.0, Stack[Reverse Polarity]

(Figure 2.5). Queenston A is defined as a zone with relatively low gamma, electron density, and neutron porosity values. This zone is not represented in the Delaney core, but due to the low gamma, density, and porosity values, it is interpreted to be relatively clean, tight sandstone. Queenston B has gamma, neutron porosity, and density values that are higher than Queenston A. Queenston C has gamma values similar to Queenston B, with peaks at the top and bottom of the zone and a trough in the middle, and density and porosity values are also similar to those of Queenston B. Queenston D also has a cyclic gamma pattern similar to Queenston C. Relative to zone D, Queenston E generally has higher gamma, porosity, and density signatures. Queenston F shows gamma values that decrease with depth while neutron porosity values increase with depth.

Queenston petrophysical zones V (Queenston Formation top to top of zone W), W, X, Y, and Z were mapped in western New York (Figure 2.7). Queenston V has a relatively consistent high gamma signature and variable density. Queenston W and X both have gamma peaks at the top and bottom of the zone and a trough in the middle. Gamma values in Queenston Y and Z generally increase toward the top of each zone, though the gradient of increase for Queenston Y is greater than that of Queenston Z.

For the central New York focus area, isopachs were made with well log data for each petrophysical zone, A-F (Figure 2.6). Zone A thickness ranges from 0 to 5 feet (0 to 2 meters) in Seneca, Tompkins, Cortland, and Broome counties to approximately 140 feet (40 meters) in Livingston County and up to nearly 200 feet (60 meters) in Steuben County, where it is thickest. This zone does not extend as far north and east as zones B-E, which are found throughout the study area except for Chenango County. Queenston B isopach is thinnest in the eastern portion of the study area (Cortland and Broome counties), where it ranges between 10 to 40 feet (3 to 12 meters), and is up to 200 feet (60 meters) thick in Seneca and Tompkins counties.

Queenston B is generally greater than 100 feet (30 meters) thick in the western portion of the study area. Queenston C isopach is also relatively thick in Seneca and Tompkins counties (175 to 240 feet; 50 to 70 meters). This zone is thinnest in Broome County (20 feet; 6 meters) and thickest in Steuben County (275 feet; 80 meters). Queenston D generally thickens to the southwest portion of the study area, and thickness ranges from 40 feet (12 meters) in Broome County to nearly 330 feet (100 meters) in Yates County. Queenston E is also thinnest in Broome County (20 feet; 6 meters), and this zone is approximately 375 feet (115 meters) thick in Chemung County. Zone F occurs only in Steuben, Yates, and Livingston counties, where thickness ranges from 50 to160 feet (15 to 50 meters; Figure 2.6).

Regional Variations in Porosity

Spatial variations in Queenston Formation lithology affect NFSG10 distribution. Generally, average Queenston Formation gamma log values increase to the west of the study area, suggesting silt and clay content increases westward (Figure 2.4). Gamma values also decrease in the southern study area, indicating clay content decreases southward, and average neutron porosity values for the entire formation generally increase to the south, from 8% in central Yates County to 17% in southern Chemung County. Though clay content increases westward, well logs suggest there are zones with relatively low gamma values and high neutron porosity values interbedded within the more clay dominated zones even in the western sector of the central New York study area. Because the Queenston Formation thins to the east, net feet of porous sandstone also thins eastward even though the formation is of more homogenous sand content in the east.

The greatest thickness of rocks of favorable high neutron porosity is in southern Steuben and Chemung Counties, where NFSG10 reaches 120 feet (40 meters; Figure 2.8), and this area corresponds to highest average neutron porosity

values for the entire thickness of the formation (17%). NFSG10 for the entire formation is also relatively high in Tompkins and southern Cayuga Counties, where it reaches nearly 70 feet (20 meters), and average total formation neutron porosity is 13% in this area. Zones Queenston A and F have the lowest NFSG10 (Figure 2.9). For both zones A and F, the thickness of strata with porosity greater than 10% increases to the south with maximum values of 15 and 20 feet (5 and 6 meters), respectively, in Steuben County (Figure 2.9), and both zones have the highest average neutron porosities in this area (8% and 14%, respectively). Zones B, C, and D all have NFSG10 patterns similar to that of the entire Queenston Formation, with the thickest zones in Cayuga/Tompkins and Steuben/Chemung Counties (Figure 2.9). NFSG10 does not exceed 30 feet (9 meters) for zones B, C, D, or E individually. Queenston B has highest average neutron porosity in southern Steuben and Chemung Counties (19%), and zones C and D have highest average neutron porosity in southern Cayuga County (16% and 17%, respectively). Queenston E NFSG10 is thickest in southern Steuben County (29 feet, 9 meters), and average neutron porosity is highest in northern Schuyler County (17%).

A histogram (Figure 2.10) displays the frequency of occurrences of porosity values in the log data. The distribution of the total porosity data set is not a Gaussian distribution because porosity data exist as high as 61% (though the frequency of the porosity data is not visible at the scale of the graph; Figure 2.10). Though there are some very high porosity values recorded throughout the study area, it is possible that high values occur in fractured zones, and if this is the case, these high porosities must be recognized in the best fit distribution function as they may greatly affect CO_2 storage potential. A gamma probability density function best fits the frequency distribution for every well log neutron porosity data point from the study area, with $k = 8$ and $\theta = 1.3$ (Figure 2.10). Based on the gamma distribution for the porosity

frequency, mean porosity is 14.3, the porosity mode is 13.0, variance is 18.6, and skewness is 0.6. This density distribution function may differ from the Gaussian distribution function reported for the Delaney well porosity by Tamulonis (2010) because the porosity data points for the entire study area are greater than those reported from the Delaney core by approximately a factor of 1,000.

Outcrop

Over 70 feet (20 meters) of the Queenston Formation directly underlying the Cherokee Unconformity are exposed at the Lewiston, New York outcrop in the Niagara Gorge, though not all horizons in the entire vertical section of the outcrop are safely or legally accessible. It is likely that this exposure is part of western New York petrophysical zone V (Figure 2.7). The overlying Whirlpool Sandstone of the Medina Group is exposed at this location. Underlying the Whirlpool Sandstone, the Queenston Formation is a reddish brown, blocky, massively bedded siltstone, at least 20 feet (6 meters) thick. Vertical ENE trending fractures are present, and pale green coloration indicates that the siltstone is chemically reduced along portions of this fracture set. Below this massive siltstone, the formation reveals interlayered reddish brown siltstone and resistant chemically-reduced sandstone layers, with approximately 5 feet (1.5 meters) of siltstone between sandstone beds. Over (2009) reports mudcracks and *Skolithos* in one sandstone bed.

At Lockport, where approximately 20 feet (6 meters) of the Queenston Formation directly underlies the Cherokee Unconformity, there is no equivalent to the thick interval of massive reddish brown siltstone that directly underlies the Whirlpool Sandstone at the Lewiston outcrop. Rather, at Lockport the Queenston Formation is similar to the lower portion of the Lewiston outcrop, with interbedded massive reddish brown siltstone and fine-grained sandstone layers (Figure 2.11), some of which are laterally discontinuous, as well as some claystone layers directly underlying the

Whirlpool Sandstone. The massive siltstone beds are up to 5 feet (1.5 meters) thick, whereas the fine-grained sandstone and claystone layers are inches (centimeters) thick. While the great majority of the strata are reddish brown in color, a few percent of the horizontal laminae in the siltstone as well as in the fine sandstone are reduced to a pale greenish gray. It is likely that this outcrop occurs in petrophysical zone V.

The Queenston Formation consists primarily of reddish brown, laminated, fine-grained sandstone interbedded with siltstone layers at the Golden Hills State Park on the south shore of Lake Ontario (Figure 2.12). Approximately 7 feet (2 meters) of the formation are exposed at this outcrop, and the vertical location of this exposure within the Queenston Formation is unknown. Some layers are reduced, and parallel, symmetric, straight ripples up to 8 inches (20 centimeters) in length are present, as well as rip-up clasts.

Fossils were not observed at any of the outcrops. A set of vertical ENE trending fractures is present at all outcrops.

Core and Seismic Data

A detailed examination of the Delaney core is reported by Lugert et al. (2006) and Tamulonis (2010). The cored strata are primarily composed of fine to medium-grained quartz sandstone with hematite cement, cross and planar horizontal beds are the dominant sedimentary structures, and mudstone rip-up clasts are common (Figure 2.13; Tamulonis, 2010). The accommodation characterized by these vertical successions of lithologic changes is interpreted to define a series of base level cycles. Three distinct intervals can be recognized from facies properties in the Delaney Well, based on either specific lithofacies or sequential patterns of lithofacies: 1) a massively bedded medium-grained sandstone is located at 1646 to 1652 feet (502 to 504 meters) depth interpreted to be a paleosol; 2) a burrowed siltstone is at 1510 to 1520 feet (460 to 462 meters) depth interpreted to be flood deposits, and 3) and an interbedded

sandstone and mudstone layer is at 1580 to 1600 feet (482 to 488 meters) depth, also interpreted to be flood deposits (Tamulonis, 2010). These features are interpreted to suggest a general base level rise occurred between the deposition of the paleosol and the two overlying flood deposits. The Delaney core petrophysical zones correspond to lithologic changes representing base level cycles, and zones B, C, and D all represent a cycle of base level fall followed by base level rise. These zones and the respective base level cycles can be mapped throughout the central New York study area.

Petrophysical zones B, C, and D had similar average core plug porosity values, ranging from 9.9% to 10.7%. In the Delaney core, petrophysical zone Queenston B is composed of fine-grained sandstone with the burrowed siltstone interval at the top and the interbedded sandstone and mudstone interval at the bottom (Figure 2.13), and this zone has the lowest average core plug porosity of 9.9%. Zone C is primarily fine- to medium-grained sandstone with several interbedded clay layers throughout the zone, and the paleosol interval is located within this zone (Figure 2.13). Zone C has the highest average core plug porosity of 10.7%. Zone D is also a fine to medium grained sandstone with several interbedded mudstone layers, and has an average core plug porosity of 10.0% (Figure 2.13).

The seismic data were also compared to petrophysical zones B, C, D, and E. Channel geometries and channel fill are distinguishable locally, which extend greater than 1 mile (1.6 kilometers) laterally and hundreds of feet (tens to hundreds of meters) of thickness (Figure 2.14). There is at least one prominent surface of internal unconformity located in zone Queenston C, marked by erosional truncation of underlying units and a strong horizontal reflection above the truncation surface (Tamulonis, 2010).

Analysis

Three types of geologic models are needed for a carbon dioxide storage assessment: 1) a model of the depositional environments is valued as a framework for prediction of rock properties where there are no wells, 2) a stratigraphic model to predict the interconnectivity among reservoir units laterally from a borehole, and 3) a petrophysical model is needed to estimate expected pore volumes and permeabilities. From our data set, we are able to address all model types needed, though a significant amount of uncertainty is associated with these assessments due to the scarceness of subsurface and outcrop data.

Petrophysical, Seismic, and Core Properties

Based on the geometry of seismic reflections, sedimentary structures revealed in core, and lack of fossils, Tamulonis (2010) interpret that the Queenston Formation of central New York was deposited in a fluvial setting. The criteria for fluvial environments published by Miall (1977, 1996) and Allen (1970) allow for a more specific interpretation: the Queenston Formation in central New York is the product of steady stream flow and sheet flooding, with 20% of the beds indicating conditions of waning flow (Tamulonis and Jordan, 2010). The key factors for this classification are: fine- to medium-grained sandstone, the presence of cross beds and cross lamination, planar horizontal bedding, and rip-up clasts in core (Figure 2.13); general lack of fining-upward successions of beds in core; relatively few mudstone interbeds in core; evidence of mound-like features in seismic sections that are interpreted as longitudinal or lingoidal bars thousands of feet (hundreds to thousands of meters) long (Figure 2.14); and what appear to be sandstone sheetflood deposits in the core. Sandstone sheet deposits develop in a series of coalescing, broad, virtually unconfined channels, and there is little differentiation of channel and overbank facies flood deposits (Campbell, 1976; Miall, 1996).

The Queenston Formation of central and western New York lacks gravel-size sediment. Ettensohn (1991) interpreted that the Queenston Delta complex was fine-grained because it was eroded from a low relief highland and was recycled from a parent sedimentary rock. Also, central New York was relatively distant (~150 miles, 240 km) from the Taconic uplands (Figure 2.3) and coarser material was deposited in proximal positions (i.e., Juniata Formation) in the Appalachian basin to the south and east. The original texture of more proximal time equivalents of the Queenston Formation farther to the east in New York is not known because these sediments have been removed by erosion.

The vertical succession of lithologic patterns in the rock of the Delaney core represents small-scale changes in depositional environments, and thus subtle changes in base level (Tamulonis and Jordan, 2010). The massively bedded sandstone at 1646 to 1652 feet (504 meters) depth is interpreted to be a paleosol, and the two relatively fine-grained zones at 1510 to 1520 feet (460 to 463 meters) and 1580 to 1600 feet (482 to 488 meters) depth are interpreted to be high base level deposits topped by flooding surfaces (Tamulonis and Jordan, 2010; Figure 2.13). These base level changes represented in the Delaney core are integrated with the respective well log suite. Though this core is a relatively homogenous fine- to medium- grained sandstone, subtle variations in the clay content correspond to high gamma log values (Figure 2.13). This suggests that several base level cycles occurred between the deposition of the paleosol and the uppermost high base level deposit, which are located at the top and bottom of petrophysical zone B (Figure 2.13).

To interpret base level cycles in zones Queenston A, E, and F in the Delaney well and in the other wells without core, we use gamma logs to map subtle base level rises and falls. This method is rooted in the interpretation of depositional environment and corresponding log patterns established in the Delaney well cored interval (Figure

2.13; Tamulonis, 2010). Key information includes shale content variation, assuming increased shale content is equivalent to a muddier depositional environment, whether it be a fluvial or marine setting. Generally, the Queenston Formation pattern of gamma log variation in central New York is a decrease in gamma value with height above the base of the unit, corresponding to a general increase in sand proportion upward and a base level-fall trend. However, subtle log variations within each petrophysical zone signify that a higher frequency but lower magnitude of base level fluctuations exists within the petrophysical zones. Integrated seismic, core, and well log data for zones B, C, and D suggest that each of these zones shows a cycle of base level fall and rise from base to top. For zones B and C, internal unconformities revealed in seismic data from Tompkins and Cayuga counties represent base level fall of higher frequency cycles. Of zones without core, Queenston F from base to top shows a steady, gradual gamma ray increase upward, and Queenston E generally displays a relatively lower gradient of upward gamma ray increase compared to zone F (Figure 2.5). This implies that Queenston F represents a gradual base level rise, and zone E shows a decreased gradient of rise. Zone A displays a sudden decrease in the gamma ray signature compared to Queenston B, suggesting a sharp base level fall.

Isopach maps for each zone indicate that Queenston Formation depocenters in central New York shifted spatially with time (Figure 2.6). These spatial variations in Queenston Formation rock volume greatly impact the CO_2 sequestration potential near any specific power plant CO_2 point source. Queenston F appears to represent a base level rise, deposited only in the western study area. By proximity of the Queenston F region to the muddier facies of western New York, this base level rise is interpreted as a true transgression. The gamma signature of Queenston E also signifies increased shale content with passing time and, whereas the gradient of base level rise may have been small, the net effect was more widespread accommodation space and deposition

throughout the entire study area, leading to a depocenter in Chemung County. Three major base level cycles correspond to zone D, C, and B gamma signatures (Figure 2.5). The top of each of these zones represents the maximum base level, and within each zone, there is a gamma trough. These zones all represent a base level fall to rise cycle. Zone D depocenter is in Yates County. Zones C and B both have elongated depocenters in Seneca, Tompkins, and Cayuga Counties, which could possibly represent paleo-river channels, since these N-NW depocenters are oriented in the same direction as the Juniata paleocurrent direction (Yeakel, 1962). Queenston A marks a large magnitude base level fall, and is not present in the northern and western sectors of the study area.

The entire Queenston Formation has greatest NFSG10 (between 70 and 120 feet (20 to 40 meters) of porous sandstone) in a small area (6,000 acres, 2.5 kilometers^2) in southeastern Steuben County and southwestern Chemung County (Figure 2.8), where the Queenston Formation isopach is thickest (nearly 1,000 feet (300 meters) thick). Only two wells, however, control this NFSG10 pattern in the southern study area. The entire formation also has relatively high NFSG10 in Tompkins, Cayuga, and Seneca Counties (approximately 21,000 acres (850 kilometers^2) with greater than 50 feet (15 meters) of porous sandstone), and this area has better well control (12 wells) than the southern area with high NFSG10.

In general, the NFSG10 isopachs for each petrophysical zone correspond to areas that have the highest average porosity. Petrophysical zones B and C (Figure 2.9) have the greatest NFSG10 where the respective zone isopach maps are thickest in N-NW trending depocenters in Seneca, Tompkins and Cayuga Counties (up to 20 feet (6 meters) of porous sand thickness in zone B in Tompkins County, and up to 30 feet (9 meters) of porous sand thickness in zone C in southern Cayuga County; Figure 2.9). Zone D also has greatest net porous sand thickness in Tompkins and Cayuga Counties

(up to 20 feet (6 meters); Figure 2.9), rather than in this zone's depocenter in Yates County. Zone E has the highest NFSG10 in Schuyler and Chemung Counties (up to 30 feet (9 meters); Figure 2.9), which coincides with that zone's depocenter. NFSG10 generally increase to the south in zones A and F (which have up to 10 feet and 18 feet (3 to 5 meters), respectively; Figure 2.9).

Outcrops

The massively bedded siltstone of the Queenston Formation at the Lewiston and Lockport outcrops (Figure 2.11) indicates there was a high degree of bioturbation. The particularly thick top layer of massively bedded siltstone of the Lewiston outcrop is missing at the Lockport outcrop, suggesting this siltstone unit was eroded from the Lockport area. The location of the Golden Hills outcrop within the Queenston Formation stratigraphy is not known (Figure 2.12). Long, parallel, symmetric ripples observed only at Golden Hills Park are interpreted as wave ripples, and the occurrence of reduced zones along fractures indicates that the chemical reduction was a secondary effect from fluid flow through fractures. Some sandstone and siltstone layers are reduced also, though it is uncertain whether this is due to primary chemical variations in the depositional environment or is a secondary feature from fluid flow.

It is difficult to determine whether the massively bedded siltstone at the top of the Queenston Formation outcrops in western New York originated primarily in subaerial or marine environments, although the lack of fossils suggests it was not deposited in a subtidal environment. In contrast, Brett et al. (1996) interpret Queenston Formation subtidal marine deposits by the presence of bryozoans fossils. A high degree of siltstone bioturbation is usually indicative of marine origin and Brett et al. (1996) interprets bioturbated sandstones to be of peritdal origin. Mudcracks reported by Over (2009) suggest an alternating wet and dry environment. The discontinuous nature of the underlying sandstone beds and the presence of *Skolithos*

(Over, 2009) within the Niagara Gorge outcrop are indicative of high energy shoreface to backshore environments (Pemberton et al., 1992). We interpret the top siltstone directly underlying the Whirlpool sandstone in outcrop to have been deposited in a tidal flat environment, and the discontinuous sandstone layers with *Skolithos* were likely deposited in a shoreface environment. Base level fluctuations and periods of exposure are recorded in the outcrop facies.

Stratigraphic Models

Several interpretations of the Queenston Formation depositional system may be made based on sparse well log, core, and seismic data from central and western New York. Here, we present three alternative qualitative models for the depositional system of what is, overall, a distributary fluvial system that transitions westward to a delta. Queenston petrophysical zones V-Z from western New York were used to correlate the western New York and Ontario, Canada data to central New York subsurface data.

Parameters necessary for a static CO_2 storage calculation such as porosity, reservoir thickness, and reservoir area can be estimated from a stratigraphic model. Specifically, by understanding the Queenston Formation depositional system, predictions can be made of locations with relatively coarser-grained Queenston Formation facies even for regions with sparse data. Stratigraphic models consequently aid in assessing regional CO_2 storage potential for the Queenston Formation. Though a single model may not be definitively determined to be the 'correct' model, a range of models demonstrates the uncertainty of CO_2 storage potential still associated with Queenston Formation variability.

It is believed the Queenston Formation was deposited in a foreland basin during a relatively quiescent period prior to the final compressional stage of the Taconic Orogeny (Fisher, 2006; Ettensohn, 1991), during which mountains continued

to erode and isostatically adjust (Figure 2.3). In active foreland basins, a large amount of accommodation space is available on the proximal side of the basin due to lithospheric flexure from crustal thickening. During times of tectonic quiescence, sedimentation becomes more widespread throughout the basin (Flemings and Jordan, 1990). Distal to the mountain belt margin of a foreland basin, marine processes may play a dominant role in sedimentation. Large-scale relative sea level changes result from a combination of sediment supply, subsidence, and global sea level variation (Jordan and Flemings, 1991). Jordan and Flemings (1991) modeled the impact of foreland basin geometry and sediment source on stratigraphy during a period of quiescence and determined that genetically related strata can be defined by marine-flooding surfaces, which undergo minor erosion during transgression and pass into condensed sections in deep water. Flemings and Jordan (1990) numerically modeled foreland basins during episodic thrusting. During a period of quiescence in their model, the simulation revealed that a foreland basin will widen and the forebulge will migrate away from the thrust load, whereas at the onset of thrusting, the generally prograding facies will be punctuated by retrogradations toward the thrust. In a similar manner, the interaction between uplift, basin evolution, sea level change, and sediment supply caused variations in Queenston Formation sediment distribution in central and western New York.

In general, a distinct lithologic change from sand-dominated strata in the east to silt- and clay-dominated strata in the west is recorded by the gamma log signature of the Queenston Formation in central New York. This change occurs west of the north-trending pink dashed line in Figure 2.4. We interpret the change in gamma log signatures to indicate a major change in lithology and depositional environment (Figure 2.15). The pattern of vertical trends in gamma log values has been synthesized in the mapped petrophysical zones, and the characteristics of these zones

Figure 2.15. Queenston Formation depositional system and stratigraphic Model 1. The Queenston Formation grades from high velocity, sandstone and conglomerate braided fluvial deposits in central Pennsylvania, to lower velocity braided fluvial sandstone deposits in central New York, to coastal plain deposits in western New York beach, to beach and shallow marine deposits in Canada. The thickness of the strata equivalent to the Queenston Formation in Pennsylvania, the Juniata Formation, was obtained from Brett et al. (1996).

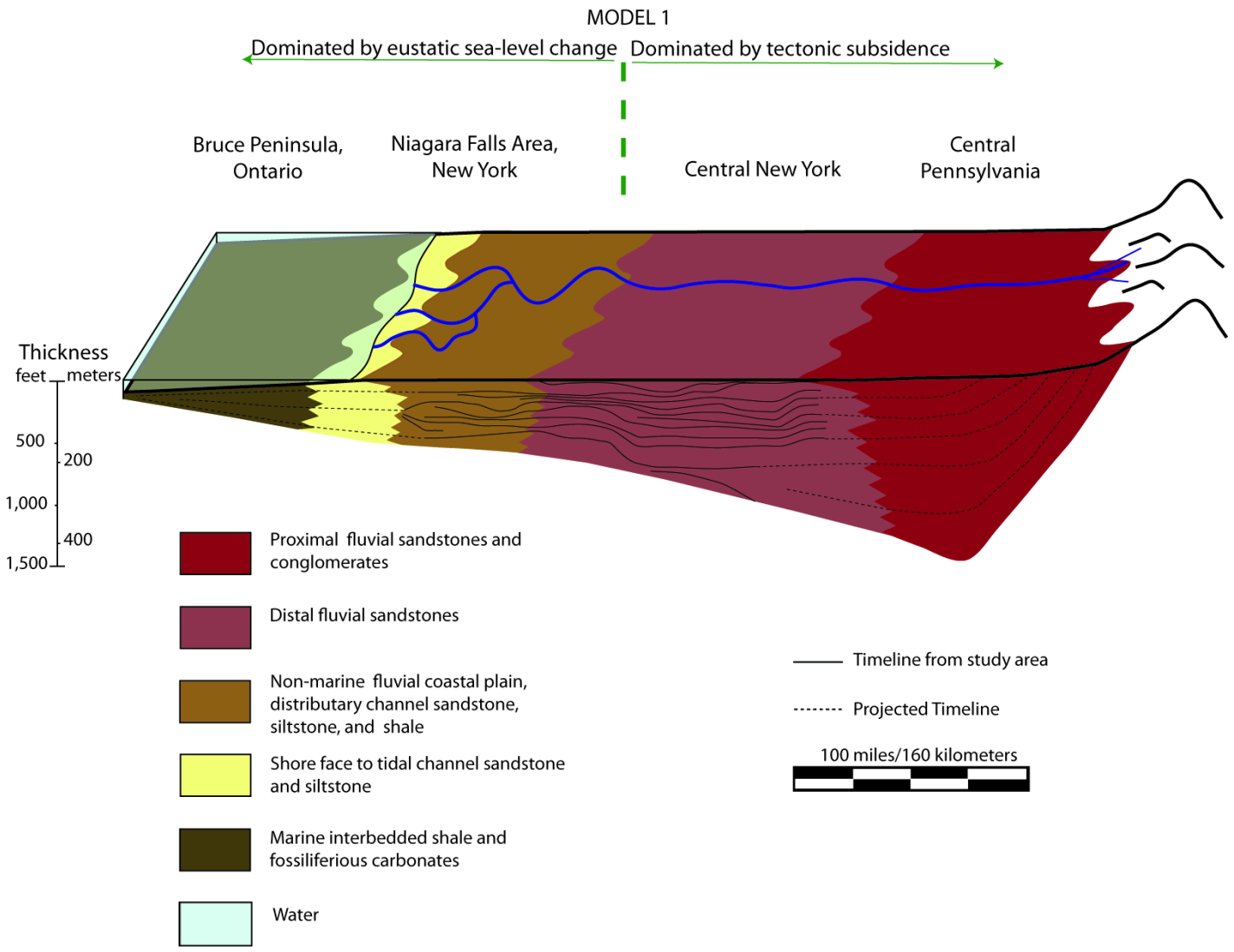
MODEL 1
Dominated by eustatic sea-level change
Dominated by tectonic subsidence
Bruce Peninsula, Ontario
Niagara Falls Area, New York
Central New York
Central Pennsylvania
Thickness
feet
meters
500
200
1,000
400
1,500
Proximal fluvial sandstones and conglomerates
Distal fluvial sandstones
Non-marine fluvial coastal plain, distributary channel sandstone, siltstone, and shale
Shore face to tidal channel sandstone and siltstone
Marine interbedded shale and fossiliferious carbonates
Water
Timeline from study area
Projected Timeline
100 miles/160 kilometers

change from western to central New York. We interpret these petrophysical zones to reveal base level trends (based on variations of core lithology), whose characteristics change west of Livingston County. This change in base level trends suggests spatially varying mechanisms were affecting sediment deposition during Queenston time.

In central New York, Tamulonis (2010) interpret that the Queenston Formation formed in a distributary fluvial system with mobile channels and no stable, long-lived floodplains, and there is little lithologic differentiation between channel sandstone and sheetflood sandstone. A westward increase in the formation shale content implies a progressive distal trend toward more floodplain deposits. As summarized earlier, it has been controversial whether the western New York Queenston Formation shale and siltstone were deposited in a fluvial coastal plain environment or a shallow marine environment. Based on well log, core, cutting, seismic, and outcrop data, as well as previous work completed in western New York and Canada, we interpret that the Queenston fluvial sandstone in central New York grades westward into coastal plain, tidal flat, and shoreface deposits in western New York and then marine deposits in Ontario, Canada (Brett et al., 1996; Brogly et al., 1998; Figure 2.15, Model 1).

Based on this environmental model, a series of base level variations can be traced from central New York to western New York. The correlations across the east to west facies gradient is built on the hypothesis that a base level rise is recorded by muddier distributary channel, coastal plain, and tidal channel deposits (increased gamma values), and base level fall is recorded by better-sorted, more homogenous fluvial sandstone deposits represented by decreased gamma values. Ambrose et al. (2009) interpreted fluvial deposits in east Texas in a similar manner. The central New York fluvial sandstone is dominated by base level fall (regressive) trends and the western New York coastal plain deposits are dominated by base level rise (transgressive) trends (Figure 2.16), with numerous high-frequency and low

Figure 2.16. Correlation of gamma logs (GR) and cores and cuttings data from central New York (highlighted yellow), to those of western New York (between vertical black and blue dashed lines) and Ontario, Canada, with base level trends noted. Endpoints (B-B') are marked on Figure 2.1. Petrophysical zones in the east (QA-QF) and west (QV-QZ) are labeled just below the top of the zone (Queenston A extending from the top of the Queenston Fromation to Queenston B, QB; Queenston V extending from top of Queenston to top of Queenston W, QW). The Milton core was described by Brogly et al. (1998); cuttings from the Schaffer, Fee, and Hooker wells were described by Hughes (1976); and the Delaney well was described by Lugert et al. (2006) and Tamulonis (2010). Well numbers assigned in Figure 2.1 are above the well name.

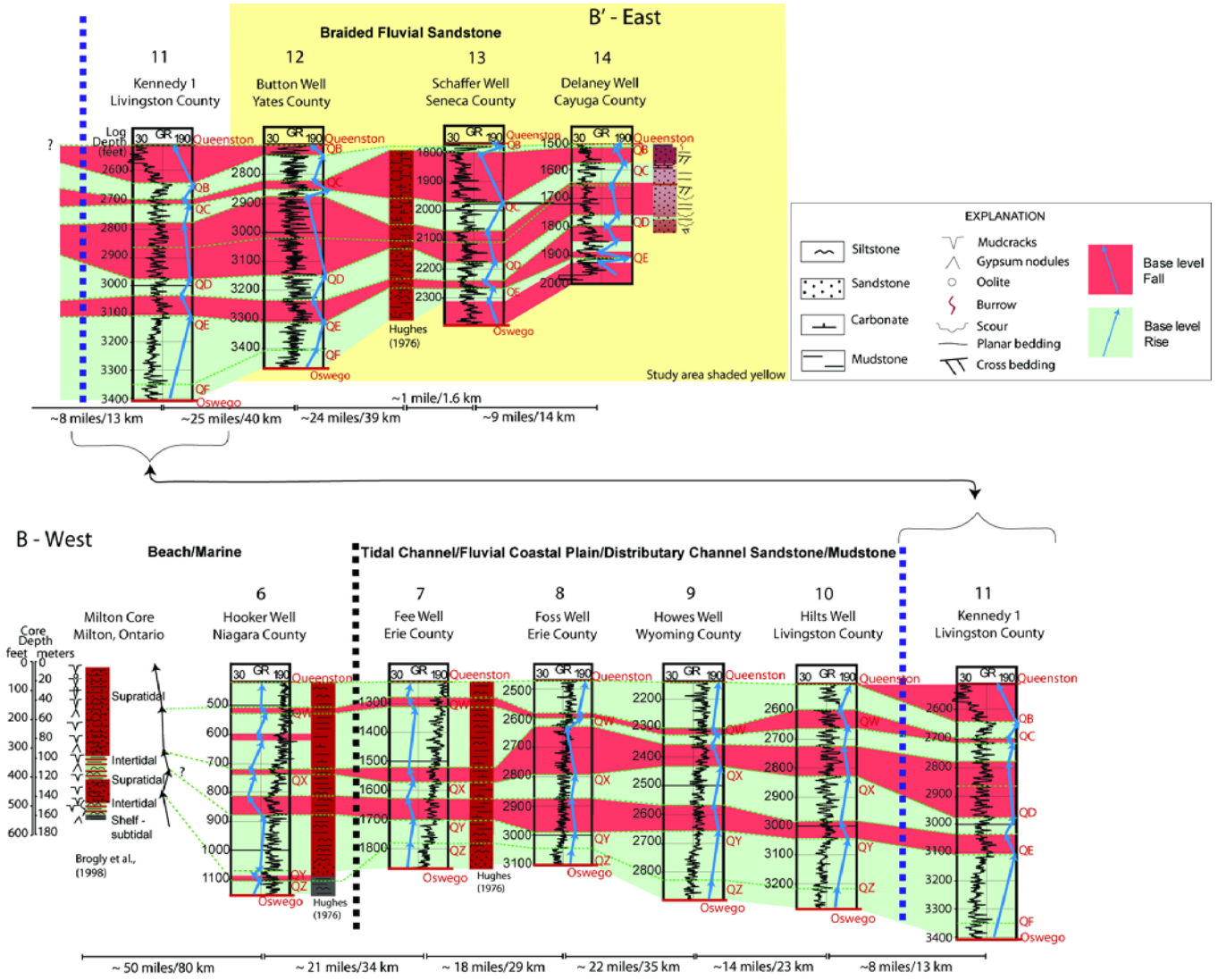
B′ - East
Braided Fluvial Sandstone
11
Kennedy 1
Livingston County
12
Button Well
Yates County
13
Schaffer Well
Seneca County
14
Delaney Well
Cayuga County
Log Depth (feet)
Queenston
QB
QC
QD
QE
QF
Oswego
Hughes (1976)
Study area shaded yellow
~8 miles/13 km
~25 miles/40 km
~24 miles/39 km
~1 mile/1.6 km
~9 miles/14 km
EXPLANATION
Siltstone
Sandstone
Carbonate
Mudstone
Mudcracks
Gypsum nodules
Oolite
Burrow
Scour
Planar bedding
Cross bedding
Base level Fall
Base level Rise
B - West
Beach/Marine
Tidal Channel/Fluvial Coastal Plain/Distributary Channel Sandstone/Mudstone
6
Hooker Well
Niagara County
7
Fee Well
Erie County
8
Foss Well
Erie County
9
Howes Well
Wyoming County
10
Hilts Well
Livingston County
11
Kennedy 1
Livingston County
Milton Core
Milton, Ontario
Core Depth
feet meters
Supratidal
Intertidal
Supratidal
Intertidal
Shelf - subtidal
Brogly et al., (1998)
QW
QX
QY
QZ
~ 50 miles/80 km
~ 21 miles/34 km
~ 18 miles/29 km
~ 22 miles/35 km
~14 miles/23 km
~8 miles/13 km

magnitude base level cycles embedded within the Queenston Formation. These cycles support previous studies suggesting that the importance of sea level changes diminish with increasing distance from shoreline, and that tectonic subsidence plays a more significant role in areas closer to the sediment source (Ethridge et al., 1998; Jordan and Flemings 1991; Posamentier and James, 1993; Posamentier and Vail, 1988;). Base level trends are less ambiguous where there is a wide range of grain sizes in western New York and are more ambiguous where grain size is more homogenous in the central New York focus area.

The contrast in long-term base level trends between the eastern area and western area reveals that somewhat different factors control accommodation space in the east compared to the west. The regional thickness and isopach pattern (Figure 2.4) show greater accommodation to the southeast, which we interpret to reflect enhanced tectonic subsidence in the southeast, close to the Taconic Mountains. Local depocenters within the basin varied spatially with time (Figure 2.6), which may reflect tectonic subsidence. The trend in the west of rising base level during Queenston time, however, contradicts Dennison's (1976) interpretation that the formation was deposited during a time of glacio-eustatic sea level fall. A final regressive trend in western New York may have been lost to the overlying Cherokee Unconformity.

One alternative Queenston Formation depositional system and stratigraphic model is only moderately different (Figure 2.17, Model 2) and interprets that the braided fluvial sandstone deposits of central New York grade into shallow marine facies in western New York (Hughes, 1976; Saroff, 1987), as opposed to muddier tidal flats and distributary channels as in Model 1. Hughes (1976) interpreted the Queenston Formation of western New York to be marine deposits. The same series of base level fluctuations interpreted in Figure 2.16 could be drawn on Model 2, with the assumption that transgression is recorded by muddier shallow marine deposits and

Figure 2.17. Queenston Formation depositional system and stratigraphic Model 2. The Queenston Formation grades from proximal sandstone and conglomerate deposits of braided fluvial origin in central Pennsylvania, to distal braided fluvial sandstone deposits in central New York, to marine deposits in western New York and Canada (modified from Saroff (1987) and Lugert et al. (2006)).

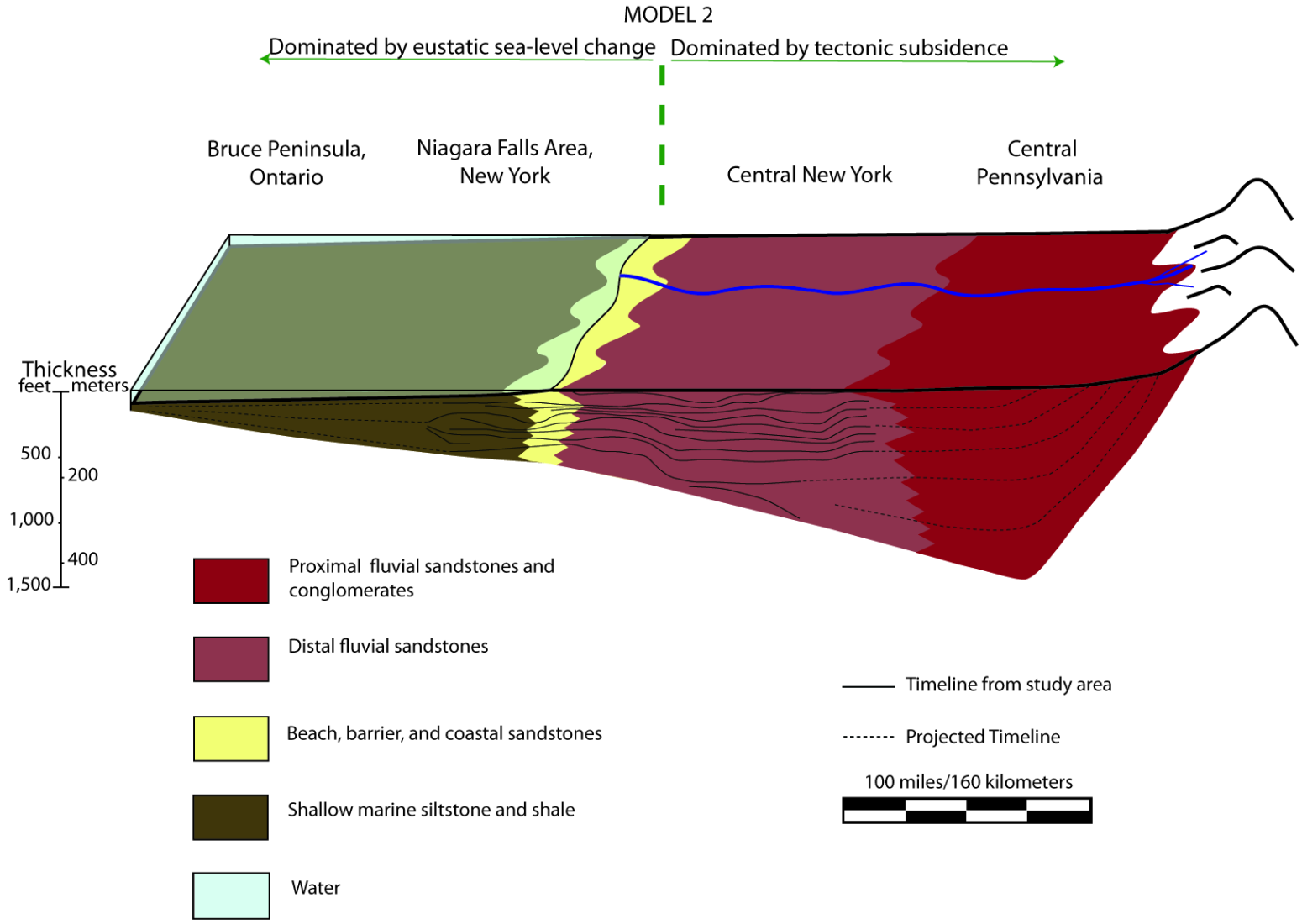
MODEL 2
Dominated by eustatic sea-level change
Dominated by tectonic subsidence
Bruce Peninsula, Ontario
Niagara Falls Area, New York
Central New York
Central Pennsylvania
Thickness
feet
meters
500
200
1,000
400
1,500
Proximal fluvial sandstones and conglomerates
Distal fluvial sandstones
Beach, barrier, and coastal sandstones
Shallow marine siltstone and shale
Water
Timeline from study area
Projected Timeline
100 miles/160 kilometers

regressions are recorded by better sorted fluvial sandstone deposits. Problems with this model are the lack of nearshore and beach environment evidence in the area between central and western New York.

Models 1 and 2 share a major stratigraphic characteristic. The correlation of Figure 2.16 suggests that, during any given region-wide short-term base level cycle, the more proximal part of the basin (central New York) accumulated the most volume of sediment during the base level fall time intervals, consequently starving the sediment supply to western New York. In turn, during the short-term intervals of base level rise, there was little sediment trapping in the more proximal area of central New York and sediment bypassing to western New York, where it could be accommodated by the base level rise. While this stratigraphic scenario makes sense in western New York, we do not recognize a cause for preferential accumulation in central New York during times of falling base level in the high frequency base level cycles.

A third Queenston Formation stratigraphic model (Figure 2.18, Model 3) displays a greater difference from Model 1 because it interprets the western New York/Ontario Queenston Formation to be diachronous to much of the central New York Queenston Formation. This diachroneity occurs across an unconformity that separates central New York sandstones from the western New York mudstones. If so, the sandstones and mudstones are not time equivalent, and an alternative regional well log correlation is needed (Figure 2.19). Changes in base level trends from east to west and variations of the color boundary separating the Queenston and Oswego Formation (Hughes, 1976) suggest that a diachroneity may exist, though additional subsurface and outcrop evidence does not exist to suggest there is an unconformity. Due to the sparse nature of subsurface and outcrop data, Model 3 must be recognized as a possibility. In Figure 2.18, the unconformity is depicted to dip northwest, although theoretically the unconformity could dip in any direction. If there is such an

Figure 2.18. Queenston Formation stratigraphic Model 3. The Queenston Formation grades from proximal sandstone and conglomerate braided fluvial deposits in central Pennsylvania to distal braided fluvial sandstone deposits in central New York. An unconformity separates the Queenston Formation in western New York from the central New York Queenston Formation.

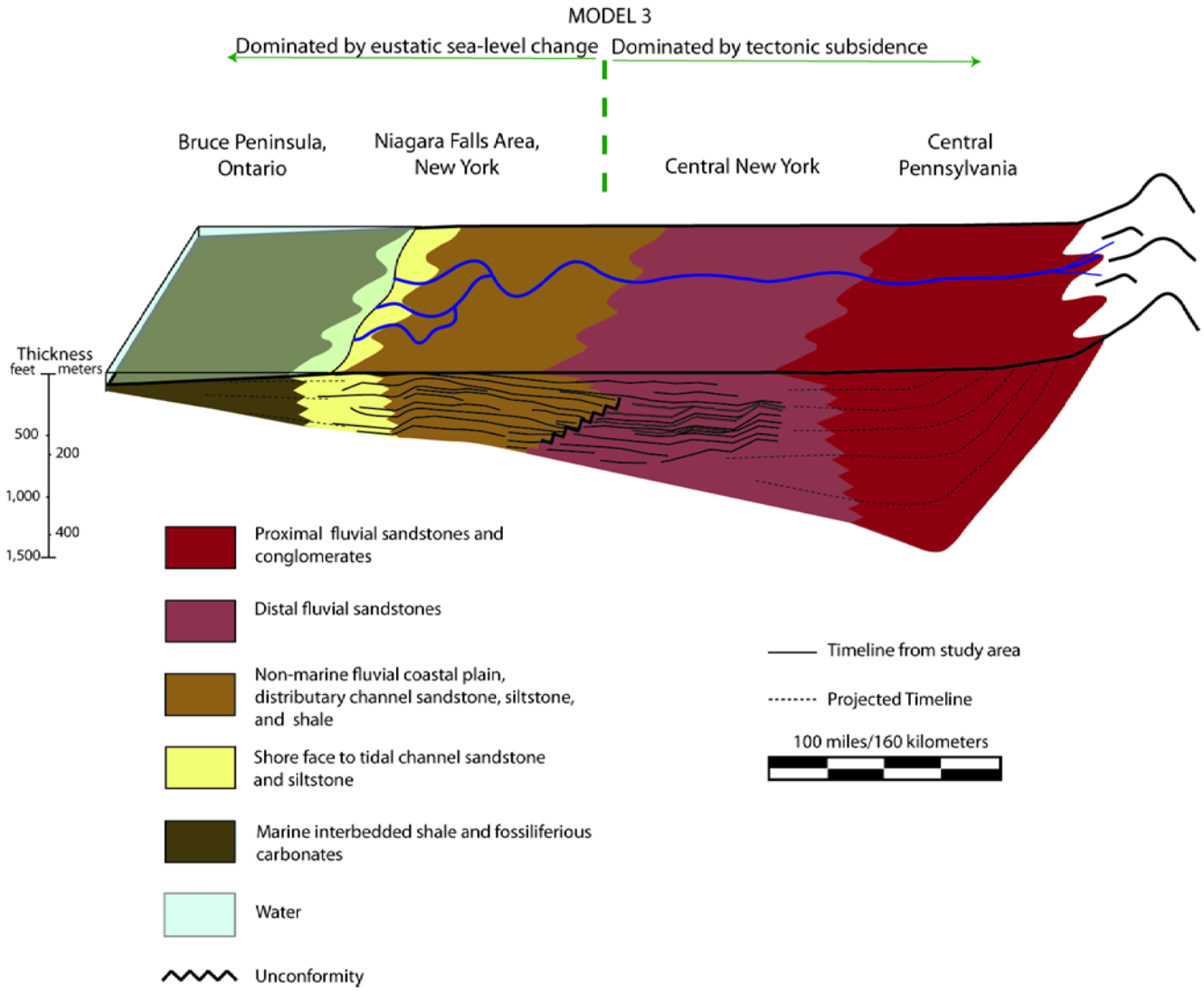
MODEL 3
Dominated by eustatic sea-level change
Dominated by tectonic subsidence
Bruce Peninsula, Ontario
Niagara Falls Area, New York
Central New York
Central Pennsylvania
Thickness
feet
meters
500
200
1,000
400
1,500
Proximal fluvial sandstones and conglomerates
Distal fluvial sandstones
Non-marine fluvial coastal plain, distributary channel sandstone, siltstone, and shale
Shore face to tidal channel sandstone and siltstone
Marine interbedded shale and fossiliferious carbonates
Water
Unconformity
Timeline from study area
Projected Timeline
100 miles/160 kilometers

Figure 2.19. Alternative regional correlation with gamma logs and data from cores and cuttings from central New York (right of vertical blue line), western New York (between black and blue dashed lines) and Ontario, Canada, with base level trends noted. In this model, an unconformity separates two regions in which base level trends can be mapped separately, but whose local trends could not be joined to establish a high resolution regional correlation. Petrophysical zones in the east (QA-QF) and west (QV-QZ) are labeled just below the top of the zone (Queenston A extending from the top of the Queenston Formation to Queenston B, QB; Queenston V extending from the top of the Queenston Formation to the top of Queenston W, QW).

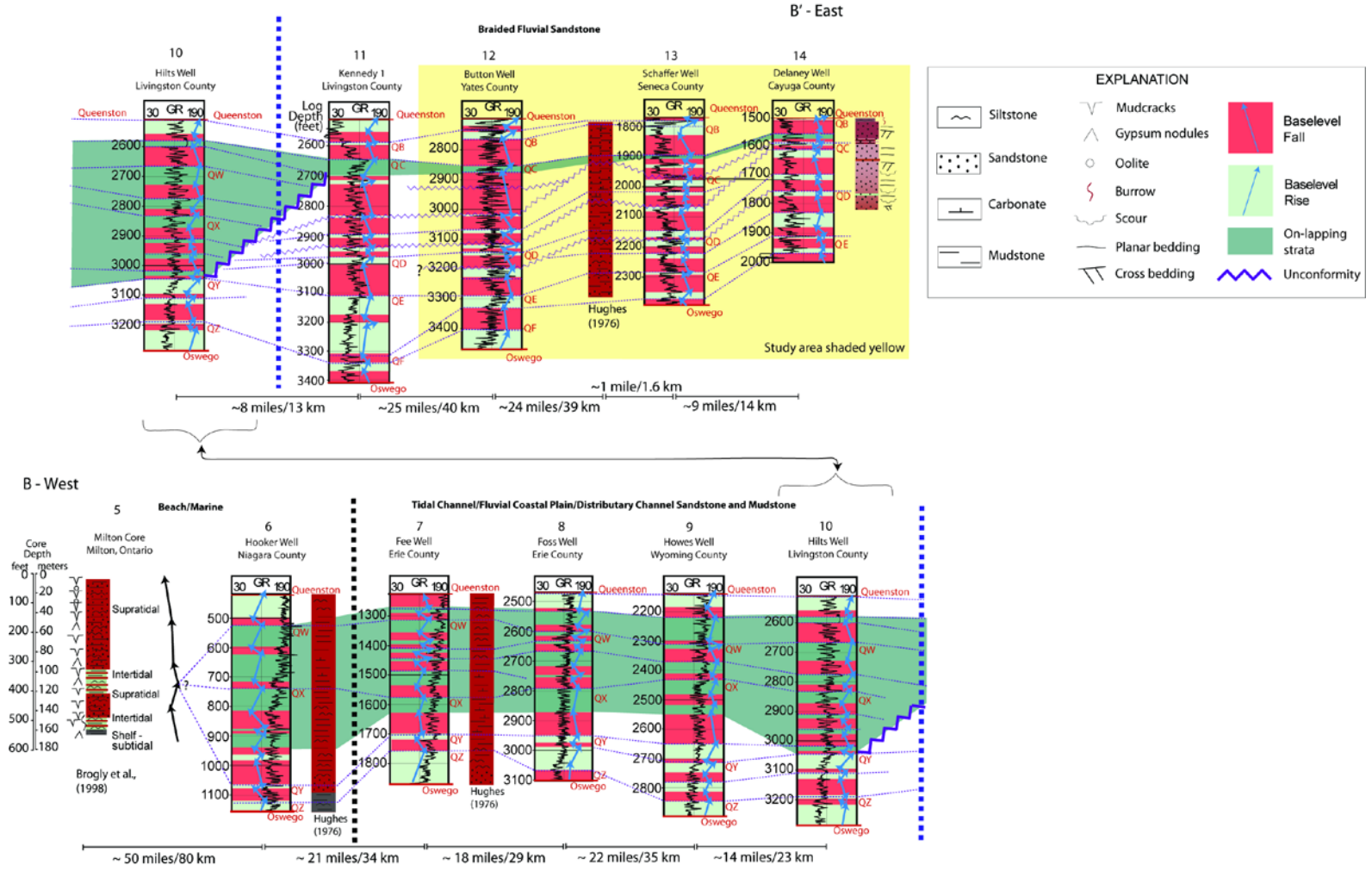
B′ - East
Braided Fluvial Sandstone
10
Hilts Well
Livingston County
11
Kennedy 1
Livingston County
12
Button Well
Yates County
13
Schaffer Well
Seneca County
14
Delaney Well
Cayuga County
Log Depth (feet)
Queenston
Oswego
QW
QX
QY
QZ
QB
QC
QD
QE
QF
Hughes (1976)
Study area shaded yellow
~8 miles/13 km
~25 miles/40 km
~24 miles/39 km
~1 mile/1.6 km
~9 miles/14 km
EXPLANATION
Siltstone
Sandstone
Carbonate
Mudstone
Mudcracks
Gypsum nodules
Oolite
Burrow
Scour
Planar bedding
Cross bedding
Baselevel Fall
Baselevel Rise
On-lapping strata
Unconformity
B - West
5
Beach/Marine
Milton Core
Milton, Ontario
Core Depth
feet meters
Supratidal
Intertidal
Supratidal
Intertidal
Shelf - subtidal
Brogly et al., (1998)
6
Hooker Well
Niagara County
Tidal Channel/Fluvial Coastal Plain/Distributary Channel Sandstone and Mudstone
7
Fee Well
Erie County
8
Foss Well
Erie County
9
Howes Well
Wyoming County
10
Hilts Well
Livingston County
~ 50 miles/80 km
~ 21 miles/34 km
~ 18 miles/29 km
~ 22 miles/35 km
~14 miles/23 km

unconformity, the base level trends of opposing characteristics for the central New York sandstone and the western New York mudstone are not correlative. However, the lowest 100 to 300 feet (30 to 90 meters) of the Queenston Formation may be correlative from central New York to Ontario. This may also be true for the top of the Queenston Formation.

If stratigraphic Model 3 is correct, one possibility for the change of Queenston Formation base level trends from east to west may be related to the interaction of the Queenston Formation sediment supply with faults in western New York that were active in the Ordovician. The Leroy, Retsof, and Hemlock faults bracket the transition from the western region with predominant base level rise trends and the eastern region with predominant base level fall trends. The Clarendon-Linden fault system is located west of the transition zone (Jacobi, 2002; Jacobi and Fountain, 2002; Figure 2.20). The Leroy fault was noted in well logs by Rickard (1973), who interpreted the existence of an Ordovician growth-fault with down-on-the-east offset, and this offset corresponds to lineaments mapped by Jacobi (2002). The gravity gradient surrounding the Leroy fault suggests that the fault affects the Precambrian basement, as does the Clarendon-Linden fault system (Jacobi, 2002). The Retsof and Hemlock faults were mapped by Jacobi (2002) based on outcrop, gravity gradients, lineaments, stratigraphic, well, and proprietary seismic data, and are related to basement trends. The Retsof fault is north-striking and has an exposed west-dipping thrust ramp (Jacobi, 2002). The Hemlock fault is a NNW striking fault and relatively little is known about this particular fault, though other NNW striking faults in western New York are thought to be anchored in the Precambrian basement (Jacobi, 2002).

The seismically active Clarendon-Linden fault system has been well documented by Jacobi and Fountain (2002), using a relatively abundant data set surrounding the system. It has as many as ten parallel, segmented faults across the

Figure 2.20. Map of western and central New York with Clarendon-Linden, Leroy, Retsof, and Hemlock faults mapped (Jacobi (2002); Jacobi and Fountain (2002)). The transition between well logs with base level rise trends and base level fall trends occurs between well numbers 10 and 11 (well names in Figure 2.1 caption).

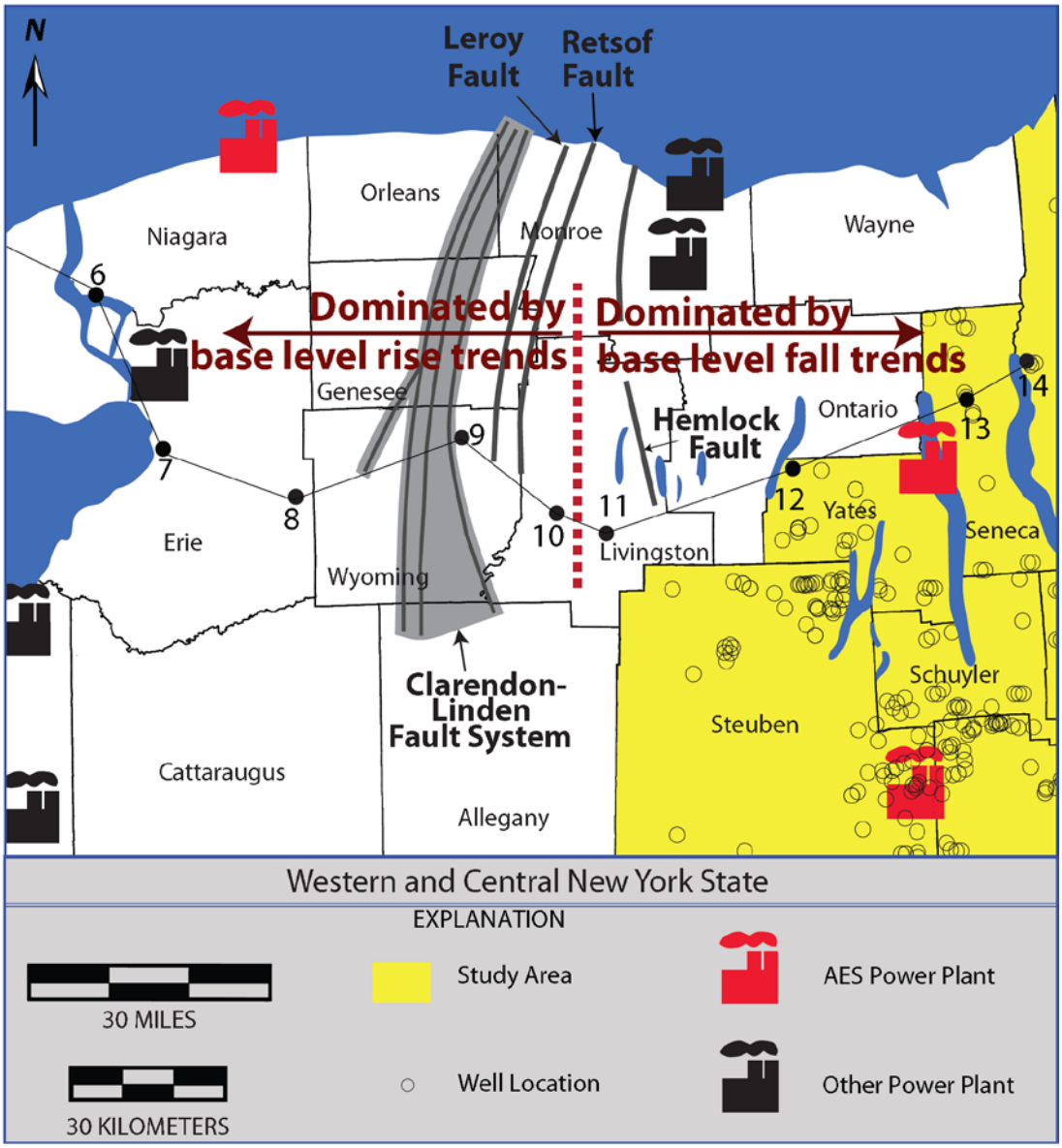
N
Leroy Fault
Retsof Fault
Orleans
Niagara
Monroe
Wayne
6
Dominated by base level rise trends
Dominated by base level fall trends
Genesee
Hemlock Fault
Ontario
14
13
9
7
8
12
11
10
Yates
Seneca
Erie
Wyoming
Livingston
Schuyler
Clarendon-Linden Fault System
Steuben
Cattaraugus
Allegany
Western and Central New York State
EXPLANATION
30 MILES
Study Area
AES Power Plant
30 KILOMETERS
Well Location
Other Power Plant

system, which form fault blocks with semi-independent fault histories and as much as 550 feet (170 meters) of throw on an individual fault. These deep Precambrian faults were reactivated as the Appalachian Basin developed during Taconic and Acadian times, and the type of faulting along the Clarendon-Linden fault system changed along strike and with time. East dipping reflectors in the Precambrian basement are indicative of thrusts of the Grenvillian Elzevir-Frontenac Boundary Zone, which were reactivated as normal growth faults (down on the east) during Black River to Trenton time as a result of basin loading and subsidence. Thrusting on the same east-dipping reflectors occurred during later Taconic time (post-Trenton).

If this fault system, along with the Leroy, Retsof, and Hemlock Faults, were indeed active in Queenston time, offsets at the set of faults (or any one fault) may have interacted with the paleo-drainage network associated with Queenston Formation deposition (Figure 2.21) as follows. I hypothesize that initially, sediment supply was continuous from (south)east to (north)west (time: Queenston E). During time Queenston D, reactivated faults disrupted the sediment supply. Tectonic subsidence in the east led to fluvial aggradation. Meanwhile, to the west of the faults, sediment was supplied either from along-strike transport by streams or by streams that breached the low relief fault block. Sedimentation west of the fault was primarily controlled by sea level fluctuations and accumulated mostly during times of rising base level during times Queenston D and C. As time progressed (time: end of Queenston C), sea level rise allowed sufficient aggradation west of the fault block *or* sediment supply overfilled the sub-basin east of the fault block, resulting in the burial of the fault block. This allowed the Queenston Formation sediment to overcome fault offset. Once sediment overcame fault offset, sediment supply and depositional environment were continuous from east to west during the final regression during Queenston Formation time (time: Queenston B and A).

Figure 2.21. Conceptual model of western New York fault systems (Figure 2.20) and sediment supply interaction during Queenston Formation deposition. Time Queenston E: Drainage from (south)east to (north)west is continuous. Time Queenston D: basement faults are reactivated and sediment supply is interrupted; tectonic activity controls base level fluctuations to the east and sea level controls base level fluctuations to the west. Time end of Queenston C: sediment deposition and base level rise overcome fault offset and Queenston Formation deposition is continuous. Time Queenston B: sediment supply is continuous during regression.

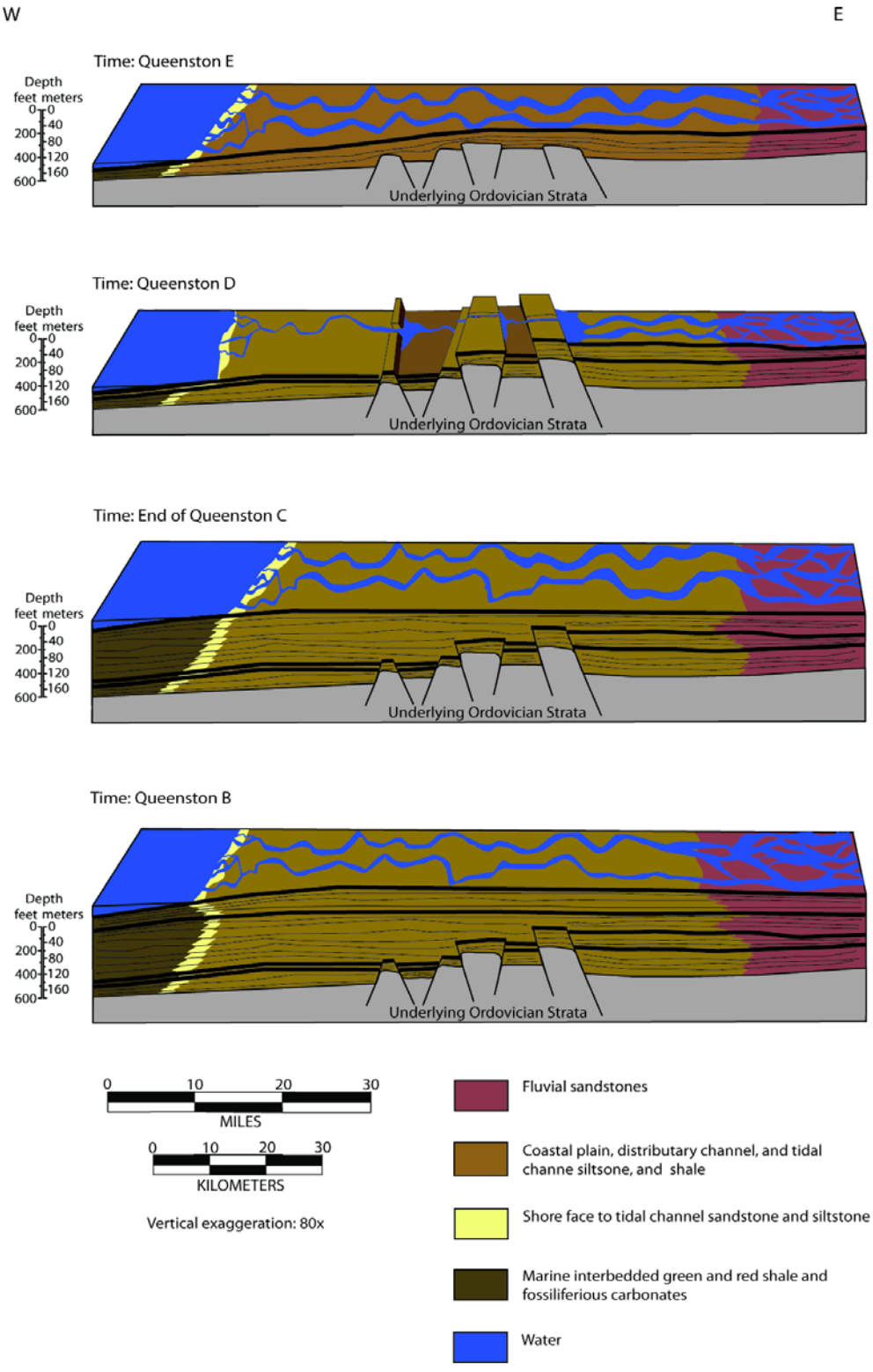
W
E
Time: Queenston E
Depth
feet meters
0 0
200 40
400 80
600 120
160
Underlying Ordovician Strata
Time: Queenston D
Depth
feet meters
0 0
200 40
400 80
600 120
160
Underlying Ordovician Strata
Time: End of Queenston C
Depth
feet meters
0 0
200 40
400 80
600 120
160
Underlying Ordovician Strata
Time: Queenston B
Depth
feet meters
0 0
200 40
400 80
600 120
160
Underlying Ordovician Strata
0 10 20 30
MILES
0 10 20 30
KILOMETERS
Vertical exaggeration: 80x
Fluvial sandstones
Coastal plain, distributary channel, and tidal channe siltsone, and shale
Shore face to tidal channel sandstone and siltstone
Marine interbedded green and red shale and fossiliferious carbonates
Water

Uncertainty

Paucity of subsurface data, particularly seismic and core data, for the Queenston Formation in central New York is the major contributor to geologic uncertainty. Because the well log data set was collected over a 60 year period, lack of consistency in data collection is likely a source of error because the techniques and tools used changed over time, and there is no known record of how to inter-calibrate among multiple generations of unspecified logging tools. Most of the data set for this study is geophysical measurements of the Queenston Formation in the subsurface, and the lack of actual intact rock samples severely affects the accuracy of both the paleoenvironmental and the petrophysical interpretations. Our tactic to overcome this obstacle has been to relate the Delaney core to its respective well log suite (Tamulonis and Jordan, 2010), and then relate the Delaney well logs to well logs within the seismic grid. Additional core data would increase our confidence in the integration of these data sets.

The seismic grid provided by Anschutz Exploration Corporation provides much insight into the vertical and lateral variability of the Queenston Formation in southern Cayuga County and northern Tompkins County. The lack of similar seismic data elsewhere severely limits the quality and resolution of the depositional system and stratigraphic models. For example, relatively small scale lateral variability was noted in the Anschutz seismic data (on the scale of hundreds of feet (meters) to miles (kilometers), as opposed to tens of miles (kilometers) from the well log data) and that observed variability is at a scale too small to be recognized in the well log correlations. Yet the vertical scale of the seismically resolved channels is sufficient to remove over half of a single petrophysical zone, which would impact correct correlations.

Interpolation between data points is the method used for contouring isopachs and porosity maps, and this technique has limitations. Often times the contouring method used generates a smooth interpolation between data points, which does not capture local variations, and confidence is highest only where the spacing of boreholes with data is dense.

Geological uncertainty associated with the stratigraphic model can cause inaccurate CO_2 storage estimation and potentially lead to an unsuccessful storage project. The geologic models aid in defining reservoir thickness, porosity, and lateral variability, as well as predicting rock properties where there are no wells, the interconnectivity within and among reservoir units, and the petrophysical properties of the rock. In the static CO_2 storage calculation (below), reservoir thickness, area, and porosity are several of the factors needed to calculate the amount of supercritical CO_2 that can be stored in a given reservoir area, and these factors can be estimated from the geologic models. Methodologies for quantifying geologic uncertainty and risk have been developed, but this data set is so sparse that additional data are needed to further refine the geologic model before uncertainty can be accurately calculated. Based on equation 2.1 (below), errors associated with the rock properties of a defined reservoir (thickness and porosity) affect the calculated storage mass, though uncertainties associated with CO_2 density (as predicted by geothermal and pressure gradients) and the reservoir efficiency factor (a function of reservoir area, porosity, and permeability) appear to have the greatest influence in the calculation.

Carbon Storage Calculation

CO_2 storage capacity for the net thickness of sandstone whose porosity exceeds 10% (NFSG10) was calculated for the entire Queenston Formation and for each petrophysical zone within the eleven county study area using Equation 2.1.

Equation 2.1. Equation for calculating CO_2 storage mass (Jarell et al., 2002; DOE, 2008).

$$CO_2 \text{ Sequestration Mass} = \frac{CO_2 \text{ Density} \times \text{Reservoir Thickness} \times \text{Reservoir Area} \times \text{porosity} \times (\text{Reservoir Storage Efficiency Factor})}{2200}$$

2200: Conversion factor (1 metric ton = 2200 lbs)

Based on any of the stratigraphic and depositional models, the Queenston Formation located in the CO_2 storage calculation area (Figures 2.8 and 2.9) was interpreted to be relatively proximal fluvial sandstones facies. As the central New York Queenston Formation grades into muddier facies west of Steuben County (whether interpreted to be fluvial coastal plain, tidal channel, or marine), the necessary pore volume for storage of a significant mass of CO_2 is not available in western New York.

Queenston Formation pore volume was calculated with NFSG10 isopachs and the respective porosity values with Petra software (Table 2.1) and pore volume variance (standard deviation^2) based on bulk Queenston Formation bulk neutron porosity variance (13.5%) reported in Figure 2.10. This pore volume was only calculated for areas where the top of the formation or zone is at least at 3,000 feet (900 meters) below the surface. An average supercritical CO_2 density of 46 lbs/ft^3 was used, which is supercritical CO_2 density at 3,000 feet (900 meters; Jarrell, 2002), with a range of 42 to 50 lbs/ft^3(Table 2.1). From our Queenston Formation data and previously published reports, average reservoir efficiency is assigned to be 0.12, with a range of 0.10 - 0.14 (Burruss et al., 2009; Zhou et al., 2007; DOE, 2008; Medina and Rupp, 2009; Tables 2.1 and 2.2). This reservoir storage efficiency factor is greater

Table 2.1. Potential CO_2 mass storage for the Queenston Formation and Queenston petrophysical zones A-F with uncertainities.

Interval	CO_2 Density		Pore Volume (acre-feet)		E		CO_2 Stored metric tons		
	Average	Variance	Average	Variance	Average	Variance	Average	Variance	Standard deviation
Queenston Formation	46	16	4.E+07	3.E+15	0.12	0.02	5.E+09	4.E+17	6.E+08
Queenston A	46	16	1.E+06	1.E+13	0.12	0.02	1.E+08	3.E+14	2.E+07
Queenston B	46	16	9.E+06	8.E+13	0.12	0.02	1.E+09	2.E+16	1.E+08
Queenston C	46	16	1.E+07	1.E+13	0.12	0.02	1.E+09	3.E+16	2.E+08
Queenston D	46	16	1.E+07	1.E+13	0.12	0.02	1.E+09	2.E+16	2.E+08
Queenston E	46	16	1.E+07	9.E+13	0.12	0.02	1.E+09	2.E+16	1.E+08
Queenston F	46	16	1.E+06	1.E+13	0.12	0.02	2.E+08	4.E+14	2.E+07

Table 2.2. Reservoir storage efficiency parameter description with averages and ranges.

Terms	Average	Range	Description
Terms used to define the entire basin or region pore volume			
Net to total area	0.7	0.2-0.8	Fraction of total basin or region that has a suitable formation present. From facies map (Chapter 2, Figure 2.4).
Net to gross thickness	0.9	0.25-0.9	Fraction of total geologic unit that meets minimum porosity and permeability requirements for injection. Fraction of formation with NFSG10.
Effective to total porosity ratio	0.9	0.6-0.9	Fraction of total porosity that is effective, i.e., interconnected. From percentage of Delaney well with >10% porosity.
Terms used to define the pore volume immediately surrounding a single well CO_2 injector			
Areal displacement efficiency	0.8	0.5-0.8	Fraction of immediate area surrounding an injection well that can be contacted by CO_2; most likely influenced by areal geologic heterogeneity such as faults or permeability anisotropy. Estimated to be 0.8 due to formation's areal homogeneity in the study area.
Vertical displacement efficiency	0.6	0.6-0.9	Fraction of vertical cross section (thickness), with the volume defined by the area (A) that can be contacted by the CO_2 plume from a single well; most likely influenced by variations in porosity and permeability between sublayers in the same geologic unit. If one zone has higher permeability than others, the CO_2 will fill this zone quickly and leave the other zones with less CO_2 or no CO_2 in them. From Delaney well with >10% porosity.
Gravity	0.9	0.2-0.9	Fraction of net thickness that is contacted by CO_2 as a consequence of the density difference between CO_2 and in-situ water. In other words, 1-Eg is that portion of the net thickness not contacted by CO_2 because the CO_2 rises within the geologic unit. Assuming CO_2 is injected into bottom of the Queenston Formation
Microscopic displacement efficiency	0.5	0.5-0.8	Portion of the CO_2-contacted, water-filled pore volume that can be replaced by CO_2. E_d is directly related to irreducible water saturation in the presence of CO_2. From water saturation reported by Lugert et al. (2006)for Queenston Auburn gas field.
	0.12 Average	0.01-0.3 Range	

than that reported by Tamulonis (2010) because only the porous sandstone intervals are taken into account with the NFSG10 maps. Based on the above average density and reservoir efficiency values and reported pore volumes, the portion of Queenston Formation with >10% porosity can sequester approximately **5×10^9 metric tons of CO_2**, with a standard deviation of 6×10^8 metric tons. Zones B, C, D, and E have the greatest potential for CO_2 storage where there is >10% porosity (Table 2.1).

Variance for the variables in Equation 2.1, as well as the storage capacity variance, is calculated with Equation 2.2.

Equation 2.2. Equation for propagating variance.

$$\frac{\sigma_x^2}{x^2} = \frac{\sigma_u^2}{u^2} + \frac{\sigma_v^2}{v^2} + 2\frac{\sigma_{uv}^2}{uv}$$

In Equation 2.2, σ_x^2 is the variance for a function *x*, *u* and *v* are variables (with respective σ^2 variances), and σ_{uv}^2 is the covariance (for which if the uncertainties in the two variables u and v are uncorrelated, as in this case, the covariance approaches 0 and is ignored; Pittman (1993)).

New York State power plants emitted approximately 42 million metric tons of CO_2 into the atmosphere in 2008 (U.S. EPA Clean Air Markets Data, 2009). According to this datum, the NFSG10 for the entire Queenston Formation in the central New York study area could store approximately 120 years (+/- 15 years) of state-wide power plant CO_2 emissions in its pore space.

Conclusions

Though sparse, subsurface data from central and western New York and western New York outcrops supply information about the Upper Ordovician Queenston Formation, which can be applied to a geologic carbon dioxide storage assessment. In central New York, well log, core, and seismic data reveal that the

Queenston Formation was deposited in a distributary fluvial setting with mobile channel bars, sheet floods, and no stable, long-lived flood plain (Tamulonis, 2010). Of the six stacked petrophysical zones, Queenston A (top) to Queenston F (bottom), zones B, C, and D are laterally continuous throughout central New York and have the highest porosity and permeability values within the formation. Seismic data suggest there are internal unconformities within zones B and C, and well core data imply that zones B and C represent a series of base level changes. Zones B, C, and D are all thickest in NW-SE trending "channels" in the study area. Well log data suggest that the Queenston Formation would not have adequate porosity for CO_2 storage west of Livingston County, where the formation begins to grade into muddier facies.

Maps of net sandstone thickness with >10% porosity show that zones Queenston B, C, and D offer the greatest pore volumes within the depocenter 'channels' in Tompkins, Cayuga, and Seneca Counties, as well as in the southern part of the study area. This suggests that the best sorted sand was deposited in channelized depocenters within the study area and at more proximal locations in the southern part of the study area.

Alternative stratigraphic models can be made for the Queenston Formation. Models 1 and 2 interpret the central New York Queenston Formation to be fluvial deposits that grade into tidal flat, beach, and marine deposits in western New York and Ontario, Canada. They also treat Queenston Formation sediment deposition as spatially continuous throughout New York State. An alternative and novel model suggests that an unconformity separates the Queenston Formation central New York sandstones from the western New York shale (Model 3). Western New York fault systems may have affected paleo-drainage and sediment supply during Queenston time.

Based on gross approximations, zones B, C, D, and E offer the greatest storage potential in porous zones within the central New York study area, each with a potential to store approximately 10^8 metric tons of CO_2. The Queenston Formation could potentially store 5×10^9 metric tons of CO_2 in porous zones throughout the study area. Uncertainties associated with this regional calculation, such as reservoir geometry, porosity, water saturation, and CO_2 density must be further explored in order to gain more accurate estimates of static CO_2 storage potential.

REFERENCES

Allen, J.R.L. 1970. Studies in fluviatile sedimentation; a comparison of fining-upwards cyclothems, with special reference to coarse-member composition and interpretation. Journal of Sedimentary Petrology. 40(1): 298-323.

Ambrose, W.A., Tucker, F.H., Bonaffé, F., Loucks, R.G., Brown, L.F., Jr., Wang, F.P., and Potter, E. 2009. Sequence-stratigraphic controls on complex reservoir architecture of highstand fluvial-dominated deltaic and lowstand valley-fill deposits in the Upper Cretaceous (Cenomanian) Woodbine Group, East Texas field: regional and local perspectives. AAPG Bulletin. 93(2): 231-269.

Asquith, G., and Krygowski. 2004. Basic well log analysis. In collaboration with S. Henderson and N. Hurley. AAPG Methods in Exploration Series. 16. 224 pp.

Brett, C.E., Goodman, W.M., LoDuca, S.T., and Lehmann, D.F. 1996. Upper Ordovician and Silurian strata in western New York; sequences, cycles and basin dynamics. *In* Upper Ordovician and Silurian sequence stratigraphy and depositional environments in western New York: a field guide for the James Hall Symposium, second international symposium on the Silurian System. C.E. Brett and W.M. Goodman, Co-leaders. 71-120 pp.

Brogly, P.J., Martini, I.P., and Middleton, G.V. 1998. The Queenston Formation; shale-dominated, mixed terrigenous-carbonate deposits of Upper Ordovician, semiarid, muddy shores in Ontario, Canada. Canadian Journal of Earth Sciences. 35(6): 702-719.

Burruss, R.C., Brennan, S.T., Freeman, P.A., Merrill, M.D., Ruppert, L.F., Becker, M.F., Herkelrath, W.N., Kharaka, Y.K., Neuzil, C.E., Swanson, S.M., Cook, T.A., Klett, T.R., Nelson, P.H., and Schenk, C.J. 2009. Development of a probabilistic assessment methodology for evaluation of carbon dioxide storage:

U.S. Geological Survey Open-File Report 2009–1035. 81 pp. Available only online at *http://pubs.usgs.gov/of/2009/1035/.*

Campbell, C.V. 1976. Reservoir geometry of a fluvial sheet sandstone. America Association of Petroleum Geologists Bulletin. 60(7): 1009-1020.

Caley, J.F. 1940. Paleozoic geology of the Toronto-Hamilton area. Geological Society of Canada, Memoir 224. 284 pp.

Colton, G.W. 1970. The Appalachian Basin; its depositional sequences and their geologic relationships. *In* Studies of Appalachian geology: central New York. G.V. Fisher, F.J. Pettijohn, and K.N. Weaver Eds. 5-47 pp.

Cotter, E. 1978. The evolution of fluvial style, with special reference to the Central Appalachian Paleozoic. *In* Fluvial Sedimentology Memoir - Canadian Society of Petroleum Geologists 5. A.D. Miall Ed. Canadian Society of Petroleum Geologists, Calgary, Canada. pp. 361-383.

Dennison, J. 1976. Appalachian Queenston Delta related to eustatic sea level drop accompanying late Ordovician glaciation centered in Africa. *In* The Ordovician System; Proceedings of a Palaeontological Association Symposium, Birmingham, UK. University of Wales Press and National Museum of Wales. Cardiff, Wales, United Kingdom. pp. 107-120.

Department of Energy (DOE). 2008. Methodology for development of geological storage estimates for carbon dioxide. http://www.netl.doe.gov/technologies/carbon_seq/refshelf/methodology2008.pdf

Dyer, W.S. 1925. The stratigraphy and paleontology of Toronto and vicinity. Part 6B: The stratigraphy and correlation of the Credit River section. Ontario Deptartment of Mines, 32nd Annual Report. pp.117-134.

Engelder, T., and Gash, G. 2008. Marcellus shale play's vast resource potential creating a stir in Appalachia. The American Oil and Gas Reporter. 51(6): 76-87.

Ethridge, F.G., Wood, L.J., and Schumm, S.A. 1998. Cyclic variables controlling fluvial sequence development; problems and perspectives. *In* Relative role of eustasy, climate, and tectonism in continental strata. K.W. Shanley and P.J. McCabe, Eds. SEPM Special Publication 59. Tulsa, OK. pp. 17-29.

Ettensohn, F.R. 1991. Flexural interpretation of relationships between Ordovician tectonism and stratigraphic sequences, central and southern Appalachians, U.S.A. *In* Advances in Ordovician Geology. C.R. Barnes and S.H. Williams Eds. Geological Survey of Canada, Ottawa, ON, Canada. pp. 213-224.

Fisher, D.W. 2006. The rise and fall of the Taconic Mountains: a geological history of eastern New York. Donald W. Fisher: in collaboration with Stephen L. Nightingale. Black Dome Press Corporation. 184 pp.

Flemings, P.B., and Jordan, T.E. 1990. Stratigraphic modeling of foreland basins: interpreting thrust deformation and lithosphere rheology. Geology. 18: 430-434.

Friedman, G.M. 1987. Deep burial diagenesis: its implication for vertical movements of crust, uplift of lithosphere, and isostatic unroofing – a review. Sedimentary Geology. 50: 67-94.

Grabau, A.W. 1913. Early Paleozoic delta deposits of North America. Geological Society of America. 24: 299-528.

Hughes, S.E.M. 1976. The paleogeography and subsurface stratigraphy of the Late Ordovician Queenston coastal complex in New York. Master's of Science Thesis, Cornell University. 127 pp.

Intergovernmental Panel on Climate Change (IPCC). 2005. Carbon Dioxide Capture and Storage. 442 pp.

Jacobi, R.D. 2002. Basement faults and seismicity in the Appalachian basin of New York State. Tectonophysics. 353: 75-113.

Jacobi, R.D., and Fountain, J.C. 2002. The character and reactivation history of the southern extension of the seismically active Clarendon-Linden fault system, western New York State. Tectonophysics. 353: 215-262.

Jarrell, P., Fox, C., Stein, M., and Webb, S. 2002. Practical Aspects of CO_2 Flooding. SPE Monograph Series. 22. 220 pp.

Johnson, M.E. 1985. Cyclic carbonates in the Lower Silurian of the Michigan Basin; applications in paleobathymetry and interregional correlation. The Geological Society of America, North-Central Section, 19th annual meeting Abstracts with Programs - Geological Society of America. 17(5): 293.

Jordan, T.E., and Flemings, P.B. 1991. Large-scale stratigraphic architecture, eustatic variation, and unsteady tectonism: a theoretical evaluation. Journal of Geophysical Research. 96(B4): 6681-6699.

Krygowski, D. 2009. Personal Communication.

Lugert, C., Smith, L., and Nyahay, R. 2006. Systematic technical innovations initiative for brine disposal in the northeast. New York State Energy Research and Development Authority (NYSERDA) Report, Contract number 6940. 269 pp.

Medina, C.R. and Rupp, J.A. 2009. Carbon dioxide storage capacity in the Upper Cambrian basal sandstone of the Midwest region: a county-based analysis. AAPG Eastern Section 2009 meeting, Evansville Indiana.

Miall, A.D. 1977. A review of the braided-river depositional environment. Earth-Science Reviews. 13(1): 1-62.

Miall, A.D. 1996. The geology of fluvial deposits; sedimentary facies, basin analysis, and petroleum geology. Berlin, Germany, Springer-Verlag. 587 pp.

Over, D.J. 2009. Personal communication.

Patchen, D.G. 1965. Petrology of the Oswego (Upper Ordovician), Queenston (Upper Ordovician), and Grimsby (Lower Silurian) formations, Oswego County, New York. Master's of Science Thesis, SUNY Binghamton. 191 pp.

Pemberton, S.G., MacEachern, J.A., and Frey, R.W. 1992. Trace fossil facies models: environnmental and allostratigraphic significance. *In* Facies models; response to sea level change. R.G. Walker and N.P. James Eds. Geological Association of Canada, Alberta, Canada. pp. 47-72.

Pitman, J. 1993. Probability. Springer-Verlag Press. 559 pp.

Posamentier, H.W., and James, D.P. 1993. An overview of sequence-stratigraphic concepts; uses and abuses. *In* Sequence stratigraphy and facies associations, 18. H.W. Posamentier, C.P. Summerhayes, B.U. Haq, and G.P. Allen, Eds. Blackwell, Oxford, England. pp. 3-18 pp.

Posamentier, H.W. and Vail, P.R. 1988. Eustatic controls on clastic deposition; II, Sequence and systems tract models. *In* Sea level changes: an integrated approach. C.K. Wilgus, B.S. Hastings, C.G.St.C. Kendall, H.W. Posamentier, C.A. Ross and J.C. Van Wagoner Eds. SEPM special publication 42. Tulsa, OK. pp. 125-154.

Rickard, L.V. 1973. Stratigraphy and the structure of the subsurface Cambrian and Ordovician carbonates of New York. New York State Museum Map and Chart 12. 55 pp., 14 plates.

Robinson, J.E. 1987. Upper Ordovician and Silurian sandstone facies of central New York State. Twelfth Appalachian Basin Industrial Associates Program; spring meeting. 12: 93-106.

Saroff, S.T. 1987. Subsurface structure and nature of gas production of the Upper Ordovician Queenston Formation, Auburn gas field, Cayuga County, New York. Thirteenth Appalachian Basin Industrial Associates Program; fall meeting. 13: 38-58.

Schlumberger. 1991. Formation Log Interpretation Principles/Applications. Schlumberger Educational Services. 198 pp.

Schlumberger. 1996. Improved recovery in the naturally-fractured Queenston Formation using geologic/engineering analysis and deviated well technology. New York State Energy Research and Development Authority (NYSERDA) Report, contract number 4307. 58 pp.

Smith, L.B. Jr. 2006. Origin and reservoir characteristics of Upper Ordovician Trenton-Black River hydrothermal dolomite reservoirs in New York. AAPG Bulletin. 90(11): 1691-1718.

Smith, L.B. Jr. 2007. Carbon dioxide capture and storage (CCS) potential in New York State. PowerPoint slides. Retrieved from http://esogis.nysm.nysed.gov/esogis/talks.cfm.

Tamulonis, K.L. 2010. Site specific carbon dioxide storage potential for the Queenston Formaton at the AES Cayuga coal-fired power plant in Tompkins County, New York. Chapter 1 of this dissertation.

Thompson, A.M. 1970. Geochemistry of color genesis in red-bed sequence, Juniata and Bald Eagle Formations, Pennsylvania. Journal of Sedimentary Petrology. 4: 599-615.

United States Environmental Protection Agency (U.S. EPA) Clean Air Markets Data. http://camddataandmaps.epa.gov/gdm/index.cfm?fuseaction=emissions.wizard

Van der Voo, R. 1988. Paleozoic paleogeography of North America, Gondwana, and intervening displaced terranes; comparisons of paleomagnetism with

paleoclimatology and biogeographical patterns. Geological Society of America Bulletin. 100(3): 311-324.

Woodrow, D.L., Brett, C. E., Selleck, B., and Hanshaw, P.M. 1989. Sedimentation and basin analysis in siliciclastic rock sequences; Sedimentary sequences in a foreland basin; the New York System. Field trips for the 28th international geological congress. 43 pp.

Yeakel, L.S., Jr. 1962. Tuscarora, Juniata, and Bald Eagle paleocurrents and paleogeography in the Central Appalachians. Geological Society of America Bulletin. 73(12): 1515-1539.

Zhou, Q., Birkholzer, J., Rutqvist, J., and Tsang, C. 2007. Sensitivity study of CO_2 storage capacity in brine aquifers with closed boundaries: Dependence on hydrogeologic properties. Sixth annual conference on carbon capture and sequestration –DOE/NETL. 37 pp.

CHAPTER 3

CAUSES AND MOVEMENT OF LANDSLIDES AT THE RAINBOW CREEK AND RATTLESNAKE GULF IN THE TULLY VALLEY, ONONDAGA COUNTY, NEW YORK*

Abstract

Two landslides in the Tully Valley of central New York are moving slowly toward their respective streams (Rainbow Creek and Rattlesnake Gulf). Data on soil displacement (landslide movement), ground-water levels in both landslide areas, and precipitation on the Tully Valley floor were collected from June 2006 through June 2008. Analyses of the data indicate the displacement of shallow, weathered soils in upslope areas is related to heavy rainstorms and the associated rise in ground-water levels above the unweathered soil layer, whereas shallow-soil displacement on the lower, steepest parts of these landslide areas is due to stream-generated erosion of the landslide toe and to decreased stability of the soil through saturation by groundwater. The upslope progression of soil displacement results in slope failure, which in turn undermines small landmasses in the shallow zone and causes further slope failure.

Introduction

In 2006, the U.S. Geological Survey (USGS), in cooperation with the Onondaga Lake Partnership and Onondaga Environmental Institute, began a 2-year

---

*Originally published as: Tamulonis, K.L., Kappel, W.M., and Shaw, S.B. 2009. Causes and movement of landslides at Rainbow Creek and Rattlesnake Gulf in the Tully Valley, Onondaga County, New York. U.S. Geological Survey Scientific Investigations Report 2009–5114. 18 pp. Available online at *http://pubs.usgs.gov/sir/2009/5114/*. Reprinted with permission of individual copyright owners.

study to determine the cause and progression of landslides in the two major tributary valleys to the Tully Valley. This report describes the landslides and their rate of movement, discusses the field methods, and interprets the probable causes of these landslides. It also includes geotechnical data from analyses of weathered and unweathered soil samples collected from both landslide areas and compares these results to previous geotechnical data analyzed from the floor of the Tully Valley.

Tully Valley Study Area

The Tully Valley, near Tully, New York, is six miles long and forms the southern part of the Onondaga Creek valley, which extends 25 miles from the Tully Moraine through Onondaga Lake, near Syracuse (Figure 3.1). Unlike other valleys in the Finger Lakes region, the Onondaga Creek valley does not contain a lake but contained proglacial lakes when ice sheets advanced and retreated across the region between 1.6 million and 11,000 years ago (Rogers, 1991). The movement of glaciers widened and deepened the bedrock valleys of this region and, during their recession, left deposits of glacially derived sediment. As much as 400 feet of glacial (unsorted), lacustrine (lake-bottom), and fluvial (stream-related) deposits of clay, silt, sand, and gravel blanket the Tully Valley floor. The walls of the Onondaga Creek valley consist of Middle Devonian Hamilton Group shale and siltstone that gently dip to the south (40–50 feet per mile) and are covered with a thin layer of till.

Onondaga Creek flows northward through the Tully Valley, and two east-west trending tributaries--Rattlesnake Gulf on the west and Rainbow Creek on the east--enter the valley nearly opposite each other (Figure 3.1). These side valleys contain fine-grained lacustrine deposits laid down in side-valley glacial lakes that were impounded when the main ice mass occupied the Tully Valley.

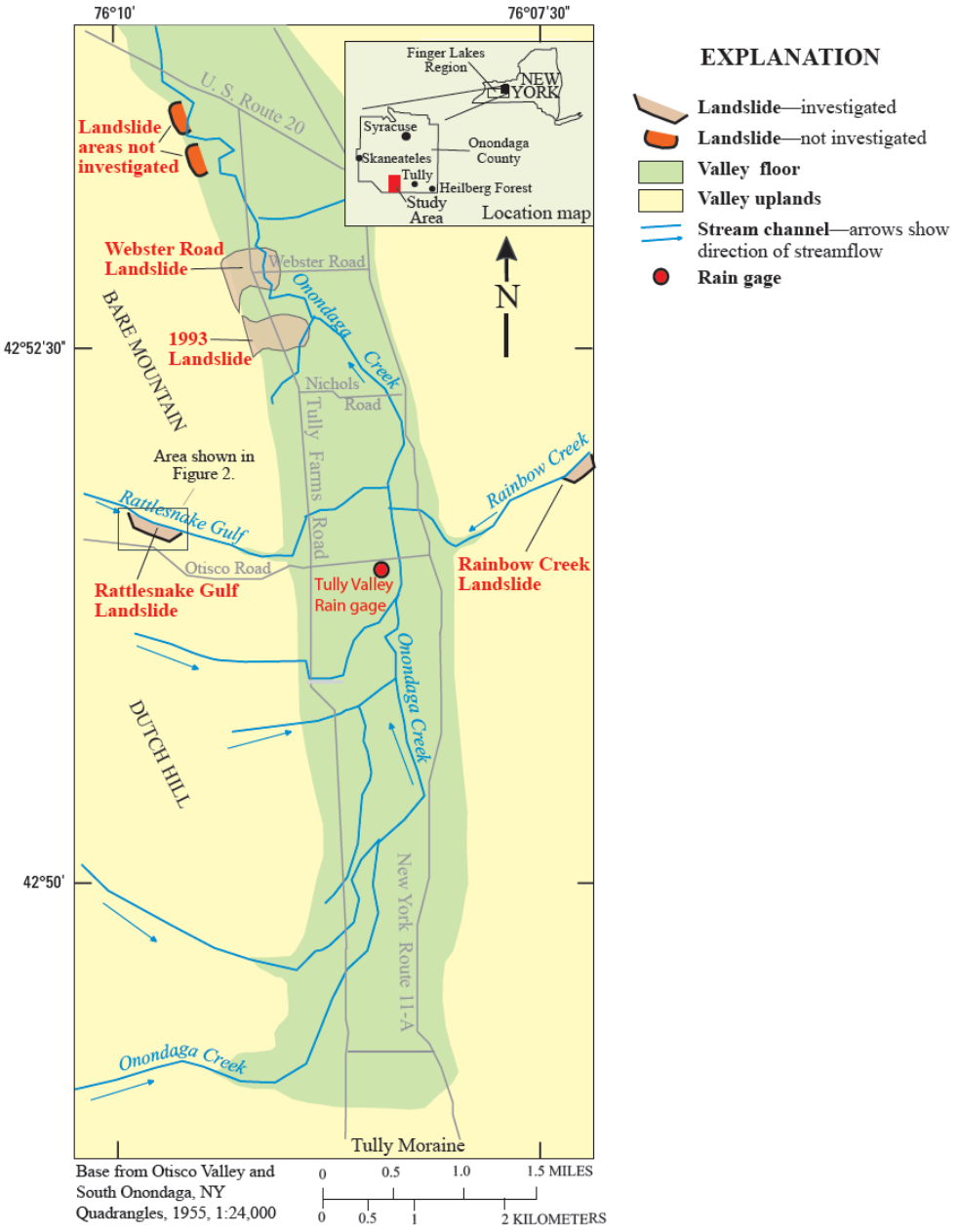

Figure 3.1. Physiographic features in the Tully Valley, Onondaga County, New York with landslide locations and rain gage mapped.

Landslides in the Tully Valley

On April 27, 1993, the largest landslide in New York State since the early 1900s occurred on the west wall of the Tully Valley (Figure 3.1). The landslide covered about 50 acres and destroyed three homes; it also buried about 1,400 feet of Tully Farms Road (Figure 3.1) with 12 to 15 feet of mud and associated debris (Fickies, 1993; Pair et al., 2000). The probable causes of this landslide were twofold--slowly developing slope failure (movement) on the lower hillside, which was first reported 3 years earlier (Wieczorek et al., 1998), and increasing pore-water pressure within clay interbeds resulting from rapid snowmelt from a record-breaking snowfall during the winter of 1992-93, followed by 7.5 inches of precipitation in early April 1993 (Pair et al., 2000). Several researchers evaluated the landslide shortly after it occurred, including Burgmeier (1998) and Morales-Muniz (2000), who completed geotechnical investigations of the landslide area, and Jäger and Wieczorek (1994), who constructed a landslide-susceptibility map of the Tully Valley and five adjacent valleys on the basis of clay distribution, former extent of proglacial lakes, and slope steepness.

Two much-older landslides, one overlying the other, were identified near Webster Road (Figure 3.1) just north of the 1993 landslide. These two slides were dated through Carbon-14 age-dating methods; the lower slide occurred about 9,800 Carbon-14 years before present (^{14}C yr B.P.) or 11,200 calibrated years before present (Cal BP years), and the overlying slide occurred about 6,100 ^{14}C yr B.P. or 7,000 Cal BP years ago (Pair et al., 2000; Kappel and Teece, 2007). The ages of two other suspected landslides further to the north have not been evaluated.

In 2005, an active, slow-moving landslide was found on the south side of the Rainbow Creek valley, and another was found on the south side of the Rattlesnake Gulf valley (Figure 3.1). The locations of these slides are consistent with the

landslide-susceptibility map by Jäger and Wieczorek (1994). Soil displacement has occurred at both locations in the top layer of sediment (just below the root zone at the interface between weathered and unweathered soil) as small "islands" of soil and trees that slowly creep downhill then break loose and slide over the steep hillside into the stream channel.

Both of these slow-moving landslides are on north-facing, forested slopes that have been logged multiple times; the forest on the Rattlesnake Gulf landslide was selectively logged in 2007, and the forest on the Rainbow Creek landslide was last cut in the late 1990's. Average annual precipitation in this part of New York is about 40 inches per year, and the rainiest months are usually May, June, and July; monthly average precipitation for those 3 months is 3.5 to 4.0 inches. Soils are typically wettest before the trees 'leaf-out', and after evapotranspiration has declined with plant dormancy (leaf-fall). Soil displacement and ground-water levels within the two landslides and precipitation on the floor of the Tully Valley between the mouths of the two streams were measured from the summer of 2006 through the summer of 2008.

Rainbow Creek Landslide

The Rainbow Creek landslide is on the southeastern slope of the creek (Figure 3.1); it was indicated by Jäger and Wieczorek (1994) to extend eastward along the creek from an altitude of about 800 feet at the creek to about 1,200 feet just west of the I-81 corridor (Figure 3.2). The active part of this landslide lies between altitude 840 and 950 feet and covers about 34 acres. The steep landslide surface faces northwest, and the material is primarily laminated clay and silt and well-sorted fluvial sand and gravel. The underlying bedrock on the valley slopes is stable, Middle-Devonian shale and siltstone of the Hamilton Group. Observations made throughout the summer and fall of 2006 indicated the landslide material consisted of more than 10 feet of laminated clay and silt overlain by 40 feet of interbedded, well-sorted silt, sand, and

Figure 3.2. Rainbow Creek orthoimage with 100-foot contour lines, showing location of current landslide areas on the north and south sides of the Rainbow Creek valley, Onondaga County, New York (location is shown in Figure 3.1). Based on New York State Orthoimagery Program, 2004, Universal Transverse Mercator Projection, Zone 18.

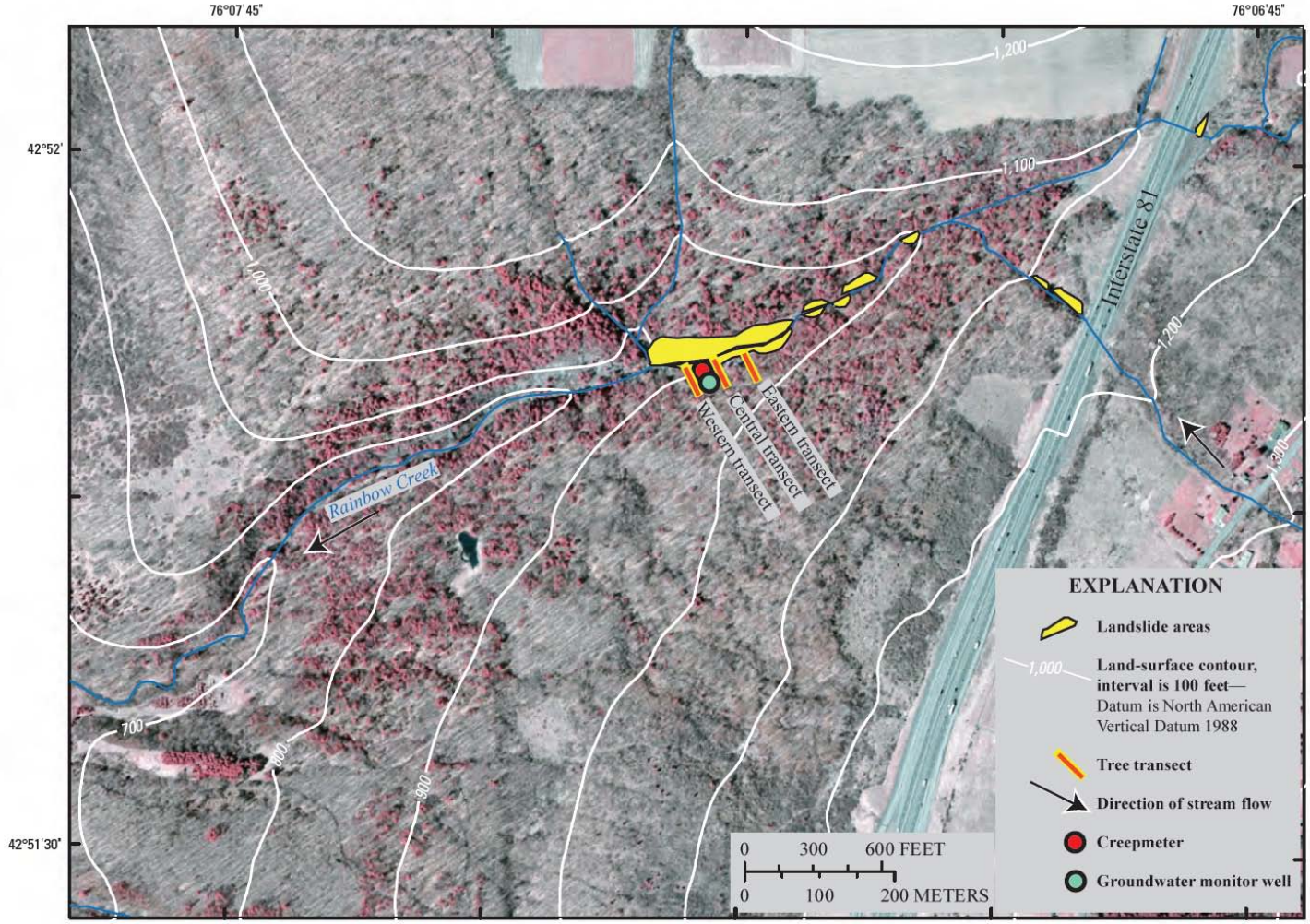
76°07'45"
76°06'45"
42°52'
42°51'30"
1,200
1,100
1,000
900
800
700
Interstate 81
Rainbow Creek
Eastern transect
Central transect
Western transect
0 300 600 FEET
0 100 200 METERS
EXPLANATION
Landslide areas
1,000
Land-surface contour, interval is 100 feet— Datum is North American Vertical Datum 1988
Tree transect
Direction of stream flow
Creepmeter
Groundwater monitor well

Figure 3.3. Hillside exposure of a rotated sand and gravel unit overlying fine-grained silt and clay in the Rainbow Creek landslide area, Onondaga County, New York. Photo is looking southeastward and side movement is toward the northwest (left in photo), toward Rainbow Creek. Photograph courtesy of Mark Schaub, Onondaga County Soil/Water Conservation District.

Trend of rotating block
Bedding orientation within sand and gravel unit

gravel that coarsen upward. This upper, interbedded material was rotated slightly upward from the horizontal position (Figure 3.3) and, after the 2006-07 winter, some of the sand and gravel unit had slumped into Rainbow Creek, exposing a scarp about 25 feet high that consisted of laminated silt and clay overlain by 8 feet of poorly sorted till. The layer of laminated silt and clay was also rotated from the horizontal--an indication that this layer was part of a larger landslide area. Smaller landslides of displaced material are evident on both sides of Rainbow Creek for at least 0.5 mile upstream (east of the present landslide area), and several landslide scars along the streambanks below the main landslide reveal the shale bedrock.

Groundwater discharges throughout the Rainbow Creek landslide, and several springs and seeps feed areas of standing water within the landslide scarps. Many of these ponded areas remain wet throughout the year, but the amount of standing water varies seasonally.

Rattlesnake Gulf Landslide

The Rattlesnake Gulf landslide is on the south slope of Rattlesnake Gulf Creek (Figure 3.1) and extends from an altitude of about 750 feet along the creek to an altitude of 1,250 feet (Jäger and Wieczorek, 1994). The active part of this landslide slopes steeply from altitude 740 to 850 feet and covers about 23 acres. Additional scarps and fractures extend to an altitude of 950 feet (Figure 3.4). Landslide material is mostly laminated silt and clay (Figure 3.5), although some well-sorted fluvial sand and gravel layers are exposed at several locations within the active landslide and are found covering the slopes above the landslide. As in the Rainbow Creek landslide, the silt and clay component is rotated from horizontal and overlies the stable Middle Devonian Hamilton Group shale and siltstone. Unlike the Rainbow Creek landslide, however, the Rattlesnake Gulf landslide does not have smaller, active components upstream from the main body, although several older landslide scars can be found

Figure 3.4. Rattlesnake Gulf orthoimage with 100-foot contour lines, showing location of current landslide areas on the north and south sides of the Rattlesnake Gulf valley, Onondaga County, New York (location is shown in Figure 3.1.). Based on New York State Orthoimagery Program, 2004, Universal Transverse Mercator Projection, Zone 18.

EXPLANATION
Landslide area
Land-surface contour—Interval is 100 feet. Datum is North American Vertical Datum 1988
1,000
Scarp
Tree transect
Active rock slide
Direction of stream flow
Creepmeter
Stratigraphic test hole
Groundwater monitor well
Rattlesnake Gulf
Otisco Road
1,300
1,200
1,100
1,000
900
800
76°10'15"
76°09'30"
42°51'45"
42°51'30"
0 300 600 FEET
0 100 200 METERS

Figure 3.5. Slide materials in the Rattlesnake Gulf landslide area, Onondaga County, New York. View is looking south (location is shown in Figure 3.1).

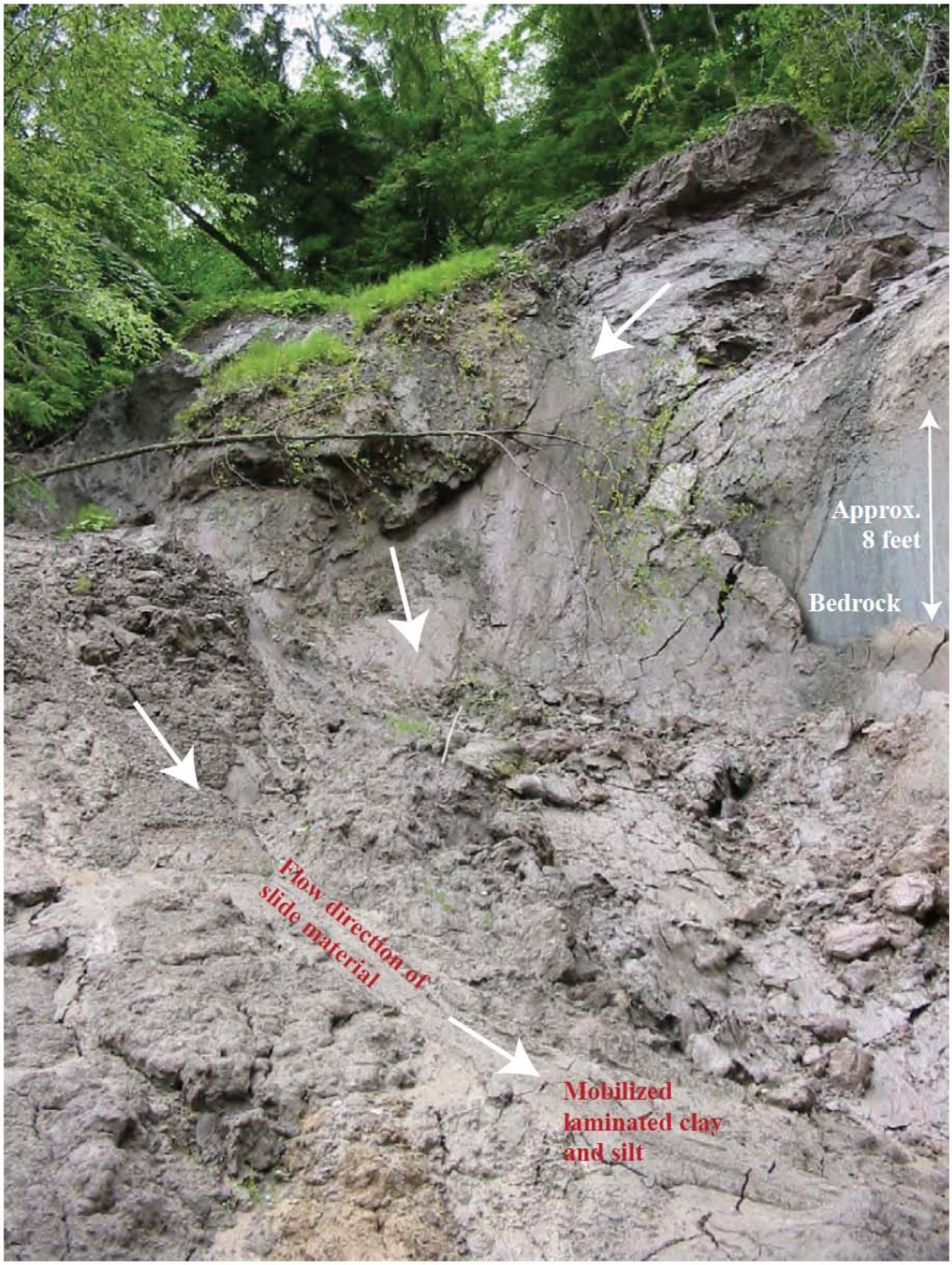
Approx.
8 feet
Bedrock
Flow direction of
slide material
Mobilized
laminated clay
and silt

upstream, and bedrock slides are seen on the north wall of the valley directly across from the active slide.

In January 2008, a test hole was drilled within the Rattlesnake Gulf landslide between small, active displacement scarps above the steep slopes adjacent to the stream. The stratigraphic log for this test hole (Figure 3.6) indicates the materials grade from sand and gravel to silt near land surface to fine sand and clay at depths below 20 feet. The bedding dips steeply near the surface, and the angle decreases with depth (Figure 3.6). The sediment color changes from reddish brown to grayish brown, and the bedding appears to be horizontal below a depth of about 70 feet. The shallow, rotated material appears to be similar to that in the main landslide area mapped by Jäger and Wieczorek (1994); the deeper sediments are not rotated and are not affected by past landslide movement.

Surface water at the Rattlesnake Gulf site drains mostly into two channels along the western and eastern edges of the active slide area; the flow in these channels varies seasonally in response to precipitation. Shallow groundwater appears as seeps and pockets of standing water within some of the displacement scarps of the slide.

Landslide Monitoring

Landslide-motion detectors (creepmeters) were constructed from old Stevens Type-F analog (paper and pen) water-level (drum) recorders (Figure 3.7) to record the timing and magnitude of land-surface displacement in both stream valleys. Land-surface displacement or movement measured at specific locations within a landslide cannot be used to compute displacement for the entire landslide but can be used to indicate relative movement and its timing within localized areas. Landslide displacement was further characterized by changes in the distance between an upgradient baseline tree and successive trees along a transect perpendicular to the active landslide slope.

Figure 3.6. Stratigraphic log of unconsolidated sediment upgradient of active slide face at the Rattlesnake Gulf landslide area, Onondaga County, New York (location of test hole is shown in Figure 3.4).

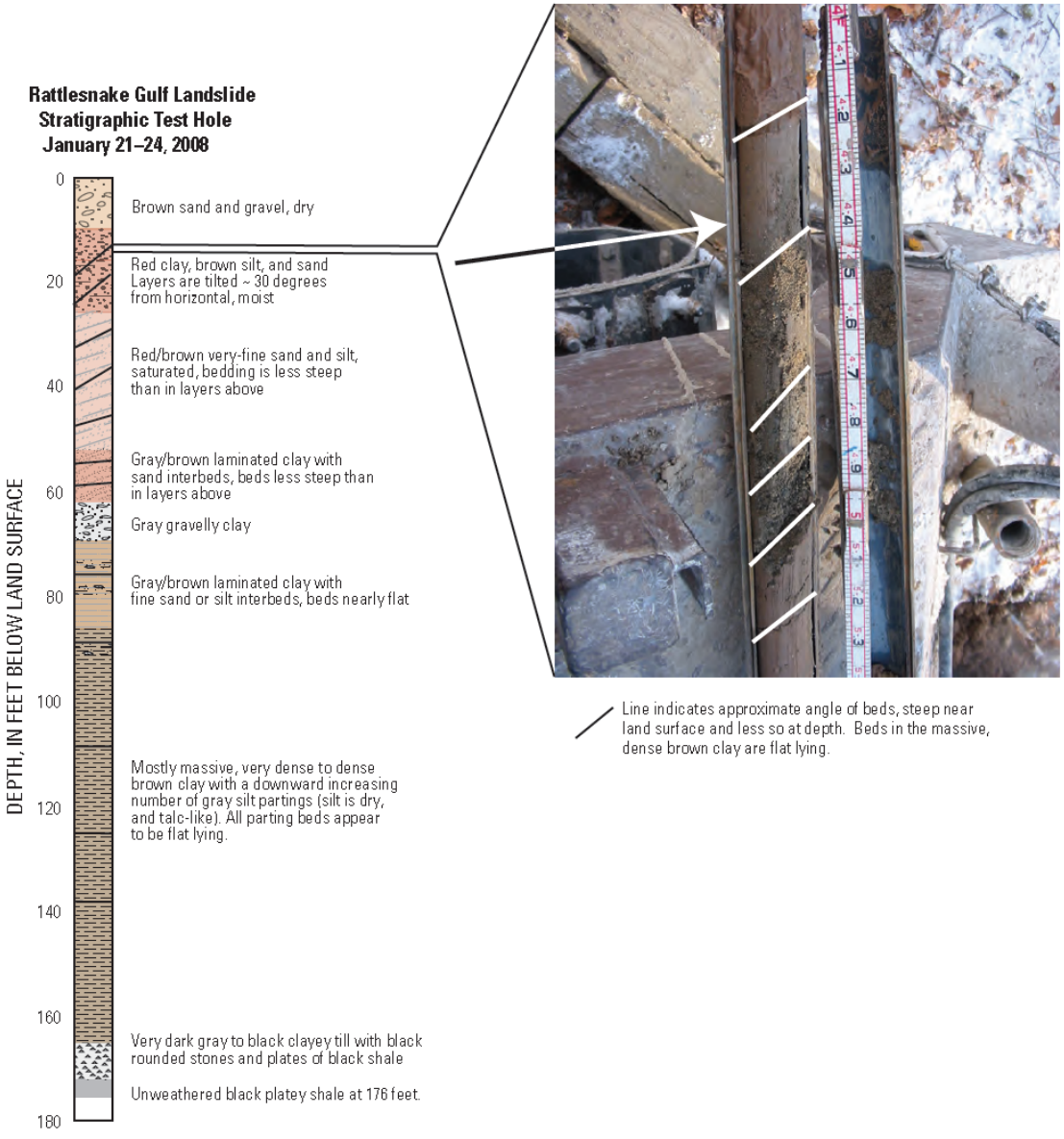
Rattlesnake Gulf Landslide
Stratigraphic Test Hole
January 21–24, 2008
DEPTH, IN FEET BELOW LAND SURFACE
0
20
40
60
80
100
120
140
160
180
Brown sand and gravel, dry
Red clay, brown silt, and sand
Layers are tilted ~ 30 degrees
from horizontal, moist
Red/brown very-fine sand and silt,
saturated, bedding is less steep
than in layers above
Gray/brown laminated clay with
sand interbeds, beds less steep than
in layers above
Gray gravelly clay
Gray/brown laminated clay with
fine sand or silt interbeds, beds nearly flat
Mostly massive, very dense to dense
brown clay with a downward increasing
number of gray silt partings (silt is dry,
and talc-like). All parting beds appear
to be flat lying.
Very dark gray to black clayey till with black
rounded stones and plates of black shale
Unweathered black platey shale at 176 feet.
Line indicates approximate angle of beds, steep near
land surface and less so at depth. Beds in the massive,
dense brown clay are flat lying.

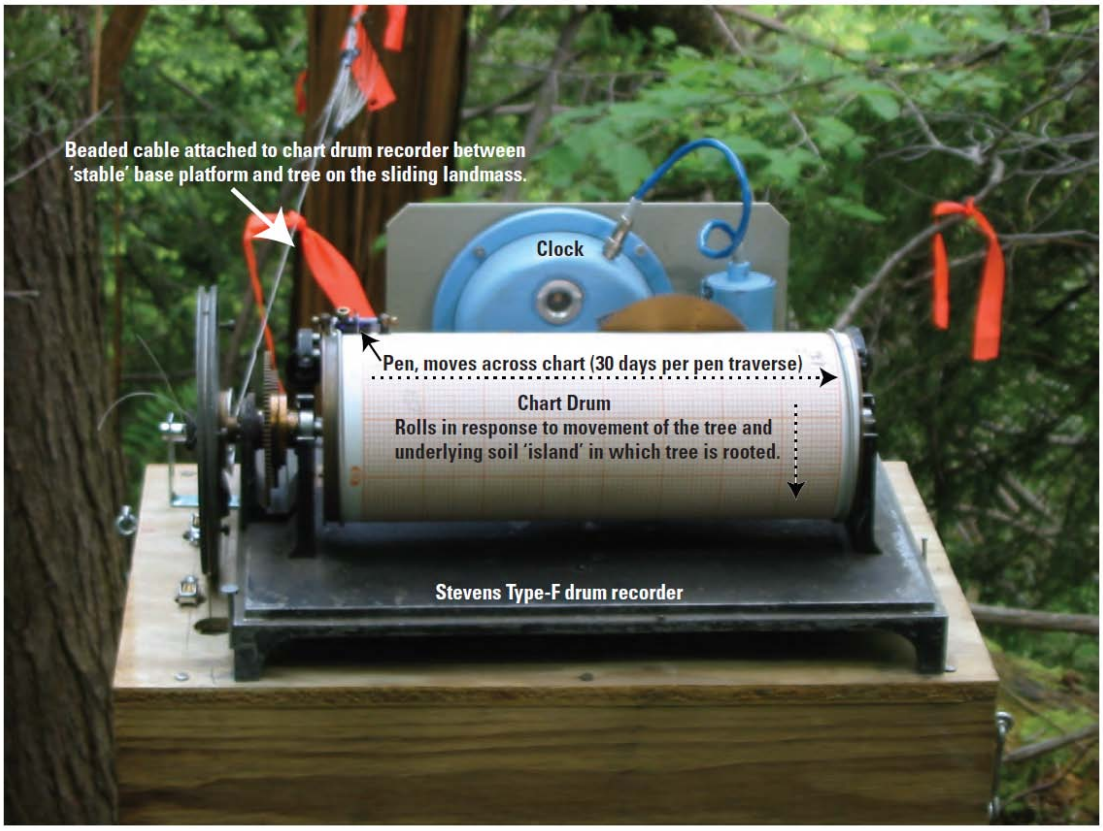

Figure 3.7. Principal components of creepmeter used at Rattlesnake Gulf and Rainbow Creek landslide areas to detect and record rates of landmass movement.

Measurement of Precipitation and Ground-Water Levels

Precipitation was measured hourly on the Tully Valley floor (Figure 3.1) between the Rattlesnake Gulf and Rainbow Creek landslide areas throughout the stud by an automated tipping-bucket rain gage. Ground-water levels at each site were measured in 2-inch-diameter wells installed in August 2006 and augured to the unweathered-soil zone. A transducer was placed in each well to record the ground-water level every 15 minutes from August 2006 through June 2008.

Creepmeters

Creepmeters span active-displacement scarp fractures. The upgradient (and assumed stable) side of the scarp holds the creepmeters, which are attached by a cable to a firm object downgradient on the moving landmass, typically a tree. Creepmeters were installed at both landslides in June 2006 to record land-surface movement (soil displacement) at specific locations where movement was observed as ground cracks or as tilted or split trees. One creepmeter was installed along the steep, eroding slope of the Rainbow Creek landslide (Figure 3.2), and two creepmeters were installed at the Rattlesnake Gulf landslide: one to record movement along a new displacement scarp in the central part of the landslide, and the other about 1,500 feet to the northwest, along the steep, eroding slope above Rattlesnake Gulf (Figure 3.4). The cumulative displacement values are plotted in Figure 3.8 along with cumulative precipitation values and hourly ground-water levels.

From June 2006 through June 2008, the Rainbow Creek creepmeter recorded 1.2 feet of displacement during the first 16 months, after which the slope completely failed in November 2007 (Figure 3.8A). The northwest Rattlesnake Gulf creepmeter recorded 6.5 feet of total displacement, and the central Rattlesnake Gulf creepmeter recorded 3.5 feet of total displacement (Figure 3.8B). Slope displacement generally occurs in small increments on consecutive days, even during periods of the most rapid

Figure 3.8. Cumulative creepmeter displacement and precipitation within the two landslide areas in relation to ground-water levels, June 2006 through June 2008. A. Rainbow Creek site, and B. Rattlesnake Gulf site (locations are shown in Figures 2 and 4, respectively).

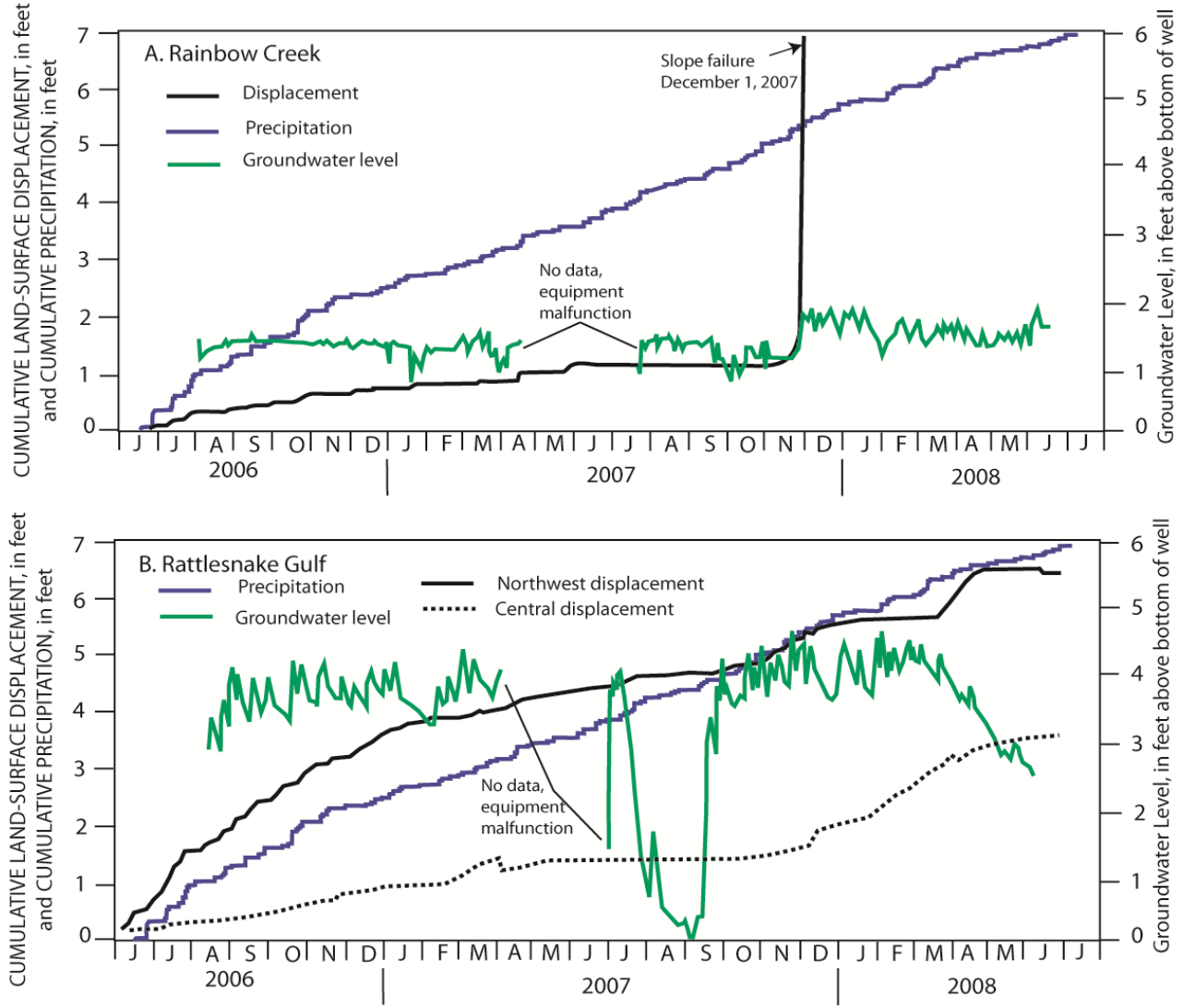
A. Rainbow Creek
Displacement
Precipitation
Groundwater level
Slope failure
December 1, 2007
No data,
equipment
malfunction
CUMULATIVE LAND-SURFACE DISPLACEMENT, in feet
and CUMULATIVE PRECIPITATION, in feet
Groundwater Level, in feet above bottom of well
J J A S O N D J F M A M J J A S O N D J F M A M J J
2006
2007
2008
B. Rattlesnake Gulf
Precipitation
Groundwater level
Northwest displacement
Central displacement
No data,
equipment
malfunction
CUMULATIVE LAND-SURFACE DISPLACEMENT, in feet
and CUMULATIVE PRECIPITATION, in feet
Groundwater Level, in feet above bottom of well
J J A S O N D J F M A M J J A S O N D J F M A M J J
2006
2007
2008

displacement (for instance, April 2008 at the northwest creepmeter, Figure 3.8B).

From June 2006 through June 2008, the Rainbow Creek landslide showed little correlation between ground-water levels and slope displacement, other than the period of rapid ground-water rise in November 2007 that preceded the slope failure (Figure 3.8A). The creepmeter records for Rattlesnake Gulf indicate that movement at the northernmost scarp was greater than in the center of the landslide through the spring and summer of 2008. While full-scale data collection had ended in June, 2008, observations of slide movement continued at both side areas through the end of 2008. During the fall of 2008, the rate of movement increased in the central area of the Rattlesnake Gulf slide because of the slow, upward progression of slope failure and movement into the central part of this landslide, while during the same period of time the northwestern area did not move at all. The timing of slope displacement at the two creepmeters at Rattlesnake Gulf was similar through most of the study period however, in that most of the movement occurred during periods of high ground-water levels (and thus greater soil moisture) than during dry periods with the exception of the central area during the fall of 2008.

Tree Displacement Transects

Three displacement transects were installed above Rainbow Creek (Figure 3.2), and one at Rattlesnake Gulf (Figure 3.4). Any change in distance between the trees reflects soil movement in response to active erosion at the landslide face. The baseline tree for each transect was assumed to be stable over the 2-year study period, but a new scarp developed on the Rattlesnake Gulf slide adjacent to the baseline tree in the spring of 2007 and may have caused this tree to move, or at least tilt, downslope. This movement may have affected the interpretation of the data along this transect, although the tree-displacement transect data from both sites supported the

creepmeter data in indicating land-surface movement near the active scarp and further upslope.

Rainbow Creek Landslide

Most of the trees along the western-most transect were adjacent to an ephemeral and quickly eroding stream channel, and many of these trees were incrementally lost over a period of 3 to 5 months as the slope continued to erode rapidly. The other two transects (central and eastern) at this landslide indicated the upper slope was slowly responding (inches per year) to erosion of the landslide face. Most of the trees were moving apart (positive movement of one tree in the central transect is plotted in Figure 3.9A), but some were moving closer to each other (negative movement of one tree in the eastern transect is plotted in Figure 3.9B). The trees with negative movement tended to lean uphill; several of these trees were anchored by their roots to the stable, upslope land surface such that the movement of the unstable, underlying soil caused these trees to tilt uphill. Many of these trees were later lost through slope failure, which ripped the remaining anchor roots and sent the trees toppling down the steep slope of the landslide. The average rate of positive movement of all trees along these two Rainbow Creek transects was 2.1 inches per year.

Rattlesnake Gulf Landslide

Only one tree-displacement transect was established at the Rattlesnake Gulf landslide (Figure 3.4) because trees within the landslide area were being selectively harvested in 2006-07. This transect was within the central and more-active part of the slide and recorded mostly positive movement, including the baseline tree. The average rate of movement along this transect over the 2-year study was 1.8 feet.

Figure 3.9. Tree movement along transects in the Rainbow Creek landslide area: (A) positive (increasing distance) movement, and (B) negative (decreasing distance) movement (note differing scales for 9A and 9B, and transect locations are shown in figs. 2 and 4, respectively).

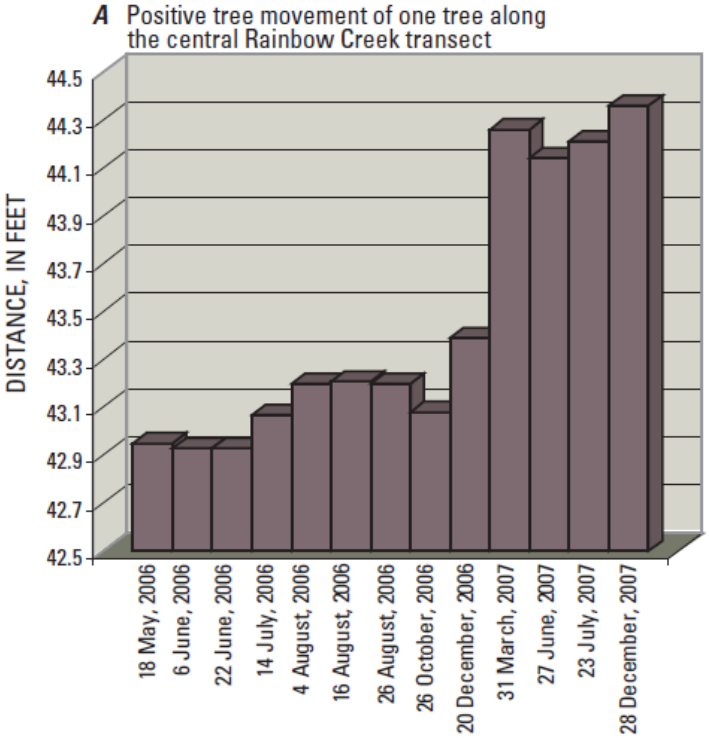
A Positive tree movement of one tree along the central Rainbow Creek transect
DISTANCE, IN FEET
44.5
44.3
44.1
43.9
43.7
43.5
43.3
43.1
42.9
42.7
42.5
18 May, 2006
6 June, 2006
22 June, 2006
14 July, 2006
4 August, 2006
16 August, 2006
26 August, 2006
26 October, 2006
20 December, 2006
31 March, 2007
27 June, 2007
23 July, 2007
28 December, 2007

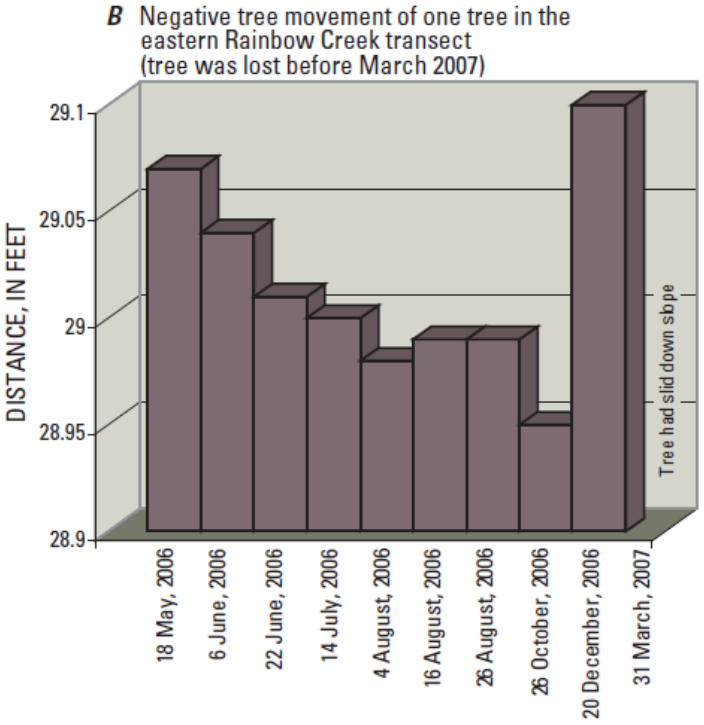
B Negative tree movement of one tree in the eastern Rainbow Creek transect (tree was lost before March 2007)
DISTANCE, IN FEET
29.1
29.05
29
28.95
28.9
18 May, 2006
6 June, 2006
22 June, 2006
14 July, 2006
4 August, 2006
16 August, 2006
26 August, 2006
26 October, 2006
20 December, 2006
31 March, 2007
Tree had slid down slope

Precipitation

Total precipitation on the Tully Valley floor in the first year (June 2006 through May 2007) was nearly 43 inches and in the second year (June 2007 through May 2008) was 40 inches. Precipitation in this part of New York is fairly uniform over the course of the year, except for occasional, high-intensity storms.

Ground-Water Levels

Two-inch-diameter wells were installed at both sites in August 2006. The well at the Rainbow Creek landslide (Figure 3.2) was augered adjacent to the creepmeter through 2.75 feet of weathered, unconsolidated clay, silt, sand, and gravel to unweathered material (dense, fine-grained silt and clay with stones). The well at the Rattlesnake Gulf landslide (Figure 3.4) was installed along the northwestern landslide scarp and was augered through 5.8 feet of unconsolidated clay, silt, and sand before encountering the unweathered fine-grained silt-clay soil.

Rainbow Creek Landslide

Ground-water levels at the Rainbow Creek landslide remained relatively stable from June 2006 through August 2007, after which they dropped and then sharply rebounded in mid-November 2007 (Figure 3.8A). The ground-water levels responded to individual precipitation and snowmelt events with little or no lag time. A perennial seep upgradient from the creepmeter and the well probably affected ground-water levels in this area and would account for the short lag time between a storm and a rise in ground-water level.

Rattlesnake Creek Landslide

Ground-water levels at the Rattlesnake Creek landslide generally fluctuated within a one foot interval, except from July through October 2007, when water levels sharply dropped more than four feet (Figure 3.8B). Ground-water levels appeared to

respond to storms within two to three days. Ground-water seepage in slump areas on either side of the well indicates the water in this well comes from upgradient areas.

Landslide activity in the Tully Valley since the late 1930's

The initial cause of the Rainbow Creek and Rattlesnake Gulf landslides is impossible to ascertain, but a review of aerial photographs from 1937, when the first aerial photos were taken in this part of New York State, indicate some landslide activity along the southern slope of Rattlesnake Gulf. Aerial photographs of the Rainbow Creek valley show no indication of landslides until the 1980s, although dense vegetation and the orientation of the photographs might mask earlier activity. A local resident who has lived next to Rainbow Creek most of his life reported that little landslide activity or sedimentation occurred in the Rainbow Creek channel along the eastern wall of the Tully Valley before the 1970s but recalled that a 30- to 40-foot waterfall over shale bedrock (Figure 3.10) just downstream from the current landslide area collapsed in the early 1970s. The resulting change in the stream channel could not be confirmed from the aerial photographs, but a narrow, 30-foot-high notch in the shale just downstream from the current landslide (Figure 3.10) marks the location of the former waterfall in the still-eroding stream channel. Coarse gravel, boulders, and fine-grained sediment behind (upstream from) this shale exposure are rapidly being eroded through the shale notch, causing an abrupt change in channel slope (generalized in Figure 3.11) upstream from the former waterfall.

The account by this resident and the physical evidence of the waterfall location indicate that landslide activity here was initiated by (1) failure of the shale bedrock at the waterfall, (2) the subsequent steepening of the upstream channel bed as streambed material eroded and moved downstream after the waterfall collapse, and (3) destabilization of the steep, fine-grained slopes along both sides of the eroding stream channel upstream from the waterfall during high-flow periods.

Figure 3.10. Location of the former bedrock waterfall along Rainbow Creek, downstream from the active landslide area.

Figure 3.11. Conceptual progression of degradation of the Rainbow Creek channel behind the bedrock waterfall which initiated landslide activity: A—plan view of the former and present stream channel with accompanying conceptual geologic section through the two channels; B—section view (B-B') of stream channel prior to failure of the waterfall; C—sectional view (B-B') of the stream channel in its current configuration, showing down-cutting of the glacial deposits which initiated ongoing landslide activity.

A Plan and cross-section views of Rainbow Creek channels

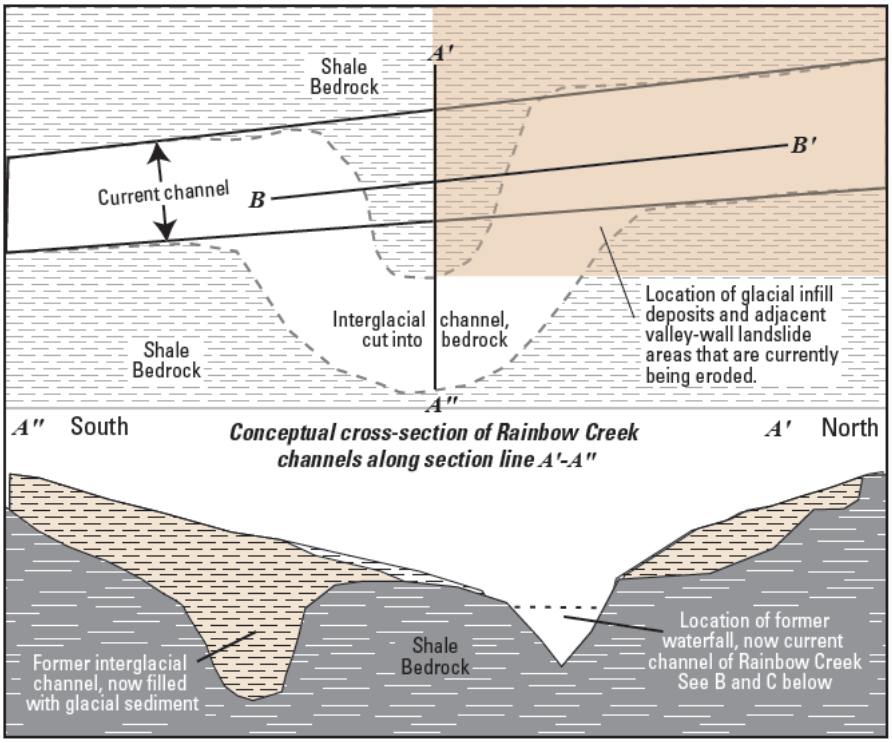

B Rainbow Creek prior to 1970s along section line *B-B′*

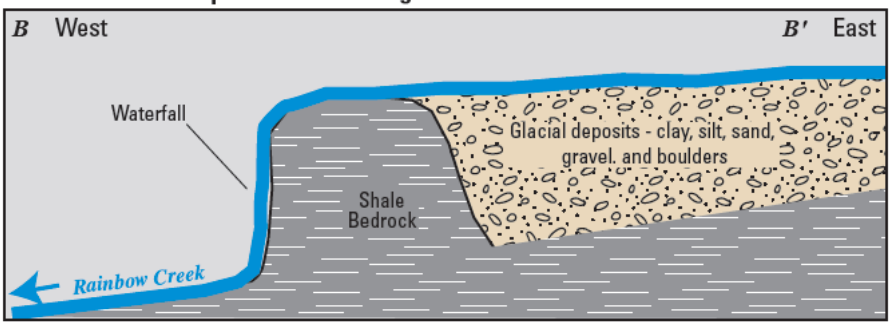

C Rainbow Creek today along section line *B-B′*

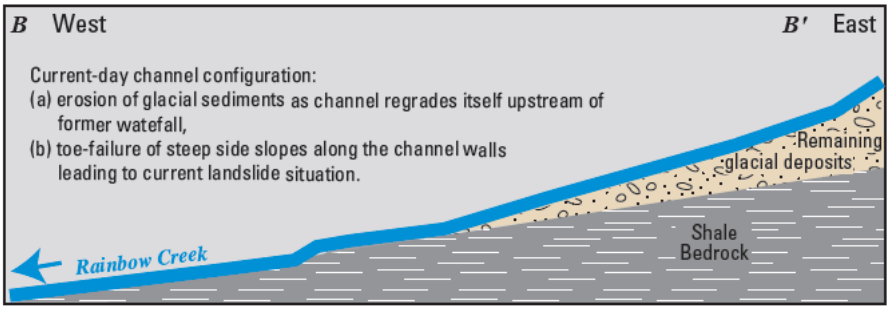

Landslides in Relation to Precipitation and Ground-Water Levels

Many factors can lead to landslides or can affect their extent and severity; among these factors are slope steepness, type of unconsolidated material, precipitation amount and intensity, hydrologic regime (streamflow characteristics), and water-table conditions. Individual storms can cause shallow slides of loose soil and rocks (Wieczorek and Sarmiento, 1988), whereas deep (rotational) slides of underlying material may not occur until days or months after a heavy storm (Varnes, 1978).

Rainbow Creek Landslide

The largest amount of movement at the Rainbow Creek landslide during the study occurred in November 2007, when the tree and landmass holding the measurement point for the creepmeter failed. The preceding summer was relatively dry, but several heavy storms in early November triggered a rapid rise in ground-water levels, which resulted in the displacement and eventual loss of the tree connected to the creepmeter. These November storms also caused a rapid increase in surface-water runoff, which quickly undermined the slope adjacent to the creepmeter landmass and contributed to the loss of the monitoring tree. Continued measurement of the remaining tree transects showed continued displacement along the upper slope of the Rainbow Creek landslide and the continued loss of trees on the remaining transects.

Rattlesnake Gulf Landslide

Several factors appear to have affected the landslide and soil displacement at Rattlesnake Gulf. The relatively rapid rate of soil movement at the location of the northwestern creepmeter coincided with wet months (Figure 3.8B), and the attendant rise in ground-water levels may have induced sliding as well as increased rates of stream erosion at the toe of the landslide below the creepmeter. In contrast, the center of this landslide is not adjacent to a major scarp but is upslope from an actively eroding landslide toe, and the displacement record for this central location (Figure

3.8B) suggests a longer response time for soil displacement here than at the northwestern location. For example, a large landslide in February 2008 blocked and continues to block the channel of Rattlesnake Gulf. As a result, land-surface movement is slowly propagating upslope to the center of the slide and was noted at the central creepmeter during the fall of 2008, even though ground-water conditions were relatively dry. This gradual upslope propagation of displacement from the stream channel and the movement of the baseline tree for the tree-measurement transect above the creepmeter support this hypothesis. The displacement and precipitation data (Figure 3.8B) also indicate, however, that shallow movement in the center of the landslide is facilitated by individual storms.

Except for the rapid slope failure at the Rainbow Creek creepmeter in November 2007, the northwestern Rattlesnake Gulf landslide scarp and the Rainbow Creek landslide scarp typically underwent the greatest displacement as the snowpack was melting and before tree 'leaf-out', which are typically the wettest months of the year, during which the steep, unstable soils on these slopes become saturated. The coarse-grained sediment within the rotated, laminated clays and silts exposed along scarps and stream channels in both valleys may also provide a path for infiltration of water into the landslides.

Geotechnical Properties of Rainbow Creek and Rattlesnake Gulf Landslide Soils

The geotechnical properties of soils provide an indication of the degree to which a soil is prone to movement. The Atterberg Limits test measures soil consistency in relation to its water content and defines the limits for four stages: solid, semi-solid, plastic, or liquid. A diagram of Atterberg Limits and indices is shown in Figure 3.12.

Soils from the Rainbow Creek and Rattlesnake Gulf landslides were sampled

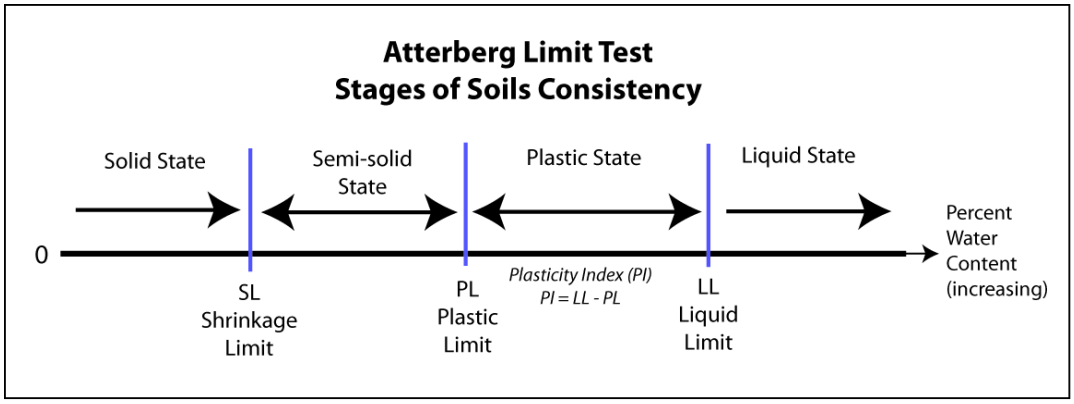

Figure 3.12. Atterberg limits for soil consistency.

in June 2007 for analysis of their geotechnical properties. Emphasis was placed on fine-grained soils (silt and clay) at each landslide, because the strength of this type of sediment is a primary factor in landslide-failure analysis. Sediment-size distribution for weathered and unweathered fine-grained sediment from each slide is reported in Table 3.1, and Atterberg limits and water content of each sample are reported in Table 3.2.

The numbers from this study were compared with Atterberg-limit testing results from the 1993 Tully Valley landslide (Burgmeier, 1998) and with geotechnical data from samples collected 30 to 104 feet below the floor of the Tully Valley along Onondaga Creek near Nichols Road (Kappel et al., 1996). The results of these nearby studies (Table 3.3) indicate the Atterberg limits for soils that blanket the side valleys are similar to those for soils on the Tully Valley floor. The only difference is the slightly greater water content for the valley-floor deposits, where the soils are saturated because the potentiometric surface within the clay is above land surface, whereas the landslide soils in the side-valley locations are partly drained.

Summary and Conclusions

Displacement of shallow soils at the Rainbow Creek landslide and the northwestern part of the Rattlesnake Gulf landslide was greatest during wet periods, and the largest displacement was at the Rainbow Creek creepmeter and in the northwestern part of the Rattlesnake Gulf landslide, probably as a result of the scarps above an unstable landslide toe that had been eroded by the adjacent stream. The center of the Rattlesnake Gulf landslide was most active after the failure of the lower slope; increased land-surface movement was noted at the centrally located creepmeter several months later. Ground-water levels at the weathered/unweathered soil interface of both landslides responded to precipitation and snowmelt within 2 or 3 days. Ground-water levels in scarps adjacent to the landslide toes were high in March 2007

Table 3.1. Grain-size distribution of landslide sediment from Rainbow Creek and Rattlesnake Gulf, Onondaga County, New York.

Sample source	Type of material, as a percent of total soil mass			
	Gravel	**Sand**	**Silt**	**Clay**
Rattlesnake Gulf				
Weathered soil	22	12	48	18
Unweathered soil	0	2	34	64
Rainbow Creek				
Weathered soil	6	44	33	17
Unweathered soil	2	2	54	42
Landslide soil	28	17	32	23

Table 3.2. Atterberg limits and indices for weathered- and unweathered-soil samples from Rainbow Creek and Rattlesnake Gulf, Onondaga County, N.Y.

Sample source	Water content (percent)	Plastic limit	Liquid limit	Plasticity index
Rattlesnake Gulf				
Weathered soil	17.1	23	33	10
Unweathered soil	34.1	26	45	19
Rainbow Creek				
Weathered soil	32.5	28	38	10
Unweathered soil	21.1	22	36	14
Landslide soil	8.9	18	32	14

Table 3.3. Average water content, plastic limits, liquid limits, and plasticity indices for soil samples from Rainbow Creek, Rattlesnake Gulf, and Tully Valley in Onondaga County, N.Y.

Sample source	Average water content (percent)	Average plastic limit	Average liquid limit	Average plasticity index
Rainbow Creek landslide soil	26.8	25.0	37.0	12.0
Rattlesnake Creek landslide soil	25.6	24.5	39.0	14.5
1993 Tully Valley landslide soil	32.5	20.6	36.2	15.6
Tully Valley floor soil (composite)	32.7	23.4	37.2	13.8

in response to infiltration of snowmelt and spring precipitation. Displacement at the center of the Rattlesnake Gulf landslide may be facilitated by soil movement that begins at the toe of the landslide and may take several months to propagate upslope to the center of the landslide. Most of the soil material at both landslides is silt and clay, and the deeper, unweathered material at both sites has substantially less coarse-grained sediment than the weathered samples.

REFERENCES

Burgmeier, P. 1998. A geotechnical investigation of the 1993 Tully Valley landslide: Syracuse, N.Y., Department of Engineering, Syracuse University, unpublished Master of Science Thesis. 55 pp.

Fickies, R.H. 1993. A large landslide in Tully Valley, Onondaga County, New York: Association of Engineering Geologists News. 36(4): 22-24.

Jäger, Stephan, and Wieczorek, G.F. 1994. Landslide susceptibility in the Tully Valley area, Finger Lakes Region, New York. U.S. Geological Survey Open-File Report 94-0615, 1 plate.

Kappel, W.M., and Teece, M.A. 2007. Paleoenvironmental assessment and deglacial chronology of the Onondaga Trough, Onondaga County, New York: U.S. Geological Survey Open-File Report 2007-1060. 12 pp.

Kappel, W.M., Sherwood, D.A., and Johnston, W.H. 1996. Hydrogeology of the Tully Valley and characterization of mudboil activity, Onondaga County, New York: U.S. Geological Survey Water-Resources Investigations Report 96-4043. 71 pp.

Morales-Muniz, P. J. 2000. The Tully Valley flowslide of 1993, Lafayette, New York: unpublished Master's Thesis, Purdue University, West LaFayette, Indiana. 176 pp.

Pair, D.L., Kappel, W.M., and Walker, M.S. 2000. History of landslides at the base of Bare Mountain, Tully Valley, Onondaga Valley, New York: U.S. Geological Survey Fact Sheet 190-99. 6 pp.

Rogers, W. B. 1991. The missing record - Tertiary Period, *In* Isachsen, Y.W., Landing, E., Lauber, J.M., Rickard, L.V., and Rogers, W.B., Eds. Geology of

New York - A simplified account: Albany, N.Y., New York State Museum, Educational Leaflet 28: 157-160.

Varnes, D.J. 1978. Slope movement types and processes, Landslides - analysis and control: *in,* Schuster, R.L., and Krizek, R.J. eds., Washington, D.C., National Academy of Science, Transportation Research Board Special Report 176: 12-33.

Wieczorek, G.F., Negussey, Dawit, and Kappel, W.M. 1998. Landslide hazards in glacial lake clays-Tully Valley, New York: U.S. Geological Survey Fact Sheet 013-98, 4 pp.

Wieczorek, G.F., and Sarmiento, J. 1988. Rainfall, piezometric levels and debris flows near La Honda, California in the January 3-5, 1982, and other storms between 1975 and 1983, *in* Ellen, S.D., and Wieczorek, G.F., eds., Landslides, floods, and marine effects of the January 3-5, 1982 storm in the San Francisco Bay region, California: U.S. Geological Survey Professional Paper 1434: 48-62.

CHAPTER 4

DENDROGEOMORPHIC ASSESSMENT OF THE RATTLESNAKE GULF LANDSLIDE IN THE TULLY VALLEY, ONONDAGA COUNTY, NEW YORK*

Abstract

Dendrogeomorphic techniques were used to assess soil movement within the Rattlesnake Gulf landslide in the Tully Valley of central New York during the last century. This landslide is a postglacial, slow-moving earth slide that covers 23 acres and consists primarily of rotated, laminated, glaciolacustrine silt and clay. Sixty-two increment cores were obtained from thirty hemlock (*Tsuga canadensis)* trees across the active part of the landslide and from three control sites to interpret the soil-displacement history. Annual growth rings were measured and reaction wood was identified to indicate years in which ring growth changed from concentric to eccentric, on the premise that soil movement triggered compensatory growth in displaced trees. These data provided a basis for an "event index" to identify years of landslide activity over the 108 years of record represented by the oldest trees. Event-index values and total annual precipitation increased during this time, but years with sudden event-index increases did not necessarily correspond to years with above-average precipitation. Multiple-regression and residual-values analyses indicated a possible

---

*Originally published as: Tamulonis, K.L., and Kappel, W.M. 2009. Dendrogeomorphic assessment of the Rattlesnake Gulf landslide in the Tully Valley, Onondaga County, New York. U.S. Geological Survey Scientific Investigations Report 2009–5134. 18 pp. Available online at *http://pubs.usgs.gov/sir/2009/5134/*. Reprinted with permission of individual copyright owners.

correlation between precipitation and movement within the landslide and a possible cyclic (decades-long) tree-ring response to displacement within the landslide area from the toe upward to, and possibly beyond, previously formed landslide features. The soil movement is triggered by a sequence of factors that include (1) periods of several months with below-average precipitation followed by persistent above-average precipitation, (2) the attendant increase in streamflow, which erodes the landslide toe and results in an upslope propagation of slumping, and (3) the harvesting of mature trees within this landslide during the last century and continuing to the present.

Introduction

The Tully Valley represents the upper (southern) 6 miles of Onondaga Creek in Onondaga County, New York. (Figure 4.1), and has had a history of landslides (Pair et al., 2000; Fickies, 1993; Jäger and Wieczorek, 1994). Two of its tributary valleys, the Rainbow Creek and Rattlesnake Gulf, drain forested uplands and enter the main stream from the east and west, respectively; each tributary valley contains an area with active landslides (Figure 4.1). The landslide material within the western tributary valley, Rattlesnake Gulf (the focus of this report), covers 23 acres and consists of unconsolidated, laminated, glaciolacustrine clay and silt that has undergone massive movement and (or) rotation in the past. Information on the age and history of this landslide would provide a basis for interpretation of current landslide processes and possibly could be used elsewhere in the Tully Valley. A technique commonly used to study landscape evolution that occurs through such processes as floods, landslides, and debris flows (Sigafoos, 1964; Hupp, 1983; Hupp et al, 1987) is dendrogeomorphology, a term derived from dendrochronology (the science of dating changes in the environment through tree-ring analysis) and geomorphology (the science of landform configuration and change). Dendrogeomorphology is based on the premise that landmass movement, expressed as slope failure, can cause trees to tilt,

Figure 4.1. Physiographic features of Tully Valley, Onondaga County, New York with landslide, rain gage, and tree sample locations.

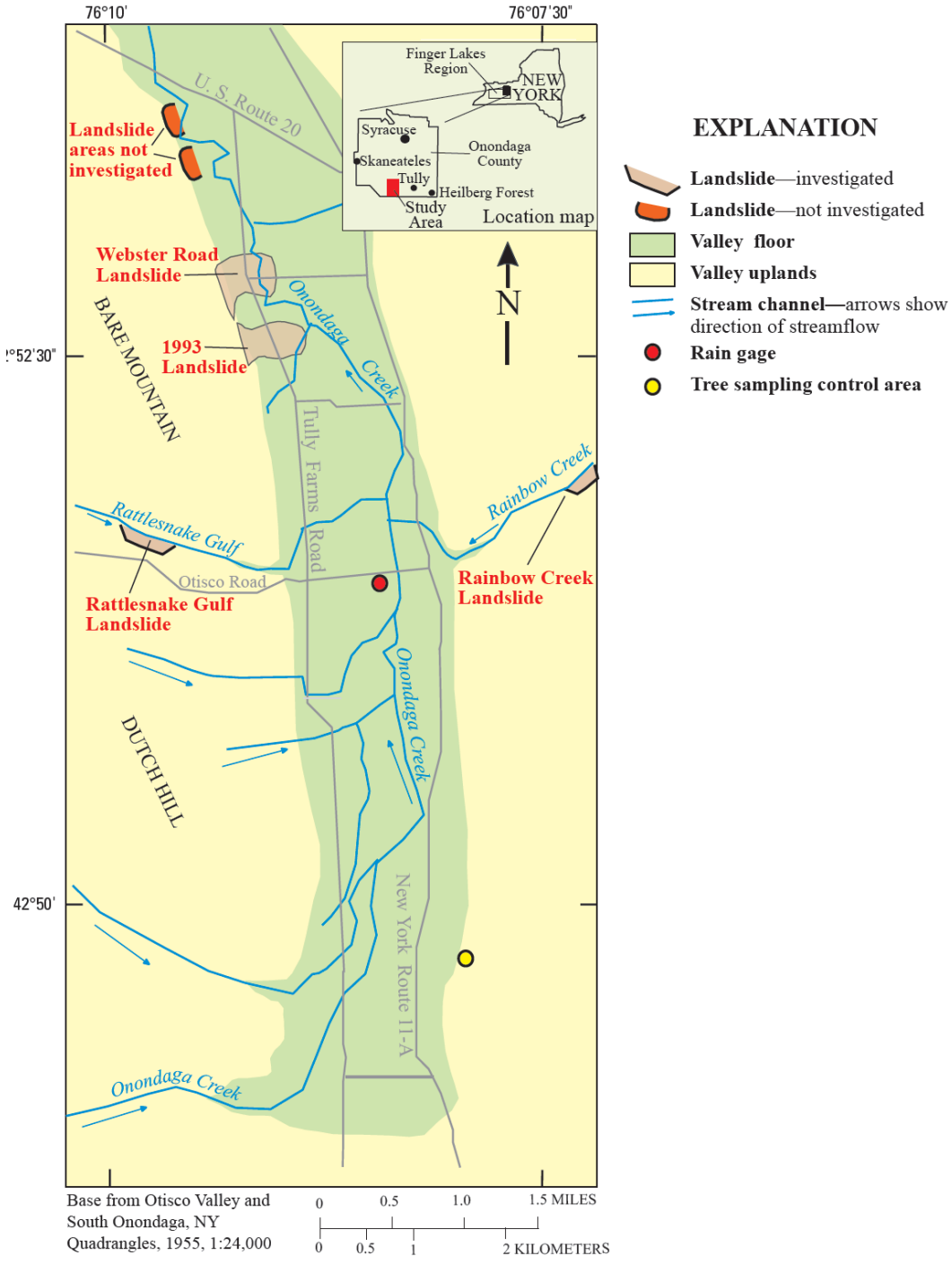
76°10'
76°07'30"
42°52'30"
42°50'
U. S. Route 20
Landslide areas not investigated
Webster Road Landslide
1993 Landslide
BARE MOUNTAIN
Onondaga Creek
Tully Farms Road
Rattlesnake Gulf
Otisco Road
Rattlesnake Gulf Landslide
Rainbow Creek
Rainbow Creek Landslide
DUTCH HILL
Onondaga Creek
New York Route 11-A
Onondaga Creek
Finger Lakes Region
NEW YORK
Syracuse
Skaneateles
Tully
Onondaga County
Heilberg Forest
Study Area
Location map
N
EXPLANATION
Landslide—investigated
Landslide—not investigated
Valley floor
Valley uplands
Stream channel—arrows show direction of streamflow
Rain gage
Tree sampling control area
Base from Otisco Valley and South Onondaga, NY Quadrangles, 1955, 1:24,000
0 0.5 1.0 1.5 MILES
0 0.5 1 2 KILOMETERS

which in turn can trigger a response in tree growth that is seen as an alteration in the thickness of new wood added around the trunk yearly to compensate for the shift away from vertical. The tree rings formed during the years in which tilting occurs are thicker on the downward facing side (of hemlock trees in this study) rather than on the upward facing side, and this asymmetry indicates the years in which the land movement occurred. Therefore, the dendrochronology of the Rattlesnake Gulf landslide may provide information on soil movement within this landslide during the life of the oldest trees, which have stood for more than 100 years, and supports geomorphic evidence gained from nearby landslide studies that the development and movement of a landslide are determined by a combination of environmental factors. For example, a rise in ground-water levels from prolonged precipitation increases pore-water pressure in clay interbeds and may thereby facilitate soil movement on affected slopes (Hupp, 1983; Pair et al, 2000; Lollino et al., 2002; Lollino et al., 2006). The increased pore-water pressure in landslides in response to rising ground water may occur immediately or it may lag by hours to several days (Lollino et al., 2006) or by months to years (Ibsen and Casagli, 2004), depending on the geology and hydrology of a particular site.

Estimation of the potential for current and future landslide activity at this and nearby locations requires information on (1) the frequency and severity of landslides as indicated by the tree-ring analyses, (2) the composition of the soils (weathered and unweathered) that form the landslide material, and (3) interaction among precipitation, ground-water levels, and the landslide material.

In 2006, the U.S. Geological Survey, in cooperation with the Onondaga Lake Partnership and the Onondaga Environmental Institute, began a two year study to evaluate the cause and progression of landslides in two tributary valleys to the Tully Valley. This report (1) describes the physiographic setting of the Rattlesnake Gulf

landslide and the geomorphic processes that shaped it, (2) explains the application of dendrogeomorphic techniques to interpret the history of the slide during the last century, and (3) summarizes the probable causes of landslide movement at this location.

Physiography of the Tully Valley

The Tully Valley is a six mile long glacial trough at the head of Onondaga Creek, which flows 15 miles northward to the city of Syracuse (Figure 1). Multiple glacial advances and retreats between 1.6 million and 11,000 years ago (Rogers, 1991) widened and deepened the river valleys of New York and left behind deposits of clay, silt, sand, gravel, and till of varying thickness on the sides and floors of these valleys (Kappel and Miller, 2003). The last major ice advance in central New York was about 14,000 years before present (B.P.), and its eventual retreat northward about 11,000 years B.P. resulted in the deposition of unconsolidated material that blocked the southern (upper) ends of the river valleys. Glacial meltwater filled these valleys to form proglacial lakes; layers of silt and clay gradually accumulated on the floor of these lakes, and streams of meltwater from the retreating ice deposited a variety of sediments along the floors and sides of the tributary valleys. One of these tributary valleys is the Rattlesnake Gulf valley, about five miles northwest of the village of Tully (Figure 4.1).

In April 1993, the largest landslide in New York since the early 1900s occurred on the west wall of the Tully valley (Fickies, 1993, Pair et al., 2000; Figure 4.1). Debris from this landslide covered about 50 acres and destroyed several homes (Pair et al., 2000); it also buried a 1,400-foot length of Tully Farms Road (Figure 4.1). Evidence of two other landslides, one overlying the other, was found just north of the 1993 landslide near Webster Road (Figure 4.1); the lower landslide has been dated at 11,200 calibrated years before present (Cal BP years), and the other at 7,000 Cal BP

years (Kappel and Teece, 2007). These slides are much older than the Rattlesnake Gulf landslide and the process of landslide movement appears to be much different in regard to their geographic position at their respective locations.

Rattlesnake Gulf Landslide

The Rattlesnake Gulf landslide is on the south slope of Rattlesnake Gulf and covers about 23 acres (Figure 4.2). An older, larger landslide lies between altitudes 1,250 and 750 feet on the south slope of Rattlesnake Gulf (Jäger and Wieczorek, 1994), and several landslide scars are visible on the bedrock wall of the north slope, directly opposite the active landslide. The current landslide, between altitudes 950 and 740 feet, consists primarily of rotated, laminated silt and clay that dips steeply to the southwest. The clay was deposited in a proglacial lake that occupied the Rattlesnake Gulf valley west of the glacial ice mass in the Tully Valley.

Shallow-soil displacement (movement) occurred adjacent to a steep scarp on the northwest side of the landslide area, and shallow displacement and slump propagation from the toe of the slide upwards into and beyond the central part of the landslide occurred during this study (July 2006 through June 2008) (Figure 4.3). Ground-water levels were recorded adjacent to the scarp during that time, and precipitation data were collected from a rain gage on the floor of the Tully Valley (Figure 4.1). The shallow-soil displacement roughly coincided with snowmelt and rainstorms and with the attendant rises in ground-water levels that lagged these precipitation events by as much as 2 days (Tamulonis et al., 2009).

Shallow-soil displacement is greatest in the northwestern part of the landslide, where scarps are oversteepened as a result of erosion by the stream. Shallow-soil displacement at the center of the landslide area may be facilitated by sustained high ground-water levels as well as by the slow upslope propagation of shallow stress

Figure 4.2. Rattlesnake Gulf orthoimagery with 100-foot contours, showing the location of current landslide areas, scarps, sampled trees, creepmeters, and a ground-water-level monitoring well in Onondaga County, New York (location is shown in Figure 4.1). Based on New York State Orthoimagery Program, 2004, Universal Transverse Mercator Projection, Zone 18.

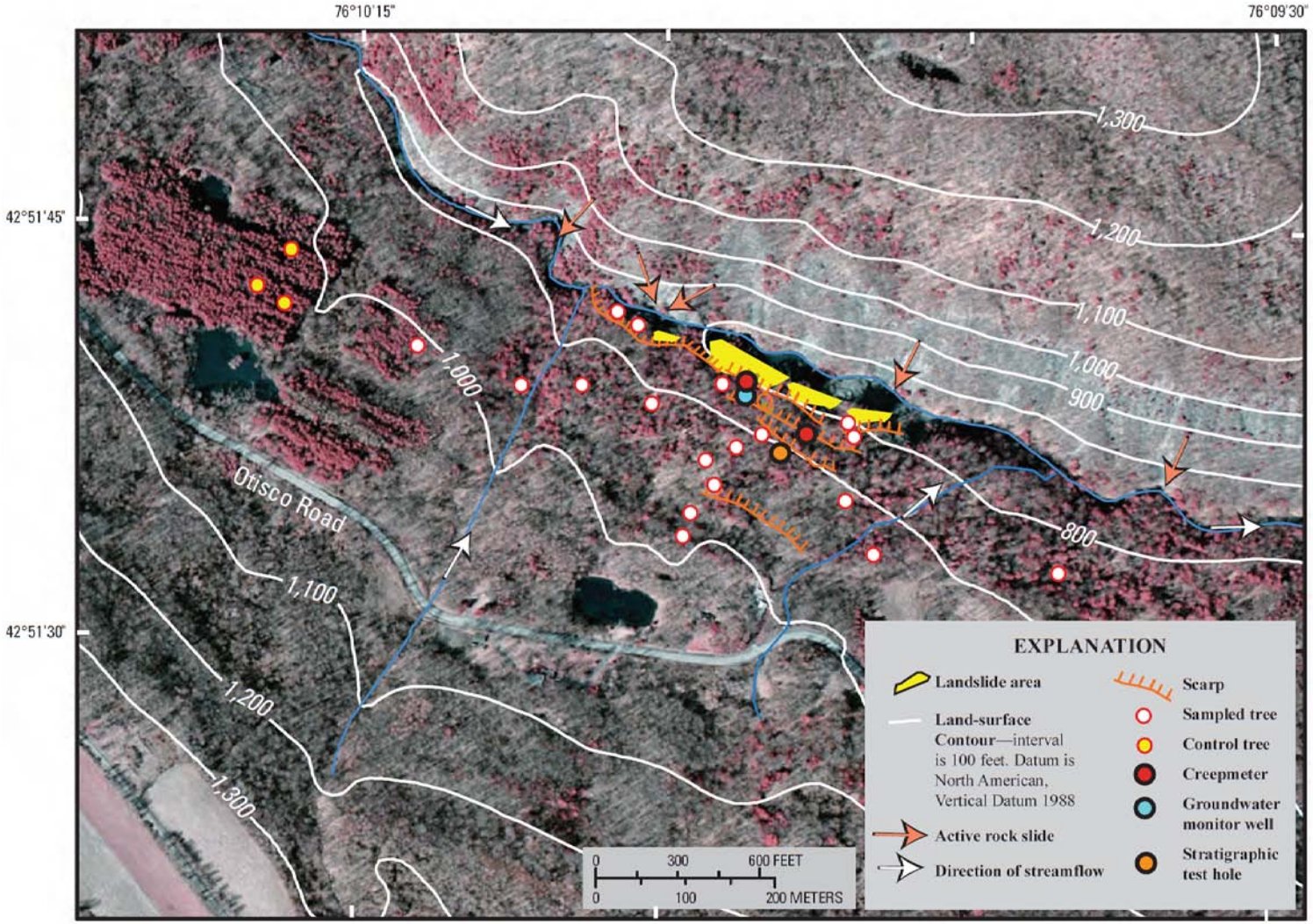
76°10'15"
76°09'30"
42°51'45"
42°51'30"
1,300
1,200
1,100
1,000
900
800
Otisco Road
0 300 600 FEET
0 100 200 METERS
EXPLANATION
Landslide area
Land-surface Contour—interval is 100 feet. Datum is North American, Vertical Datum 1988
Active rock slide
Direction of streamflow
Scarp
Sampled tree
Control tree
Creepmeter
Groundwater monitor well
Stratigraphic test hole

Figure 4.3. Cumulative creepmeter displacement and precipitation in relation to ground-water level within the Rattlesnake Gulf landslide area from June 2006 through June 2008 (Location shown in Figure 4.2).

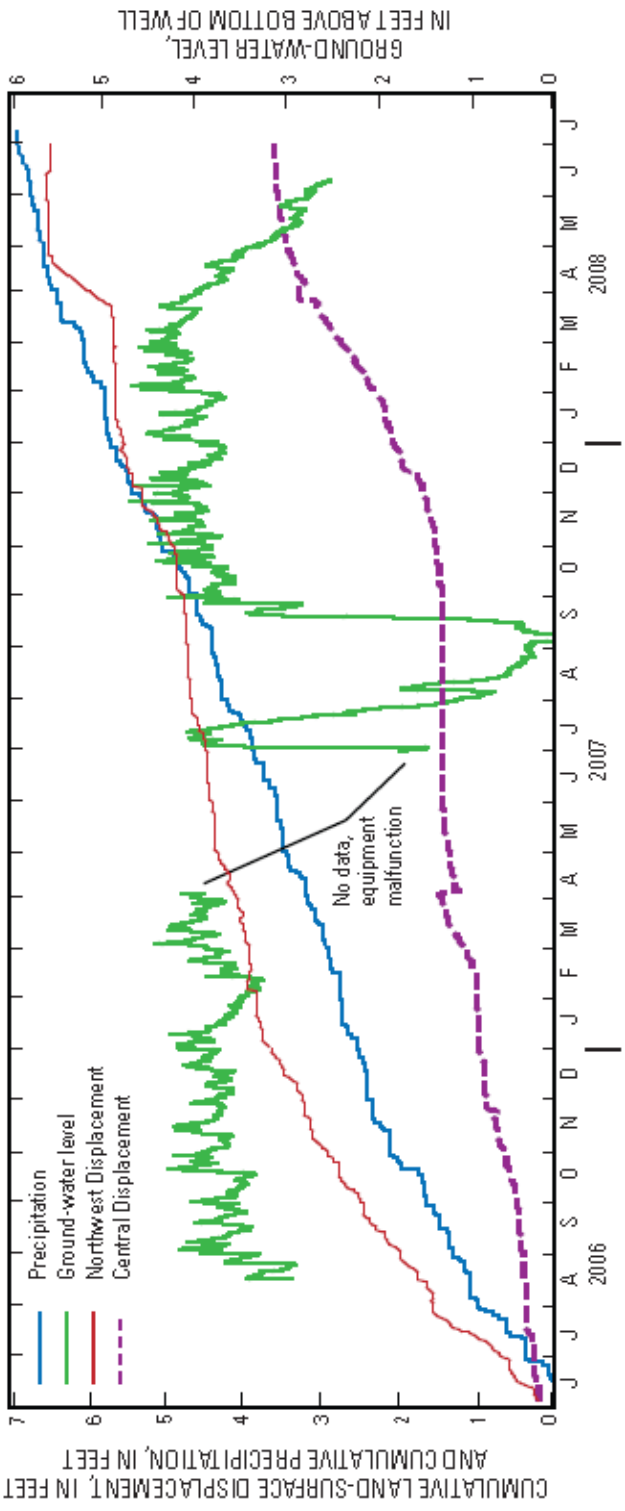
CUMULATIVE LAND-SURFACE DISPLACEMENT, IN FEET
AND CUMULATIVE PRECIPITATION, IN FEET
GROUND-WATER LEVEL,
IN FEET ABOVE BOTTOM OF WELL
Precipitation
Ground-water level
Northwest Displacement
Central Displacement
No data,
equipment
malfunction
2006
2007
2008

release from the toe of the slope up and into the center of the landslide (Tamulonis et al., 2009).

Surface water in the landslide area drains mostly into two channels along the western and eastern sides of the landslide where discharge varies seasonally. Ground water also collects in depressions along scarp areas and within the slide mass. The water table at a monitoring well installed on the northwestern scarp of the landslide (Figure 4.2) averaged less than 2 feet below land surface during the study. Forest cover at the site is mostly oak (*Quercus* L. sp.) and maple (*Acer* L. sp.); the understory is mostly Eastern hemlock (*Tsuga canadensis*) and tulip poplar (*Liriodendron tulipifera*). The landslide area has been logged in the past and was selectively cut in 2007. Average annual precipitation, as recorded at long-term meteorologic stations at Skaneateles, New York, and Tully Forest, New York (both within a 16 mile radius of the study site), is 40.2 inches per year, and the wettest months are usually May, June, and July, when monthly average precipitation is 3.5 to 4.0 inches.

Tree Sampling and Data Collection

Tree-ring widths from 18 sampled trees in the landslide area and from 12 trees in thre control areas: adjacent to the Rattlesnake landslide, adjacent to the Rainbow Creek landslide, and near the southeastern end of the Tully Valley (Figure 4.1) were measured, and comparisons of reaction-wood thickness were made to identify the years of growth-rate change at the landslide.

Geotropism and Reaction Wood

Tropism is the orientation assumed by an organism through turning, curving, or differential growth in response to a stimulus. *Geotropism* is the response of a plant to gravity. Tree growth under normal conditions is vertical, against the pull of gravity, and produces nearly concentric rings around the center of a tree trunk. A change in a tree's angle from vertical, such as through persistent high wind, bending beneath the

weight of a fallen tree, or soil erosion or earth movement at the roots, typically results in eccentric (asymmetrical) tree-ring growth and the production of reaction wood as extra ring thickness on one side of the tree trunk as it tries to regain vertical growth. Reaction wood is produced by the cambium, the thin layer of growing tissue around a tree, just inside the bark. Reaction wood in coniferous (evergreen) trees is termed "compression" wood and is found on the downward facing side of a tilted tree (Figure 4.4), whereas reaction wood in deciduous trees (those that lose their leaves each year) is called "tension" wood and is found on the upward facing side of a tilted tree (Aestello, 1971; Schroeder, 1980). Counting and measuring tree-ring widths reveals the date of tilting (Aestello, 1971).

Methods

A total of 34 increment cores and tree sections were collected from 18 *Tsuga canadensis* sp. (Eastern hemlock) trees within the landslide area. Sample-collection transects were made parallel to the active-landslide slope and perpendicular to it (Figure 4.2); trees with visible bends in the trunk (an indication of soil movement) were also sampled, regardless of their location. Samples from affected trees were collected at the bend in the trunk, where reaction-wood growth (Figure 4.4) was expected to be greatest, and samples from trees not obviously affected by soil movement were collected 4.5 feet above the ground. Of the 30 trees sampled, 13 had visibly tilted trunks; the remaining 17 did not. Trees disturbed by other processes, such as wildlife browsing, tilting from the weight of fallen trees, or human factors such as vehicle damage during timber harvesting, were not sampled, although the presence of such disturbance indicates that factors other than landslides may have caused some of the tilting. Generally, two increment borings were collected from each tree: one on the upslope side, and one on the downslope side. In addition, an entire cross section was recovered as a continuous core from one tree and one entire cross-

section was collected from another tree because a complete cross section reveals the asymmetry of the tree-ring pattern, as well as differences in tree-ring widths from one radius to the next throughout the section, and thereby provides a more reliable record of disturbance than the cores alone (Potter, 1969).

In addition, increment cores were collected from each of 12 control trees [*Tsuga canadensis sp.*] from three different control sites; three of these trees (eight cores) were adjacent to the Rattlesnake landslide, and three additional trees (eight cores) were collected adjacent to the Rattlesnake landslide in areas with surface slopes of less than 10% (Figure 4.2). The other six control trees (12 cores) were collected in a forested area 6.5 miles from the study site in the southeastern part of the Tully Valley (labeled "control area" in Figure 4.1). These six control trees were on a steep slope similar to that of the landslide, but the thin soils that blanket that slope are underlain by apparently stable shale bedrock. Trees growing on slopes typically have asymmetrical ("eccentric") growth patterns that are probably unrelated to surface displacement, but rather reflect the natural response to the slope itself and also to shade cast by neighboring trees (Phipps, 1974). Abrupt shifts in tree-ring eccentricity, however, are likely to be indicative of slope movement. Therefore, the purpose of the control trees was to distinguish eccentricity caused by non-landslide causes from that associated with soil displacement.

Core analysis entailed surface sanding to provide a clear surface for measurement of tree-ring (increment) thickness (resolution to 0.01 millimeter) on an increment-measurement machine under a binocular microscope with Corina software (Cornell University, 2008a). Each increment-core sample was measured twice, and duplicate measurements with greater than 3% discrepancy and cores with missing rings, were cross dated (Cleaveland, 1980) through comparison of a third measurement with the values from other samples (Cornell University, 2008b). Ring

Figure 4.4. Tree affected by soil movement at the Rattlesnake Gulf landslide, Onondaga County, New York: (A) 'J'-shaped profile of the tree and up- and down-slope sampling locations; (B) ring and reaction-wood growth pattern which creates the 'J'-shaped tree trunk; and (C) reaction wood on the downslope side of a tree representing years 2003-06 growth.

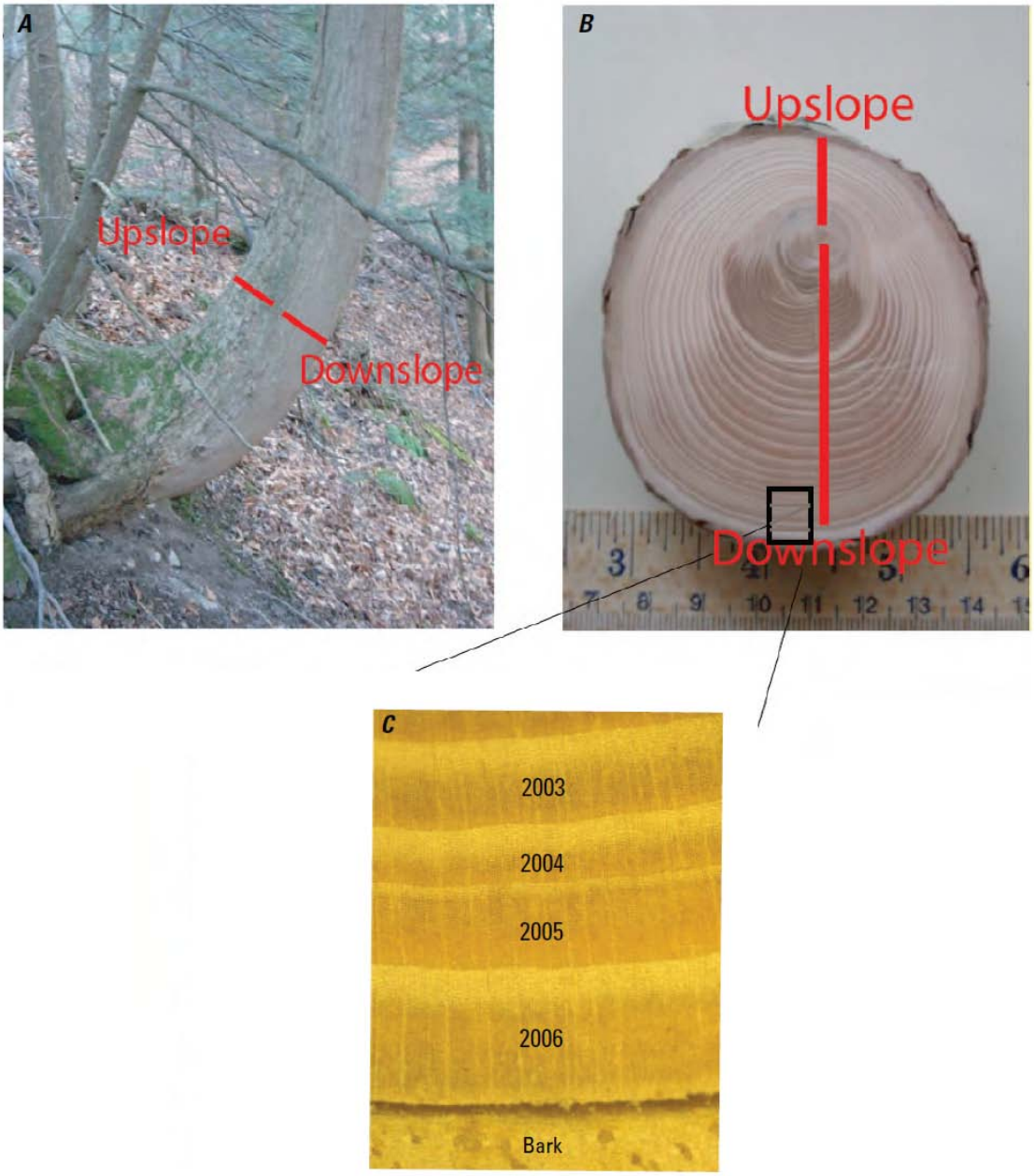
A
Upslope
Downslope
B
Upslope
Downslope
C
2003
2004
2005
2006
Bark

widths in cores from upslope and downslope sides of the same tree were plotted together. The date of the oldest tree ring, as indicated by both cores from a single tree, was A.D. 1877.

Reaction-wood growth and tree-ring eccentricity were the main indicators used in this analysis because the landslide is relatively slow moving. A ring-width ratio (larger width divided by the smaller width) was calculated for every year of each core sample for each tree, including the control trees. Of the 14 control trees, nine had a ring-width ratio greater than two, and none had a ratio greater than 3; therefore, a ring-width ratio greater than three was designated to distinguish landslide activity from normal hillside creep to which the control trees were probably exposed (Phipps, 1974). Years in which trees within the landslide area had a ring-width ratio of at least three were considered to be years when the tree moved (tilted) in response to some form of landslide movement. The largest ring-width ratio for any tree at the landslide was 77.7.

Shallow-soil-displacement data by creepmeter and tree-displacement transects collected in a companion study (Tamulonis et al., 2009) within the landslide indicate the landslide surface is moving continuously, although slowly (inches per year). The ring-width ratios, which represent many decades of tree growth, are consistent with continuous movement, as described by Phipps (1974), rather than indicative of a single, large event with progressive recovery of trees to a near-vertical position. This continuous movement is also supported by the presence of reaction-wood growth on both the upslope and downslope sides of individual trees within the landslide area. The presence of reaction wood in upslope cores of evergreen trees can be attributed to upslope tilting and was found in several of the landslide-area trees, whereas reaction wood on the downslope side is indicative of downslope movement, which is found in

most of the trees within the slide area. It should be noted though that not every year with a ring-width ratio greater than three has reaction-wood growth.

Event-Response Curve and Precipitation Data

An "event-response curve" (graph) of tree-ring data was first used by Schroeder (1978) to analyze landslide-movement frequency over time. The event (a landslide or soil displacement) causes a response (change in tree-ring growth pattern) in effected trees within a landslide; thus, the years indicated by anomalous tree-ring thickness can be plotted to reveal the timing of the displacement. Several studies worldwide have used this method to estimate the timing of debris flows and landslide displacement and to date historic avalanches (Bollschweiler et al., 2006; Stefanini, 2004; Potter, 1969). A difficulty with the Rattlesnake Gulf data is that timber harvesting in the landslide area since the late 19th century has decreased the number of old trees (and hence the amount of event-response data) backward through time and thereby decreased the numbers of early samples available. The earliest tree-ring indication of landslide activity was in 1877, but few trees dating from that period were available. The need for at least two trees (four sample cores) reflecting an event resulted in a starting date of 1899 for the Rattlesnake Gulf event-response curve, rather than 1877 (Figure 4.5A).

The graph of annual precipitation through time (Figure 4.5b) is based on data from two long-term meteorological sites rather than from the floor of the Tully Valley, which only has a 15-year precipitation record. Precipitation data from 1900 to 1997 were recorded at Skaneateles, New York, 16 miles northwest of the study area, and data from 1998 through 2007 were recorded in Tully Heiburg Forest, eight miles southeast of the study site. Linear-regression trend lines for annual precipitation data were calculated through a least-squares fit and indicate a slight upward trend over the

Figure 4.5. Event-response curve for Rattlesnake Gulf landslide, Onondaga County, New York: (A) Event-response curve, number of samples, and trend line; and (B). total annual precipitation and trend line for the period 1899 through 2007. (Location of rain gage shown in Figure 4.1.)

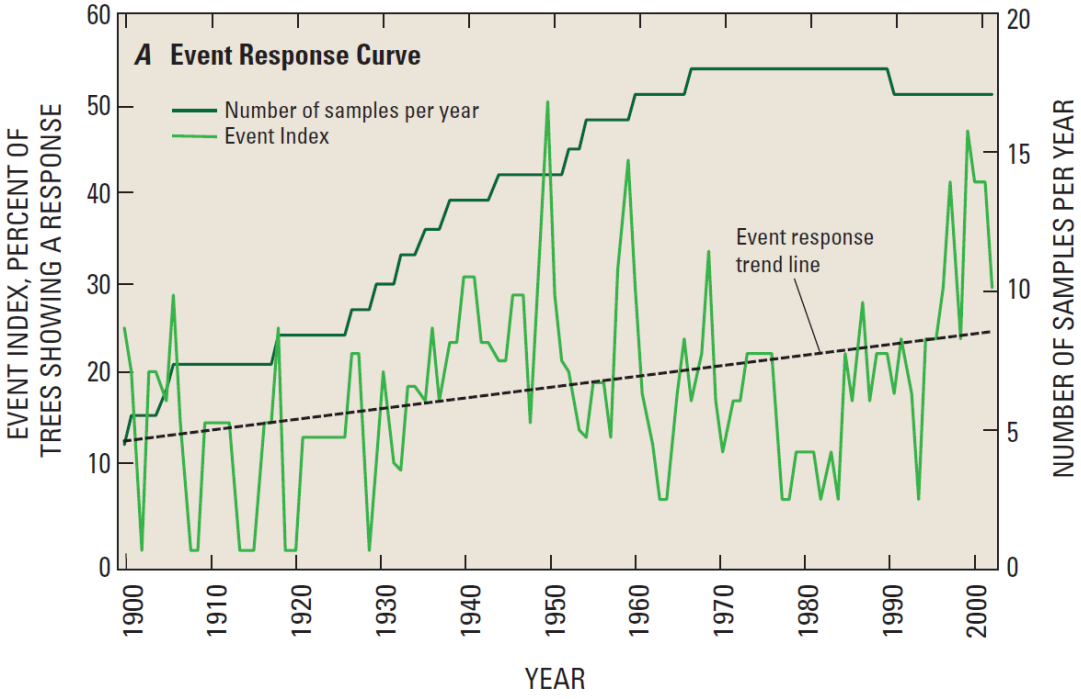
A Event Response Curve
Number of samples per year
Event Index
Event response trend line
EVENT INDEX, PERCENT OF TREES SHOWING A RESPONSE
NUMBER OF SAMPLES PER YEAR
YEAR
0
10
20
30
40
50
60
0
5
10
15
20
1900
1910
1920
1930
1940
1950
1960
1970
1980
1990
2000

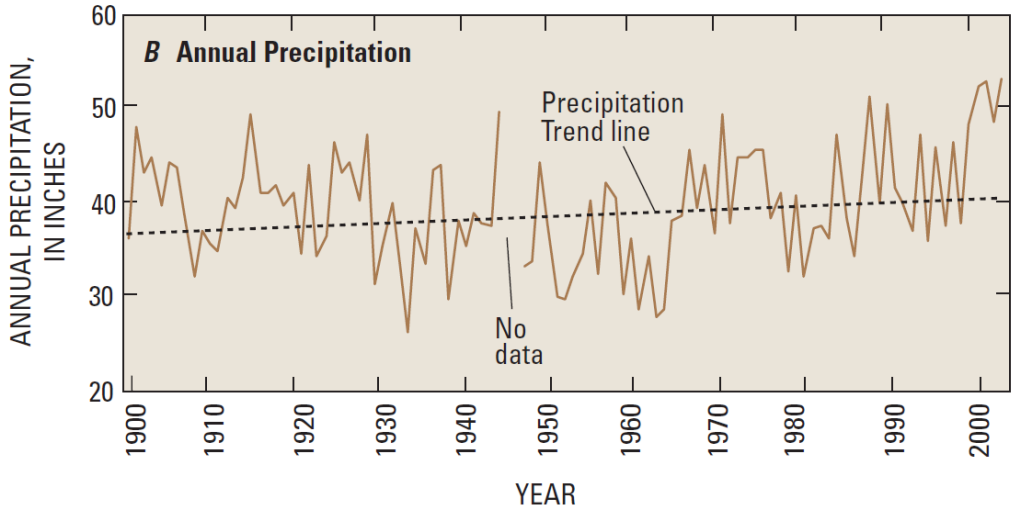
B Annual Precipitation
Precipitation Trend line
No data
ANNUAL PRECIPITATION, IN INCHES
YEAR
20
30
40
50
60
1900
1910
1920
1930
1940
1950
1960
1970
1980
1990
2000

107 year period of record (Figure 4.5b).

Historic Landslide Activity In Relation To Precipitation and Timber Harvesting

The Rattlesnake Gulf event-response curve (Figure 4.6A) indicates that the number of years without landslide activity (those years with an event index of zero; that is, no tree-ring indication of land movement) was lowest at the beginning of the analysis period. The 30 year period from 1899 through 1929 has nine years with an event-index value of zero, whereas the 76 year period from 1930 through 2008 has an index value greater than zero every year. Individual years with a large spike in the event index, as opposed to a gradual change over several years, are considered years with substantial landslide movement (Figure 4.6A).

Correlation with Short-Term Precipitation Patterns

A comparison of the 13 years with a sudden increase in event index (Figure 4.6A) with annual precipitation data (Figure 4.6B) indicates that seven of these 13 years had above-average precipitation (1905, 1916, 1918, 1927, 1990, 1998, and 2003), but the analysis did not adequately relate the event index to the annual amount of precipitation, therefore a different approach was taken to determine if another precipitation period and the event index could be better correlated.

Three- and Five-Year Moving Averages

A multiple linear regression equation was developed to reveal any correlation between the three or five year moving-average annual precipitation and event-index years. Results indicate that the three and five year moving averages were better correlated with the years of landslide movement than annual precipitation (Figure 4.6A), but this analysis did not fully correlate the precipitation data to landslide events at this site.

Figure 4.6. Event-response index and annual precipitation data for the Rattlesnake Gulf landslide, Onondaga County, New York for the period 1899 through 2008: (A) event index and years with substantial movement; and (B) total and average mean annual precipitation. (Location of rain gages is shown in Figure 4.1, inset map).

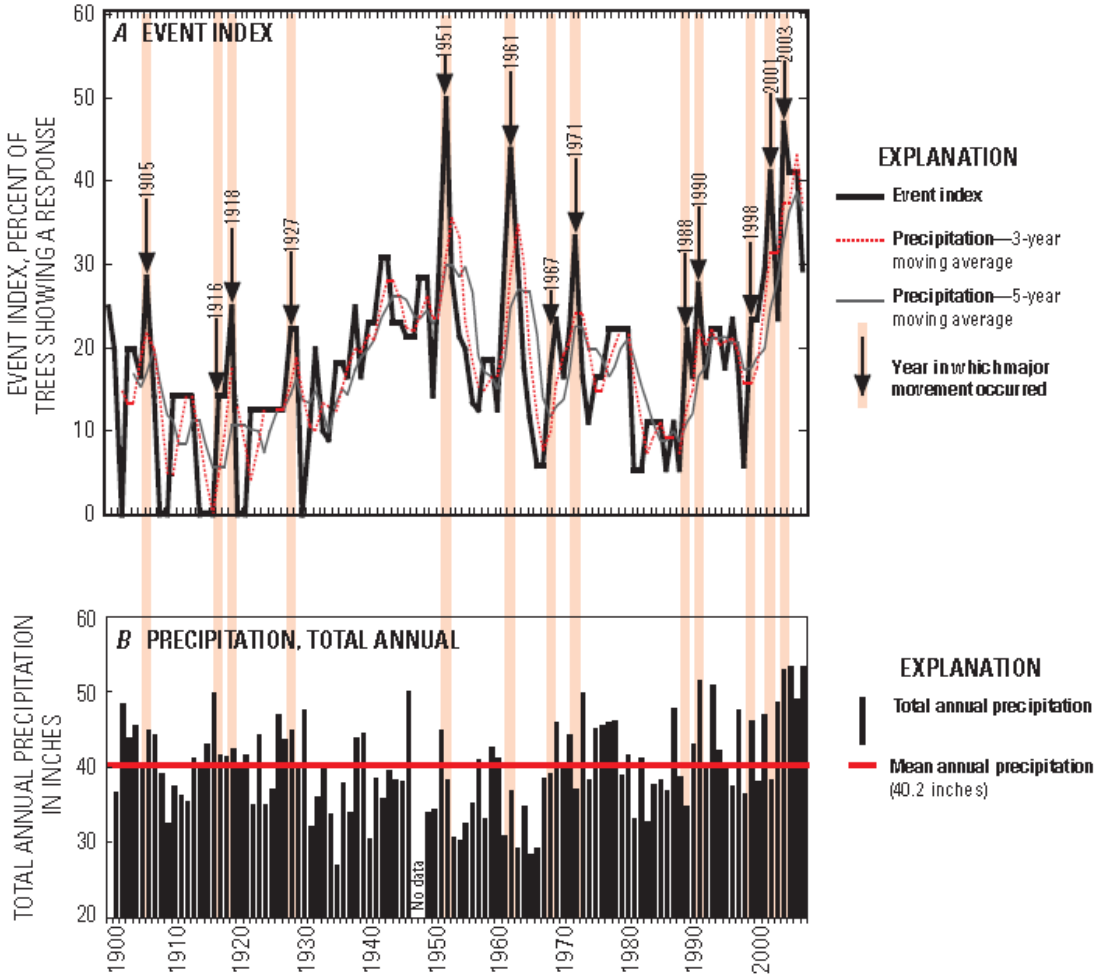
A EVENT INDEX
EVENT INDEX, PERCENT OF TREES SHOWING A RESPONSE
1905
1916
1918
1927
1951
1961
1967
1971
1988
1990
1998
2001
2003
EXPLANATION
Event index
Precipitation—3-year moving average
Precipitation—5-year moving average
Year in which major movement occurred
B PRECIPITATION, TOTAL ANNUAL
TOTAL ANNUAL PRECIPITATION IN INCHES
No data
EXPLANATION
Total annual precipitation
Mean annual precipitation (40.2 inches)

Dry Periods Followed by Wet Periods

Monthly precipitation prior to a substantial event response (landslide) was reviewed to determine if there was any correlation between periods of drought followed by above-normal precipitation as a possible cause for landslide movement. The monthly-precipitation assessment indicates that extended periods with below-average monthly precipitation followed by a month or more with above-average precipitation might be a trigger for landslide movement. The process may begin with the formation of desiccation cracks, which commonly develop in silty-clay soils during dry periods and can act as conduits through which precipitation readily flows downward to the poorly permeable, unweathered soil where it forms a water table that rises and saturates the overlying shallow, weathered soil. This saturation in turn decreases soil cohesion and allows thick masses of the loose, weathered soil to move downslope. This is consistent with a favored hypothesis for landslides in Tertiary sediments in New Zealand (McSaveny and Griffiths, 1987). Concurrent erosion of the landslide toe by high flows in the adjacent stream channel during relatively wet months may further destabilize the landslide material as hillside slumping propagates upslope. A comparison of wet periods that were preceded by a prolonged dry period in which a substantial event response occurred (Figure 4.6A) revealed that many, but not all, of the event years were consistent with this theory.

Long-Term Patterns Related to Precipitation and Timber Harvesting

A residual-value analysis of the linear-regression results discussed above was done to identify any long-term pattern of landslide occurrence and to discern whether such a pattern might also be related to long-term precipitation trends. The residual-value analysis entailed calculating the difference between observed event-index values and the index values predicted by the regression equation, then plotting the values (residuals) on a time scale through a periodic Fourier function (Figure 4.7).

Figure 4.7. Residual-value analysis curve of event index residuals for Rattlesnake Gulf in relation to a Fourier function curve for the period 1899 through 2006.

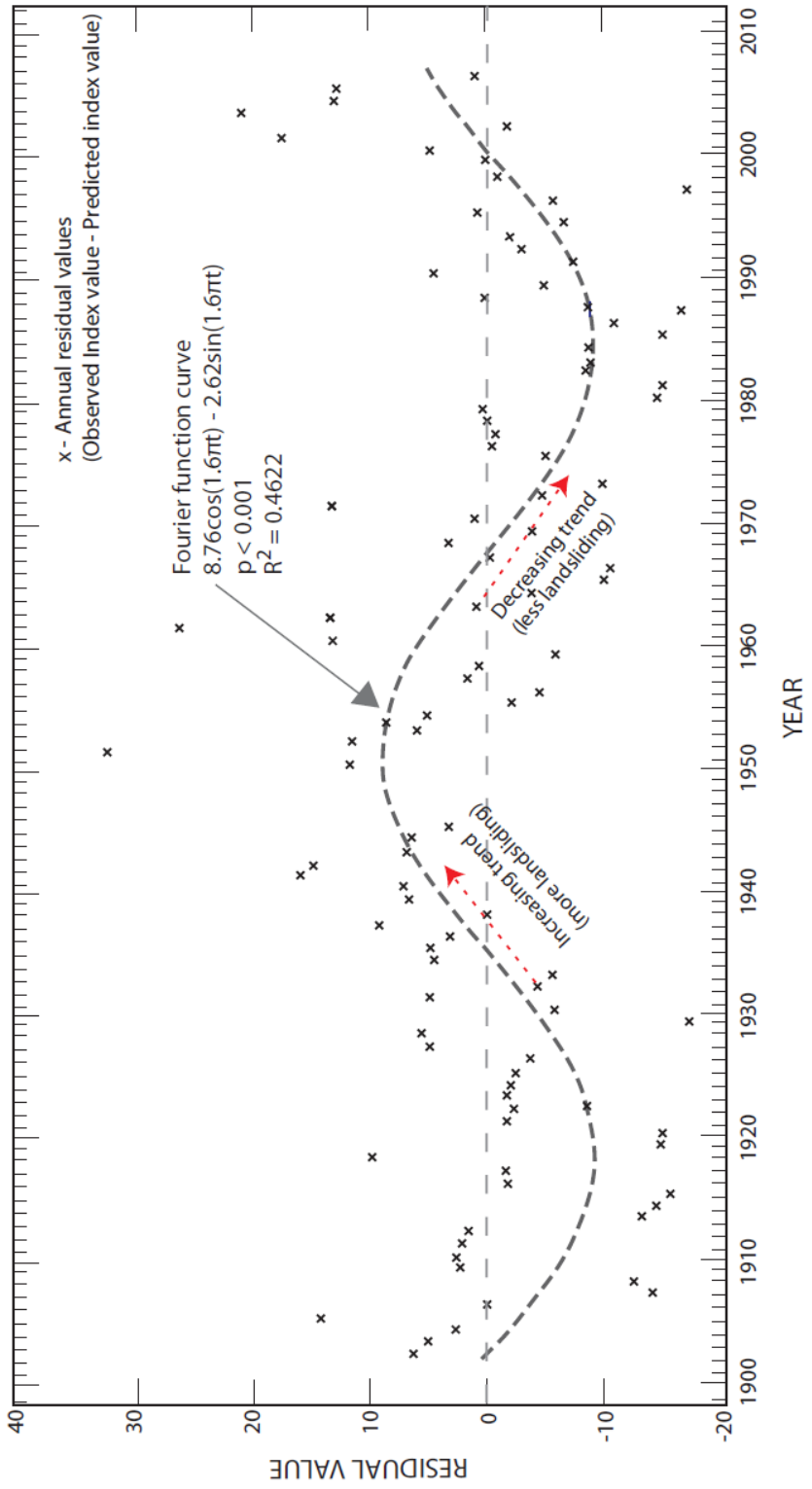
x - Annual residual values
(Observed Index value - Predicted index value)
Fourier function curve
8.76cos(1.6πt) - 2.62sin(1.6πt)
p < 0.001
R2 = 0.4622
Decreasing trend
(less landsliding)
Increasing trend
(more landsliding)
RESIDUAL VALUE
YEAR
40
30
20
10
0
-10
-20
1900
1910
1920
1930
1940
1950
1960
1970
1980
1990
2000
2010

Gradual Movement within Deep, Unweathered Soil

The residuals appear to indicate recurring decades-long cycles in landslide activity, wherein the frequency changes every 30 or so years (Figure 4.7). The residual values show an inflection point (change in slope) just before 1920, where the slope (representing landslide frequency) changes from downward to upward. The upward trend is consistent with slide occurrence recorded in the tree rings (see Event Response Curve, Figure 4.5A). This trend peaks just after 1950, then declines until the mid-1980's, when it reverses and again continues upward through the present. This cyclic pattern may be indicative of movement within the deep, unweathered, clayey soil of the landslide--movement that probably results from the continuous erosion of the landslide toe by the stream, as observed during several high flows during the study. This erosion of the toe results in an oversteepening of the slope, which in turn causes large blocks of soil to slump incrementally. The slumping slowly propagates uphill through the active landslide and possibly further upslope during the ensuing years and eventually results in a more stable slope configuration. Meanwhile, the shorter-term pattern of precipitation followed by shallow-soil movement above the unweathered layer continues.

Deforestation and Timber Harvesting

An additional factor in the longer-term cyclic nature of landslide activity in Rattlesnake Gulf is deforestation, which has occurred in this area over the last 150 years and is considered to be a landslide trigger in the western United States and the Philippines (De la Fuente et al., 2002). Tree roots reinforce the soil, and the presence or absence of trees also affects ground-water levels, which in turn affect soil moisture and soil cohesion. Thus, the cutting of forests sharply decreases evapotranspiration and typically allows ground-water levels to rise until forest cover is re-established,

while the gradual decay of roots destabilizes the hillside and further facilitates erosion of the soil and hillslope slumping.

About 80% of the original forests in central New York had been cleared for agriculture by the late 1800's (Singleton et al., 2001), but much of this region has undergone regrowth and reforestation over the past century; the oldest post-agriculture forests in central New York are about 75 years old (Singleton et al., 2001). The earliest aerial photographs of the Tully Valley (from 1937) show deforested areas upslope from several landslide areas, which were smaller than the present Rattlesnake Gulf landslide. By 1951, the deforested area surrounding the Rattlesnake Gulf landslide had expanded, but then substantially decreased through reforestation by 1978. The present landowner reported that trees within the landslide area were selectively harvested in the mid-1990s. Tree harvesting in the early part of the 20th century may have affected landslide activity in Rattlesnake Gulf at that time, and the increase in landslide activity in 2000 may coincide with the selective harvesting that began when the forest again reached maturity in the 1990s.

Summary

Dendrogeomorphologic study has provided a record of landslide activity that has occurred along Rattlesnake Gulf in the Tully Valley since 1899. Calculation of the event-response index (from trees whose rings indicate years of land movement) revealed 14 years during which landslide activity increased. Those years do not necessarily correspond to years with above-average precipitation, however, but the tree-ring data can be used to support the apparent correlation between years of increased landslide activity and months of extended drier than normal precipitation followed by months of greater than normal precipitation.

Slope stability is directly related to climate, soil composition and condition, and presence of forest cover. An event-response index curve, based on the tree-ring

data, identified the years in which landslide frequency was greatest, and a multiple linear regression analysis of the results, followed by an analysis of the residual values through a Fourier function, indicates that landslide activity is loosely related to the 3- and 5-year moving-average annual precipitation and that a lag-time of several years may occur between a period of heavy precipitation and landslide movement above the unweathered-soil layer. Residual-value assessment of the event-response index also indicates that the Rattlesnake Gulf landslide activity is cyclic and possibly related to large-scale, long-term deep landslide movement that propagates uphill from the toe of the landslide at the stream into and beyond previously formed landslide-movement features. Shallow landslide activity may also result from desiccation cracks that form during periods of below-average precipitation and provide conduits through which subsequent precipitation can flow downward to the poorly permeable, unweathered layer and saturate the overlying shallow, weathered soil. Still another destabilizing factor for landslide soils could be the harvesting of trees above and within the landslide area; the removal of trees decreases evapotranspiration and thereby allows ground-water levels to rise during the growing season, which increases soil saturation above the weathered-soil layer. The concurrent decay of roots may facilitate further hillslope movement.

REFERENCES

Aestello, J. 1971. Dendrochronological interpretation of geomorphic processes. Fennia. 105: 1-140.

Bollschweiler, M., Stoffel, M., and Schneuwly, D. 2006. Assessing the spacio-temporal debris-flow activity on a forested cone using tree-ring data. Iin Marui, H., Ed. Proceedings International Symposium "Disaster Mitigation of Debris Flows, Slope Failures and Landslides", September 25–27, 2006, Niigata, Japan: Tokyo, Universal Academic Press: 597–604.

Cleaveland, M.K. 1980. Dating tree rings in eastern United States, dendrology in the eastern deciduous forest biome: Blacksburg, Va., Virginia Polytechnic Institute and State University Publication FWS-2-80: 110-124.

Cornell University. 2008a. Corina: Ithaca, N.Y., Cornell Tree-Ring Laboratory, accessed May 2008 at *http://dendro.cornell.edu/corina/index.php*

Cornell University. 2008b. Laboratory procedures: Ithaca, N.Y., Cornell Tree-Ring Laboratory, accessed May 2008 at *http://dendro.cornell.edu/procedures.php*

De la Fuente, J., Elder, D., and Miller, A. 2002. Does deforestation influence the activity of deep-seated landslides? The Geological Society of America, Cordilleran Section meeting Abstracts with Programs – Geological Society of America. 34, 1 p.

Fickies, R.H. 1993. A large landslide in Tully Valley, Onondaga County, New York. Association of Engineering Geologists News. 36(4): 22-24.

Hupp, C.R. 1983. Geo-botanical evidence of late Quaternary mass wasting in block field areas of Virginia. Earth Surface Processes. 8: 439-450.

Hupp, C.R., Osterkamp, W.R., and Thornton, J.L. 1987. Dendrogeomorphic evidence and dating of recent debris flows on Mount Shasta, Northern California: U.S. Geological Survey Professional Paper 1396-B, 39 pp.

Ibsen, M.L., and Casagli, N. 2004. Rainfall patterns and related landslide incidence in the Porretta-Vergato region, Italy. Landslides. 1: 43-150.

Jäger, S., and Wieczorek, G.F. 1994. Landslide susceptibility in the Tully Valley area, Finger Lakes Region, New York: U.S. Geological Survey Open-File Report 94-0615, one plate.

Kappel, W.M., and Miller, T.M. 2003. Hydrogeology of the Tully Trough - southern Onondaga County and northern Cortland County, New York: U.S. Geological Survey Water-Resource Investigations Report 03-4112 16 pp.

Kappel, W.M., and Teece, M.A. 2007. Paleoenvironmental assessment and deglacial chronology of the Onondaga Trough, Onondaga County, New York. U.S. Geological Survey Open-File Report 2007-1060, 12 pp.

Lollino, G., Arattano, M., and Cuccureddu, M. 2002. The use of the Automatic Inclinometric System (AIS) for landslide early warning--the case of Cabella Ligure (North-Western Italy). Physics and Chemistry of the Earth. 27(36): 1545-1550.

Lollino, G., Arattano, M., Allasia, P., and Giordan, D. 2006. Time response of a landslide to meteorological events. Natural Hazards and Earth System Science. 6: 179-184.

McSaveny, M.J., and Griffiths, G.A., 1987, Drought, rain, and movement of a recurrent earthflow complex in New Zealand. Geology. 15(7): 643-646.

Pair, D.L., Kappel, W.M., and Walker, M.S. 2000. History of landslides at the base of Bare Mountain, Tully Valley, Onondaga County, New York: U.S. Geological Survey Fact Sheet 190-99. 6 pp.

Phipps, R.L. 1974. The soil creep – curved tree fallacy. Journal of Research of the U.S. Geological Survey. 2: 371-377.

Potter, N., Jr. 1969. Tree-ring dating of snow avalanche tracks and the geomorphic activity of avalanches, northern Absaroka Mountains, Wyoming. Geological Society of America Special Paper 123: 141-165.

Rogers, W.B. 1991. The missing record – Tertiary Period, in Isachsen, Y.W., Landing, E., Lauber, J.M., Rickard, L.V., and Rogers, W.B., eds., Geology of New York--A simplified account. Albany, N.Y., New York State Museum, Education Department, Educational Leaflet 28. 284 pp.

Schroeder, J.F. Jr. 1978. Dendrogeomorphological analysis of mass movement on Table Cliffs Plateau, Utah. Quaternary Research. 9: 168-185.

Schroeder, J.F. Jr. 1980. Dendrogeomorphology—Review and new techniques of tree-ring dating. Progress in Physical Geography. 4: 161-188.

Sigafoos, R.S. 1964. Botanical evidence of floods and flood-plain deposition. U.S. Geological Survey Professional Paper 485-A, 35 pp.

Singleton, R., Gardescu, S., Marks, P.L., and Geber, M.A. 2001. Forest herb colonization of postagricultural forests in central New York State, USA: Journal of Ecology. 89(3): 325-338.

Stefanini, M.C. 2004 Spatio-temporal analysis of a complex landslide in the Northern Apennines (Italy) by means of dendrochronology. Geomorphology. 63: 191-202.

Tamulonis, K.L., Kappel, W. M., and Shaw, S.B. 2009. Causes and movement of landslides at Rainbow Creek and Rattlesnake Gulf in the, Tully Valley, Onondaga County, New York: U.S. Geological Survey Scientific Investigations Report 2009-5114. 16 pp.